United Arab Emirates University
Scholarworks@UAEU

Dissertations | Electronic Theses and Dissertations

Summer 5-2014

RESOURCE ALLOCATION FOR WIRELESS RELAY NETWORKS

Hanan Hassan Al-Tous

Follow this and additional works at: https://scholarworks.uaeu.ac.ae/all_dissertations

Part of the Electrical and Computer Engineering Commons

Recommended Citation

Al-Tous, Hanan Hassan, "RESOURCE ALLOCATION FOR WIRELESS RELAY NETWORKS" (2014). *Dissertations*. 20.
https://scholarworks.uaeu.ac.ae/all_dissertations/20

This Dissertation is brought to you for free and open access by the Electronic Theses and Dissertations at Scholarworks@UAEU. It has been accepted for inclusion in Dissertations by an authorized administrator of Scholarworks@UAEU. For more information, please contact fadl.musa@uaeu.ac.ae.

United Arab Emirates University

College of Engineering

RESOURCE ALLOCATION FOR WIRELESS RELAY NETWORKS

Hanan Hassan Al-Tous

This dissertation is submitted in partial fulfillment of the requirements for the degree of Doctor of Philosophy

Under the direction of Dr. Imad Barhumi

May 2014

DECLARATION OF ORIGINAL WORK

I, Hanan Al-Tous, the undersigned, a graduate student at the United Arab Emirates University (UAEU) and the author of the dissertation titled "Resource Allocation for Wireless Relay Networks", hereby solemnly declare that this dissertation is an original work done and prepared by me under the guidance of Dr. Imad Barhumi, in the College of Engineering at UAEU. This work has not been previously formed as the basis for the award of any degree, diploma or similar title at this or any other university. The materials borrowed from other sources and included in my dissertation have been properly acknowledged.

Student's Signature ..... Date .....

COPYRIGHT

Copyright © 2014 by Hanan Al-Tous

All Rights Reserved

Approved by

PhD Examining Committee:

1) Advisor (Committee Chair): Dr. Imad Barhumi
   Title: Associate Professor
   Department of Electrical Engineering
   College of Engineering
   Signature ..... Date .....

2) Member: Dr. Mohammed Abdel-Hafez
   Title: Associate professor
   Department of Electrical Engineering
   College of Engineering
   Signature ..... Date .....

3) Member: Dr. Khaled Shuaib
   Title: Associate professor
   Department of Information Security
   College of Information Technology
   Signature ..... Date .....

4) Member (External Examiner): Prof. K. J. Ray Liu
   Title: Christine Kim Eminent Professor of Information Technology
   Department of Electrical and Computer Engineering
   Institution: University of Maryland, USA
   Signature ..... Date .....

Accepted by

Dean of the College of Engineering: Prof. Amr Salah El-Dieb

Signature ..... Date .....

Dean of the College of Graduate Studies: Prof. Nagi Wakim

Signature ..... Date .....

Copy of

ABSTRACT

In this thesis, we propose several resource allocation strategies for relay networks in the context of joint power and bandwidth allocation and relay selection, and joint power allocation and subchannel assignment for orthogonal frequency division multiplexing (OFDM) and orthogonal frequency division multiple access (OFDMA) systems. Sharing the two best ordered relays with equal power between the two users over Rayleigh flat fading channels is proposed to establish full diversity order for both users. Closed form expressions for the outage probability, and bit error probability (BEP) performance measures for both amplify and forward (AF) and decode and forward (DF) cooperative communication schemes are developed for different scenarios. To utilize the full potentials of relay-assisted transmission in multi user systems, we propose a mixed strategy of AF relaying and direct transmission, where the user transmits part of the data using the relay, and the other part is transmitted using the direct link. The resource allocation problem is formulated to maximize the sum rate. A recursive algorithm alternating between power allocation and bandwidth allocation steps is proposed to solve the formulated resource allocation problem. Due to the conflict between limited wireless resources and the fast growing wireless demands, Stackelberg game is proposed to allocate the relay resources (power and bandwidth) between competing users, aiming to maximize the relay benefits from selling its resources. We prove the uniqueness of Stackelberg Nash Equilibrium (SNE) for the proposed game. We develop a distributed algorithm to reach SNE, and investigate the conditions for the stability of the proposed algorithm. We propose low complexity algorithms for AF-OFDMA and DF-OFDMA systems to assign the subcarriers to the users based on high SNR approximation aiming to maximize the weighted sum rate. Auction framework is proposed to devise competition based solutions for the resource allocation of AF-OFDMA aiming to maximize either

the sum rate or the fairness index. Two auction algorithms are proposed; sequential and one-shot auctions. In sequential auction, the users evaluate the subcarrier based on the rate marginal contribution. In the one-shot auction, the users evaluate the subcarriers based on an estimate of the Shapley value and bids on all subcarriers at once.

Keywords: Relay Networks, Amplify and Forward (AF), Decode and Forward (DF), Resource Allocation, Optimization, Stackelberg Game, OFDM/OFDMA, Auction Framework.

ACKNOWLEDGMENTS

All praise and thanks be to Allah, for blessing me with the strength and enthusiasm to seek knowledge and to complete this work.

Foremost, I would like to express my sincere appreciation and gratitude to my advisor Dr. Imad Barhumi, for his academic guidance and enthusiastic encouragement throughout this PhD. His constant encouragement was vital in making this dissertation a reality. He spent endless hours proofreading my research papers and giving me excellent suggestions, which always resulted in improved versions of the documents. He also supported me during the difficult times in my research. He believed in me when I doubted myself, and always preserved his confidence in my ability to complete my PhD. Doing a PhD is always challenging, and I will not forget how Dr. Imad assisted me. I cannot thank him enough for all the encouragement and advice, helping to make it an enjoyable experience.

I owe my deepest gratitude to the United Arab Emirates University (UAEU) for its generosity in supporting me financially during my PhD study.

I would like to thank Dr. Mohammad Hayajneh, Dr. Qurban Ali, and Prof. Noafal Al-Dahir for serving as my PhD Advisory Committee.

I would like to thank Prof. K.J. Ray Liu, Dr. Mohammed Abdel-Hafez, Dr. Khaled Shuaib for serving as my PhD Examining Committee.

I would like to thank all the faculty and staff in the Electrical Engineering Department in UAEU for their continuous encouragement.

I would like to acknowledge the help of all the people who have contributed to my education, especially, my professors in Jordan University and colleagues in Amman Al-Ahliyyah University.

I would like to thank friends at UAEU; Salam, Assha, Hanifa, Razan, Shumma, Taghreed, Sawsan, Nedaa, Reem, Maysara, Dr. Maysa, Hanan, Hana, and Swzen. Thank you for the true positive experiece we had during my PhD research.

I would like to thank my friends Rana, Ymna, Lubna, Lena, Lamiss, Abir, Huda, Maram, Ahlam, and Angham. Your friendship and prayers gave me strength to overcome difficulties throughout this endeavor. All thanks to Alah for blessing me with good friends.

My heartiest thanks go to my parents, brothers and their families, thank you for everything, for your support, love, and care.

DEDICATION

I would like to dedicate this dissertation to my parents for their love and support in all my endeavors, and to my dearest friend *Rana*

TABLE OF CONTENTS

LIST OF TABLES

LIST OF FIGURES

LIST OF NOMENCLATURE

Roman Symbols

$\mathrm{E}[\cdot]$, $\mathrm{E}_x[\cdot]$ Expectation Operator

Δ Gradient Operator

$(x)^+$ $(x)^+ = \max\{x, 0\}$

$\mu(y)$ Unit Step Function

sig Sigmoid Function

$sign$ Sign Function

$(\,)^T$ Vector Transpose Operation

Greek Symbols

e Euler Constant

Γ Capacity Gap

$\jmath$ $\sqrt{-1}$

$\mathcal{N}(0, \sigma^2)$ The Normal distribution with Zero-Mean and σ^2 Variance

σ_0^2 The Noise Variance

Other Symbols

$\mathcal{C}$ Decoding Set

inf Infimum

N_0 The AWGN Power Spectral Density

Pr Probability

sup Supremum

Acronyms / Abbreviations

3GPP-LTE Third-Generation Partnership Project-Long Term Evolutions

ABRD Asynchronous Best Response Dynamics

AF Amplify and Forward

AWGN Additive White Gaussian noise

BA Beamforming Amplify and Forward

BC Broadcast Channel

BD Beamforming Decode and Forward

BEP Bit Error Probability

SEP Symbol Error Probability

BF Beamforming

BR Best Response

CDF Cumulative Density Function

CDMA Code Division Multiplexing

CoMP Coordinated Multiple Point

CR Cognitive Radio

CSI Channel State Information

DAS Distributed Antenna System

DC Direct Communications

DF Decode and Forward

DFT Discrete Fourier Transform

DSC Diagonal Strict Concavity

FDMA Frequency Division Multiple Access

FDM Frequency Division Multiplexing

FIR Finite Impulse Response

GBD Generalized Benders Decomposition

GIRG Gaussian Interference Relay Game

GRWNET Green Wireless Network

HETNEt Heterogeneous Network

IDFT Inverse Discrete Fourier Transform

IEEE-SA IEEE Standard Association

iid Independent Identically Distributed

ISI Inter-Symbol-Interference

KKT Karush-Kuhn-Tucker

LHS left Hand Side

LOS Line-Of-Sight

LP Linear Programming

MAC Multiple Access Channel

MANET Mobile Ad-Hoc Network

MBWA Mobile Broadband Wireless Access

MGF Moment Generating Function

MILP Mixed Integer Linear Programming

MIMO Multiple-Input Multiple-Output

MINLP Mixed Integer Non-Linear Programming

MQAM M-Quadrature Amplitude Modulation

MRC Maximal Ratio Combiner

MRC Maximal Ratio Combining

NE Nash Equilibrium

NP-hard Non-Deterministic-Polynomial-Hard

OFDMA Orthogonal Frequency Division Multiple Access

OFDM Orthogonal Frequency Division Multiplexing

PDF Probability Density Function

ΠG Prices Game

PO Pareto Optimal

PSD Power Spectral Density

M-PSK M-Array Phase Shift Keying

PSO Particle Swarm Optimization

PU Primary User

PWG Power Bandwidth Game

M-QAM M-Array Quadrature Amplitude Modulation

QoS Quality of Service

RHS Right Hand Side

SBRD synchronous Best Response Dynamics

SCFSC Single Carrier Frequency Selective Channel

SC Selective Combining

SDF Selective Decode and Forward

SENET Sensor Network

SNE Stackelberg Nash Equilibrium

SNR Signal-to-Noise-Ratio

STBC Space Time Block Coding

SU Secondary User

TDM Time Division Multiplexing

TC Threshold Combining

TU Transferable Utility

UAVR Unmanned Aerial Vehicle Relay

VANET Vehicular Ad-Hoc Network

WiFi Wireless Fidelity

WiMax Worldwide Interoperability for Microwave Access

CHAPTER1

INTRODUCTION

Wireless communications have seen unpredictable growth during the past few decades and will continuously evolve in the future. The exploding growth of wireless data traffic is far beyond the growth of wireless capacity. Wireless spectrum is very limited and overly crowded, and wireless channels suffer from random variations of channel quality in time, frequency, and space due to multipath fading, shadowing, and path loss effects. The introduction of multiple-input multiple-output (MIMO) communication constitutes a breakthrough in the design of wireless communication systems [14, 94]. MIMO systems could potentially increase the system capacity as well as system reliability. Such systems provide significant improvement in link reliability and spectral efficiency through the use of multiple antennas at the transmitter and/or the receiver sides. Multiple-antenna techniques are very attractive for deployment in cellular systems at the base stations and have already been included in third generation cellular standards. Variations of MIMO techniques are now considered in many existing and emerging wireless standards, such as IEEE 802.11 wireless fidelity (WiFi), IEEE 802.16 worldwide interoperability for microwave access (WiMax), and IEEE 802.20 mobile broadband wireless access (MBWA) [14, 62].

Size and power constraints limit the deployment of MIMO techniques in cellular mobile devices, as well as in wireless sensor and ad-hoc networks, which are gaining popularity in recent years. An innovative approach to

gain spatial diversity without deploying multiple antennas is cooperative diversity, also known as cooperative communications. Instead of a classical network with isolated communicating pairs, cooperative communication techniques take advantage of the broadcast nature of wireless transmission, creating virtual antenna array through cooperating nodes. This new transmission paradigm promises significant performance gains in terms of link reliability, spectral efficiency, system capacity, and transmission range. Cooperative communication builds upon a network architecture in which nodes help each other in relaying information to realize spatial diversity advantages, thereby improving their own performance and that of the whole network [35, 62, 144].

An overview of cooperative communications; history and milestones, state-of-the-art, application areas, and pros and cons are presented in Section 1.1. The motivations behind this dissertation and the addressed problems are presented in Section 1.2. A chapter by chapter overview and summary of contributions of this dissertation will be given in Section 1.3.

1.1 Cooperative Communications

It is expected that the served data rate of the next generation mobile system will be 100 to 1000 times more than the current ones. The limitations of traditional cellular systems to achieve high data rates in future mobile systems can be discussed as : (1) cellular networks can not meet the desired high data rate due to limited transmit power, (2) high speed mobile environment requires high frequency handover, which makes the system complex and expensive, (3) at frequencies higher than 2GHz, the cell edge effect becomes more serious due to the larger attenuation of radio signals.

However, a new paradigm has emerged to overcome these limitations and turn the traditional cellular system into a cooperative system. A cooperative communication system may contain one or more of the following

techniques: relaying, distributed antenna systems (DASs), multicell coordination, group cell, and coordinated multiple point transmission and reception (CoMP). In relaying cooperative transmission, a relay is used to forward the overheard information after processing. DAS was introduced to improve the indoor coverage performance of wireless communication systems, in which two or more information sources simultaneously transmit a common message. Multicell coordination was introduced to increase the capacity of cellular mobile communications by using microcells and advanced power control techniques. A group cell is characterized by several adjacent cells that use the same resources to communicate with a specific user and different resources to communicate with different users. CoMP entails dynamic coordination among multiple geographically separated transmission points. It was proposed to improve the coverage at the cell-edge and/or to improve the system throughput at high data rates [140, 171].

In this dissertation, our main concern is cooperative communication using relaying; other cooperation techniques are beyond the scope of this dissertation. In the following subsections, we trace the history and mention some milestones of relay networks, then present the state of the art and explore some application areas. Finally, the advantages and disadvantages of relay networks are discussed.

1.1.1 History and Milestones

Information theoretical development of the simplest form of cooperative communications stems back to the groundbreaking contributions by van der Meulen in 1968 [145] and by Cover and Gamal in 1979 [29]. In particular, they determined the capacity region of a three node network consisting of a source, a destination, and a relay. It was assumed that all nodes can operate in the same band, so the system can be decomposed into a broadcast channel (BC) and a multiple access channel (MAC) from the viewpoint of

the source and destination nodes, respectively. Cooperative relaying where two users help each other to boost each other's performance was introduced by Sendonaris et al. in [119, 120]. Specifically, each of the two users is responsible for transmitting not only her own information, but also the information of her partner, which she receives and detects.

Harrold and Nix [54, 55] were the first to prove that by cooperating, every user gains in the long run, whilst sometimes short-term gains were unfavorable. They also showed that coverage holes in a cellular system could be largely closed by using simple relaying.

Laneman [84, 86] in his seminal work formalized various types of supportive and cooperative communication protocols and proved that significant gains in performance can be achieved using cooperation. Cooperative schemes based on channel coding, and special code designs were proposed by Hunter et al. and Stefanov et al. [69, 132]. Space-time relaying key contributions emerged from the works of Dohler et al. and Laneman and Stefanov in [34, 85, 133].

Huang et al. [66] proposed auction framework to sell the relay power to source nodes, where the relay allocates its transmission power proportional to the source nodes' bids. Wang et al. [149] formulated the trade between a source node and multiple relay nodes as Stackelberg market with the source node as the leader and relay nodes as followers. Yang et al. [161] proposed an auction mechanism to allocate the relay nodes and charge the source nodes aiming to maximize the revenue of the base station.

Zhang et al. [174] proposed a cooperation strategy among two users communicating with an access point to allocate the bandwidth using the Nash bargaining model. Chen et al. [24] proposed a reputation based mechanism to provide incentives for nodes to serve as relay nodes using repeated game framework. Gao et al. [42] introduced a game theoretical approach to stimulate user cooperation using indirect reciprocity game.

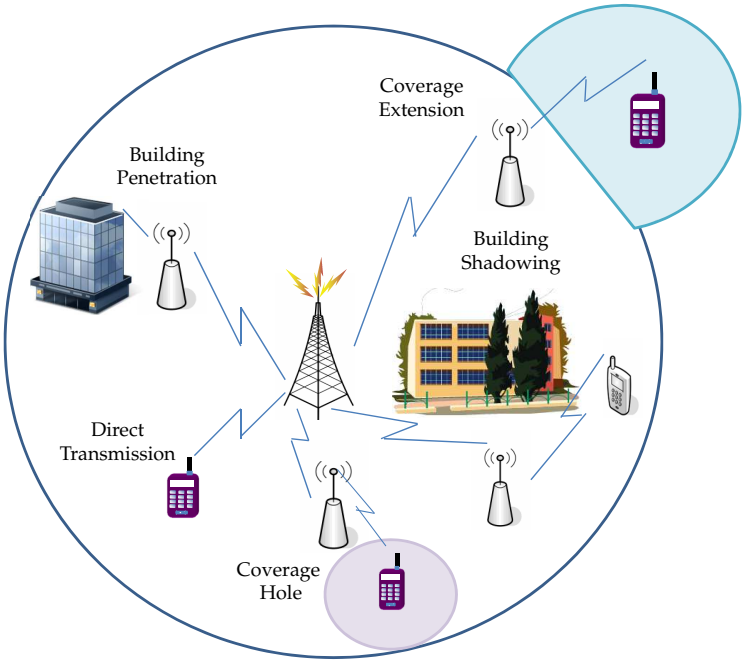

Figure 1.1 Use Cases for 802.16j [43].

1.1.2 State of the Art

Multihop wireless systems have the potential to offer improved coverage and capacity over single-hop radio access systems. The relay has been adopted by many international communication standards, such as IEEE 802.16j and the third-generation partnership project-long term evolution (3GPP-LTE). The IEEE 802.16j standard has been developed to provide performance enhancement to existing IEEE 802.16 networks by incorporating relay capabilities to the system as shown in **Figure 1.1**. IEEE 802.16j was approved by the IEEE-SA Standards Association Board on 2009-05-13 as an amendment to IEEE standard 802.16-2009.

Two relaying modes are defined in the standard; transparent and non-transparent modes. In the transparent mode, the relays do not forward framing information. The main use of this mode is to facilitate capacity increase within the BS coverage area. In the non-transparent mode, the relays forward framing information or generate their own framing information based on a scheduling scheme (distributed or centralized). The relays

are used in this mode to provide an increase in the coverage area. Non-transparent relays can support more than two hops in either centralized or distributed scheduling modes, leading to different levels of complexity at the relay node.

Relay is one of the key features of the 3GPP LTE-Advanced standard. Relays are introduced to reduce the cost of wired back-haul. Similar to IEEE 802.16j standard, the relay in 3GPP LTE-Advanced standard can operate in two operational modes; transparent and non-transparent. Only simple relaying schemes are considered in IEEE 802.16j and LTE-Advanced standards. However, more complicated and advanced cooperative communication techniques are expected in later versions and other future wireless systems [63].

1.1.3 Application Areas

Cooperative communication is one of the promising wireless technologies, and it has promising applications in many wireless systems and networks as shown in **Figure 1.2**. A brief overview of some application areas is presented as follows.

- **Mobile Ad-Hoc Networks (MANETs)**: Two potential architectures for cooperative MANETs are proposed for improving the connectivity; the clustered infrastructure where cooperative relays are centrally controlled by cluster head and the decentralized architecture, where cooperative links are formed by request of a source node [116].

- **Sensor Networks (SENETs)**: Multiple relay nodes can be used to improve energy-saving compared to direct transmission as proposed in [178]. In addition, cooperative transmission among sensor nodes can be used for maximizing the network lifetime under maximum bit-error-rate constraint. The network lifetime can be maximized by choosing the optimum location of each relay and optimally allocating the

power at the relay and sensor nodes [61]. Furthermore, unmanned aerial vehicle relays (UAVRs) can be used to increase the transmission reliability of sensor nodes under real-world impairments such as distance or obstructed line of sight between the nodes [25].

- **Vehicular Ad-Hoc Networks (VANETs)**: Cooperative communication can be used to enhance the quality of service (QoS) performance of VANETs; through the cooperation of a set of dynamically selected relay nodes, high speed content downloading can be achieved [93, 179].

- **Heterogeneous Networks (HETNETs)**: It is expected that the relay nodes will constitute the basis of HETNETs. The efficiency of large-scale HETNETs mainly depends on the deployment of relay nodes; relays can be employed to provide a cost-effective coverage [63].

- **Cognitive Radios (CRs)**: In overlay cognitive networks, the secondary users (SUs) can transmit simultaneously with the primary users (PUs). The interference to the PUs can be offsett by using part of the SU's power to relay the PUs' data [15, 91, 168]. In addition, sensing diversity gain in cognitive communications can be utilized by employing a CR that is located near the PU as a relay. Hence, the signal of the PU can be detected reliably by far users. Furthermore, the so-called cognitive wireless relay network can be used to utilize the spectrum, where the relay nodes are CRs which are dispersed over a wide-band spectrum, and each cognitive radio is allowed to be chosen as a relay as proposed in [92].

- **Green Wireless Networks (GRWNETs)**: It is believed that future wireless communication networks will be powered by sustainable energy sources. The capacity and availability of green energy highly depend on the weather and location, which may lead to degradation of user performance. In this sense, joint power allocation and relay placement

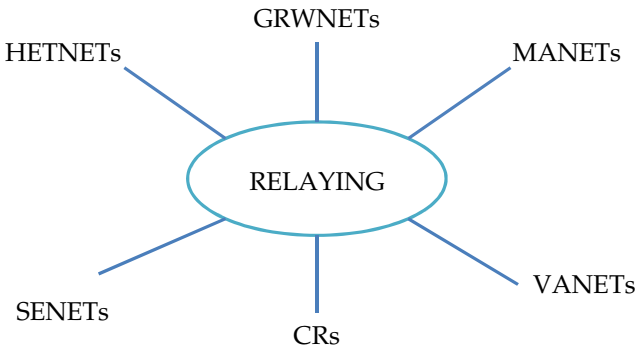

Figure 1.2 Relaying Application Areas.

can significantly increase the network throughput and the transmission performance, which will boost the construction of green wireless networks [172]. In addition, relay and cooperative networks are also promising architectures to improve energy efficiency; where the channel diversity can be exploited for potential energy savings [38].

1.1.4 Pros and Cons of Cooperation

Performance gains such as path-loss gains, diversity, and multiplexing gains are considered the key advantages of cooperative communications. These gains can be transformed into a higher capacity, better cell coverage, or reduced power transmission levels. Relaying can solve the problem of capacity and coverage at the cell edge or in shadowed areas. In addition, relaying is a cost-effective-solution to provide a given level of QoS to all users in the cell. The capital and operational costs are generally lower when relays are used [141].

The major disadvantages of cooperative communications are: complex schedulers, increased overheads, and more channel coefficient estimations to detect the signal, since relaying increases the number of wireless channels. Relaying requires sophisticated schedulers to select the relays and schedule the relayed data flow for different users in the system. Extra overheads are required to maintain synchronization in relay networks [35].

1.2 Overview of Dissertation

This section presents the context of the dissertation, introduces the investigated resource allocation problems, and presents objectives and solution approaches.

Sharing the network resources (that is, relay selection, and power and/or bandwidth) among users is one of the foremost concerns of cooperative communication systems (to be fully implemented) in future communication systems.

Resource allocation refers to the problem of allocating physical layer resources such as bandwidth and power among active users. Compared to conventional transmission, the relay-aided transmission raises more complicated resource allocation problems, since it introduces extra tasks such as deciding the transmission mode, determining assisting relay(s) and allocating power and bandwidth for each relay-aided user. In addition, resource allocation for orthogonal frequency division multiple access (OFDMA) relay-aided systems, requires subcarrier assignment and power allocation at the source and relay nodes for each subcarrier.

In a cooperative communication system, the following questions should be answered: Which nodes should be selected as relays? What relaying strategy should be used? How power and bandwidth are allocated among users? Which criterion for optimality should be considered? Clearly, the answers to these questions depend on the topology of the network, the objective and formulation of the resource allocation problem, the number of users in the network, and the power and bandwidth available at the relay and source nodes.

Our main concern in this dissertation is resource allocation in relay networks for multi user scenarios. However, we address one single user scenario in the context of relay aided orthogonal frequency division multiplex-

ing (OFDM) systems. We investigate resource allocation for relay networks to achieve different objectives; i.e. equal diversity order, maximum sum rate, maximum revenue, maximum weighted sum rate, and maximum fairness index for different scenarios and using different tools from order statistics, optimization, and game theory.

For multiple users scenarios, usually the system viewpoint is considered in allocating the system resources. One of the most likely scenarios in multiple users and multiple relays is examined, in which two users are competing for the same relay, the best relay for both users is selected. Since the relay has limited power capability, it can not satisfy the power requested by both users simultaneously. From the system viewpoint, the relay will be allocated to the user with the maximum end-to-end signal to noise ratio (SNR), and the other user will be allocated the second best ordered relay if the objective is to maximize the sum rate[1]. In the case of having the same end-to-end SNR for both users, the best and next-best relays are assigned randomly to the users. Hence, in both cases the first and second users achieve different diversity orders. In this regard, we address the problem of two users competing for the best relay by a different approach, aiming to achieve full diversity order for both users by sharing the two best ordered relays between the two users. We develop closed form expressions for the outage probability and bit error probability (BEP) performance measures, and prove that the proposed scenario achieves better performance than using the next best relay alone. In addition, sharing the two best ordered relays is studied in the context of beamforming and space time block coding (STBC) techniques to utilize the spectrum efficiently.

In the literature, most resource allocation problems investigate power allocation for a fixed bandwidth assignment, or bandwidth allocation for a fixed power allocation [57, 108, 122, 169]. To utilize the resources efficiently,

[1]The converse applies if the objective is to maximize the minimum data rate.

joint power and bandwidth needs to be investigated. In [46, 124], the authors investigated joint power and bandwidth allocation for a decode and forward (DF) cooperative communication system, where the resource allocation problem is a convex optimization problem, and the solution can be found using convex optimization techniques. Even though amplify and forward (AF) is the simplest cooperative communication protocol, joint power and bandwidth allocation for multi user systems was not addressed in the literature. This problem is a complex problem to solve since the objective function is not a jointly concave function in power and bandwidth profiles. In [98], the authors showed that the AF strategy does not necessarily benefit from the large available bandwidth in a network with many relays and a single source-destination pair. Based on this result, we modify AF cooperative protocol so that the users will use part of the bandwidth for AF transmission with diversity, and the other part is used only for direct transmission. We then formulate the optimization problem for a multiple users single relay system aiming to maximize the sum rate. The formulated problem is not convex. We propose, an iterative algorithm alternating between two steps; a power allocation step for a given bandwidth profile, and a bandwidth allocation step for a given power profile. The sum rate of the proposed algorithm coincides with the sum rate when using particle swarm optimization (PSO) method.

Joint power and bandwidth resource allocation for the improved AF relaying scheme using optimization framework relies on a system viewpoint, which requires all users to follow the resource sharing mechanism and requires the relay to belong to the system. However, in the absence of a central controller, where the relay and users may not belong to the same system, or the relay may support more than one system, then the optimization approach is no longer applicable. An alternative solution is to model the interactions between the users and the relay using a game theory framework.

Game theory is used to design incentives for cooperation in cooperative communications using different mechanisms; reputation based mechanism, resource-exchange-based mechanism, and pricing-based mechanism [28, 149, 156, 160, 161]. In this regard, we use pricing based mechanism to jointly sell the relay limited resources (i.e. power and bandwidth) to competing users using the Stackelberg framework. We investigate existence, and uniqueness of the Stackelberg Nash Equilibrium. We develop an iterative algorithm to find the equilibrium (i.e. relay prices, and power and bandwidth profiles for competing users), and study stability conditions of the proposed algorithm.

For relay-aided OFDM and relay-aided OFDMA systems, joint power and bandwidth resource allocation includes subcarrier assignment and source and relay power profiles at each subcarrier. Resource allocation in OFDM and OFDMA systems is a challenging problem, because of the mixed integer nature of the issue. In the literature, resource allocation problems for OFDMA systems are addressed using the dual domain[2], which entails a large number of iterations to find the correct Lagrange multipliers [30, 96]. Our main concern in resource allocation problems for relay-aided OFDM and relay-aided OFDMA systems is to develop low complexity algorithms or distributed competition based algorithms to solve such problems. As a result, we investigate joint subcarrier assignment and power allocation at the source and relay nodes under individual node and total power constraints for selective AF/DF-OFDM systems, aiming to maximize the symbol rate. In selective AF/DF-OFDM systems, each subcarrier can be used either for AF or DF relaying with diversity or direct transmission without diversity. We develop a low complexity subcarrier assignment algorithm based on optimal power profiles at the source and relay nodes and high SNR approximation.

[2]Resource allocation problems of multicarrier systems achieve zero duality gap for large number of subcarriers [167].

For AF/DF-OFDMA communication systems, we address joint power allocation at the source and relay nodes and subcarrier assignment in two different contexts: In the first context, we target developing a low complexity algorithm for joint subcarrier assignment and power allocation at the source and relay nodes, aiming to maximize the weighted sum rate under individual node power constraint. A low complexity algorithm is devised based on optimal source and relay power profiles and high SNR approximation.

In the second context, we target competition based distributed algorithms for joint subcarrier assignment and power allocation at the source and relay nodes aiming to maximize either the sum rate or the fairness index under individual node power constraint. In this sense, two auction algorithms are proposed to assign subcarriers among users: sequential and one-shot auction algorithms. The proposed auction algorithms are designed using a utility function to evaluate the worth of the subcarriers and bid on them. In both auction algorithms, the bidding strategies are based on optimal power profiles at the source and relay nodes. In the sequential algorithm, the user utilizes her history in the game to bid for the current subcarrier, whereas in the one-shot algorithm, the user evaluates the worth of the subcarriers at once, based on the Shapley value. A sampling approach is used to estimate the Shapley value.

1.3 Dissertation Outline and Contributions

In this section, a chapter by chapter outline is presented. In addition, the contributions associated with each chapter are listed.

- **Part One** contains the following chapters:

  Chapter 2, the basics of cooperative communication schemes and the their performance measures are explained. In particular, outage prob-

ability, diversity order and symbol error probability (SEP) are discussed. Basic concepts in optimization and game theory are introduced. In particular, the focus is put on optimality conditions, dual method, and Nash equilibrium. These concepts will be used extensively in subsequent chapters.

Chapter 3, the problem of two users sharing the same best ordered relay is investigated for different cooperative schemes. Expressions of the outage probability, BEP, and diversity order are derived for these schemes. The results of this chapter are partially incorporated in a manuscript published as:

- H. Al-Tous, I. Barhumi, *Performance Analysis of Relay Selection in Cooperative Networks Over Rayleigh Flat Fading Channels*, EURASIP Journal on Wireless Communications and Networking, (1), 1-16, December 2012.

Chapter 4, joint power and bandwidth resource allocation for a modified AF cooperative communication scheme is investigated aiming to maximize the sum rate in frequency flat and frequency selective channels. An adaptive algorithm is developed to find the optimal allocation profiles. In addition, joint power and bandwidth and relay selection is addressed using PSO method. Publications related to this chapter are:

- H. Al-Tous, I. Barhumi, *Joint Power and Bandwidth Allocation for Multiuser Amplify and Forward Cooperative Communications Using Particle Swarm Optimization*, IEEE 13th International Workshop on Signal Processing Advances in Wireless Communications (SPAWC 2012), pp. 55-59, 17-20 June 2012, Cesme, Turkey.
- H. Al-Tous, I. Barhumi, *Resource Allocation for Multiuser AF Cooperative Communications*, IEEE Transactions on Wireless Communi-

cations, Submitted for Publication.

Chapter 5, joint power and bandwidth resource allocation for a single relay AF cooperative communication system is investigated using Stackelberg game; where the relay aims to maximize its benefits by selling its resources to the users. A distributed iterative algorithm is developed to reach Nash Equilibrium. Publications related to this chapter are:

- H. Al-Tous, I. Barhumi, *Resource Allocation for AF Cooperative Communications Using Stackelberg Game*, 6th International Signal Processing and Communication Systems Conference (ICSPCS 2012), 12-14 December 2012, Gold Coast, Australia.
- H. Al-Tous, I. Barhumi, *Joint Power and Bandwidth Allocation for Amplify and Forward Cooperative Communications Using Stackelberg Game*, IEEE Transactions on Vehicular Technology, 62 (4), 1678-1691, May 2013.

- **Part Two** contains the following chapters:

  Chapter 6, basic concepts of OFDM and OFDMA systems are introduced, and resource allocation problems for AF/DF-OFDM and AF/DF-OFDMA systems are explored.

  Chapter 7, joint mode selection of AF/DF-OFDM cooperative communication and power allocation at the source and relay nodes aiming to maximize the symbol data rate under either individual node or total power constraints are investigated. Low complexity algorithms are developed to select the transmission mode. Publications related to this chapter are:

  - H. Al-Tous, I. Barhumi, *A Low Complexity Algorithm for Selective AF-OFDM System*, IEEE 79th Vehicular Technology Conference

(VTC 2014 Spring), Accepted.

Chapter 8, joint resource allocation for AF/DF-OFDMA aiming to maximize the weighted sum rate is addressed. A low complexity algorithm is developed to assign the subcarriers to the users. Publications related to this chapter are:

- H. Al-Tous, I. Barhumi, *Two Bands Subcarrier Partition Resource Allocation for Two users AF-OFDMA System*, IEEE Transactions on Mobile Computing, Revised.
- H. Al-Tous, I. Barhumi, *Resource Allocation for Two-Sources Single-Relay AF-OFDMA Systems*, SPAWC 2014, Submitted for Publication.
- H. Al-Tous, I. Barhumi, *Resource Allocation for Two-Users DF-OFDMA Systems*, IEEE VTC 2014 Fall, Accepted.

Chapter 9, auction framework is proposed for subcarrier assignment in AF-OFDMA systems, sequential and one-shot algorithms are proposed to allocate the resources aiming to maximize either the sum rate or the fairness index. Publications related to this chapter are:

- H. Al-Tous, I. Barhumi, *Resource Allocation Using Auction Framework*, IEEE Transactions on Wireless Communications, Revised.
- H. Al-Tous, I. Barhumi, *Auction Framework for Resource Allocation in AF-OFDMA Systems*, PRIMC 2014, Submitted for Publication.
- H. Al-Tous, I. Barhumi, *One-Shot Auction for Resource Allocation in AF-OFDMA Systems*, GLOBCOM 2014, Submitted for Publication.

Chapter 10, we conclude and explore further direction of research.

Part I

Relay Selection, Joint Power and Bandwidth Allocation in Relay Networks

CHAPTER2

BASIC CONCEPTS

Some basic concepts related to cooperative communications are discussed throughout this chapter, and the necessary resource allocation tools, which facilitate the understanding of the rest of this dissertation, are presented.

Wireless channel models and performance metrics are introduced in Section 2.1 and Section 2.2, respectively. In Section 2.3, the fundamental cooperative communication schemes AF and DF are introduced. We focus on the discussion of the outage probability, diversity order, and the SEP performance measures. In addition, multiple relays scenarios are presented with their performance measures.

Resource allocation problems can be addressed using two different approaches; optimization and game theory. The optimization problem is formulated to achieve a certain performance measure related to the system viewpoint. Game theory can capture the users and the system viewpoints, using utility functions. Basic concepts in optimization and game theory are reviewed in Sections 2.4 and 2.5, respectively. Conclusions are drawn in Section 2.6.

2.1 Wireless Channel

Reliable high-speed communication using the wireless radio frequency transmission as a channel is a challenging task. Wireless channels are not only

susceptible to noise, interference, and other channel impediments, but these impairments change over time in unpredictable way due to user and surrounding object movements. The variation in the received signal power over distance is due to path loss, shadowing and small scale fading. Path loss is caused by dissipation of the power radiated by the transmitter as well as effects of the propagation channel. Generally, path loss models assume that path loss is the same at a given transmit-receive distance. Shadowing is produced by obstacles between the transmitter and receiver which attenuate the signal power through absorption, reflection, scattering, and diffraction. Variation due to path loss occurs over very large distances (100 – 1000 meters), whereas variation due to shadowing occurs over distances proportional to the length of the obstructing object (10 – 100 meters). Large-scale fading effects are due to path loss and shadowing, which occur over relatively large distances. Small-scale fading effect is due to multipath propagation, which occurs over very short distance, i.e. on the order of the signal wavelength. For the design and simulation of wireless systems, models are needed to describe mathematically the basic properties of wireless channels such as, path loss, shadowing, amplitude-fading, scattering function, delay spread, etc. Three methods are used to model the wireless channel as follows [100]:

- **Realistic Channel Models**: In these models, a sounder is used to measure, digitize, and store the channel impulse response. The disadvantage of this method is that it requires a large effort to acquire the data, and it only characterizes a certain area.

- **Deterministic Channel Models**: In these models, the geographical and morphological information are used to form a database for a deterministic solution of Maxwell's equations. The main advantage is that computer simulations are easier to perform than realistic measurements, but these models are less accurate compared to realistic

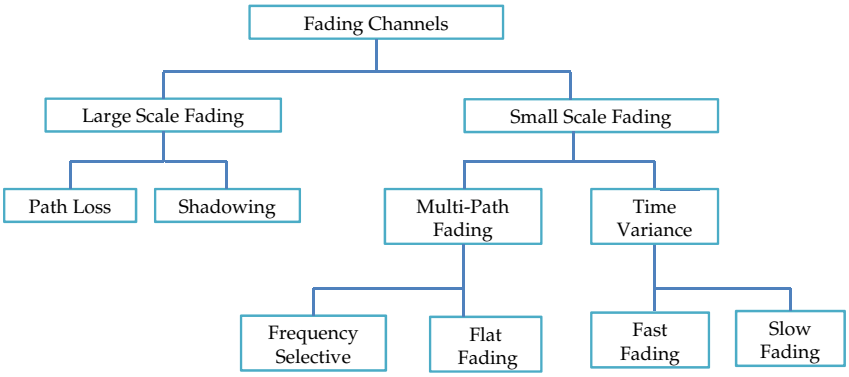

Figure 2.1 Fading Channel Classifications [26].

channel modes.

- **Stochastic Channel Models**: These methods do not attempt to correctly predict the impulse response in one specific location, but rather predict the probability density function (PDF) of the channel over a large area, an example of this approach is the Rayleigh-fading model.

In the following we will discuss some basic properties of wireless channels, and how they can be described mathematically using stochastic channel models; emphasizing on how these mathematical descriptions can be converted into simulation models, and how to parametrize these models. **Figure 2.1** shows classifications of fading channels [26].

2.1.1 Large-Scale Channel Model

It is difficult to obtain a single model that characterizes path loss accurately in different environments, due to the complexity of signal propagation. For analysis of various systems, it is sometimes best to use a simple model that captures the basics of signal propagation without resorting to complicated path loss models, which are only approximations to the real channel anyway [44]. The following simplified model for path loss as a function of distance is commonly used for system design, which is called log-scale propagation model given by:

$$PL(d) = PL(d_0)\left(\frac{d_0}{d}\right)^{\alpha}, \tag{2.1}$$

where $PL(d)$, is the path-loss at distance d, d_0 is a distance in the far-field that is used to measure $PL(d_0)$, and $\alpha \in [2, 6]$ is the path loss exponent. A table summarizing α values for different indoor and outdoor environments and antenna heights can be found in [44]. The path-loss in dB is:

$$PL(d)_{dB} = PL(d_0)_{dB} - 10\alpha \log_{10}\left(\frac{d}{d_0}\right). \tag{2.2}$$

A simple statistical model that can account for shadowing is the log-normal shadowing model in dB given as:

$$PL(d)_S = PL(d)_{dB} + X_0, \tag{2.3}$$

where X_0 is a zero-mean Gaussian random variable with variance typically from 3 to 12. The shadow path-loss is frequently referred to as log-normal fading.

2.1.2 Small-Scale Channel Model

Small scale (fading) models describe the variation in the amplitude of a signal over a small distance or time interval. Multipath fading is caused by the interference between two or more delayed versions of the transmitted signal. Several factors influence the behavior of multipath fading. One is the random presence of reflectors and scatterers between the transmitter and receiver, the second is the presence of motion; the speed of the mobile terminal and the speed of surrounding objects. The third is the transmission bandwidth of the signal. Copies of the transmitted signal; each has a different amplitude, phase and delay are added with each other at the receiver creating either constructive or destructive interference. The relation between the

transmitted signal $x(t)$ and the received signal $y(t)$ can be written as:

$$y(t) = \sum_{l=1}^{L} h_l(t)\, x\Big(t - \tau_l(t)\Big) + n(t), \tag{2.4}$$

where $h_l(t)$ is the attenuation of the lth path at time t, $\tau_l(t)$ is the delay of the lth path, and L is the number of resolvable paths at the receiver, $n(t)$ is the received additive white Gaussian noise (AWGN). Clearly, this relation describes a linear channel with an impulse response $h(t, \tau)$ given as:

$$h(t, \tau) = \sum_{l=1}^{L} h_l(t)\, \delta\Big(t - \tau_l(t)\Big). \tag{2.5}$$

If the multipath components do not change with time, the impulse response can be represented as:

$$h(t) = \sum_{l=1}^{L} h_l\, \delta(t - \tau_l). \tag{2.6}$$

The discrete-time baseband equivalent model of (2.4) can be obtained by a sampling operation at the receiver, and can be represented by a time varying finite impulse response (FIR) digital filter as [94]:

$$y(m) = \sum_{k=1}^{L_s} h_k(m)\, x(m - k) + n(m), \tag{2.7}$$

this model is frequently called tapped-delay model, all the paths with arrival time within one sampling period are combined into a single channel response coefficient h_k, and L_s is the number of resolvable paths after sampling.

In fact, it is quite common to characterize and classify wireless channels based on the power delay profile, which represents the average power associated with each path, and the power spectrum profile, which is the Fourier transform of the power delay profile. The features that can be extracted from these profiles and used to characterize the channel are as follows:

- **Delay Spread**: It represents the time difference between the arrival of the first measured path and the last. If the duration of the symbols used for signaling over the channel is more than the delay spread, then the transmitted symbols will suffer from inter-symbol-interference (ISI).

- **Coherence Bandwidth**: It is the range of frequencies over which the amplitude of two spectral components of the channel response are correlated. It is used to measure the range of frequencies over which the channel shows a flat frequency response. If the transmitted signal bandwidth is less than the channel coherence bandwidth, then all the spectral components of the signal will be affected by the same attenuation and by a linear change of phase. The channel in this case is called a flat fading channel or a narrowband channel. On the other hand, if the transmitted signal bandwidth exceeds the channel coherence bandwidth, then the spectrum component of the signal will be affected by different attenuation factors, and the channel is called a frequency selective channel or a broadband channel.

To characterize the parameters that are related to the time varying nature of the wireless channel, it is necessary to examine the variation of the frequency components over time. The correlation function between two realizations of the channel impulse response and its Fourier transform which is called the Doppler power spectrum can be used. The Doppler power spectrum provides information about the Doppler shift, i.e. if a single tone of frequency f_c is sent through a channel with a Doppler shift f_D, the Doppler spectrum will have components in the range from $f_c - f_D$ to $f_c + f_D$. The parameters that can be extracted from the correlation function and the Doppler power spectrum are as follows:

- **Coherence Time**: It is the time difference that makes the correlation between two realizations of the channel impulse response approximately zero.

- **Doppler Spread**: It represents the range of frequencies over which the Doppler power spectrum is non-zero. The Doppler spread provides information about how fast the channel changes over time. Doppler spread is proportional to the inverse of the channel coherence time. If the Doppler spread is smaller than the signal bandwidth, the channel is called slow fading channel. On the converse, if the signal bandwidth is smaller than the Doppler spread, the channel is called fast fading channel.

The channel coefficient $h(t, \tau)$ in (2.5) of a time-invariant system is modeled by a random variable, and it is modeled by a random process for a time-variant system. One of the most common models for the random channel coefficient is Clarke's model (or Jake's model). In this model, the arrived signal at the receiver is assumed to be scattered on a very large number of scatterers, which are located on a circle centered around the receiver. In addition, it is assumed that there is no line-of-sight (LOS) signal with a power notably larger than the rest. The channel coefficient for narrow-band time-invariant system based on Clarke's model can be modeled as:

$$h = h_I + \jmath h_Q, \tag{2.8}$$

where h_I and $\jmath h_Q$ represent the in-phase and quadrature-phase components, respectively. These components are modeled by zero mean Gaussian random variables; i.e. $h_I \sim \mathcal{N}(0, \sigma^2)$, and $h_Q \sim \mathcal{N}(0, \sigma^2)$, where σ^2 is the signal variance. In addition, the channel coefficient h can be written in the polar form as $h = r\, \mathrm{e}^{\jmath\theta}$, where the PDFs of r and θ are given as:

$$f_R(r) = \frac{r}{\sigma} \mathrm{e}^{\frac{-r^2}{2\sigma^2}},\ r \geq 0, \tag{2.9a}$$

$$f_\Theta(\theta) = \frac{1}{2\pi},\ 0 \leq \theta \leq 2\pi. \tag{2.9b}$$

Because the magnitude of the channel coefficient follows a Rayleigh dis-

tribution, this model is frequently called Rayleigh fading channel model. When there exists one LOS path, the magnitude of the channel coefficient is modeled using Ricean distribution. In addition, modeling the channel coefficient can be done using channels realization and using probability distributions that can be tuned to the data samples such as the Nakagami distribution [44].

It is common to model the time variation of the channel statistically using the autocrrelation function. Therefore, assuming the transmitted signal is a single tone, and the multipath components are uncorrelated, the channel correlation function can be modeled as:

$$C_h(\tau) = P_r J_0\Big(2\pi f_D \tau\Big), \tag{2.10}$$

where P_r is the received signal power, $J_0(\cdot)$ is the Bessel function of the first kind and zeroth order computed as $J_0(x) = \frac{1}{\pi}\int_0^{\pi} \mathrm{e}^{-jx\cos(\theta)} d\theta$, $f_D = \frac{v}{\lambda}$ is the Doppler frequency, v is the absolute velocity of the receiver, and λ is the wavelength. From (2.10), the auto-correlation function is zero for $f_D\tau \approx 0.4$. Thus the signal decorrelates over a distance of approximately one-half wavelength under the uniform scattering assumption. The corresponding channel power spectral density can be obtained as [44]:

$$S_h(f) = \frac{P_r}{2\pi f_D} \frac{1}{\sqrt{1 - \left(\frac{f}{f_D}\right)^2}}, \text{ if } |f| \leq f_D. \tag{2.11}$$

A common method to simulate the envelop of a narrow-band process is to pass two independent (i.e. the in-phase and quadrature phase components) white Gaussian noise sources with power spectral density (PSD) $\frac{N_0}{2}$ through a lowpass filter with frequency response $H(f)$ given as:

$$|H(f)|^2 = S_h(f). \tag{2.12}$$

2.2 Performance Metrics

In this section, the capacity of a single-user wireless channel is discussed where the transmitter and/or receiver had a single antenna. We introduce the well-known formula for capacity of a AWGN channel, then we examine capacity of time-varying flat-fading channels. For multi-users scenarios, specific points within the rate region are highlighted.

2.2.1 Single User View

The input-output relationship of a discrete-time AWGN channel is modeled as [44]:

$$y(m) = x(m) + n(m), \tag{2.13}$$

where $x(m)$ and $y(m)$ are the channel input and channel output at time m, respectively. $n(m)$ is a white Gaussian noise random process with PSD equals $\frac{N_0}{2}$. For a channel with bandwidth W and transmit power P, the channel capacity is given by Shannon's well-known formula [123]:

$$C = W \log_2 \left(1 + \frac{P}{N_0 W}\right), \tag{2.14}$$

the capacity units are bits per second (bps). Shannon's coding theorem proves that a code exists that achieves data rates arbitrarily close to the capacity with arbitrarily small probability of bit error. The converse theorem shows that any code with rate $R > C$ has a probability of error bounded away from zero.

The deterministic effect of the path-loss only scales the signal power in (2.14). The randomness in the wireless channel needs to be investigated based on the types of variation. Mainly, two types of channel variations need to be considered; ergodic (fast fading) and non-ergodic fading (slow fading). The capacity of an AWGN channel with fast flat fading, when only

the receiver has knowledge of the channel state information (CSI) is given as:

$$C = \mathrm{E}_h\Big[W \log_2\Big(1 + \frac{P|h|^2}{N_0 W}\Big)\Big], \tag{2.15}$$

where $\mathrm{E}_h[\cdot]$ is the expectation operator with respect to the channel variation h, and $|h|^2$ is the envelop of the channel attenuation. It is worth noting that the capacity-achieving code must be sufficiently long so that a received codeword is affected by all possible fading states. Using Jensen's inequality:

$$\mathrm{E}_h\Big[W \log_2\Big(1 + \frac{P|h|^2}{N_0 W}\Big)\Big] \leq W \log_2\Big(1 + \mathrm{E}_h\Big[\frac{P|h|^2}{N_0 W}\Big]\Big). \tag{2.16}$$

Therefore, Shannon capacity in (2.15) is less than Shannon capacity of an AWGN channel with the same average SNR, i.e. fading reduces Shannon capacity when only the receiver has CSI. Since Shannon capacity is not developed for wireless communications when the average channel conditions change from codeword to codeword, the concept of outage capacity was introduced to deal with non-ergodic fading, i.e. for slow flat fading channels the notion of outage capacity is used, where the instantaneous received SNR denoted as $\gamma = \frac{P|h|^2}{N_0 W}$ is constant over a large number of transmissions and then changes to a new value based on the fading distribution. With this model, data can be sent over the channel at a rate $W \log_2(1+\gamma)$ with negligible probability of error. Since the transmitter does not know the SNR value γ, it must fix a transmission rate independent of the instantaneous received SNR. Therefore, the outage condition for a realization of γ can be written as:

$$W \log_2(1 + \gamma) < R. \tag{2.17}$$

Hence, the outage probability at a required data rate R can be defined as:

$$P_{out}(R) = Pr\Big[W \log_2(1 + \gamma) < R\Big]. \tag{2.18}$$

With simple algebraic operations, the outage probability can be written as:

$$P_{out}(\gamma_{th}) = Pr\Big[\gamma < \gamma_{th}\Big]. \tag{2.19}$$

where γ_{th} is the threshold SNR computed as $\gamma_{th} = 2^{\frac{R}{W}} - 1$. The value of γ_{th} is a design parameter based on an acceptable outage probability. Typically, it is common to characterize flat fading channels by the normalized capacity $\frac{C}{W}$ versus the outage probability $P_{out}(\gamma_{th})$. The normalized capacity approaches zero for small outage probability values, and increases dramatically as the outage probability increases. However, the probability of incorrect data reception increases as the outage probability increases. The average rate correctly received over many transmission bursts is defined as:

$$\overline{C} = \Big(1 - P_{out}(\gamma_{th})\Big) W \log_2(1 + \gamma_{th}). \tag{2.20}$$

Diversity techniques are used to improve the performance of wireless communication systems in fading channels. It mitigates the fluctuations due to fading by providing more than one signal path between the source and destination nodes, so that the channel appears more like an AWGN channel. The trend is that as the number of independent paths becomes larger, the channel looks like an AWGN channel. At the receiver terminal, different techniques can be used to combine the received signals in a constructive fashion from different paths such as the maximal ratio combining (MRC), selective combining (SC), and the threshold combining (TC). The MRC combines multiple signals by first cophasing them, then weighting each signal proportionally to the corresponding path SNR, and finally adding them. SC selects the path with the best SNR. The TC scans sequentially the received signals and outputs the first signal with SNR exceeding a threshold [130].

There are many different forms of diversity; time diversity, frequency di-

versity, and spatial diversity. In time diversity, multiple copies of a symbol are sent at different time instants. In frequency diversity, multiple copies of a symbol are sent using different carrier frequencies. In spatial diversity, multiple copies of a symbol are sent using different spatial paths. Moreover, multiple diversity techniques can be combined to obtain greater performance gains, for example, time diversity with spatial diversity, and frequency diversity with spatial diversity. In this dissertation, our main focus is spatial diversity using cooperative communications. For any diversity technique, the performance improvement is revealed by the outage probability (or the symbol error probability) decreasing at high SNR at a much larger rate than a system with less or no diversity. Formally, the diversity order (gain) can be computed as:

$$d = -\lim_{\overline{\gamma}\to\infty} \frac{\log\left(P_{out}(R)\right)}{\log(\overline{\gamma})}, \tag{2.21}$$

where $\overline{\gamma} = \mathrm{E}_h[\gamma]$. Note that (2.21) illustrates a linear function between outage probability and high average SNR on a log-log scale. If $d = 0$, then with increasing SNR no decrease in outage probability is achieved. At high average SNR, diversity order is equivalent to the gradient of the outage probability (or symbol error probability) curve. Note that if the expression of $P_{out}(R)$ at high SNR can be written as:

$$\lim_{\overline{\gamma}\to\infty} P_{out}(R) \simeq c|\,\overline{\gamma}\,|^{-d}, \tag{2.22}$$

then the diversity order is d, and the coding gain is c [94].

2.2.2 System View

In multi-user communication systems, different users or terminals share the same radio channel to communicate among themselves. In the context of multi-user systems, the achievable system performance in such systems is

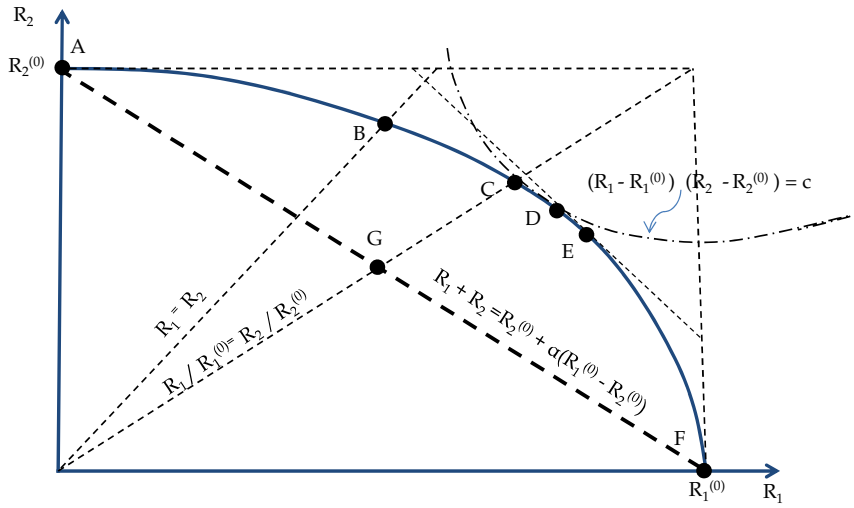

Figure 2.2 Rate Region.

characterized by the capacity region, which is defined as the set of achievable rates under limited resources. For example, the capacity region for the Gaussian *K*-users channel is a convex region in the *K* dimensional space [106].

Some specific rates on the boundary of the capacity region, corresponding to some desirable working points, can be identified. The sum-rate is one of the important points on the boundary of the rate region. The sum-rate is a single number that defines the maximum throughput of the system, regardless of fairness in terms of rate allocation between the users. It is therefore, much easier to characterize than the capacity region, and often leads to important insights.

Figure 2.2 shows the rate region for a two user scenario. Specific points on the boundary can be highlighted as follows. Points *A*, and *F* correspond to the single-user rates $R_2^{(0)}$ and $R_1^{(0)}$, that is, all the resources are allocated to either user 2 or user 1, respectively. Point *E* corresponds to the maximum sum rate. Point *B* gives the symmetric maximum rate, when single user rates are very different. Setting a common rate for all users is generally a waste of resources as it forces the users with the best channel condition to lower their rates to reach the level of the weakest users. The line *AGF* represents the rate distributions obtained by using time-division multiple-access

(TDMA), that is, the channel is allocated to user 1 solely for $0 \leq \alpha \leq 1$ of the time, and $1 - \alpha$ of the time the channel is allocated solely to user 2. Point G is obtained if time slots of equal duration are allocated to each user. Point C satisfies a fairness criterion called 'balanced rates'; that is, maximum simultaneously achievable rates (on the boundary region) that are proportional to the single user rates $R_1/R_1^{(0)} = R_2/R_2^{(0)}$. It is a compromise between the symmetric average rate B and the maximum sum rates E. Point D satisfies Nash bargaining fairness criterion, defined later in this subsection. In every scenario, a specific constrained optimization problem can be formulated to allocate the resources to achieve the system objectives, and then solved by an appropriate method.

The following are some of the criteria that are used to allocate the resources for a multi-user wireless system:

- **Equal Allocation**: The resources are allocated between the users with some control policy (for example, maximum number of users can be served). It can be used for the following cases: (1) to allocate non-dividable resources, such as time-slots, subcarriers by allocating equal number of time slots or subcarriers for each user in the system, (2) to simplify the resource allocation problem of dividable resources, that is, allocating equal power or bandwidth for all users in the system. This resource allocation criterion can be used as a benchmark for other resource allocation criterion, but it may have the disadvantage of increasing the interference as in near-far problems and/or inefficient usage of the resources.

- **Max-Weighted Sum Rate**: It is used as the basis for physical layer resource allocation; it is used for, power/rate control policy in wireless, as well as in wireline networks. It has been used extensively in joint power control and subcarrier assignment algorithms for OFDMA networks. Maximum sum rate is a special criterion, where all users have

the same priority. In multiuser systems, by introducing a time sharing argument, one can always assume that the rate region is convex. Therefore, any boundary point of the rate region can be obtained by solving a max-weighted sum rate problem for different weights [152]. Algorithmically, varying the weights allows us to prioritize different users in the system and enforce certain notions of fairness [154].

- **Max-Min Fairness**: It is used when it is required to achieve the same quality of service for all users in the system, a max-min fairness is said to be achieved by an allocation, if and only if, the allocation is feasible and an attempt to increase the allocation of any user results in the decrease in the allocation of another user with an equal or smaller allocation [108, 136].

- **Proportional Fairness**: An allocation $\boldsymbol{R}^* = [R_1^* \cdots, R_I^*]$ is said to be proportional fair, if for any other feasible allocation $\boldsymbol{R} = [R_1 \cdots, R_I]$, the following holds [81]:

$$\sum_{i=1}^{I} \frac{R_i - R_i^*}{R_i^*} \leq 0, \tag{2.23}$$

  where R_i is the rate of user i, for $i = 1, \cdots, I$. For convex sets, this point is unique and can be determined by allocating the resources to maximize the sum of logarithmic user rates. For certain nonconvex sets that are strictly convex after a logarithmic transformation, maximizing the sum of logarithmic user rates is proportionally fair [17].

- **Nash Bargaining Fairness**: It is a popular strategy for allocating resources among competing users. It is a unique Pareto optimal point that is characterized by a set of axioms called Nash Bargaining axioms. A rate distribution is said to be Pareto optimal, if and only if, there is no other rate distribution that leads to superior performance for some

users without causing performance degradation for some other users. Nash Bargaining axioms are: (1) individual rationality, (2) feasibility, (3) independence of linear transformations, (4) independence of irrelevant alternatives, (5) symmetry. The detailed explanation for these axioms can be found in [157, 174]. Nash bargaining solution (NBS) can be obtained for compact convex sets by finding the allocation that maximizes the product of user utility functions. The user utility function can be defined in terms of the user data rate, or the difference between the user data rate and a minimum acceptable data rate [50, 174]. For convex sets, Nash bargaining and proportional fairness are equivalent [17]. In addition, since NBS is Pareto optimal, it can be obtained as the solution to the maximization of the sum of the weighted utility functions [157].

- **Minimum Power** consumption subject to minimum achievable rates: This formulation tries to utilize the resources in an efficient way when it is required to maintain constant data rates for all users [108].

2.3 Cooperative Communication Schemes

Cooperative communication schemes can be characterized based on the processing done at the relay node. In AF relaying scheme, the relay scales the received signal and transmits an amplified version to the base-station. Although noise is amplified by cooperation, the destination node receives two independently faded versions of the signal and can make better decisions on the detection of the transmitted information. DF relaying is another possibility of processing at the relay node, where the relay decodes the received signal, re-encodes it, and then transmits it to the destination node. Cooperative communication protocols can be categorized into fixed relaying and adaptive relaying protocols. In fixed relaying protocols, the channel re-

sources (that is, time slots or frequency slots) are divided between the source and the relay in a fixed deterministic fashion. Fixed relaying schemes are easier to implement but have low bandwidth efficiency. This is due to allocating half the channel resources to the relay's transmission, which reduces the overall transmission rate [35]. Adaptive relaying protocols try to overcome the problem of low bandwidth efficiency in fixed relaying protocols. Adaptive relaying includes selective relaying, and incremental relaying. In selective DF relaying, the relay decodes and forwards the information only if the received SNR at the relay node exceeds a certain threshold [71]. In incremental relaying, the relay forwards the information only if the destination node does not decode the source information correctly. The destination informs the relay and the source nodes via feedback channels [94].

Most cooperative communication protocols/schemes operate in a half-duplex mode, since the relay cannot listen and transmit simultaneously in the same time-slot or frequency-band. Two orthogonal phases are used to model typical cooperative schemes, either in time division multiplexing (TDM) manner, or frequency division multiplexing (FDM) manner. In phase I (broadcast phase), the source sends its information to the destination. The information is also received at the relay node at the same time. In phase II (multi-access phase), the relay node helps the source by forwarding or retransmitting the information to the destination node [94].

2.3.1 AF Cooperative Communications

The system under consideration is depicted in **Figure 2.3**, sender (source) node S is communicating with the destination terminal D over a quasi-static channel (that is, is stable over two-time slots) with channel coefficient h_{SD}. The relay node R is used to improve the reliability of the communication between the source-destination pair using simple AF cooperative scheme. The channel coefficients between the source-relay and relay-destination pairs

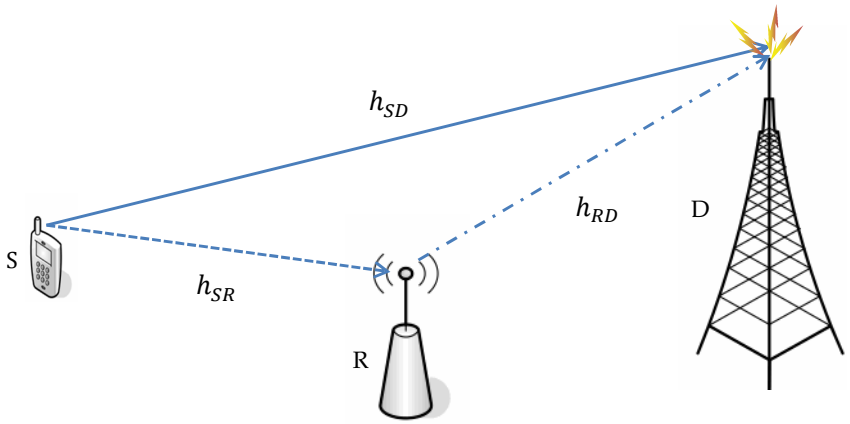

Figure 2.3 System Model.

are denoted as h_{SR} and h_{RD}, respectively. The channel coefficients are modeled by Rayleigh flat fading coefficients. The analysis of other fading channel models such as Nakagami and Ricean can be found in [72, 138]. In AF, the relay scales the received data and transmits it in the second phase. The source uses two-time slots T_1 and T_2 in a TDM manner. In the first-time slot T_1, the source broadcasts its signal to the relay and destination nodes. In the second-time slot T_2, the relay amplifies the received signal without decoding it and forwards to the destination node. The received signals in the first-time slot T_1 defined as $y_{T_1}^{(R)}$ and $y_{T_1}^{(D)}$ at the relay and at destination nodes, respectively, are obtained as follows:

$$y_{T_1}^{(R)} = \sqrt{P_S}\, h_{SR}\, x + n_1^{(R)}, \tag{2.24a}$$

$$y_{T_1}^{(D)} = \sqrt{P_S}\, h_{SD}\, x + n_1^{(D)}, \tag{2.24b}$$

where P_S is the source transmitted power. The transmitted symbol x is drawn from a constellation with unit energy. $n_1^{(R)}$ and $n_1^{(D)}$ are AWGNs received at the relay and at the destination nodes, respectively. During the second-time slot T_2, the received signal $y_{T_2}^{(D)}$ at the destination node is obtained as:

$$y_{T_2}^{(D)} = G\sqrt{P_R}\, h_{RD}\, y_{T_1}^{(R)} + n_2^{(D)}, \tag{2.25}$$

where P_R is the relay transmitted power, $n_2^{(D)}$ is the AWGN received at the destination node in the second-time slot T_2. G[1] is the normalization factor at the relay node, which is a function of the instantaneous channel gain (variable type) of the source-relay link given as [56]:

$$G = \frac{1}{\sqrt{P_S|h_{SR}|^2 + \sigma_0^2}}. \tag{2.26}$$

The end-to-end SNR for AF scheme denoted as Γ_{AF} is given as [4]:

$$\Gamma_{AF} = \frac{P_S P_R |h_{SR}|^2 |h_{RD}|^2}{\sigma_0^2(\sigma_0^2 + P_S|h_{SR}|^2 + P_R|h_{RD}|^2)}. \tag{2.27}$$

After using MRC at the destination node, the instantaneous mutual information I_{AF} for AF cooperative scheme is computed as:

$$I_{AF} = \frac{W}{2}\log_2\left(1 + \Gamma_{SD} + \Gamma_{AF}\right), \tag{2.28}$$

where $\Gamma_{SD} = \frac{P_S|h_{SD}|^2}{\sigma_0^2}$, and the factor $\frac{1}{2}$ is due to the fact that two time slots are used for cooperative transmission. The outage probability can be obtained by averaging over the channel gains as:

$$P_{out}^{AF}(R) = Pr\{I_{AF} < R\} = \mathrm{E}_{h_{SD},h_{SR},h_{RD}}[I_{AF} < R]. \tag{2.29}$$

Note that the channel gains are independent random variables. The random variable Y that is defined as the magnitude square of a Rayleigh-distribution channel coefficient (that is, ($Y = |h|^2$)) follows an exponential distribution with PDF $f_Y(y) = \frac{1}{\sigma^2}\mathrm{e}^{-\frac{y}{\sigma^2}}\mu(y)$, where $\mu(y)$ is the unit step function. By calculating the expectation in (2.29), the outage probability with $P_S = P_R = P$ can

[1]The normalizing factor can generally be of variable type as in [56], averaged type as in [58], or fixed type as in [80].

be simplified for high $SNR_0 = \frac{P}{\sigma_0^2}$ as [86]:

$$P_{out}^{AF}(R) \simeq \frac{\sigma_{SR}^2 + \sigma_{RD}^2}{2\,\sigma_{SD}^2\,\sigma_{SR}^2\,\sigma_{RD}^2}\left(\frac{2^{2R}-1}{SNR_0}\right)^2. \tag{2.30}$$

For high SNR, the outage probability $P_{out}^{AF}(R)$ decays as SNR_0^{-2}, which means that AF cooperative protocol achieves diversity order of two.

Using the moment generating function (MGF) approach to evaluate the performance over fading channels, the average SEP of AF cooperative scheme with M-array phase shift keying (M-PSK) modulation or M-array quadrature amplitude (M-QAM) modulation can be tightly approximated for high SNR as [134, 135]:

$$SEP^{AF} \simeq \frac{B\,\sigma_0^2}{b^2}\frac{1}{P_S\,\sigma_{SD}^2}\left(\frac{1}{P_S\,\sigma_{SR}^2}+\frac{1}{P_R\,\sigma_{RD}^2}\right), \tag{2.31}$$

where B is computed as:

$$B = \begin{cases} \frac{3(M-1)}{8M} + \frac{\sin(\frac{2\pi}{M})}{4\pi} - \frac{\sin(\frac{4\pi}{M})}{32\pi} & \text{M-PSK,} \\ \frac{3(M-1)}{8M} + \frac{(1-\frac{1}{\sqrt{M}})^2}{\pi} & \text{M-QAM,} \end{cases} \tag{2.32}$$

while b is computed as:

$$b = \begin{cases} \sin^2(\frac{\pi}{M}) & \text{M-PSK,} \\ \frac{3}{2(M-1)} & \text{M-QAM.} \end{cases} \tag{2.33}$$

The exact expression for the SEP^{AF} can be found in [59]. The SEP^{AF} expression in (2.31) with $P_S = P_R = P$ and $SNR_0 = \frac{P}{\sigma_0^2}$ can be simplified as:

$$SEP^{AF} \simeq \frac{B}{b^2}\frac{1}{SNR_0^2\,\sigma_{SD}^2}\left(\frac{1}{\sigma_{SR}^2}+\frac{1}{\sigma_{RD}^2}\right), \tag{2.34}$$

which reveals a diversity order of two.

2.3.2 DF Cooperative Communications

In a DF cooperative scheme, the relay decodes the received signal, re-encodes, and then transmits to the destination. DF has the advantage over AF cooperative scheme by reducing the effects of the additive noise at the relay, but it has the possibility of forwarding an erroneously detected signal to the destination node, resulting in performance degradation. The instantaneous mutual information I_{DF} for DF cooperative scheme using MRC is computed as [86]:

$$I_{DF} = \frac{W}{2} \min\left\{ \log_2\left(1 + \Gamma_{SR}\right), \log_2\left(1 + \Gamma_{SD} + \Gamma_{RD}\right)\right\}, \tag{2.35}$$

where, $\Gamma_{RD} = \frac{P_R |h_{RD}|^2}{\sigma_0^2}$, and $\Gamma_{SR} = \frac{P_S |h_{SR}|^2}{\sigma_0^2}$. The mutual information between the source and the destination is limited by the weakest link between the source-relay and the combined channel from the source-destination and relay-destination. The outage probability with $P_S = P_R = P$ can be simplified for high $SNR_0 = \frac{P}{\sigma_0^2}$ as in [86]:

$$P_{out}^{DF}(R) \simeq \frac{1}{\sigma_{SR}^2}\left(\frac{2^{2R} - 1}{SNR_0}\right). \tag{2.36}$$

For high SNR, the outage probability $P_{out}^{DF}(R)$ decays as SNR_0^{-1}, which means that DF cooperative protocol achieves diversity order one. Clearly, DF cooperative scheme has the disadvantage of low bandwidth efficiency.

Since the fading coefficient h_{SR} can be measured to high accuracy at the relaying terminal, the relay can adapt its transmission based on the realized value of h_{SR} which results in selective relaying, where the relay forwards the received information if $|h_{SR}|^2$ lies above a certain threshold. Otherwise, the relay keeps silent and the source may repeat the transmission of the information. The mutual information for selective DF (SDF) relaying is com-

puted as [86]:

$$I_{SDF} = \begin{cases} \frac{W}{2}\log_2(1+2\Gamma_{SD}) & |h_{SR}|^2 < \frac{2^{2R}-1}{SNR_0}, \\ \frac{W}{2}\log_2(1+\Gamma_{SD}+\Gamma_{RD}) & |h_{SR}|^2 \geq \frac{2^{2R}-1}{SNR_0}. \end{cases} \tag{2.37}$$

The outage probability for high SNR can be approximated as [86]:

$$P_{out}^{SDF}(R) \simeq \frac{\sigma_{SR}^2 + \sigma_{RD}^2}{2\,\sigma_{SD}^2\,\sigma_{SR}^2\,\sigma_{RD}^2}\Big(\frac{2^{2R}-1}{SNR_0}\Big)^2. \tag{2.38}$$

Clearly from (2.38), SDF cooperative scheme achieves a diversity order of two, similar to AF cooperative scheme.

The average SEP of SDF cooperative scheme with M-PSK modulation or M-QAM modulation can be tightly approximated for high SNR as in [114]:

$$SEP^{SDF} \simeq \frac{\sigma_0^4}{b^2}\frac{1}{P_S\,\sigma_{SD}^2}\left(\frac{A^2}{P_S\,\sigma_{SR}^2} + \frac{B}{P_R\,\sigma_{RD}^2}\right), \tag{2.39}$$

where A is computed as:

$$A = \begin{cases} \frac{M-1}{2M} + \frac{\sin\left(\frac{2\pi}{M}\right)}{4\,\pi} & \text{M-PSK}, \\ \frac{M-1}{2M} + \frac{\left(1-\frac{1}{\sqrt{M}}\right)^2}{\pi} & \text{M-QAM}, \end{cases} \tag{2.40}$$

B, and b are computed as in (2.32) and (2.33), respectively.

2.3.3 Multiple Relays Scenarios

In this subsection we extend the analysis of the SEP for M-PSK/M-QAM, and the diversity order for multi-relay AF/SDF cooperative schemes; the destination node is allowed to combine the received signals from all the relays using either MRC or SC. The system under investigation is depicted in **Figure 2.4**, it consists of a source, a destination, and K relays. The transmitted signal from the source in the first time slot T_1 can be overheard at

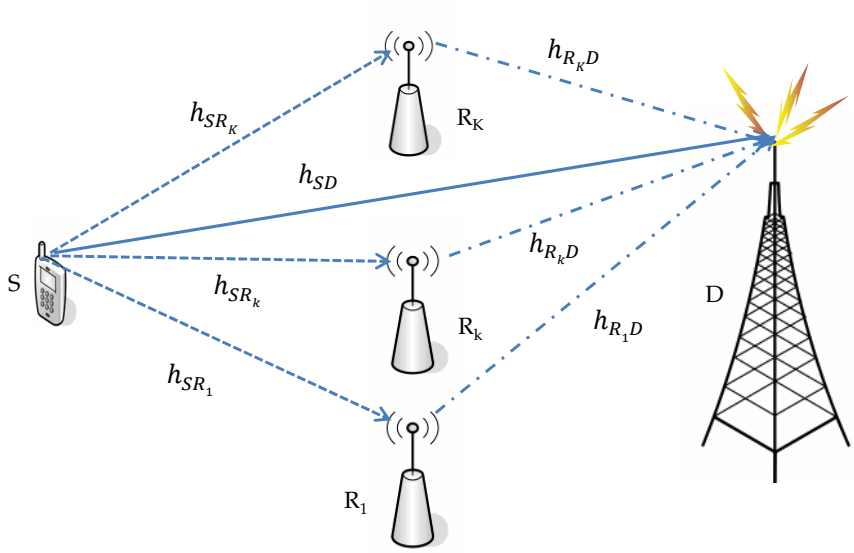

Figure 2.4 Multi Relay System Model.

the relay nodes. Using TDM each relay $k \in \{1, \cdots, K\}$ amplifies and forwards the received signal in an orthogonal fashion to the destination node. Therefore, $K+1$ time slots are required to transmit the information from the source and K relay nodes to the destination node. The end-to-end SNR at the destination node $\Gamma_{AF}^{(D)}$ after using MRC technique, can be computed as:

$$\Gamma_{AF}^{(D)} = \Gamma_{SD} + \sum_{k=1}^{K} \Gamma_{AF}^{(k)}, \tag{2.41}$$

where $\Gamma_{AF}^{(k)}$ is computed as:

$$\Gamma_{AF}^{(k)} = \frac{P_S P_{R_k} |h_{SR_k}|^2 |h_{R_kD}|^2}{\sigma_0^2(\sigma_0^2 + P_S|h_{SR_k}|^2 + P_{R_k}|h_{R_kD}|^2)}, \tag{2.42}$$

where P_{R_k} is kth relay transmitted power, h_{SR_k}, and h_{R_kD} are the channel gains between the source and relay k, and relay k and destination nodes, respectively, which are modeled as Rayleigh flat fading channels. Asymptotically tight lower and upper bounds can be found for the SEP of M-PSK and M-

QAM as in [4]:

$$SEP_K^{AF} \geq \left[\left(1+\frac{g\,P_S\,\sigma_{SD}^2}{\sigma_0^2}\right)\prod_{k=1}^{K}\left(1+\frac{g\,P_S\,P_{R_k}\,\sigma_{SR_k}^2\sigma_{R_kD}^2}{\sigma_0^2(P_S\sigma_{SR_k}^2+P_{R_k}\sigma_{R_kD}^2)}\right)\right]^{-1} W_{AF}(K,M), \tag{2.43a}$$

$$SEP_K^{AF} \leq \frac{2^K}{g^{(K+1)}}\left[\frac{P_S\,\sigma_{SD}^2}{\sigma_0^2}\prod_{k=1}^{K}\frac{P_SP_{R_k}\sigma_{SR_k}^2\sigma_{R_kD}^2}{\sigma_0^2(P_S\sigma_{SR_k}^2+P_{R_k}\sigma_{R_kD}^2)}\right]^{-1} W_{AF}(K,M), \tag{2.43b}$$

where g is computed as:

$$g=\begin{cases}\sin^2(\frac{\pi}{M}) & \text{M-PSK},\\ \frac{3}{4(M-1)} & \text{M-QAM},\end{cases} \tag{2.44}$$

and $W_{AF}(K,M)$ is computed as:

$$W_{AF}(K,M)=\begin{cases}\frac{1}{\pi}\int_0^{\frac{(M-1)\pi}{M}}\sin^{2K+2}(\phi)d\phi & \text{M-PSK},\\ \frac{4C}{\pi}\int_0^{\frac{\pi}{2}}\sin^{2K+2}(\phi)d\phi-\frac{4C^2}{\pi}\int_0^{\frac{\pi}{4}}\sin^{2K+2}(\phi)d\phi & \text{M-QAM},\end{cases} \tag{2.45}$$

where $C=1-\frac{1}{\sqrt{M}}$. Using the lower and upper bounds of the SEP, it can be shown that the system achieves full diversity order of $K+1$ for high SNR scenarios.

In a K relays SDF scheme, the relay retransmits only if the received signal exceeds certain threshold. The SEP of M-PSK and M-QAM can be approximated for high SNR as in [94]:

$$SEP_K^{DF} \simeq \frac{(\sigma_0^2)^{K+1}}{\sigma_{SD}^2(b\,P)^{K+1}}\sum_{k=1}^{K+1}\frac{W_{DF}(K-k+2,M)(W_{DF}(1,M))^{k-1}}{a_0^k\prod_{i=k}^{K}a_i\sigma_{R_iD}^2\prod_{l=1}^{k-1}\sigma_{SR_l}^2}, \tag{2.46}$$

and $W_{DF}(K,M)$ is computed as:

$$W_{DF}(K,M) = \begin{cases} \frac{1}{\pi}\int_0^{\frac{(M-1)\pi}{M}} \sin^{2K}(\phi)d\phi & \text{M-PSK,} \\ \frac{4C}{\pi}\int_0^{\frac{\pi}{2}} \sin^{2K}(\phi)d\phi - \frac{4C^2}{\pi}\int_0^{\frac{\pi}{4}} \sin^{2K}(\phi)d\phi & \text{M-QAM,} \end{cases} \tag{2.47}$$

with $P_S + \sum_{k=1}^{K} P_{R_k} = P$, $P_S = a_0 P$, and $P_{R_k} = a_k P$, for $k = 1, \cdots, K$. Using (2.46) it can be proven that K relays SDF scheme achieves the full diversity order of $K + 1$. A closed form expression for the outage probability for K relays SDF is derived in [9].

In common cooperative diversity networks with K relaying nodes, $K + 1$ orthogonal channels or time slots are used to provide $K + 1$ diversity order, which encounters bandwidth penalty [73, 111, 142, 175]. In [16], opportunistic best relay selection is used to utilize the resources efficiently; only two channels or time slots are required regardless of the number of relays, while maintaining a full diversity order of $K + 1$. The best relay is only selected to forward the data. In [86], the authors proved that best relay selection achieves full diversity order for AF and SDF cooperation schemes under flat fading Rayleigh channels. The performance is measured in terms of the outage events and the associated outage probabilities.

Performance analysis of the lth best ordered relay cooperative communication is studied in [75, 76], where one relay is selected based on ordering of the received SNRs. It is proved that the lth best ordered relay for AF/SDF provides a diversity order equals $K - l + 1$, where K is the number of relays, $l = 0$ is the best relay, $l = 1$ is the next-best relay, and so on. Closed-form expressions for the symbol error probability, outage probability and the channel capacity were derived for the lth best ordered relay for AF/SDF scheme using the MGF approach. In [79], different criteria for relay selection are investigated with their achievable diversity orders.

2.4 Optimization Concepts

Resource allocation is the action of obtaining the best result under given conditions. In this section, we present the basic formulation of resource allocation problems, investigate how to judge whether a solution is optimal, discuss the important concept of duality, and introduce non-conventional optimization techniques.

Resource allocation problems usually can be formulated as constrained optimization problems, which can be optimized from the system viewpoint. The general resource allocation problem can be written as:

$$\min_{\boldsymbol{x}\in\chi} f_0(\boldsymbol{x}), \tag{2.48a}$$

$$\text{s.t. } f_j(\boldsymbol{x}) \leq 0,\ j = 1, \cdots, m, \tag{2.48b}$$

$$g_i(\boldsymbol{x}) = 0,\ i = 1, \cdots, p, \tag{2.48c}$$

where $\boldsymbol{x} = (x_1, \cdots, x_n)$ is an n dimensional vector called the design vector defined over the feasible range χ, $f_0(\boldsymbol{x})$ is termed the objective function (optimization goal) which represents the performance or the cost, and $f_j(\boldsymbol{x})$ and $g_i(\boldsymbol{x})$ are known as inequality and equality constraints, respectively. The optimization process finds the optimal solution $\boldsymbol{x}^* \in \chi$ that satisfies all the inequality and equality constraints, and $f_0(\boldsymbol{x}^*) \leq f_0(\boldsymbol{x})$, $\forall \boldsymbol{x} \in \chi$. Linear programming (LP) is an optimization problem where the objective function, the inequality and equality constraints are all linear functions of the design vector $\boldsymbol{x}$. One of the important features of LP is the existence of a global optimal point that can be found easily using LP methods. Unfortunately, most wireless resource allocation problems are nonlinear, that is, either the objective function and/or the constraints are non-linear, and therefore fall under the category of nonlinear programming problems. Generally, nonlinear programming problems are characterized by the existence of multiple

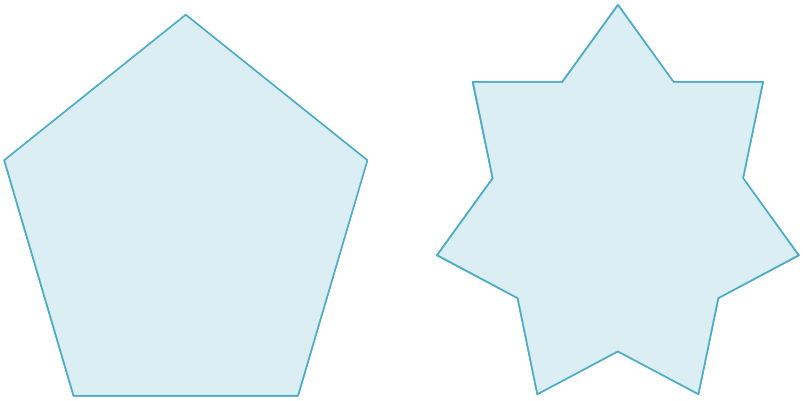

(a) Convex Set. **(b)** Non-Convex Set.

Figure 2.5 A Convex and Non-Convex Sets.

local optima, and finding the global optimum is a challenging task.

In addition, if some of the design parameters are restricted to be integers, then the problem as defined in (2.48) is called integer programming. Most integer programming can not be solved by polynomial time algorithms, and are described as non-deterministic-polynomial-hard (NP-hard) problems.

2.4.1 Convex Optimization

Convex optimization problems are a special class of nonlinear optimization problems in which the feasible set χ is a convex set, objective function $f_0(\boldsymbol{x})$ is a convex function, inequality functions $f_j(\boldsymbol{x})$, $j = 1, \cdots, m$ are convex functions, and the equality constraints $g_i(\boldsymbol{x})$, $i = 1, \cdots, p$ are linear functions. A convex set is defined as:

Definition 2.4.1 *A set $\chi \subseteq \mathbb{R}^n$ is convex if for any $\boldsymbol{x}_1$, $\boldsymbol{x}_2 \in \chi$, and for any $\theta \in [0, 1]$ the following holds:*

$$\theta \boldsymbol{x}_1 + (1 - \theta)\boldsymbol{x}_2 \in \chi. \tag{2.49}$$

Figure 2.5(a) shows an example of a convex set. Whereas, **Figure 2.5(b)** shows an example of a non-convex set. A convex function is defined as:

Definition 2.4.2 *A function f is convex over $\boldsymbol{x}$ if the feasible range χ of the vector*

$\boldsymbol{x}$ is a convex set, and if for all $\boldsymbol{x}_1, \boldsymbol{x}_2 \in \chi$, and $0 \leq \theta \leq 1$, the following holds:

$$f\Big(\theta \boldsymbol{x}_1 + (1-\theta)\, \boldsymbol{x}_2\Big) \leq \theta f(\boldsymbol{x}_1) + (1-\theta) f(\boldsymbol{x}_2). \tag{2.50}$$

A function is strictly convex if the strict inequality in (2.50) *holds strictly whenever $\boldsymbol{x}_1 \neq \boldsymbol{x}_2$, and $0 < \theta < 1$. A function is called concave if $-f$ is a convex function.*

Figure 2.6(a) shows an example of a convex function. Whereas, **Figure 2.6(b)** shows an example of a non-convex function.

Some of the important properties of convex functions are:

- **Global Bound Property**: It is also called the first-order condition, if $f(\boldsymbol{x})$ is differentiable function over χ, then it is convex over χ if and only if

  $$f(\boldsymbol{x}_2) \geq f(\boldsymbol{x}_1) + \nabla f(\boldsymbol{x}_1)^T (\boldsymbol{x}_2 - \boldsymbol{x}_1), \forall \boldsymbol{x}_1, \boldsymbol{x}_2 \in \chi. \tag{2.51}$$

  In addition, $f(\boldsymbol{x})$ is strictly convex over χ if and only if the inequality in (2.51) holds strictly when $\boldsymbol{x}_1 \neq \boldsymbol{x}_2$.

- **Hessian Related Property**: It is also called the second-order condition, if $f(\boldsymbol{x})$ is twice differentiable function over χ, then it is convex over χ if and only if

  $$\nabla^2 f(\boldsymbol{x}) \geq \boldsymbol{0}, \forall \boldsymbol{x} \in \chi. \tag{2.52}$$

  In addition, $f(\boldsymbol{x})$ is strictly convex over χ if and only if the inequality in (2.52) holds strictly.

- **Jensen's Inequality**: If $f(\boldsymbol{x})$ is a convex function over χ, then the following holds:

  $$\sum_{k=1}^{K} \theta_k f(\boldsymbol{x}_k) \geq f\Big(\sum_{k=1}^{K} \theta_k \boldsymbol{x}_k\Big). \tag{2.53}$$

  Generally, when the vector $\boldsymbol{x}$ is a random vector over χ, and the func-

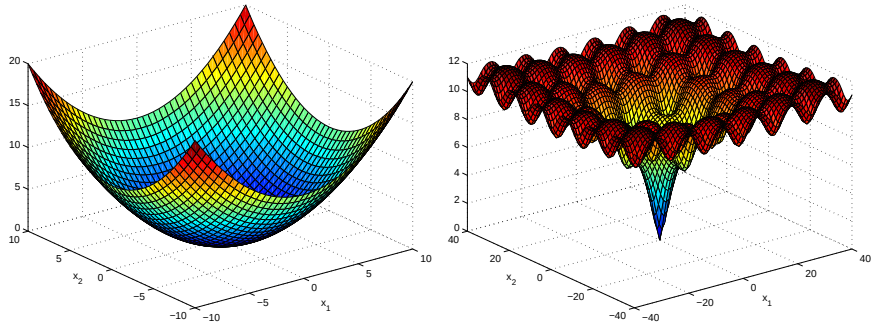

(a) Convex Function. **(b)** Non-Convex Function.

Figure 2.6 Two Dimensions Convex and Non-Convex Functions.

tion $f(\boldsymbol{x})$ is convex, then the following holds:

$$f(\mathrm{E}_x[\boldsymbol{x}]) \leq \mathrm{E}_x[f(\boldsymbol{x})]. \tag{2.54}$$

When $f(\boldsymbol{x})$ is strictly convex then the inequality in (2.54) holds strictly.

Conditions (2.51) or (2.52) can be used to check the convexity of a differential function. These methods often lead to very demanding mathematical procedures. A more efficient way to recognize a convex function is to check if that function can be transformed from certain convex functions through operations that preserve convexity. A number of typical convex and concave functions are listed in Chapter 3 of [20]. A few of them will be used in this dissertation, which are listed below:

1. **Affine Function**: $f(\boldsymbol{x})$ is an affine convex function over $\mathbb{R}^n$, if

$$f(\boldsymbol{x}) = a^T\boldsymbol{x} + b, \ \forall a \in \mathbb{R}^n, \forall b \in \mathbb{R}. \tag{2.55}$$

2. **Logarithmic Function**: $f(x)$ is a logarithmic concave function over $\mathbb{R}_{++}$, if

$$f(x) = \log(x). \tag{2.56}$$

3. **Minimum of Two Concave Functions**: $h(\boldsymbol{x}) = \min\{f(\boldsymbol{x}), g(\boldsymbol{x})\}$ is a concave function, if $f(\boldsymbol{x})$ and $g(\boldsymbol{x})$ are concave functions.

A number of typical convexity or concavity preserving operations are listed in Chapter 3 of [20]. A few of them will be used in this dissertation, which are listed below:

- **Weighted Summation**: The function $f(\boldsymbol{x})$ defined as:

$$f(\boldsymbol{x}) = \sum_i w_i f_i(\boldsymbol{x}), \tag{2.57}$$

  is convex over χ, if $\forall i$ one of the following conditions is satisfied:

  - $w_i \geq 0$ and $f_i(\boldsymbol{x})$ is convex over χ.
  - $w_i \leq 0$ and $f_i(\boldsymbol{x})$ is concave over χ.

- **Composition of Functions**: The function $f(\boldsymbol{x})$ defined as:

$$f(\boldsymbol{x}) = h\Big(z_1(\boldsymbol{x}), \cdots, z_L(\boldsymbol{x})\Big), \tag{2.58}$$

  is convex over χ, if $\forall l \in \{1, \cdots, L\}$ one of the following conditions is satisfied:

  - $h(\boldsymbol{z})$ is increasing of z_l and $z_l(\boldsymbol{x})$ is convex in χ.
  - $h(\boldsymbol{z})$ is decreasing of z_l and $z_l(\boldsymbol{x})$ is concave in χ.

- **Perspective Function**: The perspective function $g(\boldsymbol{y})$ defined as:

$$g(\boldsymbol{y}, t) = t\, f(\frac{\boldsymbol{y}}{t}), \tag{2.59}$$

  is convex over $\{(\boldsymbol{y}, t) \in \mathbb{R}^{n+1} | \frac{\boldsymbol{y}}{t} \in \chi, t > 0\}$, where $f(\boldsymbol{x})$ is convex over χ.

2.4.2 Duality Principle

Duality is an important concept that can be used to give a lower bound on the optimal value of (2.48). In addition, under some convexity assumptions

and constraint properties, the primal and dual problems have the same optimal objective values, so it is possible to solve the primal problem by considering the dual problem. In this subsection, we will start by defining the dual problem, then present the duality theorem and discuss some of its properties and applications.

Problem (2.48) is called the prime (or primal) problem using duality notation. The basic idea of duality is to augment the objective function with a weighted sum of the constraint functions. The Lagrangian function $L(\boldsymbol{x}, \boldsymbol{\lambda}, \boldsymbol{\mu}) : \mathbb{R}^n \times \mathbb{R}^m \times \mathbb{R}^p \mapsto \mathbb{R}$ is defined as:

$$L(\boldsymbol{x}, \boldsymbol{\lambda}, \boldsymbol{\mu}) = f(\boldsymbol{x}) + \sum_{j=1}^{m} \lambda_j f_j(\boldsymbol{x}) + \sum_{i=1}^{p} \mu_i g_i(\boldsymbol{x}), \tag{2.60}$$

where $\boldsymbol{\lambda} = (\lambda_1, \cdots, \lambda_m)$ and $\boldsymbol{\mu} = (\mu_1, \cdots, \mu_p)$ are called the Lagrange multipliers.

One of the essential methods to solve optimization problems analytically (in closed form) is the Lagrangian method, which is based on writing the Lagrangian function (2.60), then the optimal solution $\boldsymbol{x}^*$ can be obtained by differentiating $L(\cdot)$ over $\boldsymbol{x}$ and setting to zero as $\frac{\partial L}{\partial \boldsymbol{x}} = \mathbf{0}$, and using the inequity and equality constraints to substitute for the Lagrange multipliers [52].

The Lagrangian dual problem (dual problem) of (2.48) can be defined as:

$$\max_{\boldsymbol{\lambda} \geq \mathbf{0},\, \boldsymbol{\mu}} \beta(\boldsymbol{\lambda}, \boldsymbol{\mu}), \tag{2.61}$$

where $\beta(\boldsymbol{\lambda}, \boldsymbol{\mu}) = \inf_{\boldsymbol{x} \in \chi} L(\boldsymbol{x}, \boldsymbol{\lambda}, \boldsymbol{\mu})$, where inf stands for infimum. It is worth noting that the dual problem is convex even if the primal problem is non-convex [20]. One of the main applications of the dual problem is the duality theorem, which is stated as follows:

Theorem 2.4.1 *Weak Duality Theorem: If $\boldsymbol{x}$ is a feasible solution to the prime problem* (2.48) *and $\boldsymbol{\lambda}, \boldsymbol{\mu}$ are the feasible solution to the dual problem* (2.61)*, then*

$f_0(\boldsymbol{x}) \geq \beta(\boldsymbol{\lambda}, \boldsymbol{\mu})$. *The duality gap is defined as* $f_0(\boldsymbol{x}) - \beta(\boldsymbol{\lambda}, \boldsymbol{\mu})$.

The duality gap is zero under convexity assumption and constraint qualification (Slater's strict feasibility condition) as stated next in the strong duality theorem.

Theorem 2.4.2 *Strong Duality Theorem: Let* (2.48) *be a convex problem, suppose there exists an* $\boldsymbol{x} \in \chi$ *such that* $f_j(\boldsymbol{x}) < 0$ *, for* $j = 1, \cdots, m$ *(Slater's strict feasibility condition), and* $g_i(\boldsymbol{x}) = 0$*, for* $i = 1, \cdots, p$*. Then the optimal point of a prime problem is the same as the optimal point of a dual problem.*

When all inequality constraints of the convex problem (2.48) are linear, Slater's strict feasibility condition is refined to feasibility conditions, that is, $f_j(\boldsymbol{x}) \leq 0$, for $j = 1, \cdots, m$ [20].

The necessary and sufficient condition for zero duality gap is the existence of a saddle point for the Lagrangian function. Thus, strong duality can be expressed as [20]:

$$\sup_{\boldsymbol{\lambda} \geq \mathbf{0},\, \boldsymbol{\mu}} \inf_{x \in \chi} L(\boldsymbol{x}, \boldsymbol{\lambda}, \boldsymbol{\mu}) = \inf_{x \in \chi} \sup_{\boldsymbol{\lambda} \geq \mathbf{0},\, \boldsymbol{\mu}} L(\boldsymbol{x}, \boldsymbol{\lambda}, \boldsymbol{\mu}), \tag{2.62}$$

where sup stands for supremum. For zero-duality-gap problems, it is possible to solve the prime problem indirectly by solving the dual problem. Some times, solving the dual is easier than solving the prime problem, and this may lead to a distributed algorithm to solve the problem.

It is worth noting that a problem with zero duality gap might be non-convex. For example, the spectrum optimization of a multicarrier system is non-convex problem, but it has zero duality gap, when number of subcarriers is sufficiently large [167].

Global optimality conditions for zero-duality-gap, can be stated as [13]:

Theorem 2.4.3 *Suppose* (2.48) *has zero duality gap , then* $\boldsymbol{x}^*$, $\boldsymbol{\lambda}^*$ *and* $\boldsymbol{\mu}^*$ *are globally optimum for* (2.48) *and* (2.61)*, respectively, if and only if they satisfy the following conditions:*

- *Primal Feasibility:* $\boldsymbol{x}^*$ *is feasible for* (2.48)
- *Dual Feasibility:* $\boldsymbol{\lambda}^* \geq \mathbf{0}$.
- *Lagrangian Optimality Condition:* $\boldsymbol{x}^* = \arg\min_{\boldsymbol{x}\in\chi} L(\boldsymbol{x}, \boldsymbol{\lambda}^*, \boldsymbol{\mu}^*)$.
- *Complementary Slackness:* $\lambda_j^* f_j(\boldsymbol{x}^*) = 0$, *for* $j = 1, \cdots, m$.

For a zero-duality-gap problem without equality constraints (that is, $p = 0$), the optimal dual variables $\boldsymbol{x}^*$ and $\boldsymbol{\lambda}^*$, can be obtained iteratively using either the subgradient or ellipsoid methods [19, 21].

The sub-gradient method for the dual problem can be described as follows: For initial values of the Lagrange multipliers $\boldsymbol{\lambda}^{(t)}$ for $t = 0$, find $\boldsymbol{x}^{(t)} = \arg\min_{\boldsymbol{x}\in\chi} L(\boldsymbol{x}, \boldsymbol{\lambda}^{(t)})$. Then $\boldsymbol{\lambda}^{(t+1)}$ is updated as:

$$\boldsymbol{\lambda}^{(t+1)} = \left(\boldsymbol{\lambda}^{(t)} + \delta^{(t)} \boldsymbol{f}(\boldsymbol{x}^{(t)})\right)^+, \tag{2.63}$$

where $t = 0, 1, \cdots$, $\boldsymbol{f}(\boldsymbol{x}^{(t)}) = [f_1(\boldsymbol{x}^{(t)}), \cdots, f_m(\boldsymbol{x}^{(t)})]^T$, and $(x)^+ = \max\{x, 0\}$. Some of the used values for $\delta^{(t)}$ are $\delta^{(t)} = \kappa$, $\delta^{(t)} = \frac{\kappa}{t+1}$, and $\delta^{(t)} = \frac{\kappa}{\sqrt{t+1}}$, where κ is sufficiently small [21]. The procedure is repeated iteratively, that is, by finding the argument $\boldsymbol{x}^{(t)}$ that minimizes the Lagrangian function, and using it to update the Lagrange multipliers $\boldsymbol{\lambda}^{(t+1)}$. It is noted that the convergence of the subgradient method is very slow [143].

Ellipsoid method is a multi dimensional bisection method. It is an efficient algorithm for structured problems; that is, it is faster in convergence compared to the subgradient method [19]. It can be used to solve the dual problem by updating the dual variables. The ellipsoid method basic idea is that the optimal solution is located within an ellipsoid, then at each iteration, the volume of the ellipsoid is reduced until the optimal solution is obtained within a specified tolerance. For initial values of the Lagrange multipliers $\boldsymbol{\lambda}^{(t)}$, for $t = 0$, the value of $\boldsymbol{x}^{(t)}$ is obtained as $\boldsymbol{x}^{(t)} = \arg\min_{\boldsymbol{x}\in\chi} L(\boldsymbol{x}, \boldsymbol{\lambda}^{(t)})$.

Algorithm 2.1 Dual Method

Initialize $\boldsymbol{\lambda}^{(t)}$.
Repeat
Find $\boldsymbol{x}^{(t)}$ by solving an unconstrained optimization problem (the Lagrangian function).
Update the Lagrangian multipliers using (2.63) or (2.65).
Until $\boldsymbol{x}^{(t)}$ is feasible and $|\sum_{j=1}^{m} \lambda_j^{(t)} f_j(\boldsymbol{x}^{(t)})| \leq \epsilon$.
Return $f_0(\boldsymbol{x}^{(t)})$ and $\boldsymbol{x}^{(t)}$ as the approximate optimal value and optimal solution, respectively.

The ellipsoid $E^{(t)}$ at iteration t is defined as [167]:

$$E^{(t)} = \{\boldsymbol{\lambda} | (\boldsymbol{\lambda} - \boldsymbol{\lambda}^{(t)})^T \boldsymbol{A}_t^{-1} (\boldsymbol{\lambda} - \boldsymbol{\lambda}^{(t)}) \leq 1\}, \tag{2.64}$$

where $\boldsymbol{A}_t^{-1}$ is positive semi-definite matrix. $\boldsymbol{A}^{(t)}$ defined as the inverse matrix of $\boldsymbol{A}_t^{-1}$. $\boldsymbol{\lambda}^{(t+1)}$ and $\boldsymbol{A}^{(t+1)}$ are updated to generate a new ellipsoid $E^{(t+1)}$ as:

$$\boldsymbol{\lambda}^{(t+1)} = \boldsymbol{\lambda}^{(t)} - \frac{1}{m+1} \boldsymbol{A}^{(t)} \boldsymbol{b}^{(t)}, \tag{2.65a}$$

$$\boldsymbol{A}^{(t+1)} = \frac{m^2}{m^2 - 1} \Big(\boldsymbol{A}^{(t)} - \frac{2}{m+1} \boldsymbol{A}^{(t)} \boldsymbol{b}^{(t)} \boldsymbol{b}^{(t)T} \boldsymbol{A}^{(t)} \Big), \tag{2.65b}$$

where $\boldsymbol{b}^{(t)} = \frac{f(\boldsymbol{x}^{(t)})}{\sqrt{f(\boldsymbol{x}^{(t)})^T \boldsymbol{A}^{(t)} f(\boldsymbol{x}^{(t)})}}$. The dual method is illustrated in **Algorithm 2.1**. The termination criterion is chosen as $|\sum_{j=1}^{m} \lambda_j{}^{(t)} f_j(\boldsymbol{x}^{(t)})| \leq \epsilon$, since it is often difficult to find an $\boldsymbol{x}^{(t)}$ that satisfies simultaneously the feasibility and the complementary slackness conditions exactly.

2.4.3 Optimality Conditions

Karush-Kuhn-Tucker (KKT) first condition is a necessary condition for a point to be a local minimizer, stated as follows [27]:

Theorem 2.4.4 *Let* $f_0(\boldsymbol{x})$, $f_j(\boldsymbol{x})$, $g_i(\boldsymbol{x}) \in C^1$, *for* $j = 1, \cdots, m$, *and* $i = 1, \cdots, p$, *and let* $\boldsymbol{x}^*$ *be a regular point and a local minimizer for* (2.48). *Then, there exist* $\boldsymbol{\lambda}^* = (\lambda_1^*, \cdots, \lambda_m^*) \in \mathbb{R}^m$ *and* $\boldsymbol{\mu}^* = (\mu_1^*, \cdots, \mu_p^*) \in \mathbb{R}^p$ *such that*

1. $\boldsymbol{\lambda}^* \geq \boldsymbol{0}$.

2. $\nabla f_0(\boldsymbol{x}^*) + \sum_{j=1}^{m} \lambda_j^* \nabla f_j(\boldsymbol{x}^*) + \sum_{i=1}^{p} \mu_i^* \nabla g_i(\boldsymbol{x}^*) = \boldsymbol{0}$.

3. $\lambda_j^* f_j(\boldsymbol{x}^*) = 0$, *for* $j = 1, \cdots, m$.

where a regular point $\boldsymbol{x}^*$ is defined as:

Definition 2.4.3 *$\boldsymbol{x}^*$ is a regular point if the vectors $\nabla g_i(\boldsymbol{x}^*)$, for $i = 1, \cdots, p$, and $\nabla f_j(\boldsymbol{x}^*)$, for $j \in \mathcal{J}(\boldsymbol{x}^*)$ are linearly independent, where $\mathcal{J}(\boldsymbol{x}^*)$ is the index set of active inequality constraints, that is, $\mathcal{J}(\boldsymbol{x}^*) \stackrel{\text{def}}{=} \{j : f_j(\boldsymbol{x}^*) = 0\}$.*

The KKT condition is applied in the same way as any necessary condition. Specifically, points that satisfy the KKT condition are considered as candidate minimizer of the optimization problem (2.48). For convex optimization problems with zero duality gap, the first order KKT condition is a necessary and sufficient condition for optimality.

The KKT second order necessary condition for optimality is stated as:

Theorem 2.4.5 *Let $f_0(\boldsymbol{x})$, $f_j(\boldsymbol{x})$, $g_i(\boldsymbol{x}) \in C^2$, for $j = 1, \cdots, m$, and $i = 1, \cdots, p$, let $\boldsymbol{x}^*$ be a regular point and a local minimizer for* (2.48)*. Then, there exists $\boldsymbol{\lambda}^* = (\lambda_1^*, \cdots, \lambda_m^*) \in \mathbb{R}^m$ and $\boldsymbol{\mu}^* = (\mu_1^*, \cdots, \mu_p^*) \in \mathbb{R}^p$ such that*

1. $\boldsymbol{\lambda}^* \geq \boldsymbol{0}$.

2. $\nabla f_0(\boldsymbol{x}^*) + \sum_{j=1}^{m} \lambda_j^* \nabla f_j(\boldsymbol{x}^*) + \sum_{i=1}^{p} \mu_i^* \nabla g_i(\boldsymbol{x}^*) = \boldsymbol{0}$.

3. $\lambda_j^* f_j(\boldsymbol{x}^*) = 0$, *for* $j = 1, \cdots, m$.

4. *For all $\boldsymbol{y} \neq \boldsymbol{0}$, we have $\boldsymbol{y}^T \Psi(\boldsymbol{x}^*, \boldsymbol{\lambda}^*, \boldsymbol{\mu}^*) \boldsymbol{y} \geq 0$,*

where $\forall \boldsymbol{y} \in \mathbb{R}^n$ the following holds:

- $\boldsymbol{y}^T \nabla g_i(\boldsymbol{x}^*) = 0$, for $i = 1, \cdots, p$,
- $\boldsymbol{y}^T \nabla f_j(\boldsymbol{x}^*) = 0$, for $j \in \mathcal{J}(\boldsymbol{x}^*)$.

And $\Psi(\boldsymbol{x}, \boldsymbol{\lambda}, \boldsymbol{\mu})$ is computed as:

$$\Psi(\boldsymbol{x}, \boldsymbol{\lambda}, \boldsymbol{\mu}) = \boldsymbol{F}_0(\boldsymbol{x}) + \sum_{j=1}^{m} \lambda_j \boldsymbol{F}_j(\boldsymbol{x}) + \sum_{i=1}^{p} \mu_i \boldsymbol{G}_i(\boldsymbol{x}), \tag{2.66}$$

where $\boldsymbol{F}_0(\boldsymbol{x})$, $\boldsymbol{F}_j(\boldsymbol{x})$, and $\boldsymbol{G}_i(\boldsymbol{x})$ are the Hessian matrices at $\boldsymbol{x}$ of $f_0(\boldsymbol{x})$, $f_j(\boldsymbol{x})$, and $g_i(\boldsymbol{x})$, respectively. The Hessian matrix $\boldsymbol{F}_j(\boldsymbol{x})$ of the function $f_j(\boldsymbol{x})$, $j = 0, 1, \cdots, m$ is computed as:

$$\boldsymbol{F}_j(\boldsymbol{x}) = \begin{bmatrix} \frac{\partial^2 f_j(\boldsymbol{x})}{\partial x_1^2} & \cdots & \frac{\partial^2 f_j(\boldsymbol{x})}{\partial x_1 \partial x_n} \\ & \ddots & \\ \frac{\partial^2 f_j(\boldsymbol{x})}{\partial x_n \partial x_1} & \cdots & \frac{\partial^2 f_j(\boldsymbol{x})}{\partial x_n^2} \end{bmatrix}. \tag{2.67}$$

The second order sufficient condition for optimality is stated as:

Theorem 2.4.6 *Suppose $f_0(\boldsymbol{x})$, $f_j(\boldsymbol{x})$, $g_i(\boldsymbol{x}) \in C^2$, for $j = 1, \cdots, m$, $i = 1, \cdots, p$, and there exist a feasible point $\boldsymbol{x}^* \in \mathbb{R}^n$ and there exist vectors $\boldsymbol{\lambda}^* = (\lambda_1^*, \cdots, \lambda_m^*) \in \mathbb{R}^m$ and $\boldsymbol{\mu}^* = (\mu_1^*, \cdots, \mu_p^*) \in \mathbb{R}^p$ such that*

1. $\boldsymbol{\lambda}^* \geq \boldsymbol{0}$.
2. $\nabla f_0(\boldsymbol{x}^*) + \sum_{j=1}^m \lambda_j^* \nabla f_j(\boldsymbol{x}^*) + \sum_{i=1}^p \mu_i^* \nabla g_i(\boldsymbol{x}^*) = \boldsymbol{0}$.
3. $\lambda_j^* f_j(\boldsymbol{x}^*) = 0$, *for* $j = 1, \cdots, m$.
4. *For all* $\boldsymbol{y} \neq \boldsymbol{0}$ *we have* $\boldsymbol{y}^T \Psi(\boldsymbol{x}^*, \boldsymbol{\lambda}^*, \boldsymbol{\mu}^*) \boldsymbol{y} > 0$,

then $\boldsymbol{x}^*$ is a strict local minimizer of (2.48).

Usually, using the second order condition for optimality check is computationally expensive [104].

2.4.4 Nonlinear Programming

One of the greatest challenges for nonlinear non-convex problems is to find the global optimum, since some problems exhibit local optima, where the local optima satisfy the requirements on the derivatives of the function. First, we will introduce algorithms to find local optimum. Specifically, barrier (interior-point) and penalty methods are discussed, then we will discuss some techniques to find global optimum.

Algorithm 2.2 Barrier Method

Initialize $\beta_t > 0$, feasible $\boldsymbol{x}^{(t)}$.
Repeat
Find $\boldsymbol{x}^{(t)}$ in (2.69).
Update $\beta_{t+1} = \nu\beta_t$, $\nu > 1$.
Until tolerance is satisfied.
Return $f_0(\boldsymbol{x}^{(t)})$ and $\boldsymbol{x}^{(t)}$ as the approximate optimal value and optimal solution, respectively.

A barrier function is a continuous function whose value on a point increases to infinity as the point approaches the boundary of the feasible region. It is used to penalize the term that violates the constraints. The barrier function should be convex and smooth. One of the most common types of barrier function is the logarithmic barrier function defined as:

$$I(\boldsymbol{x}) = -\sum_{j=1}^{m} \log(-f_j(\boldsymbol{x})). \tag{2.68}$$

The barrier method stands on solving an optimization problem for a sequence of iterations $t = 1, 2, \cdots$. For each iteration t, and $\beta_t > 0$, the associated optimization problem can be written as:

$$\min_{\boldsymbol{x}\in\chi} \beta_t f_0(\boldsymbol{x}) + I(\boldsymbol{x}), \tag{2.69a}$$

$$\text{s.t. } g_j(\boldsymbol{x}) = 0,\ j = 1, \cdots, p. \tag{2.69b}$$

The barrier method computes the optimal $\boldsymbol{x}^*$ of (2.48) by solving a sequence of the associated optimization problem (2.69) by updating the value $\beta_{t+1} = \nu\beta_t$, with $\nu > 1$ until the solution is within a specified tolerance. Various modifications of interior-point method for linear and quadratic programming were proposed to cope with non-convexity of the objective function and non-linearity of the equality constraints. Generally, the interior point method starts from the center of the feasible region, then follows the central path, and finally converges to an optimal solution [20]. **Algorithm 2.2**

illustrates the barrier method.

The penalty function method for solving constrained optimization problems involves constructing and solving an associated unconstrained optimization problem, and using the solution to the unconstrained problem as the solution to the original constrained problem [104].

Definition 2.4.4 *A function* $P(\boldsymbol{x}) : \mathbb{R}^n \mapsto \mathbb{R}$ *is called a penalty function for* (2.48) *if it satisfies the following three conditions:*

- $P(\boldsymbol{x})$ *is continuous.*
- $P(\boldsymbol{x}) \geq 0$, $\forall \boldsymbol{x} \in \mathbb{R}^n$.
- $P(\boldsymbol{x}) = 0$ *if and only if* $\boldsymbol{x}$ *is feasible, that is* $f_j(\boldsymbol{x}) \leq 0$, *for* $j = 1, \cdots, m$ *and* $g_i(\boldsymbol{x}) = 0$, *for* $i = 1, \cdots, p$.

The penalty function $P(\boldsymbol{x})$ must be appropriately chosen to have a good approximation of the original problem (2.48). The penalty function is defined in terms of the constraint functions. One possible choice is the so-called Courant-Beltrami penalty function, defined as [27]:

$$P(\boldsymbol{x}) = \sum_{j=1}^{m} \max^2(f_j(\boldsymbol{x}), 0) + \sum_{i=1}^{p} g_i^2(\boldsymbol{x}). \tag{2.70}$$

The association function $q(\gamma_t, \boldsymbol{x})$ is defined as:

$$q(\gamma_t, \boldsymbol{x}) = f_0(\boldsymbol{x}) + \gamma_t P(\boldsymbol{x}), \tag{2.71}$$

where γ_t is a given positive constant for $t = 1, 2, \cdots$. The associated unconstrained optimization problem for each t can be written as:

$$\min_{\boldsymbol{x} \in \chi} q(\gamma_t, \boldsymbol{x}), \tag{2.72}$$

Let $\boldsymbol{x}^{(t)}$ be the solution of (2.72), the following theorem relates the convergence of the sequence $\boldsymbol{x}^{(t)}$ as $t \to \infty$ to the solution of (2.48) as [13]:

Algorithm 2.3 Penalty Method

Initialize γ_t, and $\boldsymbol{x}^{(t)}$.
Repeat
Find $\boldsymbol{x}^{(t)}$ in (2.72).
Update $\gamma_{t+1} = \nu\gamma_t$, $\nu > 1$.
Until the termination criterion is satisfied.
Return $f_0(\boldsymbol{x}^{(t)})$ and $\boldsymbol{x}^{(t)}$ as the approximate optimal value and optimal solution, respectively.

Theorem 2.4.7 *Let* $f_0(\boldsymbol{x}) \in C^1$, $\gamma_t < \gamma_{t+1}$, *and* $\gamma_t \to \infty$ *as* $t \to \infty$. *Then, the limit of any convergent sequence* $\boldsymbol{x}^{(t)}$ *is a solution to the constrained optimization problem* (2.48).

Algorithm 2.3 illustrates the penalty method.

The initial starting point for the optimization algorithm plays an important role in achieving the global optimum for non-convex functions. One popular approach is to use stochastic initial points; these algorithms use random or pseudo-random numbers to initialize the algorithm in the feasible region (for example, it can be used with the barrier method), so that different local optima can be obtained, by comparing the local optima. The probability of finding the global optimum is increased with the number of initialization points. In addition, there are various stochastic optimization methods that use non-conventional approaches to find the optimal such as, simulated annealing, genetic, and PSO algorithms [109].

2.4.5 Mixed Integer Programming

Mixed integer programing are formulated as follows:

$$\min_{\boldsymbol{x},\boldsymbol{y}} f_0(\boldsymbol{x}, \boldsymbol{y}), \tag{2.73a}$$

$$\text{s.t. } f_j(\boldsymbol{x}, \boldsymbol{y}) \leq 0,\ j = 1, \cdots, m, \tag{2.73b}$$

$$g_i(\boldsymbol{x}, \boldsymbol{y}) = 0,\ i = 1, \cdots, p, \tag{2.73c}$$

$$\boldsymbol{x} \in \mathbb{R}^n,\ \boldsymbol{y} \in \mathbb{Z}^N. \tag{2.73d}$$

In general, mixed integer programming are very hard to solve even for the simple linear objective and constraint functions. Enumerating all the integer solutions in the feasible region and individually solving the resulted optimization problems and checking each one for optimality, are computationally extensive. As the dimension of the problem grows, enumeration becomes NP hard. One common technique is to relax the value of the integer variables. Simply rounding the solution will often compromise optimality. Besides, the rounded solution may not be in the feasible region. For linear mixed integer programming techniques based on solving linear programming problems such as the cutting plan method, can be used to solve the problem. Mixed integer non-linear programming (MINLP) can be solved using algorithms that seek an upper and lower bound of the MINLP such as the generalized benders decomposition(GBD) algorithm. The upper bound results from the primal problem, while the lower bound results from the master problem. The primal problem corresponds to (2.73) with fixed $\boldsymbol{y}$ variables and its solution provides information about the upper bound and the Lagrange multipliers associated with the equality and inequality constraints. The master problem is derived via nonlinear duality theory, which makes use of the Lagrange multipliers obtained in the primal problem. Its solution provides information about the lower bound, as well as the next set of fixed $\boldsymbol{y}$ variables to be used subsequently in the primal problem. The termination criterion for GBD is based on the difference between the updated upper bound and the current lower bound. GBD algorithm has finite convergence if the problem has certain structures; for example, the functions $f_0(\boldsymbol{x}, \boldsymbol{y})$, $f_i(\boldsymbol{x}, \boldsymbol{y})$, and $g_j(\boldsymbol{x}, \boldsymbol{y})$ for $j = 1, \cdots, m$, and $i = 1, \cdots, p$ are separable in $\boldsymbol{x}$, and $\boldsymbol{y}$ [39].

2.4.6 Particle Swarm Optimization

PSO has been widely used to solve continuous and integer programming problems in a faster and cheaper way, compared to other stochastic optimization methods [82, 165]. The swarm is defined as a set of candidate solutions known as particles of size P. Each particle $[\mathbf{x}_p : \mathbf{y}_p]$ for $p \in \{1, \ldots, P\}$ represents a potential solution to the optimization problem:

$$\min_{\boldsymbol{x},\boldsymbol{y}} f_0(\boldsymbol{x}, \boldsymbol{y}), \tag{2.74a}$$

$$\boldsymbol{x} \in \mathbb{R}^n,\ \boldsymbol{y} \in \mathbb{Z}^N, \tag{2.74b}$$

where $\mathbf{x}_p$ represents the continuous variable vector defined as: $\mathbf{x}_p = [x_1^{(p)}, \ldots, x_n^{(p)}]$, and $\mathbf{y}_p$ represents the binary variables vector defined as: $\mathbf{y}_p = [y_1^{(p)}, \ldots, y_N^{(p)}]$. Using PSO, the continuous particle solution is updated as [82]:

$$\mathbf{x}_p^{(t+1)} = \mathbf{x}_p^{(t)} + \mathbf{v}_p^{(t+1)} \text{ for } t \geq 1, \tag{2.75}$$

where $\mathbf{v}_p^{(t)}$ is the pseudo-velocity for the continuous variables and computed as:

$$\mathbf{v}_p^{(t+1)} = \omega^{(t)}\mathbf{v}_p^{(t)} + c_1 r_1(\mathbf{x}_{p,best}^{(t)} - \mathbf{x}_p^{(t)}) + c_2 r_2(\mathbf{x}_{Gbest}^{(t)} - \mathbf{x}_p^{(t)}) \text{ for } t \geq 1, \tag{2.76}$$

the particle new velocity $\mathbf{v}_p^{(t)+1}$ depends on the previous velocity $\mathbf{v}_p^{(t)}$ and the distance of its current position $\mathbf{x}_p^{(t)}$ from its own best position $\mathbf{x}_{p,best}^{(t)}$ and the global best position $\mathbf{x}_{Gbest}^{(t)}$. The best position $\mathbf{x}_{p,best}^{(t)}$ is defined as the position at which the particle had best fitness (that is, minimum objective function), and it is checked at the end of every iteration. The global best position $\mathbf{x}_{Gbest}^{(t)}$ is defined as the best of $\mathbf{x}_{p,best}^{(t)}$ of all particles. r_1 and r_2 are uniform random numbers between 0 and 1, c_1 and c_2 are two positive constants, and $\omega^{(t)}$ is the inertia weight, which is employed to control the impact of previous history.

For integer variables, two approaches can be used to represent and update the value and the velocity of the variables. In the first approach, the integer variable is treated as a real variable; the velocity and value are updated using (2.75) and (2.76), then the value is rounded to the nearest integer. In this second approach, a suitable number of binary digits d is selected to represent the value. The velocity of particle p at time t with d binary digits is defined as $\tilde{\mathbf{v}}_p^{(t)}$, the update of the binary velocity can be computed as:

$$\tilde{\mathbf{v}}_p^{(t+1)} = \omega^{(t)}\tilde{\mathbf{v}}_p^{(t)} + c_1 r_1(\mathbf{y}_{p,best}^{(t)} - \mathbf{y}_p^{(t)}) + c_2 r_2(\mathbf{y}_{Gbest}^{(t)} - \mathbf{y}_p^{(t)}) \text{ for } t \geq 1, \tag{2.77}$$

where $\mathbf{y}_{p,best}^{(t)}$ and $\mathbf{y}_{Gbest}^{(t)}$ are analogy to $\mathbf{x}_{p,best}^{(t)}$ and $\mathbf{x}_{Gbest}^{(t)}$ for the binary variables. The binary variables $\mathbf{y}_p^{(t)}$ are then updated as [165]:

$$\text{If } \mathbf{c}_p^{(t+1)} \leq \text{sig}(\tilde{\mathbf{v}}_p^{(t)}) \text{ then } \mathbf{y}_p^{(t+1)} = 1 \text{ else } \mathbf{y}_p^{(t+1)} = 0, \tag{2.78}$$

where $\mathbf{c}_p^{(t)}$ is a vector of random numbers of $[0,1]^{dN}$, and sig$(\cdot)$ is the sigmoid function defined as $\text{sig}(x) = \frac{1}{1+\exp(-x)}$. Initially, $\mathbf{v}_p^{(0)}$ and $\tilde{\mathbf{v}}_p^{(0)}$ are random numbers within the boundary $0 \leq \mathbf{v}_p^{(0)}, \tilde{\mathbf{v}}_p^{(0)} \leq v_{\max}$. The particle then flies toward a new position according to (2.75) and (2.78). The update speed for the continuous variables could be set faster/slower than the speed of the binary variables in order to allow for convergence. The performance of each particle is measured according to the objective of the optimization problem (2.74).

For constraint optimization problems, there are efficient techniques to handle the constraints in (2.73), such as using a penalty term in the objective function or using a fitness function [109]. If the constraints are linear, there is no need to include them in the fitness function. The updated variables are selected to satisfy the constraints, otherwise they are normalized or reinitialized such that the constraints are satisfied. PSO method is illustrated in **Algorithm 2.4**.

Algorithm 2.4 PSO Method

Initialize $\mathbf{x}_p^{(t)}$, and $\mathbf{y}_p^{(t)}$, for $p = 1, \cdots, P$.
Repeat
Evaluate the objective function $f_0(\mathbf{x}_p^{(t)}, \mathbf{y}_p^{(t)})$ in (2.74) for $p = 1, \cdots, P$.
Find $\mathbf{x}_{p,best}^{(t)}$, $\mathbf{y}_{p,best}^{(t)}$, $\mathbf{x}_{Gbest}^{(t)}$, and $\mathbf{y}_{Gbest}^{(t)}$.
Update $\mathbf{x}_p^{(t)}$, and $\mathbf{y}_p^{(t)}$, for $p = 1, \cdots, P$.
Until termination criterion is satisfied.
Return $f_0(\mathbf{x}_{Gbest}^{(t)}, \mathbf{y}_{Gbest}^{(t)})$, $\mathbf{x}_{Gbest}^{(t)}$, and $\mathbf{y}_{Gbest}^{(t)}$ as the approximate optimal value and optimal solution, respectively.

2.5 Game Theory Concepts

In this section, the basic elements of game theory are defined. The celebrated Nash equilibrium (NE) solution concept is introduced. Theorems related to the existence and uniqueness of NE are reviewed. Special game types are highlighted. A brief introduction to auction terminology is given, and the Shapley value solution concept to cooperative games is introduced.

Game theory is a mathematical tool to study the interactions among decision-makers who can have conflicting or common interests. Decision-makers are called players in game theory, the meaning of a player can be very broad; it can be a human being, a machine, an automaton, etc. Interaction means that what others do has an impact on each player; what she gets from a decision does not only depend on her decision. Game theory possesses its own tools, notations and solution concepts coming from different areas such as economics, biology, and computer science. Rationality, punishments, cooperative plans, and evolutionary strategy are examples of game theory terminologies. Game theory uses interaction models, behavior models, and information assumptions aiming to predict the outcome of the interactive situation. Solution concepts and other issues like existence, uniqueness of the solution are essentials of game theory [90].

Games can be classified into two representative types non-cooperative and cooperative games as shown in **Figure 2.7**. In cooperative games, the

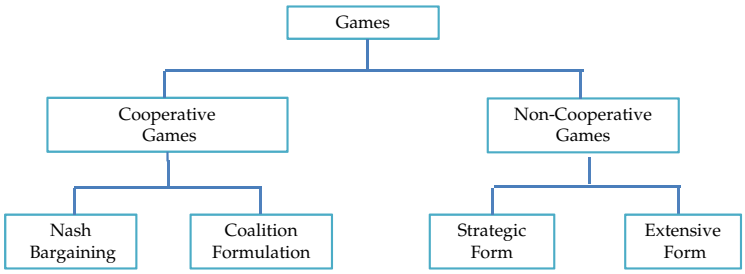

Figure 2.7 Game Classifications.

basic modeling unit is the group rather than the individual player, and the coalition model captures the capability of different groups. Solutions in cooperative games deal with distributing the profit among the users in the coalition, different solution concepts are used for cooperative games such as the core and Shapley value.

Non-cooperative games do not always infer that the players do not cooperate, but it means that any cooperation that might occur must be self-enforcing with no communications or coordination of strategic choices among the players [53]. Non-cooperative games are represented using two forms; normal (strategic) and extensive forms. The strategic form is the most used form. It is appropriate for mathematical analysis and can be used for both discrete and continuous strategy sets. Firstly, some notations and definitions in game theory will be introduced, and then solution concepts are discussed. The normal form stands on the existence of a utility function for each player, which represents the cost or payoff to the player. In some scenarios in wireless communications, performance measures e.g., QoS are used directly as utility functions.

The strategic game is defined as follows:

Definition 2.5.1 *A strategic game is an ordered triplet:*

$$G = (\mathcal{I}, \{\boldsymbol{S}_i\}_{i\in\mathcal{I}}, \{U_i\}_{i\in\mathcal{I}}), \tag{2.79}$$

where $\mathcal{I} = \{1, \cdots, I\}$ *is the set of players,* $\boldsymbol{S}_i$ *is the set of strategies of player i, and* $U_i : \boldsymbol{S} \mapsto \mathbb{R}$ *is the utility of player i, and* $\boldsymbol{S} = \boldsymbol{S}_1 \times \cdots \times \boldsymbol{S}_i \times \cdots \times \boldsymbol{S}_I$ *is the Cartesian*

product of the strategy sets.

For player i, $s_i \in \boldsymbol{S}_i$ denotes a strategy, $\boldsymbol{s}_{-i} = [s_j]_{j\in\mathcal{I},\, j\neq i}$ denotes the vector of strategies of all players except player i, and $\boldsymbol{s} = (s_i, \boldsymbol{s}_{-i}) \in \boldsymbol{S}$ is referred to as the strategy profile. The game is called finite whenever the sets of strategies $\boldsymbol{S}_i$ are finite for all $i \in \mathcal{I}$.

Extensive games are used to represent games that are played sequentially. Tree is the key feature of the extensive form, since the game is represented by a tree. At each node of the tree, a given player can make a decision, so the next node depends on the decision made of other players. Extensive game is defined as:

Definition 2.5.2 *An extensive form game is a sextuplet:*

$$G = (\mathcal{I}, \boldsymbol{V}, v_{root}, \pi, \{\boldsymbol{V}_i\}_{i\in\mathcal{I}}, \boldsymbol{U}), \tag{2.80}$$

where $\mathcal{I} = \{1, \cdots, I\}$ is the set of players, $(\boldsymbol{V}, v_{root}, \pi)$ is a tree with $\boldsymbol{V}$ is the set of vertices (nodes), v_{root} is the root node, and π is the predecessor function, that is, $\forall v \in \boldsymbol{V}, \exists\, n \geq 1, \pi^{(n)} = \pi \circ \cdots \circ \pi = v_{root}$, $\{\boldsymbol{V}_i\}_{i\in\mathcal{I}}$ is a partition of $\boldsymbol{V}$, and $\boldsymbol{U} = (U_1, \cdots, U_I)$ is a result function.

The extensive form is some times more intuitive and gives a better understanding of the game, and it can be used for computer-based analysis.

Games can be classified into two types based on the available information to the players; complete information, and non-complete information games. In complete information games, it is assumed that the data of the game are common knowledge (the actions and utility functions), that is, every player knows the data of the game, every player knows that the other players know the data of the game, and every player knows that the other players know that she knows the data of the game. Games with non-complete information (known as Bayesian games) model the case where the players have partial information about the game. Furthermore, games can

be classified into two types based on the history of the game as perfect and imperfect information games. When all the players know the history of the game perfectly, it is called perfect information game, otherwise, it is called imperfect information game.

A game is classified as static, if players take their actions only once, independent of each other. In contrast, a dynamic game is one where players may act more than once; that is, players have some information about others' actions, and time has an important role in decision-making. Game theory has been recently used extensively in communication systems and networks to model routing, flow control, power control in up-link CDMA systems, and resource allocations in cooperative communications [3, 28, 47, 60, 127, 149, 156].

2.5.1 Solution Concepts

For an optimization problem the key notion is the optimal profile, that is, a strategy that maximizes the objective function under the given constraints. However, the situation is even more complex in a game setting. In this case, the environment includes other players, all of whom are also hoping to maximize their payoffs. Thus the notion of an optimal profile for a given player is not meaningful; the best strategy depends on the choices of others. Game theory deals with this problem by identifying certain subsets of outcomes, called solution concepts, that are interesting in one sense or another. In this subsection, we describe some of the most fundamental solution concepts: dominant-strategy equilibrium, Nash equilibrium, and Pareto optimality.

One useful concept for solving non-cooperative games in strategic form is the notion of dominate-strategy equilibrium. Dominant strategy is defined as:

Definition 2.5.3 *A strategy $s_i \in \boldsymbol{S}_i$ is said to be dominant for player i if [40]*

$$U_i(s_i, \boldsymbol{s}_{-i}) \geq U_i(\acute{s}_i, \boldsymbol{s}_{-i}), \forall \acute{s}_i \in \boldsymbol{S}_i, \text{ and } \forall \boldsymbol{s}_{-i} \in \boldsymbol{S}_{-i}, \tag{2.81}$$

where $\boldsymbol{S}_{-i} = \prod_{j \in \mathcal{I},\, j \neq i} \boldsymbol{S}_j$ is the set of all strategy profiles for all players except player i.

Whenever a player has a dominant strategy, she has no incentive to choose any other strategy. If each player has a dominant strategy, then all users will choose their dominant strategies. This strategy profile denoted as dominant strategy equilibrium is defined as:

Definition 2.5.4 *A strategy profile $\boldsymbol{s}^* \in \boldsymbol{S}$ is the dominant-strategy equilibrium if every element $s_i^* \in \boldsymbol{s}^*$ is a dominant strategy for player i.*

The existence of dominant-strategy equilibrium is not guaranteed in many games.

On the other hand, strictly dominated strategies are defined as:

Definition 2.5.5 *A strategy $\acute{s}_i \in \boldsymbol{S}_i$ of a player i is said to be strictly dominated by a strategy $s_i \in \boldsymbol{S}_i$ if*

$$U_i(s_i, \boldsymbol{s}_{-i}) > U_i(\acute{s}_i, \boldsymbol{s}_{-i}), \ \forall \acute{s}_i \in \boldsymbol{S}_i, \ \acute{s}_i \neq s_i. \tag{2.82}$$

A player in a complete information game eliminates all strictly dominated strategies before making a decision. Eliminating all strictly dominated strategies leads to a concept called iterated strictly dominance, which can be used to reduce the strategy space and in some cases results in a reasonable outcome of the game.

The most accepted solution concept for a non-cooperative game is that of Nash equilibrium (NE). It is a state of a non-cooperative game where no player can improve her utility function by changing its strategy, if the other players keep their current strategies. Formally, NE is defined as:

Definition 2.5.6 *A pure strategy NE of a non-cooperative game* $G = (\mathcal{I}, \{\boldsymbol{S}_i\}_{i\in\mathcal{I}}, \{U_i\}_{i\in\mathcal{I}})$ *is a strategy profile* $\boldsymbol{s}^* \in \boldsymbol{S}$ *such that* $\forall i \in \mathcal{I}$ *the following holds:*

$$U_i(s_i^*, \boldsymbol{s}_{-i}^*) \geq U_i(s_i, \boldsymbol{s}_{-i}^*), \ \forall s_i \in \boldsymbol{S}_i, \tag{2.83}$$

where pure strategies are deterministic choices by the players. In general, a player may be able to assign a certain probability to each pure strategy, which constructs the mixed strategy concept. NE is strict if $U_i(s_i^*, \boldsymbol{s}_{-i}^*) > U_i(s_i, \boldsymbol{s}_{-i}^*), \forall s_i \in \boldsymbol{S}_i$.

When studying NE of a game, the key points of interest are existence, multiplicity (or uniqueness) and efficiency.

Static continuous kernel games are games where the strategy sets have uncountably many elements, such as subsets of a finite-dimensional Euclidean space, and the payoff functions are continuous on these sets. In other words, the strategies are intervals, or unions of sub-intervals of the real line. For static continuous kernel games, the concept of best response (BR) function is useful to solve some games, which is defined as:

Definition 2.5.7 *The BR function* $b_i(\boldsymbol{s}_{-i})$ *of a player i to the profile of strategies* $\boldsymbol{s}_{-i}$ *is a set of strategies for player i such that:*

$$b_i(\boldsymbol{s}_{-i}) = \{s_i \in \boldsymbol{S}_i | U_i(s_i, \boldsymbol{s}_{-i}) \geq U_i(\acute{s}_i, \boldsymbol{s}_{-i}), \forall \acute{s}_i \in \boldsymbol{S}_i\}, \tag{2.84}$$

NE can be characterized using the BR function, that is, it is a strategy profile for which every player's strategy is a best response to the other players' strategies. This can be stated as:

Theorem 2.5.1 *A strategy profile* $\boldsymbol{s}^* \in \boldsymbol{S}$ *is a Nash equilibrium of a non-cooperative game if and only if every player's strategy is a best response to other players' strategies; that is,*

$$s_i^* \in b_i(\boldsymbol{s}_{-i}^*), \ \forall i \in \mathcal{I}. \tag{2.85}$$

If each player i has a single best response for every strategy profile $\boldsymbol{s}_{-i}$, then (2.85) can be written as the following set of equations:

$$s_i^* = b_i(\boldsymbol{s}_{-i}^*),\ \forall i \in \mathcal{I}. \tag{2.86}$$

To find NE, one can find the BR function of each player, then the strategy profiles that satisfy (2.85) are sought, which reduces to the solution of the set of equations (2.86) for single BR function. If closed form expressions for the BR can be found, the pure strategy NE and their existence can be found by investigating the intersection of these BR functions. In particular, if the BR function can be found explicitly, the uniqueness of the pure strategy NE can be proved by the concept of a standard function, which is defined as:

Definition 2.5.8 *A function $f : \boldsymbol{S} \mapsto \mathbb{R}_+^I$ is said to be standard if it has the following properties:*

- *Monotonicity:* $\forall \boldsymbol{s}, \acute{\boldsymbol{s}} \in \boldsymbol{S},\ \boldsymbol{s} \leq \acute{\boldsymbol{s}} \Rightarrow f(\boldsymbol{s}) \leq f(\acute{\boldsymbol{s}})$.
- *Scalability:* $\forall \alpha > 0,\ \boldsymbol{s} \in \boldsymbol{S},\ f(\alpha \boldsymbol{s}) \leq \alpha f(\boldsymbol{s})$.

The standard function has a unique fixed point. This is used to prove the following theorem [164]:

Theorem 2.5.2 *If the BR functions of a non-cooperative game $G = (\mathcal{I}, \{\boldsymbol{S}_i\}_{i\in\mathcal{I}}, \{U_i\}_{i\in\mathcal{I}})$ are standard functions for all players, that is, $\forall i \in \mathcal{I}$, then the game has a unique NE in pure strategies.*

Away from the BR, some theorems exist for describing the existence of NE, the most common is the following:

Theorem 2.5.3 *Given a non-cooperative game in strategic form $G = (\mathcal{I}, \{\boldsymbol{S}_i\}_{i\in\mathcal{I}}, \{U_i\}_{i\in\mathcal{I}})$, if $\forall i \in \mathcal{I}$, every strategy set $\boldsymbol{S}_i$ is compact and convex, $U_i(s_i, \boldsymbol{s}_{-i})$ is a continuous function in the profile of strategies $\boldsymbol{s} \in \boldsymbol{S}$ and quasi-concave in s_i, then the game has at least one pure strategy NE.*

Theorem 2.5.3 can be used to show the existence of NE. It does not give any idea about the number of these equilibria. The following theorem is useful to show the uniqueness of NE [112].

Theorem 2.5.4 *Consider a strategic game* $G = (\mathcal{I}, \{\boldsymbol{S}_i\}_{i\in\mathcal{I}}, \{U_i\}_{i\in\mathcal{I}})$ *where* $\forall i \in \mathcal{I}$, *every strategy set* $\boldsymbol{S}_i$ *is compact and convex,* $U_i(s_i, \boldsymbol{s}_{-i})$ *is a continuous function in the profile of strategies* $\boldsymbol{s} \in \boldsymbol{S}$ *and concave in* s_i. *Let* $\boldsymbol{r} = (r_1, \cdots, r_I)$ *be an arbitrary vector of fixed positive parameters, if the diagonal strict concavity (DSC) property holds true, that is,*

$$\exists\, \boldsymbol{r} : (\boldsymbol{s} - \acute{\boldsymbol{s}})\Big(g(\boldsymbol{s}, \boldsymbol{r}) - g(\acute{\boldsymbol{s}}, \boldsymbol{r})\Big) > 0,\ \forall \boldsymbol{s}, \acute{\boldsymbol{s}} \in \boldsymbol{S}, \boldsymbol{s} \neq \acute{\boldsymbol{s}}, \tag{2.87}$$

with $g(\boldsymbol{s}, \boldsymbol{r}) \stackrel{\text{def}}{=} [r_1 \frac{\partial U_1(s_1, \boldsymbol{s}_{-1})}{\partial s_1}, \cdots, r_I \frac{\partial U_I(s_I, \boldsymbol{s}_{-I})}{\partial s_I}]^T$, *then the game has a pure strategy NE.*

Theorem 2.5.4 is used to prove the uniqueness of NE in many wireless communication problems as in [10]. In many cases, proving the DSC property in complicated scenarios is difficult and restrictive since the condition needs to be satisfied for all strategies [53]

One measure of the efficiency of a strategy is Pareto optimality concept, defined as:

Definition 2.5.9 *A strategy profile* $\boldsymbol{s} \in \boldsymbol{S}$ *is Pareto-superior to another strategy profile* $\acute{\boldsymbol{s}} \in \boldsymbol{S}$ *if for every player* $i \in \mathcal{I}$ *the following inequality holds:*

$$U_i(s_i, \boldsymbol{s}_{-i}) \geq U_i(\acute{s}_i, \acute{\boldsymbol{s}}_{-i}), \tag{2.88}$$

with strict inequality for at least one player. Hence, a strategy profile $\hat{\boldsymbol{s}} \in \boldsymbol{S}$ *is Pareto optimal (PO) if there exists no other strategy profile that is Pareto-superior to* $\hat{\boldsymbol{s}}$.

A PO outcome cannot be improved without hurting at least one player. In a game with multiple equilibria, it is desired to select a PO equilibrium, if possible. In general, NE is not PO.

Besides Pareto optimality, the price of anarchy[2] is another metric that can be used to evaluate the performance of NE. It is defined as the ratio of the maximum social welfare obtained by maximizing the total utility $\sum_{i\in\mathcal{I}} U_i(\boldsymbol{s})$ over $\boldsymbol{S}$ to the social welfare achieved at the worst-case equilibrium. Let $\boldsymbol{S}^{NE}$ defined as the set of NE strategy profiles of a given game $G = (\mathcal{I}, \{\boldsymbol{S}_i\}_{i\in\mathcal{I}}, \{U_i\}_{i\in\mathcal{I}})$, then the price of anarchy η is computed as [88]:

$$\eta = \frac{\min\limits_{\boldsymbol{s}\in\boldsymbol{S}^{NE}} \sum\limits_{i\in\mathcal{I}} U_i(\boldsymbol{s})}{\max\limits_{\boldsymbol{s}\in\boldsymbol{S}} \sum\limits_{i\in\mathcal{I}} U_i(\boldsymbol{s})}. \tag{2.89}$$

In general, no formal rule exists for selecting an efficient equilibrium, even though concepts such as Pareto optimality and the price of anarchy are suitable in some situations. Some techniques such as pricing and hierarchy structure are used to improve NE as in [89, 115]. In [89], the authors proposed hierarchy to improve energy-efficiency for non-cooperative power control game. In [115], the authors proposed a linear pricing function of the transmitted power to establish a Pareto optimal power solution for the uplink one-cell code division multiple access (CDMA) wireless system.

2.5.2 Special Classes of Non-Cooperative Games

In this subsection, we investigate two special classes of games: Potential and Stackelberg games. Potential games are non-zero sum games which possess a potential function that can be used to determine NE. The set of pure NE can be found by finding the maximum of the potential function. Formally a potential game is defined as:

Definition 2.5.10 *A non-cooperative strategic game $G = (\mathcal{I}, \{\boldsymbol{S}_i\}_{i\in\mathcal{I}}, \{U_i\}_{i\in\mathcal{I}})$, is an exact potential game if there exists an exact potential function $\Phi : \boldsymbol{S} \mapsto \mathbb{R}$ such that*

[2]The price of stability can be defined in a similar way using best-case equilibrium [88].

$\forall i \in \mathcal{I}$,

$$\Phi(x, \boldsymbol{s}_{-i}) - \Phi(y, \boldsymbol{s}_{-i}) = U_i(x, \boldsymbol{s}_{-i}) - U_i(y, \boldsymbol{s}_{-i}),\ \forall x, y \in \boldsymbol{S}_i,\ \forall \boldsymbol{s} \in \boldsymbol{S}. \tag{2.90}$$

An equivalent condition for the existence of an exact potential function $\Phi(\cdot)$ is [101]:

$$\frac{\partial U_i}{\partial a_i} = \frac{\partial \Phi}{\partial a_i}. \tag{2.91}$$

In a similar fashion, the ordinal potential function can be defined as:

Definition 2.5.11 *A game is a general ordinal potential game if there is an ordinal potential function* $\Phi : \boldsymbol{S} \mapsto \mathbb{R}$ *such that:*

$$sign\Big(\Phi(x, \boldsymbol{s}_{-i}) - \Phi(y, \boldsymbol{s}_{-i})\Big) = sign\Big(U_i(x, \boldsymbol{s}_{-i}) - U_i(y, \boldsymbol{s}_{-i})\Big),\ \forall x, y \in \boldsymbol{S}_i,\ \forall \boldsymbol{s} \in \boldsymbol{S}. \tag{2.92}$$

The interest in potential game is due to the following results [40]:

Corollary 2.5.1 *For infinite potential games (with a finite number of players), a pure strategy NE exists if*

1. $\boldsymbol{S}_i$ *are compact strategy sets.*
2. *The potential function* Φ *is upper semi-continuous on* $\boldsymbol{S}$.

Another interesting result for potential game that is pertained to the uniqueness of NE is:

Corollary 2.5.2 *For infinite potential games (with a finite number of players), unique pure strategy NE exists if*

1. *The strategy set* $\boldsymbol{S}$ *is compact and convex.*
2. *The potential function* Φ *is continuously differentiable on the interior of* $\boldsymbol{S}$.
3. *The potential function* Φ *is strictly concave in* $\boldsymbol{S}$.

Finding a potential function for a game is a difficult task, and in many cases a potential function may not exist. The following theorem can be used to check the existence of a potential function.

Theorem 2.5.5 *Given a strategic game where the strategy sets $\boldsymbol{S}_i$, $\forall i \in \mathcal{I}$, are intervals of $\mathbb{R}$, and assuming the utilities are twice continuous differentiable, then this game is a potential game if and only if*

$$\frac{\partial^2\Big(U_i(s_i, \boldsymbol{s}_{-i}) - U_j(s_j, \boldsymbol{s}_{-j})\Big)}{\partial s_i \partial s_j} = 0, \forall i, j \in \mathcal{I}, i \neq j. \tag{2.93}$$

Stackelberg games describe a hierarchical decision-making scheme, where one or more of the players declare and announce their strategies before the other players decide their strategies. In such games, the declaring players are called leaders, and can be in a position to enforce their own strategies upon the other players who are called the followers.

For a two player non-cooperative games between a leader and a follower, let $\boldsymbol{S}_i$, for $i = 1, 2$ denote the strategy set of player i. Each time the leader (player 1) chooses a strategy $s_1 \in \boldsymbol{S}_1$, she knows that the follower (player 2) observes her action before taking a decision $s_2 \in \boldsymbol{S}_2$. Formally, this can be stated as:

Definition 2.5.12 *Given a two player finite game, the set $R_2(s_1)$, defined for each strategy $s_1 \in \boldsymbol{S}_1$ by:*

$$R_2(s_1) = \{s_2 \in \boldsymbol{S}_2 : U_2(s_1, s_2) \geq U_2(s_1, t), \forall t \in S_2\}, \tag{2.94}$$

is the optimal response set of player 2 to the strategy $s_1 \in \boldsymbol{S}_1$ of player 1.

As the leader knows that the follower observes her action, when the follower reaction set $R_2(s_1)$ is a singleton for each $s_1 \in \boldsymbol{S_1}$, then the leader has

the following utility to maximize:

$$\max_{s_1 \in \boldsymbol{S}_1} U_1\Big(s_1, R_2(s_1)\Big). \tag{2.95}$$

The concept of Stackelberg equilibrium strategy (s_1^*, s_2^*) for a two player game is defined as:

$$s_1^* = \max_{s_1 \in \boldsymbol{S}_1} U_1\Big(s_1, R_2(s_1)\Big), \tag{2.96}$$

and,

$$s_2^* = R_2(s_1^*). \tag{2.97}$$

It is worth noting that using Stackelberg game can improve the leader utility when the followers reaction set $R_2(s_1)$ is a singleton for each $s_1 \in \boldsymbol{S_1}$ as per the following theorem.

Theorem 2.5.6 *For a given two-person finite game, let U_1^* and U_1^{NE} denote, respectively, the Stackelberg Equilibrium utility and the Nash Equilibrium utility of player* 1 *(the leader in Stackelberg formulation). If the reaction set is a singleton set for all $s_1 \in \boldsymbol{S}_1$, then the following holds:*

$$U_1^* \geq U_1^{NE}. \tag{2.98}$$

Accordingly, Stackelberg solution for a single leader multi-follower non-cooperative game describes the case where the leader maximizes her utility function given the reaction set of the follower group while the followers respond to the leader announced strategy by playing according to a certain equilibrium concept (e.g., Nash Equilibrium). The case of more than two levels of hierarchy can be treated using the concept of backward-induction from extensive games as in [89]. Stackelberg game is used extensively to perform resource allocation for relay networks as in [28, 149, 163, 170].

2.5.3 Distributed Algorithms

In this subsection, we present distributed algorithms to reach an equilibrium based on the best response correspondence (or function). Asynchronous (sequential) best response dynamics (ABRD) and synchronous (simultaneous) best response dynamics (SBRD) are discussed in [90]. For a strategic form game $G = (\mathcal{I}, \{\boldsymbol{S}_i\}_{i\in\mathcal{I}}, \{U_i\}_{i\in\mathcal{I}})$, the ABRD assumes that G starts at initial state $\boldsymbol{s}^{(0)} = (s_1^{(0)}, \cdots, s_I^{(0)})$. Player i for $i \in \mathcal{I}$ update her strategy by choosing her best response to $\boldsymbol{s}_{-i}^{(0)}$ as $s_i^{(1)} = BR_i(\boldsymbol{s}_{-i}^{(0)})$. If there is more than one best strategy, one of them is chosen randomly. The algorithm proceeds by updating the strategy of another player by choosing her best response to the new action profile, and so on. In SBRD algorithm all players update their actions synchronously. Both the ABRD and SBRD have been used in resource allocation for wireless communication problems as in [101, 118].

There are not many general results regarding the convergence of the best response dynamics, which means, that each situation needs to be investigated by itself. One of the positive properties of potential games is that SBRD dynamics converge with probability of one to a pure Nash equilibrium [90].

2.5.4 Auction Theory

An auction may take many forms, but it is described by two properties: first, it is used to sell any item. Second, the outcome of the the auction does not depend on the identity of the bidders, that is, auctions are anonymous. Auction can be defined as [53]:

Definition 2.5.13 *An auction is a market mechanism in which an object, service, or set of objects, is exchanged on the basis of bids submitted by participants. It provides a specific set of rules that will govern the sale of an object to the submitter of the most favorable bid. Specific mechanism includes: first price, second price,*

English, and Dutch auctions.

Auctions can be categorized in many ways. In general, there are four types of auctions that are used for single item allocation as follows:

1. **First Price Auction**: The bidder who submits the highest bid is awarded the object being sold and pays a price equal to the amount of the bid. First price auctions are either sealed-bid, in which bidders submit bids simultaneously, or Dutch. In first price auctions, bidders shade their bids below their true value.

2. **Second Price Auction**: The bidder who submits the highest bid is awarded the object being sold and pays a price equal to the second highest bid. Second price auctions are either sealed-bid, or English, in which bidders continue to raise each other's bids until only one bidder remains. In second price auctions, true value is a dominant strategy.

3. **English Auction**: It is a sequential second price auction, in which the auctioneer directs participants to beat a standing bid. New bids must increase the current bid by a predefined increment. The auction ends when no participant is willing to outbid the current standing bid. The participant who placed the current bid is the winner and pays the amount bid.

4. **Dutch Auction**: A clock initially indicates a price for the object for sale which is substantially higher than any bidder is likely to pay, then the clock gradually decreases the price until a bidder indicates a willingness to pay. The auction is then concluded and the winning bidder pays the amount reflected on the clock at time the process was terminated.

Most auction theory rotates around the above four basic types, other types of auction such as share auction for divisible goods, double auction, and

multi-items auction have received some importance in wireless communications as in [66, 137, 159]. Bids in some wireless communication scenarios are not used as true payments but are used as signals of willingness to pay.

2.5.5 Cooperative Games

In cooperative games, the players are allowed to form agreements among themselves, which can affect the strategic choices of these players and their utilities. Cooperative games includes two main categories bargaining and coalition games. Bargaining games are out of the scope of this dissertation. Here, we will give a brief introduction to coalition games and discuss one solution concept of a coalition game called the Shapley value. Coalition games can be defined as:

Definition 2.5.14 *A Coalition game is defined by the pair* $(\mathcal{I}, v)$*, where* v *is a mapping that determines the payoff that any coalition of players can receive in the game.*

Characteristic form game is a class of coalition games, where the value of a coalition $\mathcal{S} \subseteq \mathcal{I}$ of players depends solely on the members of that coalition, with no dependence on how the players in $\mathcal{I} \setminus \mathcal{S}$ are structured. A transferable utility (TU) game implies that the total utility can be divided in any manner between the coalition members. Formally, the value of a TU game can be defined as [113]:

Definition 2.5.15 *The characteristic function of a coalition game with transferable utility is a function* v *over the real line defined as:* $v : 2^{|\mathcal{I}|} \mapsto \mathbb{R}$*, with* $v(\varnothing) = 0$*, and* $|\mathcal{I}|$ *is the cardinality of the set* $\mathcal{I}$*.*

The characteristic function associates with every coalition $\mathcal{S} \subseteq \mathcal{I}$ a real number, that represents the value of $\mathcal{S}$. The values in TU games represent the monetary worth that members in a coalition can distribute among themselves using an appropriate rule. The amount of utility that player $i \in \mathcal{S}$ receives from the distribution of $v(\mathcal{S})$ is the player's payoff, and is denoted as

x_i. The payoff allocation for the players in the set $\mathcal{S}$ is denoted by the vector $\boldsymbol{x} \in \mathbb{R}^{|\mathcal{S}|}$. Many solution concepts are defined for coalition games such as the core, the nucleolus, and the Shapley value. The Shapley value has received interest in this research because it is a unique and fair solution that always exists. In contrast, the core suffers from three main drawbacks: it can be empty, quite large, and allocations in the core may be unfair. Furthermore, computing the Shapley value is less complex, compared with computing the nucleolus, which is unique, always exists, and it is a fair allocation (that is, achieves min-max criterion).

The Shapley value is denoted as $\boldsymbol{\Phi}(v) = [\Phi_1(v), \cdots, \Phi_i(v), \cdots, \Phi_{|\mathcal{I}|}(v)]$, where $\Phi_i(v)$ is the payoff given to player i. The Shapley value satisfies four axioms as follows:

1. **Efficiency Axiom**: $v(\mathcal{I}) = \sum_{i \in \mathcal{I}} \Phi_i(v)$.
2. **Symmetry Axiom**: If player i and player $\acute{i}$ are such that $v(\mathcal{S} \cup \{i\}) = v(\mathcal{S} \cup \{\acute{i}\})$ for every coalition $\mathcal{S}$ not containing player i and player $\acute{i}$, then $\Phi_i(v) = \Phi_{\acute{i}}(v)$.
3. **Dummy Axiom**: If player i is such that $v(\mathcal{S}) = v(\mathcal{S} \cup \{i\})$, for every coalition $\mathcal{S}$ not containing i, then $\Phi_i(v) = 0$.
4. **Additive Axiom**: If u and v are characteristics functions, then $\boldsymbol{\Phi}(v + u) = \boldsymbol{\Phi}(u + v) = \boldsymbol{\Phi}(v) + \boldsymbol{\Phi}(u)$.

The Shapley value for player i is computed as:

$$\Phi_i(v) = \frac{1}{|\mathcal{I}|!} \sum_{\pi \in \Omega} v(C_i(\pi) \cup \{i\}) - v(C_i(\pi)), \tag{2.99}$$

where Ω is the set of all possible $|\mathcal{I}|!$ permutations on $\mathcal{I}$, π is a permutation in Ω, and $C_i(\pi)$ is the set of players that precedes user i in the permutation π.

2.6 Conclusions

In this chapter, the basic concepts and notations that will be used throughout the dissertation are introduced. The basic schemes of cooperative communication, specifically AF, DF, and SDF are introduced with emphasis on the outage probability, diversity order, and SEP performance measures. Basic concepts of optimization theory such as optimality conditions, duality formulation, and solution methods are presented. Solution concepts, such as NE for non-cooperative games, and Shapley value for cooperative games are discussed. In the remainder of this dissertation, the emphasis will be in studying the performance measures of specific cooperative communication scenarios and designing resource allocation algorithms, using different formulations. Tools and concepts from optimization and game theory frameworks will be used to find the solutions.

CHAPTER3

ORDERED BEST RELAYS: PERFORMANCE ANALYSIS

This chapter addresses relay selection in multi source multi relay scenarios. Relay selection based on the highest end-to-end SNR utilizes the spectrum efficiently, when only two time slots are used. For a system with multiple users and multiple relays with limited power capability, the scenario of two users competing for the same relay is pronounced. Along this direction, the scenario of two users having the same best ordered relay is addressed for both AF and DF cooperative communication schemes. We propose sharing of the two ordered best relays over Rayleigh flat fading channel subject to relay power constraint per user to establish full diversity order for both users. We study the performance of the proposed scheme in terms of the outage probability, diversity order, and the BEP performance measures. The MGF formula of the received SNR of the two ordered best relays (the best, and the next-best) after using MRC is derived assuming equal power sharing, where each relay transmits with half power.

Introduction and related works are given in Section 3.1. The system model and notations are introduced in Section 3.2. Three-time slots, and two-time slots based cooperative relay transmission schemes with their performance measures are presented in Sections 3.3 and 3.4, respectively. Numerical results and discussions are presented in Section 3.5. Conclusions are

drawn in Section 3.6.

3.1 Introduction

As discussed in Subsection 2.3.3, using the best ordered relay achieves full diversity order using two time slots. However, for multi-user systems, the probability of two users competing for the same best relay is significant and comparable to the probability of having different best relays with similar average channel conditions as was proven in [11]. In this sense, two solutions are proposed in literature; the first solution is to use the best relay for user one, and the next-best relay for the other user. So, this solution transforms the problem to the kth best ordered relay selection problem, which was investigated in [74–76, 158], by this solution the users achieve different diversity orders. The second solution is to use the best relay for the two users with half power for each user, if this choice gives better performance than using the next-best relay alone with full power, which was proposed in [11]. However, no analytical results for the BEP, or outage probability have yet been derived because of the mathematical complexity. In summary, the two solutions are based on using only one relay for each user.

In this chapter, we propose a different solution, in which the best relay and the next-best relay are equally shared between the two users. The relays are ordered based on the instantaneous end-to-end SNR of the source-relay-destination links. Each user will have the chance to use the best and the next-best ordered relays in a predetermined manner. The relay transmit power is equally shared between the two users. Equal opportunity of using the best relay is the base to build up this scheme. Three-time-slots are used, where each user benefits from two relays as follows: the first-time-slot is used to transmit the sources' data to the relays and the destination nodes, the second-time-slot is used to relay the processed data from the best relay to the destination node, and the third-time-slot is used to relay the processed

data from the next-best relay to the destination node. In addition, sharing the two ordered best relays for both AF and DF cooperative schemes for independent identically distributed (*iid*) flat fading Rayleigh channels, utilizing two-time slots using distributed STBC or distributed beamforming (BF) are also investigated to exploit the channel efficiently. The proposed schemes place full diversity selection at the core of the design scheme, and take into consideration the limited available power at the relay. The available power at the relay is used to support both users, and it is equally split between them.

3.2 System Model

The system under consideration is depicted in **Figure 3.1**. In this model, the channel characterizing the link between source S_i and relay R_l is denoted as $h_{S_iR_l}$, and the channel characterizing the link between relay R_l and destination node D is denoted as h_{R_lD}. Moreover, the channel identifying the link between source S_i and destination node D is denoted as h_{S_iD}. The channels $h_{S_iR_l}$, h_{R_lD}, and h_{S_iD} are assumed *iid* Rayleigh random variables for $l \in \{1, \ldots, K\}$ with K is the number of relays, and $i \in \{1, 2\}$. The received noise at all links is assumed to be *iid* AWGN with zero mean and variance σ_0^2. For relay selection schemes, the channel characterizing the link between the source S_i and the jth ordered best relay R_{bj} is denoted as $h_{S_iR}^{(j)}$, and the channel characterizing the link between the jth ordered best relay and the destination is denoted as $h_{RD}^{(j)}$, where $j \in \{0, 1\}$.

In this chapter, time division multiple access (TDMA) is considered. For a two-users case, each time slot is divided into two sub-slots. Frequency division multiple access (FDMA) can also be considered in a similar fashion, where each frequency sub-band in FDMA corresponds to a time sub-slot in TDMA. The sharing scenarios are classified into two categories: three-time slots scenario (orthogonal), and two-time slots scenario (non-orthogonal).

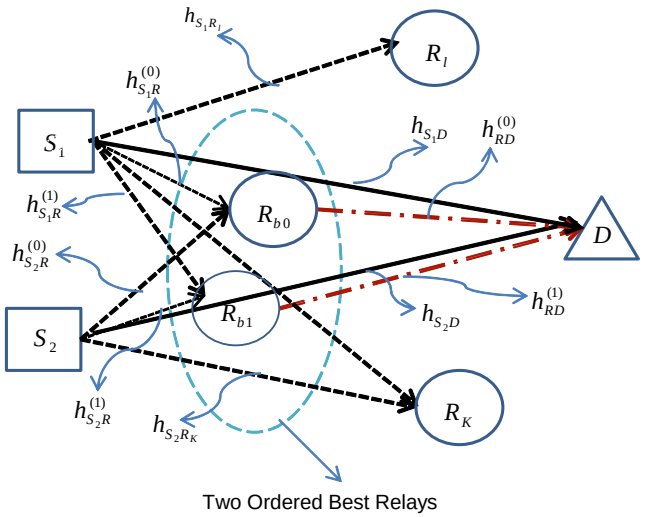

Figure 3.1 System Model.

In both scenarios, the first-time slot is used for the sources' transmission to the destination node and relay nodes (broadcast phase). Orthogonal in this context refers to relay transmission, where the best relay transmits in the second-time slot, and the next-best relay transmits in the third-time slot (no interference). The second and third time slots are subdivided into T_{m1}, and T_{m2} for $m \in \{2,3\}$ to transmit user's 1 and user's 2 data respectively. For two-time slots scenario, STBC or BF transmission schemes are used to relay the data from the two best ordered relays to the destination node for the two users simultaneously. Non-orthogonal in this context refers to the transmission in the second-time slot; the best, and the next-best relays transmit at the same time. Sub-slot T_{2i} is used by the best and next-best relays for transmitting user's i data simultaneously for BF scenarios. The instantaneous value of the phase of the CSI of the source-relay and relay-destination links are required to be available at the best, and the next-best relays to perform distributed BF. For distributed STBC the best and next-best relays transmit the re-encoded signal or the complex conjugate of the re-encoded signal in a predetermined way as will be explained in Subsection 3.4.1. The destination node for all scenarios, combines the directed and relayed signals using MRC, where the received signals from all independent paths are co-

phased, weighted, and combined, assuming the destination knows the instantaneous CSI from the sources and relays. The instantaneous CSI is kept invariant over multiple transmission intervals. So, the selection of the best, and next-best relays is performed once for multiple transmissions. Relay selection is performed before data transmission. The best and next-best relays can be determined for both AF and DF in a centralized or distributed fashion, depending on where the decision is carried out. In a centralized relay selection, the destination node based on the end-to-end SNR of the source-relay-destination links determines the best and the next-best relays, and informs the selected relays through feedback channels. In a distributed relay selection, each relay acquires the instantaneous CSI of the two links (relay-destination, and source-relay), the CSI of the relay-destination link can be acquired by allowing the destination to transmit a pilot signal. The relay then can determine the CSI of the relay-destination link assuming that the relay-destination link is symmetric. Besides, the CSI of the source-relay link can be determined at the relay from the source request to transmit. Based on CSI of the two links (relay-destination, and source-relay), the relay sets a timer and remains silent inversely proportional to the end-to-end SNR. The relay whose timer expires first or second will broadcast a signal to other relays, indicating that they can go to a sleep mode for the rest of the current transmission period. If the relay receives two signals from other relays before its timer goes to zero, it can go to a sleep mode, otherwise, it will be the best relay or the next-best relay [16, 155].

3.3 Three-Time Slots Scenario

In this scenario, three-time slots are used. The selected relays are shared between the two sources (users), where the relays transmit power is shared. The transmission scheme is illustrated in **Table 3.1**, where T_{x_i} stands for transmission of user i data x_i, and R_{x_i} stands for receiving user i (source S_i)

Table 3.1 Three-Time Slots Scenario.

Terminal	T_{11}	T_{12}	T_{21}	T_{22}	T_{31}	T_{32}
S_1	T_{x_1}	-	-	-	-	-
S_2	-	T_{x_2}	-	-	-	-
R_{b0}	R_{x_1}	R_{x_2}	T_{x_1}	T_{x_2}	-	-
R_{b1}	R_{x_1}	R_{x_2}	-	-	T_{x_1}	T_{x_2}
D	R_{x_1}	R_{x_2}	R_{x_1}	R_{x_2}	R_{x_1}	R_{x_2}

data x_i. The received signal $y_{T_{1i}}^{(D)}$ at the destination node D, in time slot T_1 is obtained as follows:

$$y_{T_{1i}}^{(D)} = \sqrt{P_S} h_{S_iD} x_i + n_{1i}^{(D)},\ i = 1, 2. \tag{3.1}$$

The received signal $y_{T_{1i}}^{(R_l)}$ at the relay node R_l, in time slot T_1 is as:

$$y_{T_{1i}}^{(R_l)} = \sqrt{P_S} h_{S_iR_l} x_i + n_{1i}^{(R_l)},\ i = 1, 2\ \&\ l = 1, \ldots, K. \tag{3.2}$$

In particular, the received signal at the ordered best relays R_{b0} and R_{b1} in time slot T_1 is obtained as:

$$y_{T_{1i}}^{(R_{bj})} = \sqrt{P_S} h_{S_iR_{bj}}^{(j)} x_i + n_{1i}^{(R_{bj})},\ i = 1, 2\ \&j = 0, 1, \tag{3.3}$$

where $n_{1i}^{(D)}$, $n_{1i}^{(R_l)}$, and $n_{1i}^{(R_{bj})}$ are the AWGNs at the destination D, at the relay R_l, and at the best ordered relay R_{bj}, respectively. The relays are ordered based on the end-to-end SNR of the source-relay-destination links as explained later in Subsections 3.3.1 and 3.3.2 for DF and AF scenarios, respectively. The transmitted symbol x_i is drawn from a constellation with unit energy, and P_S is the source transmitted power. The instantaneous received SNR at the destination node, from the source S_i through the direct link over Rayleigh flat fading channel is defined as γ_{S_iD}. It is computed

using (3.1) as $\gamma_{S_iD} = \gamma_0 |h_{S_iD}|^2$, where $\gamma_0 = \frac{P_S}{\sigma_0^2}$, and γ_{S_iD} is a random variable exponentially distributed with parameter λ_{S_iD}. To simplify the analysis, the source-destination links of user 1 and user 2 are assumed to be *iid* with $\lambda_{S_1D} = \lambda_{S_2D} = \lambda_{SD} = \frac{1}{\gamma_0 \mathrm{E}[|h_{S_iD}|^2]}$[1]. Similarly, the instantaneous received SNR at the relay R_l from source S_i is computed using (3.2) as $\gamma_{S_iR_l} = \gamma_0 |h_{S_iR_l}|^2$, where $\gamma_{S_iR_l}$ is also an exponentially distributed random variable with parameter $\lambda_{S_iR_l}$. The source relay links are assumed to have the same average value $\lambda_{S_iR_l} = \lambda_{SR} = \frac{1}{\gamma_0 \mathrm{E}[|h_{S_iR_l}|^2]}$, $\forall l \in \{1, \ldots, K\}$, and $\forall i \in \{1, 2\}$. For an exponentially distributed random variable X with parameter λ, the mean is given as $\mu_X = \mathrm{E}[X] = \frac{1}{\lambda}$. The transmission in the second and third-time slots depends on the cooperation scheme, DF or AF. The three-time slots DF scenario is investigated in Subsection 3.3.1, and the three-time slots AF scenario is investigated in Subsection 3.3.2.

3.3.1 DF Three-Time Slots Scenario

As illustrated in **Table 3.1**, the received signal $y_{T_{mi}}^{(DF)}$ at the destination node in time slot T_m for DF scheme is as:

$$y_{T_{mi}}^{(DF)} = \sqrt{\frac{P_S}{2}} h_{RD}^{(j)} \tilde{x}_{ji} + n_{mi}^{(DF)}, \; j = 0, 1, \; i = 1, 2, \; \& \; m = 2, 3, \tag{3.4}$$

where $n_{mi}^{(DF)}$ is the received AWGN at the destination node in time slot T_m, and $\tilde{x}_{ji}$ is the ith user decoded symbol at the jth relay. The jth ordered relay transmits with power $P_R^{(j)}$ equals half the source power ($P_R^{(j)} = P_S/2$) for each user. Defining $\gamma^{(0.5D)}$ as the instantaneous SNR for the ith user at the destination node after using MRC, and assuming the relays R_{b0} and R_{b1} decoded the symbol x_i correctly (i.e. $\tilde{x}_{0i} = \tilde{x}_{1i} = x_i$), then $\gamma^{(0.5DF)}$ is obtained as:

$$\gamma^{(0.5DF)} = \gamma_{S_iD} + \frac{1}{2} \gamma_{sum}^{(DF)}, \tag{3.5}$$

[1] $\mathrm{E}_X[X]$ is written as $\mathrm{E}[X]$ to simplify the notations.

where $\gamma_{sum}^{(DF)}$, is defined as $\gamma_{sum}^{(DF)} = \gamma_{b0}^{(DF)} + \gamma_{b1}^{(DF)}$, and $\gamma_{b0}^{(DF)}$, $\gamma_{b1}^{(DF)}$ are respectively the instantaneous end-to-end SNR of the best, and the next-best relays. The factor $\frac{1}{2}$ in (3.5) is due to the fact that the best and next-best relays are equally shared between the two users, where $P_R^{(j)} = P_S/2$ for $j \in \{0, 1\}$.

The best relay R_{b0} is the relay with the maximum instantaneous end-to-end SNR at the destination node, i.e. $\gamma_{b0}^{(DF)} = \max_{l}(\gamma_0|h_{R_lD}|^2)$. The next-best relay R_{b1} is the relay with the next-maximum instantaneous end-to-end SNR at the destination node, i.e. $\gamma_{b1}^{(DF)} = \max_{l,\, l\neq b0}(\gamma_0|h_{R_lD}|^2)$, where $l = 1, \ldots, K$ (l is used as an index for the relay without ordering). The selection of the best relay R_{b0} and next-best relay R_{b1} from the K available relays is determined by ordering the instantaneous end-to-end SNRs from the K relays as follows $\gamma_{b0}^{(DF)} > \gamma_{b1}^{(DF)} > \gamma_{b2}^{(DF)} > \ldots > \gamma_{bK-1}^{(DF)}$. [2] In the following, the PDF and the MGF of the end-to-end SNR $\gamma^{(0.5D)}$ are derived in order to evaluate the BEP and outage probability performance measures of the proposed scenario.

In order to find the PDF $f_{\gamma_{sum}^{(DF)}}(z)$ of the instantaneous end-to-end SNR $\gamma_{sum}^{(DF)}$, from the best and the next-best relays, we consider the following. (1) Instead of dealing with the decoding set C as in [65], we assume that the relay is selected from the K available relays. However, if a relay cannot decode the message correctly, it will not transmit and hence, the instantaneous end-to-end SNR equals zero [77]. (2)The lth relay can decode the message of user S_i, if $\gamma_0|h_{S_iR_l}|^2$ is greater than some threshold value Δ_{TH}, i.e. if $\gamma_0|h_{S_iR_l}|^2 > \Delta_{TH}$. Defining β as the probability of erroneously decoding the message, then β is computed as $\beta = \Pr(\gamma_0|h_{S_iR_l}|^2 < \Delta_{TH}) = 1 - e^{-\lambda_{SR}\Delta_{TH}}$, where $\gamma_0|h_{S_iR_l}|^2$ is an exponential random variable with a parameter λ_{SR}. Assuming the source-relay links are identical random variables, then Δ_{TH} can be computed as the value of $\gamma_0|h_{S_iR_l}|^2$ that is sufficient to satisfy a given transmission rate R. In other words, Δ_{TH} is the threshold value satisfying the inequality $\frac{1}{2}\log(1 + \gamma_0|h_{S_iR_l}|^2) \geq R$ or equivalently $\gamma_0|h_{S_iR_l}|^2 \geq \Delta_{TH} = (2^{2R} - 1)$. The re-

[2] The decoding set C is a subset of the K available relays. If a relay is not in the decoding set, the end-to-end SNR value is set to zero.

lay R_l that satisfies this condition is considered in the decoding set C [9, 77]. Defining the unordered instantaneous end-to-end SNR at the destination node from the lth relay as $\gamma_l^{(DF)}$, for $l = \{1, \ldots, K\}$, $\gamma_l^{(DF)}$ is then obtained as:

$$\gamma_l^{(DF)} = \begin{cases} 0, & \text{if } \gamma_0 |h_{S_i R_l}|^2 < \Delta_{TH}, \\ \gamma_0 |h_{R_l D}|^2 & \text{if } \gamma_0 |h_{S_i R_l}|^2 \geq \Delta_{TH}. \end{cases} \tag{3.6}$$

The PDF $f_{\gamma_l^{(DF)}}(x)$, and the cumulative density function (CDF) $F_{\gamma_l^{(DF)}}(x)$ of $\gamma_l^{(DF)}$ are given as [76]:

$$f_{\gamma_l^{(DF)}}(x) = (1-\beta)\lambda_{RD} e^{-\lambda_{RD} x} \mu(x) + \beta \delta(x), \tag{3.7a}$$

$$F_{\gamma_l^{(DF)}}(x) = \left(1 - (1-\beta) e^{-\lambda_{RD} x}\right) \mu(x), \tag{3.7b}$$

where $\mu(x)$ is the unit step function, $\delta(x)$ is Dirac delta function, and λ_{RD} is the parameter of the exponential random variable characterizing the received SNR at the destination node from the relay, assuming that all relay-destination links are *iid* random variables, with $\lambda_{RD} = \frac{1}{\gamma_0 E\{|h_{R_l D}|^2\}}$.

In order to find the PDF of the SNR of the best and next-best relays, the order statistics of random variables is used. Let $X_1, X_2, \ldots, X_K$ be defined as *iid* random variables, with PDF $f_X(x)$ and CDF $F_X(x)$. In addition, define the ordered random variables $Y_1 < Y_2 \ldots < Y_K$, where $Y_1 = \min_l X_l$, and $Y_K = \max_l X_l$ for $l \in \{1, \ldots K\}$, then the PDF of the kth ordered random variable Y_k is obtained as [31]:

$$f_{Y_k}(y) = \binom{K}{k} k \left[F_X(y)\right]^{k-1} \left[1 - F_X(y)\right]^{K-k} f_X(y), \tag{3.8}$$

and the joint PDF of the two ordered random variables (Y_r and Y_s), where

$r < s$ is given by [70]:

$$f_{Y_r,Y_s}(x,y) = \frac{K!}{(r-1)!(s-r-1)!(K-s)!}[F_X(x)]^{r-1} f_X(x) f_X(y) \times [1-F_X(y)]^{K-s}[F_X(y)-F_X(x))]^{s-r-1}. \quad (3.9)$$

From (3.8) the PDFs of the received SNR $\gamma_{b0}^{(DF)}$, and $\gamma_{b1}^{(DF)}$ from the best, and next-best relays respectively are obtained as:

$$f_{\gamma_{b0}^{(DF)}}(z) = K[F_X(z)]^{K-1} f_X(z), \quad (3.10a)$$

$$f_{\gamma_{b1}^{(DF)}}(z) = K(K-1)[F_X(z)]^{K-2}[1-F_X(z)] f_X(z). \quad (3.10b)$$

The joint PDF of the received SNR from the ordered relays (R_{b0}, R_{b1}) using (3.9) is obtained as:

$$f_{\gamma_{b1}^{(DF)},\gamma_{b0}^{(DF)}}(x,y) = K(K-1)[F_X(x)]^{K-2} f_X(x) f_X(y). \quad (3.11)$$

Substituting (3.7a) in (3.11), results in:

$$f_{\gamma_{b1}^{(DF)},\gamma_{b0}^{(DF)}}(x,y) = K(K-1)\left[\left(1-(1-\beta)e^{-\lambda_{RD}x}\right)\mu(x)\right]^{K-2}\left[(1-\beta)\lambda_{RD}e^{-\lambda_{RD}x}\mu(x)+\beta\delta(x)\right] \times \left[(1-\beta)\lambda_{RD}e^{-\lambda_{RD}y}\mu(y)+\beta\delta(y)\right]. \quad (3.12)$$

Note that, $\gamma_{b0}^{(DF)}$ and $\gamma_{b1}^{(DF)}$ are dependent random variables due to the ordering of the instantaneous end-to-end SNR. The PDF of their sum $\gamma_{sum}^{(DF)} = \gamma_{b0}^{(DF)} + \gamma_{b1}^{(DF)}$ is computed as [107]:

$$f_{\gamma_{sum}^{(DF)}}(z) = A^{(DF)}e^{-\lambda_{RD}z}\mu(z) + B^{(DF)}ze^{-\lambda_{RD}z}\mu(z) + D^{(DF)}\delta(z) + \sum_{k=3}^{K} E_k^{(DF)} e^{-k\lambda_{RD}\frac{z}{2}}\mu(z). \quad (3.13)$$

Defining c_k as:

$$c_k = \binom{K}{k} k\,(k-1)\,(-1)^{k-2}, \quad (3.14)$$

then $A^{(DF)}, B^{(DF)}, D^{(DF)}$, and $E^{(DF)}$ are computed as given in **Table 3.2**.

The MGF $\Psi_{\gamma_{sum}^{(DF)}}(s)$ of the received SNR $\gamma_{sum}^{(DF)}$ is obtained using (3.13) as:

$$\Psi_{\gamma_{sum}^{(DF)}}(s) = E\{e^{-s\,\gamma_{sum}^{(DF)}}\} = \frac{A^{(DF)}}{s+\lambda_{RD}} + \frac{B^{(DF)}}{(s+\lambda_{RD})^2} + \sum_{k=3}^{K} \frac{E_k^{(DF)}}{s+\frac{k\lambda_{RD}}{2}} + D^{(DF)}. \quad (3.15)$$

For the case of sharing the best and next-best relays, it is required to compute the MGF of $0.5\gamma_{sum}^{(DF)}$, which can be obtained simply from $\gamma_{sum}^{(DF)}$ as $\Psi_{\frac{\gamma_{sum}^{(DF)}}{2}}(s) = \Psi_{\gamma_{sum}^{(DF)}}(\frac{s}{2})$. Since the received SNR from the source-destination link γ_{S_iD} is independent of the received SNR from the relay-destination link $0.5\gamma_{sum}^{(DF)}$, the MGF $\Psi_{\gamma^{(0.5DF)}}(s)$ of the received SNR at the destination node after using MRC is $\Psi_{\gamma^{(0.5DF)}}(s) = \Psi_{\gamma_{sum}^{(DF)}}(\frac{s}{2})\Psi_{\gamma_{SD}}(s)$. Applying the partial fraction expansion, we arrive at:

$$\Psi_{\gamma^{(0.5DF)}}(s) = \frac{a^{(DF)}}{1+\frac{s}{2\lambda_{RD}}} + \frac{b^{(DF)}}{(1+\frac{s}{2\lambda_{RD}})^2} + \sum_{k=3}^{K} \frac{e_k^{(DF)}}{1+\frac{s}{\lambda_{RD}k}} + \frac{f^{(DF)}}{1+\frac{s}{\lambda_{SD}}}, \quad (3.16)$$

where $a^{(DF)}$, $b^{(DF)}$, $f^{(DF)}$, and $e_k^{(DF)}$ (assuming that $\lambda_{SD} \neq \lambda_{RD}$ or multiple of it for simplicity, but the analysis can be easily extended), are given as in **Table 3.2**. Since MRC is used at the destination node, the SEP can be calculated by averaging the multichannel conditional SEP over the PDF of the random variable representing the received end-to-end SNR at the destination node [73]. The SEP for M-PSK and M-QAM are respectively obtained by using the MGF $\Psi(s)$ of the received end-to-end SNR as follows [130]:

$$SEP_{MPSK} = \frac{1}{\pi}\int_0^{\frac{(M-1)\pi}{M}} \Psi\Big(\frac{\sin^2(\frac{\pi}{M})}{\sin^2\theta}\Big)d\theta, \quad (3.17a)$$

$$SEP_{MQAM} = \frac{4q}{\pi}\int_0^{\frac{\pi}{2}} \Psi\Big(\frac{3}{2(M-1)\sin^2\theta}\Big)\,d\theta - \frac{4q^2}{\pi}\int_0^{\frac{\pi}{4}} \Psi\Big(\frac{3}{2(M-1)\sin^2\theta}\Big)\,d\theta, \quad (3.17b)$$

where $q = 1 - \frac{1}{\sqrt{M}}$.

Here, the SEP is calculated only for BPSK modulation by substituting

Table 3.2 Coefficients of The PDF, The MGF, The BEP, and the $P_{out}(\gamma_{Th})$ for DF Sharing Scheme.

Coefficient	Value
$A^{(DF)}$	$\sum_{k=3}^{K} \lambda_{RD} c_k (1-\beta)^{k-1}\left(\beta + \frac{1-\beta}{k-2}\right) + c_2(1-\beta)\beta\lambda_{RD}$
$B^{(DF)}$	$\frac{c_2}{2}(1-\beta)^2\lambda_{RD}^2$
$D^{(DF)}$	$\sum_{k=2}^{K} c_k \beta^2 (1-\beta)^{k-2}$
$E_k^{(DF)}$	$\frac{c_k}{2}(1-\beta)^k\left(\frac{-2}{k-2}\right)\lambda_{RD}$
$a^{(DF)}$	$\frac{1}{2\lambda_{RD}}\left(\frac{2A^{(DF)}\lambda_{SD}}{-2\lambda_{RD}+\lambda_{SD}} - \frac{4B^{(DF)}\lambda_{SD}}{(-2\lambda_{RD}+\lambda_{SD})^2}\right)$
$b^{(DF)}$	$\frac{1}{4\lambda_{RD}^2}\left(\frac{4B^{(DF)}\lambda_{SD}}{-2\lambda_{RD}+\lambda_{SD}}\right)$
$f^{(DF)}$	$\frac{2A^{(DF)}}{2\lambda_{RD}-\lambda_{SD}} + \frac{4B^{(DF)}}{(2\lambda_{RD}-\lambda_{SD})^2} + \sum_{k=3}^{K} \frac{2E_k^{(DF)}}{\lambda_{RD}k-\lambda_{SD}} + D^{(DF)}$
$e_k^{(DF)}$	$\frac{1}{\lambda_{RD}k}\left(\frac{2E_k^{(DF)}\lambda_{SD}}{-\lambda_{RD}k+\lambda_{SD}}\right)$

$M = 2$ in (3.17a), but it can be easily extended to M-PSK, and M-QAM using (3.17a) and (3.17b) respectively, and can be expressed in a closed-form using the hypergeometric functions [130]. In the following we obtain the BEP for different sharing scenarios. The BEP is computed using (3.17a) as:

$$BEP = \frac{1}{\pi}\int_0^{\frac{\pi}{2}} \Psi\left(\frac{1}{\sin^2\theta}\right)d\theta. \tag{3.18}$$

Defining the function $F^n(u)$ as:

$$F^n(u) = \frac{1}{\pi}\int_0^{\frac{\pi}{2}} \frac{1}{(1+\frac{u}{\sin^2\theta})^n}d\theta = \left(\frac{1-k_u}{2}\right)^n \sum_{t=0}^{n-1}\binom{n-1+t}{t}\left(\frac{1+k_u}{2}\right)^t, \tag{3.19}$$

where $k_u = \sqrt{\frac{u}{1+u}}$ and n is an integer, the integral for $n = 1$ simplifies to $F^1(u) = \frac{1}{2}(1-k_u)$.

The $BEP_{\gamma^{(0.5DF)}}$ is obtained by substituting (3.16) into (3.18), and computing

the integral as follows:

$$BEP_{\gamma^{(0.5DF)}} = \frac{a^{(DF)}}{2}\Big(1 - \sqrt{\frac{1}{1+2\lambda_{RD}}}\Big) + b^{(DF)}F^2\Big(\frac{1}{2\lambda_{RD}}\Big) + \sum_{k=3}^{K} \frac{e_k^{(DF)}}{2}\Big(1 - \sqrt{\frac{1}{1+\lambda_{RD}k}}\Big) + \frac{f^{(DF)}}{2}\Big(1 - \sqrt{\frac{1}{1+\lambda_{SD}}}\Big). \quad (3.20)$$

The CDF $F_{\gamma^{(0.5DF)}}(x)$ of the end-to-end SNR $\gamma^{(0.5DF)}$ can be obtained from the MGF $\Psi_{\gamma^{(0.5DF)}}(s)$ given in (3.16). Hence, the outage probability $P_{out}^{(0.5DF)}(\gamma_{Th})$ can be obtained as:

$$\begin{aligned} P_{out}^{(0.5DF)}(\gamma_{Th}) &= F_{\gamma^{(0.5DF)}}(\gamma_{Th}), \\ &= \sum_{k=3}^{K} e_k^{(DF)}(1 - e^{-\lambda_{RD}k\gamma_{Th}}) + f^{(DF)}(1 - e^{-\lambda_{SD}\gamma_{Th}}) + \\ &\quad (a^{(DF)} + b^{(DF)})(1 - e^{-2\lambda_{RD}\gamma_{Th}}) - 2\lambda_{RD}\, b^{(DF)}\gamma_{Th}(e^{-2\lambda_{RD}\gamma_{Th}}). \end{aligned} \quad (3.21)$$

The diversity order of sharing the two best ordered relays can be investigated using asymptotic analysis of the BEP or the outage probability $P_{out}(\gamma_{Th})$ at high SNR values [86, 175]. Another approach, is to use the asymptotic analysis of the PDF or the MGF of the end-to-end SNR [6, 95, 151]. We follow the latter approach using the MGF of the end-to-end SNR at the output of the MRC. The MGF $\Psi_{\gamma^{(0.5DF)}}(s)$ is given in (3.16). Using the results of [151], the MGF can be approximated as $s \to \infty$ by $b|s|^{-d} + O(|s|^{-d})$ [3], where d is the diversity order, and b is related to the coding gain. Writing $\Psi_{\gamma^{(0.5DF)}}(s)$ as a division of two polynomials $\Psi_{\gamma^{(0.5DF)}}(s) = \frac{B(s)}{A(s)}$, where $B(s)$ and $A(s)$ are the numerator and denominator polynomials respectively. $A(s)$ can be written as $A(s) = (1 + \frac{s}{2\lambda_{RD}})^2(1 + \frac{s}{\lambda_{SD}}) \prod_{k=3}^{K}(1 + \frac{s}{\lambda_{RD}k})$, which can be approximated for $s \to \infty$ as $A(s) \approx (\frac{s}{2\lambda_{RD}})^2(\frac{s}{\lambda_{SD}}) \prod_{k=3}^{K}(\frac{s}{\lambda_{RD}k}) = (2\lambda_{RD}\lambda_{SD}\prod_{k=3}^{K}\lambda_{RD}k)^{-1}s^{(K+1)}$. The numerator polynomial can be found by collecting and combining the corresponding terms, which is clearly of a degree less than the denominator poly-

[3] A function $a(x)$ is written as $O(x)$ if $\lim_{x\to 0}\frac{a(x)}{x} = 0$.

nomial. Taking only the constant term of the numerator polynomial, and divide this term by the approximation of the denominator polynomial results in the term $b|s|^{-(K+1)}$. This means that the diversity order is $K+1$. Other terms which result from the division of the numerator polynomial with the approximation of the denominator polynomial contribute to $O(|s|^{-(K+1)})$.

3.3.2 AF Three-Time Slots Scenario

As illustrated in **Table 3.1**, the received signal $y_{T_{kj}}^{(AF)}$ at the destination node in time slot T_m for AF scheme is as follows:

$$y_{T_{mi}}^{(AF)} = G_{S_iR}^{(j)} \sqrt{\frac{P_S}{2}}\, h_{RD}^{(j)} y_{T_{1i}}^{(R_{bj})} + n_{mi}^{(AF)},\ j = 0,1,\ i = 1,2,\ \&\ m = 2,3, \tag{3.22}$$

where $n_{mi}^{(AF)}$ is an AWGN at the destination node, and $G_{S_iR}^{(j)}$ is the normalizing factor at the relay, which depends on the instantaneous CSI between the ith source and the jth ordered best relay. Assuming that each relay knows its instantaneous channel information $h_{S_iR}^{(j)}$, the normalizing factor using (3.3) is $G_{S_iR}^{(j)} = \frac{1}{\sqrt{P_S|h_{S_iR}^{(j)}|^2+\sigma_0^2}}$. The end-to-end received SNR at the destination node for AF scheme (with instantaneous CSI at the lth relay) with $P_{R_l} = P_S/2$, and using the normalizing factor $G_{S_iR_l} = \frac{1}{\sqrt{P_S|h_{S_iR_l}|^2+\sigma_0^2}}$ is obtained as

$$\gamma_l^{(AF)} = \frac{\frac{\gamma_{S_iR_l}\gamma_{R_lD}}{2}}{1+\gamma_{SiR_l}+\frac{\gamma_{R_lD}}{2}}, \tag{3.23}$$

which can be upper and lower bounded for high SNR as [4, 56]:

$$\frac{1}{2}\ \min(\gamma_{S_iR_l}, \frac{\gamma_{R_lD}}{2}) \le \gamma_l^{(AF)} \le\ \min(\gamma_{S_iR_l}, \frac{\gamma_{R_lD}}{2}). \tag{3.24}$$

The upper bound in (3.24) is shown to be tight, and can be used to simplify the analysis [75]. It is easy to show that the PDF of the upper bound in (3.24) for Raleigh flat fading channels is an exponential random variable,

with parameter $\lambda_{eq} = \lambda_{SR} + 2\lambda_{RD}$. The upper bound of the received end-to-end SNR $\gamma^{(0.5AF)}$ at the destination node after using MRC, and using (3.22), and (3.3) is given as:

$$\gamma^{(0.5AF)} = \gamma_{S_iD} + \gamma_{sum}^{(0.5AF)}, \tag{3.25}$$

where $\gamma_{sum}^{(0.5AF)} = \gamma_{b0}^{(0.5AF)} + \gamma_{b1}^{(0.5AF)}$ with $\gamma_{b0}^{(0.5AF)}$ and $\gamma_{b1}^{(0.5AF)}$ are the upper bound of the end-to-end SNR from the best, and next-best relays respectively. The best relay R_{b0} is selected as the relay with the maximum upper bound of the end-to-end SNR $\gamma_{b0}^{(0.5AF)}$ at the the destination node, i.e. $\gamma_{b0}^{(0.5AF)} = \max_{l}(\min(\gamma_{S_iR_l}, \frac{\gamma_{R_lD}}{2}))$, where $l = 1, \ldots, K$. Similarly, the next-best relay R_{b1} is selected as the relay with the next-maximum upper bound of the end-to-end SNR $\gamma_{b1}^{(0.5AF)}$ at the the destination node, i.e. $\gamma_{b1}^{(0.5AF)} = \max_{l,\, l\neq b0}(\min(\gamma_{S_iR_l}, \frac{\gamma_{R_lD}}{2}))$. The selection of the best, next-best relays R_{b0} and R_{b1}, respectively from the K available relays is done using the ordering of the upper bound of end-to-end SNRs from the K available relays as follows $\gamma_{b0}^{(0.5AF)} > \gamma_{b1}^{(0.5AF)} > \gamma_{b2}^{(0.5AF)} > \ldots > \gamma_{bK-1}^{(0.5AF)}$.

The joint PDF of the upper bound received SNRs from the ordered relays R_{b0} and R_{b1} using (3.9) can be obtained as:

$$f_{\gamma_{b1}^{(0.5AF)},\gamma_{b0}^{(0.5AF)}}(x, y) = K(K-1)[(1 - e^{-\lambda_{eq}x})]^{K-2}\lambda_{eq}^2 e^{-\lambda_{eq}x} e^{-\lambda_{eq}y}\mu(x)\mu(y). \tag{3.26}$$

Using (3.26), and following a similar procedure to that followed in Subsection 3.3.1, the $BEP_{\gamma(0.5AF)}$ can be derived as:

$$\begin{aligned} BEP_{\gamma(0.5AF)} =& \frac{a^{(AF)}}{2}\Big(1 - \sqrt{\frac{1}{1+\lambda_{eq}}}\Big) + b^{(AF)}F^2\Big(\frac{1}{\lambda_{eq}}\Big) + \sum_{k=3}^{K}\frac{e_k^{(AF)}}{2}\Big(1 - \sqrt{\frac{1}{1+\frac{\lambda_{eq}k}{2}}}\Big) + \\ & \frac{f^{(AF)}}{2}\Big(1 - \sqrt{\frac{1}{1+\lambda_{SD}}}\Big), \end{aligned} \tag{3.27}$$

where $A^{(AF)}$, $B^{(AF)}$, and $E_k^{(AF)}$ are defined in column 2 of **Table 3.3**, and $a^{(AF)}$, $b^{(AF)}$, $e_k^{(AF)}$ and $f^{(AF)}$ are defined in column 4 of **Table 3.3**. The outage probability $P_{out}^{(0.5AF)}(\gamma_{Th})$ of sharing the two ordered best relays for AF scheme can

Table 3.3 Coefficients of The PDF, The MGF, The BEP, and the $P_{out}(\gamma_{Th})$ for AF Sharing Scheme.

Coeff.	Value	Coeff.	Value
$A^{(AF)}$	$\sum_{k=3}^{K} c_k \lambda_{eq} \frac{1}{k-2}$	$a^{(AF)}$	$\frac{1}{\lambda_{eq}}\left(\frac{A^{(AF)}\lambda_{SD}}{-\lambda_{eq}+\lambda_{SD}} - \frac{B^{(AF)}\lambda_{SD}}{(-\lambda_{eq}+\lambda_{SD})^2}\right)$
$B^{(AF)}$	$\frac{c_2 \lambda_{eq}^2}{2}$	$b^{(AF)}$	$\frac{1}{\lambda_{eq}^2}\left(\frac{B^{(AF)}\lambda_{SD}}{-\lambda_{eq}+\lambda_{SD}}\right)$
$E_k^{(AF)}$	$-\frac{c_k \lambda_{eq}}{k-2}$	$e_k^{(AF)}$	$\frac{2}{\lambda_{eq}k}\left(\frac{E_k^{(AF)}\lambda_{SD}}{-\frac{\lambda_{eq}k}{2}+\lambda_{SD}}\right)$
		$f^{(AF)}$	$\frac{A^{(AF)}}{\lambda_{eq}-\lambda_{SD}} + \frac{B^{(AF)}}{(\lambda_{eq}-\lambda_{SD})^2} + \sum_{k=3}^{K} \frac{E_k^{(AF)}}{(\frac{\lambda_{eq}k}{2}-\lambda_{SD})}$

be computed as:

$$P_{out}^{(0.5AF)}(\gamma_{Th}) = F_{\gamma^{(0.5AF)}}(\gamma_{Th}) = \sum_{k=3}^{K} e_k^{(AF)}(1 - e^{-\frac{\lambda_{eq}k}{2}\gamma_{Th}}) + f^{(AF)}(1 - e^{-\lambda_{SD}\gamma_{Th}}) + (a^{(AF)} + b^{(AF)})(1 - e^{-\lambda_{eq}\gamma_{Th}}) - \lambda_{eq}\, b^{(AF)}\gamma_{Th}(e^{-\lambda_{eq}\gamma_{Th}}). \tag{3.28}$$

The diversity order of sharing the two ordered best relays for AF scheme is also $K + 1$, which can be found from the similarity between $BEP_{\gamma^{(0.5AF)}}$ expression in (3.27) and the $BEP_{\gamma^{(0.5DF)}}$ expression in (3.20).

It is worth noting that, for AF sharing scenario, the ordering of the best, and the next-best relays depends on the relay's transmitted power with the assumption that the relays transmit with the same power level. Therefore, the best and next-best relays in this scenario are different from the best and next-best relays without sharing. In the sharing scenario, the best relay is selected as $\max_{l}(\min(\gamma_{S_iR_l}, \frac{\gamma_{R_lD}}{2}))$ but the best relay without sharing is selected as: $\max_{l}(\min(\gamma_{S_iR_l}, \gamma_{R_lD}))$. It is clear that the factor $\frac{1}{2}$ affects the ordering of the relays. The same result holds for the next-best relay. In general the ordered best relays for sharing and without sharing AF are different (even the relays transmit with equal power). Whereas for DF scenario, the relays are ordered depending on the received SNR at the destination as given by

Table 3.4 Best Relay Selection Criterion for AF Scheme.

The Case	The Best Relay With Sharing	The Best Relay Without Sharing	Comments
$\gamma_{S_iR_l} < \frac{\gamma_{R_lD}}{2} < \gamma_{R_lD}$	$\max_l(\gamma_{S_iR_l})$	$\max_l(\gamma_{S_iR_l})$	**Same**
$\frac{\gamma_{R_lD}}{2} < \gamma_{S_iR_l} < \gamma_{R_lD}$	$\max_l(\frac{\gamma_{R_lD}}{2})$	$\max_l(\gamma_{S_iR_l})$	**Different**
$\frac{\gamma_{R_lD}}{2} < \gamma_{R_lD} < \gamma_{S_iR_l}$	$\max_l(\frac{\gamma_{R_lD}}{2})$	$\max_l(\gamma_{R_lD})$	**Different**

$\max_l(\gamma_0|h_{RD}^{(l)}|^2)$ if the relays transmit with full power, and as $\max_l(\frac{1}{2}\gamma_0|h_{RD}^{(l)}|^2)$ if the relays transmit with half power. The factor $\frac{1}{2}$ in the last expression does not affect the ordering of the relays, and it can be removed from the expression without affecting the ordering for DF. The different cases for AF ordering are illustrated in **Table 3.4**. Rows 2 and 3 illustrate that the sharing scenario may use different relays from the best and next-best relays which were ordered based on full power transmission. Simulation results show that AF sharing scenario based on half power allocation achieves full diversity order and outperforms the BEP performance of the best relay (alone) scenario. The ordering based on relay half power allocation is used for two reasons: First, the BEP performance of the sharing based on half power ordering outperforms the sharing based on full power ordering. Second, using the half power ordering simplifies deriving the PDF expression (3.26).

3.4 Two-Time Slots Scenario

So far, the transmission schemes discussed do not utilize the resources efficiently. The sources and the relays needed to wait for three-time slots to start a new retransmission. In this section, we will discuss more efficient transmission schemes where only two time slots are required. Three types of such transmission schemes will be examined. These schemes are DF with

Table 3.5 Distributed STBC-DF Scenario.

Terminal	T_{11}	T_{12}	T_{21}	T_{22}
S_1	T_{x_1}	-	-	-
S_2	-	T_{x_2}	-	-
R_{b0}	R_{x_1}	R_{x_2}	$T_{\tilde{x}_1}$	$T_{-\tilde{x}_2^*}$
R_{b1}	R_{x_1}	R_{x_2}	$T_{\tilde{x}_2}$	$T_{\tilde{x}_1^*}$
D	R_{x_1}	R_{x_2}	$R^{(DS)}_{T_{21}}$	$R^{(DS)}_{T_{23}}$

distributed STBC at the relays, DF with distributed BF at the relays, and AF with distributed BF at the relays.

3.4.1 Distributed STBC for DF Scheme

In this scenario, the selected relays are shared between the two sources equally. The two sources are assumed to have the same best and next-best relays. As illustrated in **Table 3.5**, only two-time slots are used for cooperation. Alamouti STBC [2] is used between the relays and the destination node [7]. The noiseless received signals generated using distributed STBC in time sub-slots T_{21} and T_{22} are denoted as $R^{(DS)}_{T_{21}}$ and $R^{(DS)}_{T_{22}}$, respectively. The received signals $y^{(DS)}_{21}$ and $y^{(DS)}_{22}$ at the destination node in sub-slots T_{21} and T_{22} respectively, are given as:

$$y^{(DS)}_{21} = \sqrt{\frac{P_S}{2}} h^{(0)}_{RD} \tilde{x}_{01} + \sqrt{\frac{P_S}{2}} h^{(1)}_{RD} \tilde{x}_{12} + n^{(DS)}_{21}, \tag{3.29a}$$

$$y^{(DS)}_{22} = -\sqrt{\frac{P_S}{2}} h^{(0)}_{RD} \tilde{x}^*_{02} + \sqrt{\frac{P_S}{2}} h^{(1)}_{RD} \tilde{x}^*_{11} + n^{(DS)}_{22}, \tag{3.29b}$$

where $\tilde{x}_{ji}$ is the decoded symbol of the transmitted symbol x_i at the best relay R_{bj}. The superscript $(^*)$ stands for complex conjugate. $n^{(DS)}_{2i}$ is the additive noise at the destination in time sub-slot T_{2i} for $i = 1, 2$. The estimated symbols $\hat{x}_1$ and $\hat{x}_2$ at the destination node in time sub-slots T_{21} and T_{22} can be found with the assumption that the transmitted symbols are correctly

Table 3.6 Distributed BF Scenarios.

Terminal	T_{11}	T_{12}	T_{21}	T_{22}
S_1	T_{x_1}	-	-	-
S_2	-	T_{x_2}	-	-
R_{b0}	R_{x_1}	R_{x_2}	$T_{\tilde{x}_1}$ / T_{x_1}	$T_{\tilde{x}_2}$ / T_{x_2}
R_{b1}	R_{x_1}	R_{x_2}	$T_{\tilde{x}_1}$ /T_{x_1}	$T_{\tilde{x}_2}$ / T_{x_2}
D	R_{x_1}	R_{x_2}	$R_{T_{21}}^{(BD)}$ / $R_{T_{21}}^{(BA)}$	$R_{T_{22}}^{(BD)}$ / $R_{T_{22}}^{(BA)}$

decoded at the relays (i.e. $\tilde{x}_{0i} = \tilde{x}_{1i} = x_i$) as [2]:

$$\hat{x}_1 = h_{RD}^{*(0)} y_{21}^{(DS)} + h_{RD}^{(1)} y_{22}^{*(DS)}, \tag{3.30a}$$

$$\hat{x}_2 = h_{RD}^{*(1)} y_{21}^{(DS)} - h_{RD}^{(0)} y_{22}^{*(DS)}. \tag{3.30b}$$

The end-to-end SNR at the destination node after using MRC is computed as $\gamma^{(DS)} = \gamma_{S_iD} + \gamma_{sum}^{(DS)}$, with $\gamma_{sum}^{(DS)} = (\gamma_{b0}^{(DS)} + \gamma_{b1}^{(DS)})$, which is similar to the SNR expression obtained in (3.5). Hence, the same analysis can be carried out, which results in the same BEP performance as (3.20). The goal of this analysis is not to investigate the distributed STBC, but to examine the BEP performance of sharing the two ordered best relays. A detailed analysis of distributed STBC for multi-relay systems using pairwise error probability can be found in [78].

The two best order relays STBC-AF requires greater investigation for the selection criterion, and the amplification gain at the relays, using the instantaneous CSI. This however, is a topic for further research.

3.4.2 Distributed BF for DF Scheme

In this scenario, two-time slots are used as in the previous scenario, except that the best and the next-best relays transmit the same information at the same time. As illustrated in **Table 3.6**. The noiseless received signals using

DF distributed BF in time sub-slots T_{21}, and T_{22} are denoted as $R_{T_{21}}^{(BD)}$ and $R_{T_{22}}^{(BD)}$, respectively. For DF scheme, it is referred to as BF-DF (BD). The received signals at the destination node in the second-time slot for BD are:

$$y_{2i}^{(BD)} = \sqrt{\frac{P_S}{2}}\left(|h_{RD}^{(0)}|\tilde{x}_{i0} + |h_{RD}^{(1)}|\tilde{x}_{i1}\right) + n_{2i}^{(BD)}\ i = 1, 2, \tag{3.31}$$

where $\tilde{x}_{i0}$ and $\tilde{x}_{i1}$ are the decoded symbols of the ith user at the relays R_{b0} and R_{b1} respectively, and $n_{2i}^{(BD)}$ is the AWGN received at the destination node. From (3.31) and using MRC with the assumption that the signal is decoded correctly at both relays R_{b0} and R_{b1} ($\tilde{x}_{i0} = \tilde{x}_{i1}$), the SNR $\gamma^{(BD)}$ at the destination node is computed as:

$$\gamma^{(BD)} = \gamma_{S_iD} + 0.5\left(\sqrt{|\gamma_{b0}^{(DB)}|} + \sqrt{|\gamma_{b1}^{(DB)}|}\right)^2. \tag{3.32}$$

It is rather complicated to obtain the PDF and/or the MGF of $\gamma^{(BD)}$ in (3.32) at the destination node analytically. In this respect, we obtain the PDF and MGF of the bounded SNR as follows. Defining $\gamma_B = 0.5\left(\sqrt{\gamma_{b0}^{(BD)}} + \sqrt{\gamma_{b1}^{(BD)}}\right)^2$, then γ_B can be lower and upper bounded as:

$$\frac{1}{2}(\gamma_{b0}^{(BD)} + 3\gamma_{b1}^{(BD)}) \leq \gamma_B \leq \frac{1}{2}(3\gamma_{b0}^{(BD)} + \gamma_{b1}^{(BD)}). \tag{3.33}$$

Now, defining $Z_1 = \frac{1}{2}(\gamma_{b0}^{(BD)} + 3\gamma_{b1}^{(BD)})$ and $Z_2 = \frac{1}{2}(3\gamma_{b0}^{(BD)} + \gamma_{b1}^{(BD)})$, the PDF of Z_1, and the PDF of Z_2 can be easily computed using the joint PDF of $f_{\gamma_{b1}^{(BD)},\gamma_{b0}^{(BD)}}(x, y)$ given in (3.12). The MGF of the lower and upper bounds follow easily. Based on the MGF $\Psi_{\gamma_{S_iD}}(s)\Psi_{Z_1}(s)$ and the MGF $\Psi_{\gamma_{S_iD}}(s)\Psi_{Z_2}(s)$ (note that the random variables γ_{S_iD} and Z_1, and γ_{S_iD} and Z_2 are independent), the upper and lower bounds of the $BEP^{(BD)}$ can be computed using (3.18). Applying partial fraction expansion, the $BEP^{(BD)}$ is upper bounded

Table 3.7 Coefficients of the PDF, the MGF and the BEP for the Upper and the Lower Bounds of BD.

Coeff.	$S = U$	$S = L$
$A^{(S)}$	$\frac{\lambda_{RD}}{3}\sum_{k=2}^{K} c_k(1-\beta)^{k-1}\Big(\frac{1-\beta}{k-\frac{4}{3}}+\beta\Big)$	$c_4(1-\beta)^3\beta\lambda_{RD}+$ $\lambda_{RD}\sum_{\substack{k=2\\k\neq 4}}^{K} c_k(1-\beta)^{k-1}\Big(\frac{1-\beta}{k-4}+\beta\Big)$
$B^{(S)}$	-	$\frac{c_4(1-\beta)^4\lambda_{RD}^2}{4}$
$E_k^{(S)}$	$\frac{c_k(1-\beta)^k\lambda_{RD}}{4}\Big(1-\frac{k}{k-\frac{4}{3}}\Big)$	$\frac{c_k(1-\beta)^k\lambda_{RD}}{4}\Big(1-\frac{k}{k-\frac{4}{3}}\Big),\ k\neq 4$
$a^{(S)}$	$\frac{3}{2\lambda_{RD}}\Big(\frac{2A^{(S)}\lambda_{SD}}{\frac{-2\lambda_{RD}}{3}+\lambda_{SD}}\Big)$	$\frac{1}{2\lambda_{RD}}\Big(\frac{2A^{(S)}\lambda_{SD}}{-2\lambda_{RD}+\lambda_{SD}}-\frac{4B^{(S)}\lambda_{SD}}{(-2\lambda_{RD}+\lambda_{SD})^2}\Big)$
$b^{(S)}$	-	$\frac{1}{4\lambda_{RD}^2}\Big(\frac{4B^{(S)}\lambda_{SD}}{-2\lambda_{RD}+\lambda_{SD}}\Big)$
$e_k^{(S)}$	$\frac{2}{\lambda_{RD}k}\Big(\frac{2E_k^{(S)}\lambda_{SD}}{-\frac{\lambda_{RD}k}{2}+\lambda_{SD}}\Big)$	$\frac{2}{\lambda_{RD}k}\Big(\frac{2E_k^{(S)}\lambda_{SD}}{\frac{-\lambda_{RD}k}{2}+\lambda_{SD}}\Big)$
$f^{(S)}$	$\frac{2A^{(S)}}{\frac{2\lambda_{RD}}{3}-\lambda_{SD}}+\sum_{k=2}^{K}\frac{2E_k^{(S)}}{(\frac{\lambda_{RD}k}{2}-\lambda_{SD})}+$ $D^{(DF)}$	$\frac{2A^{(S)}}{2\lambda_{RD}-\lambda_{SD}}+\frac{4B^{(S)}}{(2\lambda_{RD}-\lambda_{SD})^2}+$ $\underbrace{\sum_{k=2}^{K}}_{k\neq 4}\frac{2E_k^{(S)}}{\frac{\lambda_{RD}k}{2}-\lambda_{SD}}+D^{(DF)}$

as:

$$BEP^{(BD)} \leq \frac{a^{(U)}}{2}\Big(1-\sqrt{\frac{1}{1+\frac{2\lambda_{RD}}{3}}}\Big)+\frac{f^{(U)}}{2}\Big(1-\sqrt{\frac{1}{1+\lambda_{SD}}}\Big)+\sum_{k=2}^{K}\frac{e_k^{(U)}}{2}\Big(1-\sqrt{\frac{1}{1+\frac{\lambda_{RD}k}{2}}}\Big), \tag{3.34}$$

where $A^{(U)}$, $E_k^{(U)}$, $a^{(U)}$, $f^{(U)}$ and $e_k^{(U)}$ are as defined in **Table 3.7**. Similarly, the $BEP^{(BD)}$ is lower bounded as:

$$\begin{aligned} BEP^{(BD)} \geq & \frac{a^{(L)}}{2}\Big(1-\sqrt{\frac{1}{1+2\lambda_{RD}}}\Big)+b^{(L)}F^2\Big(\frac{1}{2\lambda_{RD}}\Big)+ \\ & \frac{f^{(L)}}{2}\Big(1-\sqrt{\frac{1}{1+\lambda_{SD}}}\Big)+\sum_{\substack{k=2\\k\neq 4}}^{K}\frac{e_k^{(L)}}{2}\Big(1-\sqrt{\frac{1}{1+\frac{\lambda_{RD}k}{2}}}\Big), \end{aligned} \tag{3.35}$$

where $A^{(L)}$, $B^{(L)}$, $E_k^{(L)}$, $a^{(L)}$, $f^{(L)}$, and $e_k^{(L)}$ are as defined in **Table 3.7**. A tighter upper bound for the end-to-end SNR $\gamma^{(BD)}$ can be obtained by comparison

with the optimal power allocation under total relay power constraint as [87]:

$$\gamma^{(BD)} \leq \gamma_{Op}^{(BD)} = \gamma_{S_jD} + \gamma_{b_0}^{(BD)} + \gamma_{b_1}^{(BD)}, \tag{3.36}$$

where $\gamma_{Op}^{(BD)}$ is defined as the maximum received SNR using optimum power assignment for distributed BF scenario, using the best and the next-best relays under the constraint $P_R^{(0)} + P_R^{(1)} = P_S$. This upper bound can also be used to compute the $BEP_{Op}^{(BD)}$ using (3.20) by replacing $2\lambda_{RD}$ with λ_{RD} in all terms. Hence, the $BEP^{(BD)}$ can be lower bounded by $BEP_{Op}^{(BD)}$, i.e. $BEP_{Op}^{(BD)} \leq BEP^{(BD)}$. However, in this research we are only concerned with equal power sharing to simplify the analysis.

3.4.3 Distributed BF for AF Scheme

In this scenario, two-time slots are used as in the previous scenario, as illustrated in **Table 3.6**. The noiseless received signals using AF distributed BF in time sub-slots T_{21}, and T_{22} are denoted as $R_{T_{21}}^{(BA)}$, and $R_{T_{22}}^{(BA)}$, respectively. For the distributed BF-AF scheme, it is referred to as (BA). The received signal at the destination node for BA in the second-time slot is as [87]:

$$y_{2i}^{(BA)} = \sqrt{P_S}\sqrt{\frac{P_S}{2}}x_i\frac{|h_{RD}^{(0)}||h_{S_iR}^{(0)}|}{\sqrt{\sigma_0^2 + P_S|h_{S_iR}^{(0)}|^2}} + \sqrt{P_S}\sqrt{\frac{P_S}{2}}x_i\frac{|h_{RD}^{(1)}||h_{S_iR}^{(1)}|}{\sqrt{\sigma_0^2 + P_S|h_{S_iR}^{(1)}|^2}} + \sqrt{\frac{P_S}{2}}\frac{|h_{RD}^{(0)}|n_{0i}}{\sqrt{\sigma_0^2 + P_S|h_{S_iR}^{(0)}|^2}} + \sqrt{\frac{P_S}{2}}\frac{|h_{RD}^{(1)}|n_{1i}}{\sqrt{\sigma_0^2 + P_S|h_{S_iR}^{(1)}|^2}} + n_{2i}^{(BA)},\ i = 1, 2, \tag{3.37}$$

where n_{0i}, n_{1i} and $n_{2i}^{(BA)}$ are AWGNs at the best, next-best relays in time slot T_1 and the destination node at time slot T_2, respectively.

The SNR $\gamma^{(BA)}$ at the destination node using MRC and using the best and

next-best relays can be computed as:

$$\gamma^{(BA)} = \gamma_{S_iD} + \frac{\Big(\sum_{j=0}^{1} \sqrt{\frac{|\gamma_{RD}^{(j)}||\gamma_{S_iR}^{(j)}|}{1+|\gamma_{S_iR}^{(j)}|}}\Big)^2}{2\Big(1+\sum_{j=0}^{1}\frac{|\gamma_{RD}^{(j)}|}{2(1+|\gamma_{S_iR}^{(j)}|)}\Big)}, \tag{3.38}$$

where $\gamma_{S_iR}^{(j)} = \gamma_0|h_{S_iR}^{(j)}|^2$, and $\gamma_{RD}^{(j)} = \gamma_0|h_{RD}^{(j)}|^2$. It is also difficult here to compute analytical expressions for the PDF and the MGF of $\gamma^{(BA)}$ at the destination node. Therefore, the upper bound for the SNR $\gamma^{(BA)}$ is given as [87]:

$$\begin{aligned}\gamma^{(BA)} \leq \gamma_{Op}^{(BA)} &= \gamma_{S_iD} + \frac{\gamma_{S_iR}^{(0)}\gamma_{RD}^{(0)}}{1+\gamma_{S_iR}^{(0)}+\gamma_{RD}^{(0)}} + \frac{\gamma_{S_iR}^{(1)}\gamma_{RD}^{(1)}}{1+\gamma_{S_iR}^{(1)}+\gamma_{RD}^{(1)}},\\ &\leq \gamma_{S_iD} + \gamma_{b_0}^{(BA)} + \gamma_{b_1}^{(BA)},\end{aligned} \tag{3.39}$$

where $\gamma_{Op}^{(BA)}$ is defined as the maximum received SNR using optimum power assignment for the best, and the next-best ordered relays under the constraint $P_R^{(0)} + P_R^{(1)} = P_S$, $\gamma_{b_0}^{(BA)} = \max_{l}(\min(\gamma_{S_iR_l}, \gamma_{R_lD}))$ and, $\gamma_{b_1}^{(BA)}$ is given as $\gamma_{b_1}^{(BA)} = \max_{l,\, l\neq b_0}(\min(\gamma_{S_iR_l}, \gamma_{R_lD}))$. Hence, the lower bound of the $BEP^{(BA)}$ can be found using (3.27) by replacing $\lambda_{eq} = 2\lambda_{SR} + \lambda_{RD}$ with $\lambda_{eq} = \lambda_{SR} + \lambda_{RD}$.

It is worth noting that the weights for BF-AF and BF-DF are chosen as $w_1 = 1$ and $w_2 = 1$ for the following reasons. First, the weights w_1 and w_2 can be considered as power adjustment factors, and in this study optimal power adjustment is not considered, only equal power assignment is investigated in all scenarios. Second, the weights are not similar to the weights given by [79, 87] which were derived for one user scenario. The weights for this problem need to be selected to maximize the minimum received SNR of the two users under individual relay power constraint and user sum power constraint. Finally, if power adjustment is to be used, there is no benefit from relay ordering. Relay ordering in this paper is based on relays' equal power transmission.

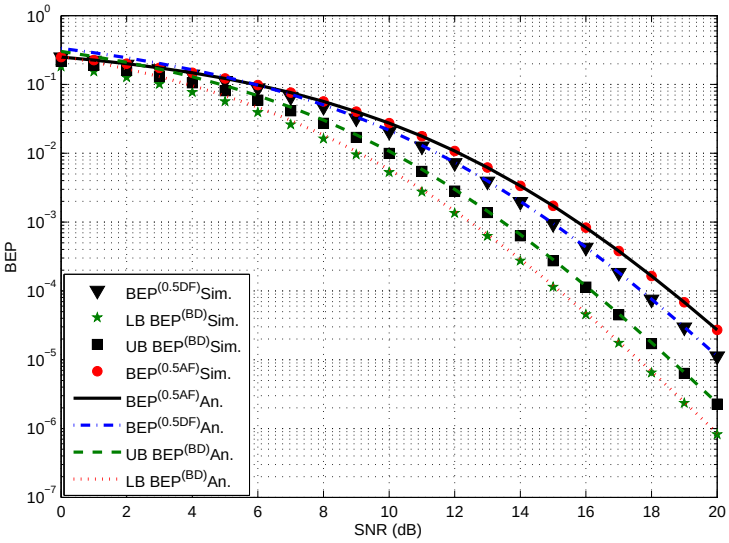

Figure 3.2 Comparison of the BEP Performance Using Derived Formulas and Simulations for the Sharing of the Best Ordered Relays R_{b0}, R_{b1}.

3.5 Numerical Results and Discussion

In this section, we provide the results of the BEP and the outage probability performance measures for sharing the two ordered best relays, and compare them with the performance of the best ordered and next-best ordered relays using Monte Carlo simulations for $K = 4$.

In all the simulations and the analytical expressions $\lambda_{SD} = 10$, $\lambda_{RD} = 7.5$ and $\lambda_{SR} = 6.0$ are used to simulate a better average source-relay and relay-destination channel links than a source-destination link except in **Figure 3.6** where three different conditions are considered, as explained later.

In **Figure 3.2**, the analytical BEP performance is compared to the simulated BEP performance for both DF and AF schemes in both two-time slots and three-time slots scenarios. As can be seen clearly from this figure, the BEP curves using simulations exactly coincide with those obtained analytically for orthogonal DF (3.20), the upper bound of the distributed BF-DF (3.34), the lower bound of BF-DF (3.35), and the lower bound of AF (3.27). An SNR gain of 0.85dB for the case of DF cooperation scheme is observed, compared to AF cooperation scheme computed at BEP= 10^{-4}.

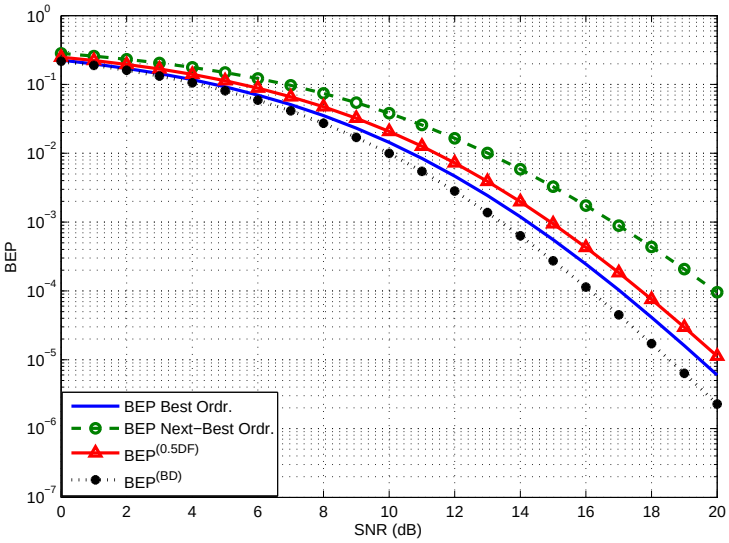

Figure 3.3 The BEP Performance For The sharing DF Scenario Using Simulation.

In **Figure 3.3** simulation results of the BEP performance for sharing the two ordered best relays in a DF cooperation scheme are shown, and compared with the BEP performance of the best and the next-best ordered relays. As shown in this figure, sharing the two best ordered relays outperforms the next-best relay by 2.27dB at BEP= 10^{-4}. The best ordered relay BEP performance outperforms the sharing BEP performance by 0.71dB at BEP= 10^{-4}. We also compare the BEP performance of the three time slots DF with the BEP performance of the two-time slots BF-DF scenario. An SNR gain of 0.82dB for BF-DF is observed compared to DF best relay at BEP= 10^{-4}.

For distributed BF-DF cooperation schemes, the exact BEP performance is obtained and compared with the BEP performance upper bound, BEP performance lower bound and BEP performance with optimal power allocation strategy. The simulation results are shown in **Figure 3.4**. As can be seen clearly from this figure, the upper and lower bounds are very close. The SNR gain of the BEP performance with optimal power strategy is very marginal. The SNR gain of the optimal power strategy is 0.16dB compared to equally sharing the best and next best ordered relays at BEP= 10^{-4}.

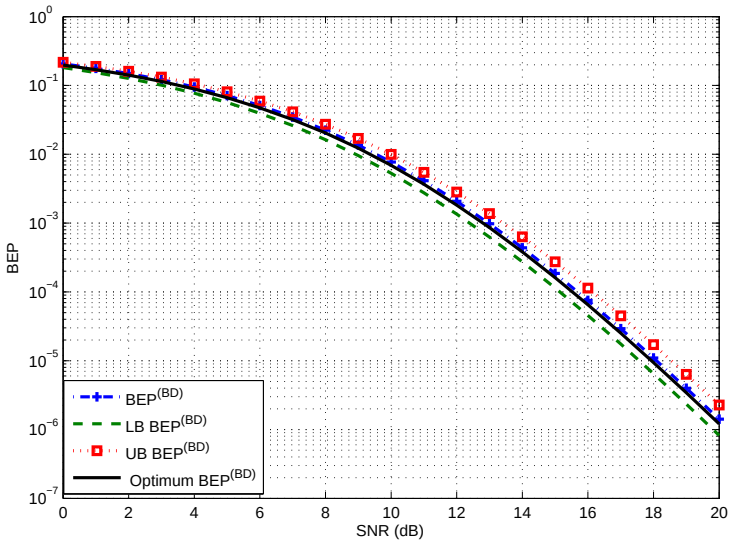

Figure 3.4 The BEP Performance for DF Distributed BF scenario with Lower & Upper Bounds.

In **Figure 3.5**, the BEP performance of sharing the two ordered best relays in AF scheme is obtained and compared to the BEP performance of the best and next-best ordered relays. The BEP performance of the sharing scenario outperforms the best relay by 0.18dB at BEP= 10^{-4}. In addition, we simulate the BEP performance of BA, which approaches that of the best ordered relay at high SNR. The BEP performance of BF-AF using optimal power allocation under total power constraint is also shown. The SNR gain of the BEP performance with optimal power allocation is 0.7dB compared to sharing the best and next best ordered relays at BEP= 10^{-4}.

Figure 3.6 shows results of the analytical BEP performance for three channel conditions for DF with sharing the best and next-best ordered relays. In setup 1, $\lambda_{SD} = 10.14$, $\lambda_{RD} = 7.58$ and $\lambda_{SR} = 6.01$. In setup 2, $\lambda_{SD} = 7.58$, $\lambda_{RD} = 10.14$ and $\lambda_{SR} = 6.01$, and finally, in setup 3, $\lambda_{SD} = 7.58$, $\lambda_{RD} = 5.40$ and $\lambda_{SR} = 6.01$. The BEP performance of the channel in setup 3 outperforms the BEP performance of the other setups. An SNR gain of 1.30dB and 1.93dB is observed compared to setup 2 and setup 1 respectively, computed at BEP= 10^{-4}. It is well observed that, a better BEP performance is achieved when the source-relay and the relay-destination links are in better

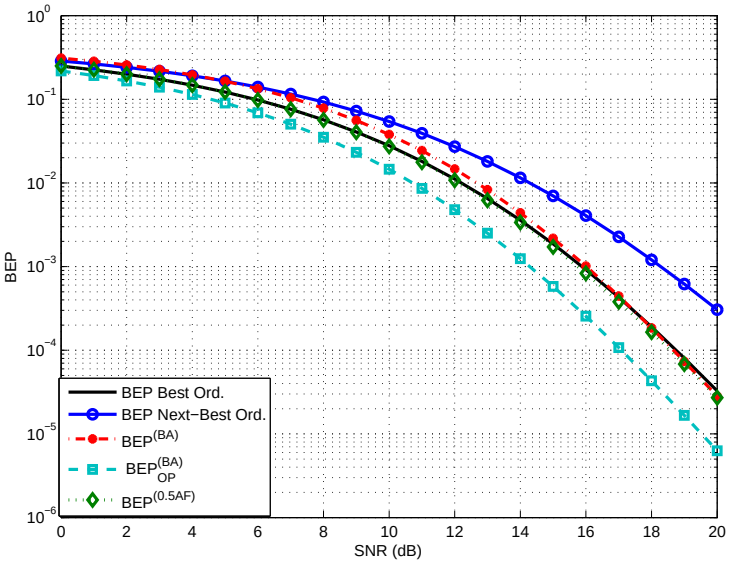

Figure 3.5 The BEP Performance for AF Sharing Scenario Using Simulation.

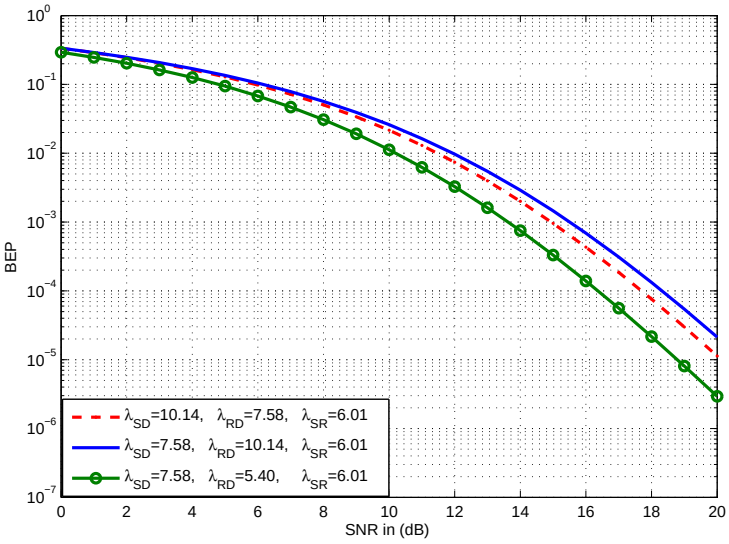

Figure 3.6 The BEP Performance for the sharing DF scenario for Different Channels' Conditions Using Analytical Formula.

channel conditions than source-destination links.

In **Figure 3.7**, the BEP performance is shown at high SNR range from 25dB to 30dB for sharing the best and next-best relays, the best relay alone, and the next-best relay alone for both AF and DF schemes. In all schemes, analytically a diversity order 5 is expected, except for the next-best relay where a diversity order 4 is expected. The diversity order is calculated using simulation results as shown in **Table 3.8**. As shown in this table, the

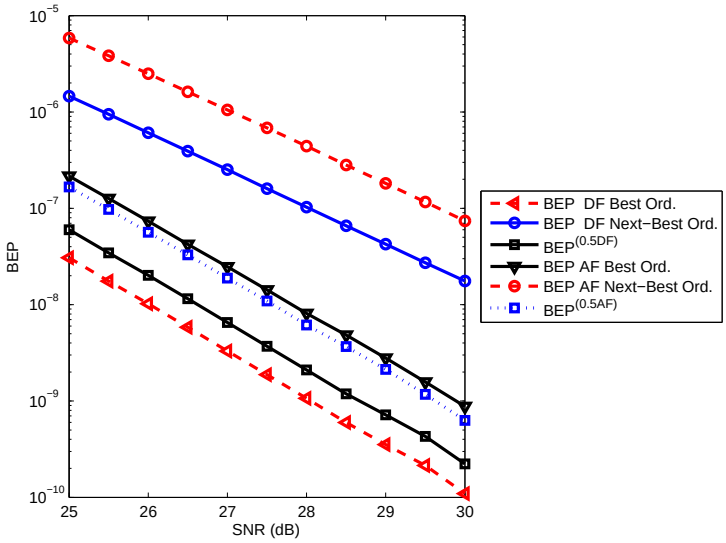

Figure 3.7 The BEP Performance for Diversity Calculations for the Orthogonal Sharing AF and DF Schemes Using Simulations.

Table 3.8 Diversity Calculations.

Scheme	BEP_1	BEP_2	Diversity Order
Best AF	2.4777×10^{-8}	8.7832×10^{-10}	4.8181
Next-Best AF	1.0507×10^{-6}	7.4121×10^{-8}	3.8253
Sharing AF	1.8862×10^{-8}	6.2973×10^{-10}	***4.9046***
Best DF	3.3840×10^{-9}	1.0909×10^{-10}	4.9551
Next-Best DF	2.5017×10^{-7}	1.6573×10^{-8}	3.9160
Sharing DF	6.6892×10^{-9}	2.0673×10^{-10}	***5.0160***

diversity order of sharing the two ordered best relays for both DF and AF schemes is the same as the diversity order of the best relay. The slope of the BEP performance of sharing the best and next best relays is approximately the same as the slope of the BEP performance of the best relay. Two SNR values are considered for comparison purpose (SNR_1 = 27dB and SNR_2 = 30dB). The diversity order is computed in the last column of **Table 3.8**.

In **Figure 3.8** the outage probability performance for R = 1bps/Hz is shown for sharing the best and next-best relays, distributed beamforming,

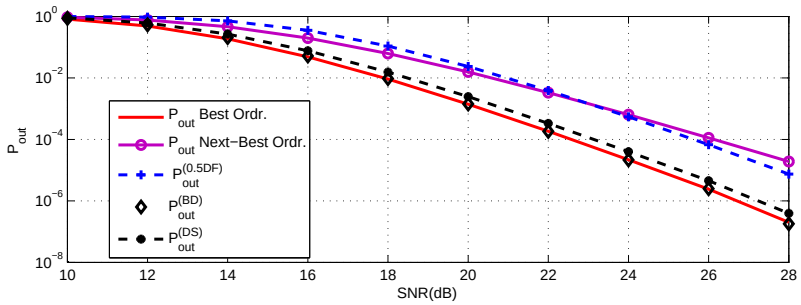

(a) DF Outage Probability

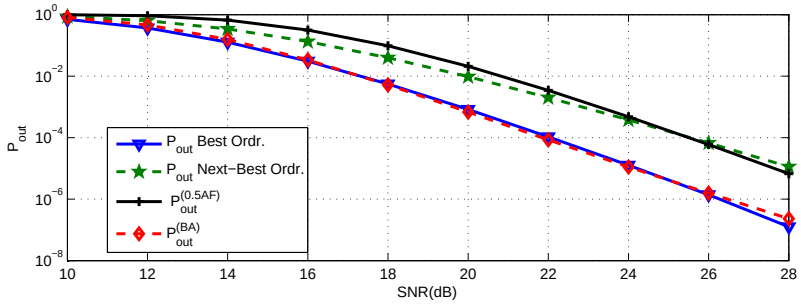

(b) AF Outage Probability

Figure 3.8 The Outage Probability Performance for AF/DF Scenarios

the best relay alone, and the next-best relay alone for both DF and AF schemes. In addition, the outage probability performance for distributed STBC for DF scheme is shown. It is clear from the these curves that the sharing scenarios achieve full diversity order as expected and as proved by the BEP performance. Furthermore, distributed beamforming and distributed STBC scenarios utilize the resources efficiently.

3.6 Conclusions

In this chapter, relay selection for cooperative communication systems is investigated. Assuming two users scenario, and the availability of K relays, BEP is computed for the case of sharing the two ordered best relays for AF and DF relaying schemes. Analytical expressions for the BEP and the outage probability are derived for the different scenarios. Simulation results validate the analytical expressions of the BEP and outage probability performance measures. The BEP performance of the proposed schemes are also

compared with the BEP performances of the best and the next-best relays. In DF scheme, the BEP performance of the best relay outperforms the BEP performance of the sharing. But, the BEP performance of BF-DF scenario outperforms the BEP performance of the best ordered relay. As a result, the BEP performance of equally sharing the two best ordered relays for AF outperforms the BEP performance of the best ordered relay. Efficient channel utilization can be achieved by using STBC and BF schemes.

CHAPTER4

JOINT RESOURCE ALLOCATION FOR AF RELAY NETWORKS

Conventional resource allocation strategies based on equal or optimal allocation of the relay power between users with full bandwidth relaying may not be efficient. In this sense, this chapter, considers joint power and bandwidth allocation for an uplink multi-user improved AF cooperative communication scheme. This improved AF cooperative scheme is proposed to utilize the spectrum efficiently. In this system, each user can adapt to a mixed strategy transmission where FDM is used; part of the data is transmitted using the relay with diversity, and the other part is transmitted using the direct link without diversity. This mixed strategy targets improving the user rate compared to full bandwidth relaying. Joint power and bandwidth allocation is proposed for the improved AF cooperative communication scheme aiming to maximize the sum rate of all users under relay node power constraint. The formulated optimization problem is non-convex and difficult to solve. In order to find the optimal power and bandwidth profiles, we propose a recursive algorithm that solves iteratively either power allocation for a given bandwidth profile or bandwidth allocation for a given power profile. The attained solution using the proposed algorithm is compared to the solution obtained using PSO. The resource allocation problem is solved using PSO, because of its simplicity in tuning its parameters and the high

possibility of obtaining a global solution. The two solutions coincide with negligible difference as shown by numerical simulations. Moreover, joint power and bandwidth allocation with relay selection for the improved AF scheme aiming to maximize the sum rate is addressed using the PSO algorithm because of the MINLP nature of the problem.

The introduction and related research are presented in Section 4.1. Section 4.2, presents the formulation of the optimization problem and the proposed algorithm for power and bandwidth allocation. In Section 4.3, AF resource allocation problem is extended to frequency selective fading channels. In Section 4.4, relay selection and joint power and bandwidth are addressed using the PSO algorithm. Numerical results are presented and discussed in Section 4.5. Finally, conclusions are drawn in Section 4.6.

4.1 Introduction

Efficient management of relay resources becomes a critical issue for increasing transmission rate for multiple users scenarios. In [108], the authors developed power allocation schemes for AF multi-user system, using different objectives such as maximizing the minimum rate, maximizing the sum rate, and minimizing the total power consumption with a constrained minimum transmission rate. In [176], the authors studied relay assignment and power allocation for AF relay system aiming to maximize the sum-rate of all users subject to individual and total power constraints at the relays.

Joint power and bandwidth allocation for transmission nodes are equally important. For multi-user DF relay networks, joint power and bandwidth allocation was addressed in [46, 124]. In [46], the optimization problem was transformed into an equivalent convex optimization problem. Whereas in [124], the optimization problem was transformed into an equivalent no-relaying broadcast channel optimization problem, where each user was substituted by two virtual users having different channel quantities and mul-

tiplexing weights. AF joint power and bandwidth allocation problem for multi source-destination pairs is more difficult compared to DF, since the transmission rate is not a jointly concave function in the power and bandwidth profiles. Therefore, convex optimization techniques cannot be used to solve this problem. In [99], joint power and bandwidth allocation for two users cooperative relaying is addressed aiming to maximize the achievable rate region using AF and DF cooperative schemes. In [98], joint power and bandwidth allocation for multi-relay and a single source-destination pair was investigated. It was shown that an AF strategy cannot benefit necessarily from large bandwidth.

In this chapter, the sum rate for multi-user AF relay assisted network is maximized in the presence of source-destination direct link. The ith user is willing to seek cooperative transmission only if the data rate achieved through cooperation is not lower than the data rate achieved through non cooperation using direct link only. Full cooperative transmission may not be always beneficial or even necessary if direct transmission from the source to the destination results in the best achievable transmission rate. If cooperation is sought, it should result in a higher rate than using the direct link only. To gain the benefits of the two approaches user i can adapt to a mixed strategy transmission; part of her data can be transmitted using the direct link only, and the other part is transmitted using AF cooperative communication scheme. With this strategy, we ensure that the ith user rate is maximized, and the relay's resources are used more efficiently. Admission control is considered inherently in the formulated problem in the sense that the user who cannot benefit from cooperation will use direct transmission, and will not waste the relay's resources. In this chapter, we show that by seeking the optimal relaying power and bandwidth profiles, we are able to improve the system sum rate when compared to full bandwidth relaying.

Joint power and bandwidth allocation is investigated for a single relay

for both flat and frequency selective fading channels using the improved AF cooperative communication scheme. Resource allocation for the improved AF scheme with frequency selective fading channels is different from selective AF-OFDM, since here the issue is to determine the range of frequencies that are used for relaying, i.e. adjacent subcarriers are used for relaying or for direct transmissions. Whereas, in selective AF-OFDM transmission each subcarrier solely can be used for AF relaying or direct transmission without looking at its adjacent subcarriers [30, 36, 49, 126]. Selective AF-OFDM is addressed in Section 7.2.

An iterative two-step recursive algorithm is proposed to solve the problem, which separates the joint power and bandwidth allocation problem into two subproblems; power allocation for a given bandwidth profile, and bandwidth allocation for a given power profile. Simulation results show that the power and bandwidth profiles of the proposed algorithm coincide with the power and bandwidth profiles obtained using PSO and the exterior penalty methods. Furthermore, simulation results show the fast convergence of the proposed algorithm and the possibility of implementing it in a distributed fashion.

Joint power and bandwidth allocation and relay selection are investigated to maximize the sum rate for a system with I users and K relays using the improved AF cooperative communication scheme. The problem at hand, is a mixed integer optimization problem, which is computationally intensive to solve using an exhaustive search. In this sense, PSO is used to solve the formulated problem without the need for the convexity and differentiability of the objective function, nor the relaxation of the integer variables, which are associated with conventional optimization techniques. Modified versions of the PSO method are developed to handle the nature of the formulated problem. Asynchronized PSO velocity update is used to guarantee the convergence of the mixed integer problem. A distributed

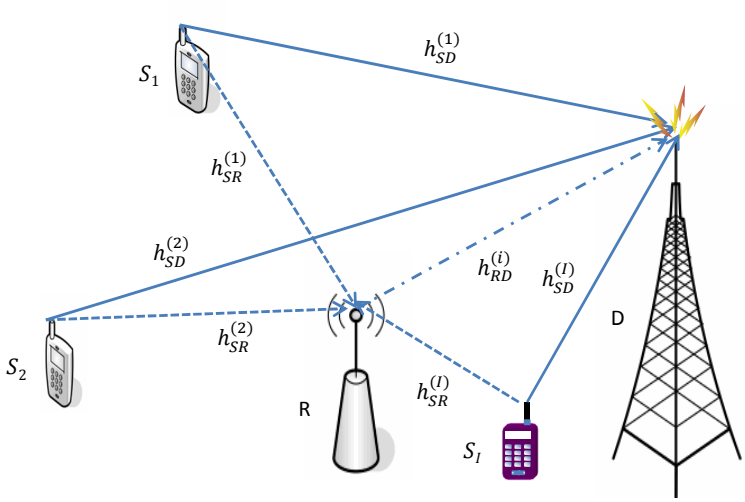

Figure 4.1 System Model: AF Multiple Users Single Relay System.

PSO algorithm is also developed to allocate the resources in a distributed fashion. The key feature towards this is the use of a fitness function with a penalty factor and then applying the PSO algorithm at the user side.

4.2 Flat Fading Improved AF Cooperative Communication

The system under consideration is depicted in **Figure 4.1**. Let $\mathcal{I} = \{1, ..., I\}$ denote the set of active users. Sender (Source) nodes S_i for $i \in \mathcal{I}$ are communicating with the destination terminal D over stable channels with coefficients $h_{SD}^{(i)}$. The relay station R is used to improve the reliability of the communication between the source-destination pairs using simple AF cooperative scheme. $h_{SR}^{(i)}$, and $h_{RD}^{(i)}$ are the channel gains of source-relay and relay-destination links of user S_i. In AF, the relay scales the received data and transmits it in the relaying phase. Considering FDMA and assuming no interference between the users, each active user utilizes a different frequency band. Each user will use two-time slots T_1 and T_2 in a TDM manner. The received signals of user S_i in the first-time slot T_1 defined as $y_{T_1}^{(R_i)}$ and $y_{T_1}^{(D_i)}$ at the relay and destination nodes, respectively are obtained as follows:

$$y_{T_1}^{(R_i)} = \sqrt{P_S} h_{SR}^{(i)} x_i + n_1^{(R_i)}, \tag{4.1a}$$

$$y_{T_1}^{(D_i)} = \sqrt{P_S} h_{SD}^{(i)} x_i + n_1^{(D_i)}, \tag{4.1b}$$

where P_S is the source transmitted power, which is assumed to be the same for all users in the system. The transmitted symbol x_i is drawn from a constellation with unit energy, and $n_1^{(R_i)}$ and $n_1^{(D_i)}$ are AWGNs in the first-time slot T_1 received at the relay and destination nodes, respectively. During the second-time slot T_2, the received signal $y_{T_2}^{(D_i)}$ of user S_i at the destination node is obtained as:

$$y_{T_2}^{(D_i)} = G^{(i)} \sqrt{P_R^{(i)}}\, h_{RD}^{(i)} y_{T_1}^{(R_i)} + n_2^{(D_i)}, \tag{4.2}$$

where $P_R^{(i)}$ is the relay transmitted power for user S_i, and $n_2^{(D_i)}$ is the AWGN received at the destination node in the second-time slot T_2. The noise variance is expressed as $\sigma_i^2 = N_0 W_i$, where $\frac{N_0}{2}$ is the PSD per dimension of the AWGN, N_0 is assumed to be the same at all nodes in the system, and W_i is the relaying bandwidth for user S_i. $G^{(i)}$ is the normalization factor at the relay station given as [56]: $G^{(i)} = \frac{1}{\sqrt{P_S |h_{SR}^{(i)}|^2 + \sigma_i^2}}$. The end-to-end SNR $\Gamma_{AF}^{(i)}$ of user S_i using the relay is given by [4]:

$$\Gamma_{AF}^{(i)} = \frac{P_S P_R^{(i)} |h_{SR}^{(i)}|^2 |h_{RD}^{(i)}|^2}{\sigma_i^2 (\sigma_i^2 + P_S |h_{SR}^{(i)}|^2 + P_R^{(i)} |h_{RD}^{(i)}|^2)}, \tag{4.3}$$

which can be written in a simplified form as [149]:

$$\Gamma_{AF}^{(i)} = \frac{A_i P_R^{(i)}}{W_i (B_i + P_R^{(i)} + C_i W_i)}, \tag{4.4}$$

with $A_i = \frac{P_S |h_{SR}^{(i)}|^2}{N_0}$, $B_i = \frac{P_S |h_{SR}^{(i)}|^2}{|h_{RD}^{(i)}|^2}$ and $C_i = \frac{N_0}{|h_{RD}^{(i)}|^2}$. The SNR of user S_i at the destination node is denoted as $\Gamma_{SD}^{(i)}$, that resulted from direct transmission between the ith source-destination pair in the first time slot T_1, which can

be expressed as [149]:

$$\Gamma_{SD}^{(i)} = \frac{P_S |h_{SD}^{(i)}|^2}{N_0 W_i}. \tag{4.5}$$

The achievable data rate $R_{AF}^{(i)}$ of AF cooperative communication scheme at the destination node with the aid of the relay node using relaying power $P_R^{(i)}$ and relaying bandwidth W_i and using MRC technique, can be computed as:

$$R_{AF}^{(i)} = \frac{W_i}{2} \log_2 \Big(1 + \frac{\Gamma_{SD}^{(i)} + \Gamma_{AF}^{(i)}}{\Gamma}\Big), \tag{4.6}$$

where the factor $\frac{1}{2}$ is due to the fact that two time slots are used for cooperative transmission, and Γ is a constant representing the capacity gap as in [45].

Assuming no interference between the users; each user S_i for $i \in \mathcal{I}$ is assigned a bandwidth W, and transmits with source power P_S. The relay can offer user S_i relaying power $P_R^{(i)}$ depending on the channel conditions and the other users in the system, to relay her information or part of it in a bandwidth $0 \leq W_i \leq W$ in the second time slot. To benefit from all available degrees of freedom, user S_i uses the remaining bandwidth $W - W_i$ to transmit her message directly to the destination node without the help of the relay node (no diversity). The SNR of user S_i at the destination node that results from direct transmission between the ith source-destination pair is the same as in (4.5) with W_i being replaced by $W - W_i$. The achievable data rate $R_{SD}^{(i)}$ using direct transmission without diversity is given as:

$$R_{SD}^{(i)} = (W - W_i) \log_2 \Big(1 + \frac{P_S |h_{SD}^{(i)}|^2}{\Gamma N_0 (W - W_i)}\Big). \tag{4.7}$$

Following the proposed protocol, depending on the availability of the resources, user S_i may operate in different transmission modes; for example user S_i can use direct transmission for all the bandwidth achieving a data

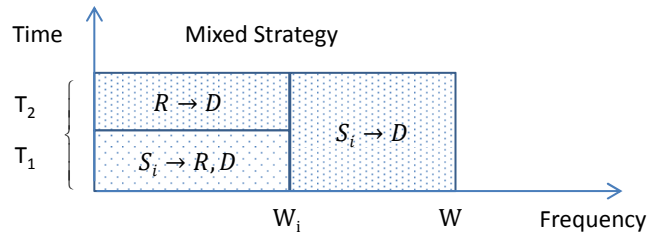

Figure 4.2 Mixed Strategy AF Scheme for User S_i.

rate $R_{SD0}^{(i)}$ given as:

$$R_{SD0}^{(i)} = W \log_2 \left(1 + \frac{P_S |h_{SD}^{(i)}|^2}{\Gamma N_0 W}\right), \tag{4.8}$$

In general, user S_i uses a mixed strategy transmission achieving a date rate $R^{(i)}$ given as:

$$R^{(i)} = R_{AF}^{(i)} + R_{SD}^{(i)}. \tag{4.9}$$

This mixed strategy transmission is illustrated in **Figure 4.2**. Note that: direct transmission with achievable rate $R_{SD0}^{(i)}$ is a special case of the mixed strategy with $W_i = 0$. From now on, the mixed strategy transmission is denoted as the improved AF cooperative communication scheme.

One criterion for resource allocation is to maximize the overall network performance. This criterion is sometimes denoted as the efficient resource allocation criterion, which appears in applications without delay constraints, where high data rate from any user is preferable. Since the user has a source-destination link, the resources allocated to this user need to achieve a transmission rate higher than the rate achieved using direct transmission. The user needs to determine the relaying bandwidth to maximize her data rate by using the improved AF scheme. Therefore, the maximum sum rate problem (effective resource allocation) can be formulated as follows[1]:

$$\max_{\boldsymbol{P}, \boldsymbol{W}} \sum_{i \in \mathcal{I}} R^{(i)}, \tag{4.10a}$$

$$\text{s.t.} \sum_{i \in \mathcal{I}} P_R^{(i)} \leq P_{\max}^{(R)}, \tag{4.10b}$$

[1]The case of additional relaying bandwidth constraint $\sum_{i \in \mathcal{I}} W_i \leq W_{\max}$ is addressed in the simulations.

$$W_i \leq W, \ \forall i \in \mathcal{I}, \tag{4.10c}$$

$$W_i \geq 0, \ P_R^{(i)} \geq 0, \ \forall i \in \mathcal{I}, \tag{4.10d}$$

where $\boldsymbol{P} = [P_R^{(1)}, \cdots, P_R^{(I)}]$, and $\boldsymbol{W} = [W_1, \cdots, W_I]$ are the relay power and bandwidth profiles respectively, for all users S_i for $i \in \mathcal{I}$. Constraint (4.10b) means that the total power allocated to forward the data of all users assisted by the relay is limited to $P_{\max}^{(R)}$. Whereas, constraint (4.10c) indicates that the bandwidth allocated for user S_i is limited to W. The achievable data rate (4.9) for user S_i is not a joint concave function with respect to the power and bandwidth profiles, since $\exists W_i \in [0, W]$ and/or $\exists P_R^{(i)} > 0$, such that $\frac{\partial^2 R^{(i)}}{\partial {W_i}^2} \frac{\partial^2 R^{(i)}}{\partial {P_R^{(i)}}^2} < (\frac{\partial^2 R^{(i)}}{\partial W_i \partial P_R^{(i)}})^2$. To solve this problem we adapt an iterative recursive algorithm that is repeated until convergence is obtained. The joint resource allocation problem is implemented into two recursive steps; power allocation step for a given bandwidth profile and bandwidth allocation step for a given power profile as described below.

1. **Power Allocation Step**: in this step, given the relaying bandwidth profile **W** for all users S_i for $i \in \mathcal{I}$, the effective power allocation problem can be formulated as:

$$\max_{\boldsymbol{P}} \sum_{i \in \mathcal{I}} R_{AF}^{(i)}, \tag{4.11a}$$

$$\text{s.t.} \sum_{i \in \mathcal{I}} P_R^{(i)} \leq P_{\max}^{(R)}, \tag{4.11b}$$

$$P_R^{(i)} \geq 0, \ \forall i \in \mathcal{I}. \tag{4.11c}$$

   The power allocation problem (4.11) can be considered as a weighted-sum rate allocation, which is a convex optimization problem. The objective function is a concave function with respect to the power profile as can be proved by the second order derivative test (Hessian matrix is positive definite). The constraints are also linear.

The KKT conditions for (4.11) are as follows:

$$P_R^{(i)2}(W_i(\Gamma+\Gamma_{SD}^{(i)})+A_i)+P_R^{(i)}\Big(A_iB_i+C_iW_iA_i+2W_i(\Gamma+\Gamma_{SD}^{(i)})(B_i+C_iW_i)\Big)+$$
$$W_i(\Gamma+\Gamma_{SD}^{(i)})(B_i+C_iW_i)^2-\frac{A_iW_i(B_i+C_iW_i)}{2\lambda_R\ln(2)}=0,\ \forall i\in\mathcal{I}, \tag{4.12a}$$

$$\sum_{i\in\mathcal{I}}P_R^{(i)}=P_{\max}^{(R)}, \tag{4.12b}$$

$$P_R^{(i)}\geq 0,\ \forall i\in\mathcal{I}, \tag{4.12c}$$

$$\lambda_i\geq 0,\ \forall i\in\mathcal{I}, \tag{4.12d}$$

$$\lambda_iP_R^{(i)}=0,\ \forall i\in\mathcal{I}, \tag{4.12e}$$

where, λ_is are the Lagrange multipliers of the non-negativity power constraint (4.11c), and λ_R is the Lagrange multiplier associated with the total relaying power constraint (4.11b). To simplify the forthcoming notations, we define $\alpha_2^{(i)}$, $\alpha_1^{(i)}$, and $\alpha_0^{(i)}$ as:

$$\alpha_2^{(i)}=W_i(\Gamma+\Gamma_{SD}^{(i)})+A_i, \tag{4.13a}$$

$$\alpha_1^{(i)}=A_iB_i+C_iW_iA_i+2W_i(\Gamma+\Gamma_{SD}^{(i)})(B_i+C_iW_i), \tag{4.13b}$$

$$\alpha_0^{(i)}=W_i(\Gamma+\Gamma_{SD}^{(i)})(B_i+C_iW_i)^2-\frac{A_iW_i(B_i+C_iW_i)}{2\lambda_R\ln(2)}, \tag{4.13c}$$

then, the optimal solution $P_R^{*(i)}$ can be obtained by solving the KKT conditions given as:

$$P_R^{*(i)}=\max\Big(0,\frac{\sqrt{\alpha_1^{(i)2}-4\alpha_2^{(i)}\alpha_0^{(i)}}-\alpha_1^{(i)}}{2\alpha_2^{(i)}}\Big), \tag{4.14}$$

and λ_R is chosen such that the total power constraint $\sum_{i\in\mathcal{I}}P_R^{*(i)}=P_{\max}^{(R)}$ is satisfied.

The optimal relaying power $P_R^{*(i)}$ for user S_i can be obtained in an independent manner using the dual decomposition approach. In this sense, the Lagrangian function can be written by relaxing the total

power constraint (4.11b) as:

$$\boldsymbol{L}(\boldsymbol{P}, \lambda_R) = \sum_{i \in \mathcal{I}} R_{AF}^{(i)} - \lambda_R (\sum_{i \in \mathcal{I}} P_R^{(i)} - P_{\max}^{(R)}), \tag{4.15a}$$

$$\text{s.t. } P_R^{(i)} \geq 0, \ \lambda_R \geq 0, \tag{4.15b}$$

then, with a little algebra, we can rearrange the Lagrangian function as:

$$\boldsymbol{L}(\boldsymbol{P}, \lambda_R) = \sum_{i \in \mathcal{I}} (R_{AF}^{(i)} - \lambda_R P_R^{(i)}) + \lambda_R P_{\max}^{(R)}. \tag{4.16}$$

The associated dual problem can be written as:

$$g(\lambda_R) = \max_{\boldsymbol{P} \geq 0} \boldsymbol{L}(\boldsymbol{P}, \lambda_R). \tag{4.17}$$

Since problem (4.11) is convex with linear constraints, strong duality holds. Hence, the solution of the problem can be obtained from the solution of the corresponding dual problem which is given as:

$$\min g(\lambda_R), \tag{4.18a}$$

$$\text{s.t. } \lambda_R \geq 0. \tag{4.18b}$$

The dual problem can be solved iteratively using the gradient or sub-gradient methods as [21]:

$$\lambda_R^{(t+1)} = \left(\lambda_R^{(t)} - \epsilon (P_{max}^{(R)} - \sum_{i \in \mathcal{I}} P_R^{t(i)})\right)^+, \tag{4.19}$$

where ϵ is a small step size, t is the iteration index, and $(\cdot)^+$ denotes the projection operator in the set of non-negative numbers. The relaying power $P_R^{t(i)}$ at iteration t is computed using (4.14) with λ_R substituted with $\lambda_R^{(t)}$.

2. **Bandwidth Allocation Step**: in this step, given the relaying power

profile $P_R^{(i)}$ for all users S_i for $i \in \mathcal{I}$, the effective bandwidth allocation problem can be formulated as:

$$\max_{W} \sum_{i \in \mathcal{I}} R^{(i)}, \tag{4.20a}$$

$$\text{s.t. } 0 \leq W_i \leq W, \ \forall i \in \mathcal{I}, \tag{4.20b}$$

since the users are assigned orthogonal frequency bands, the bandwidth allocation problem (4.20) can be decomposed into $|\mathcal{I}|$ bandwidth allocation problems, where each user S_i for $i \in \mathcal{I}$ finds her optimal bandwidth profile W_i^* without affecting other users as:

$$W_i^* = \arg \max_{0 \leq W_i \leq W} R^{(i)}. \tag{4.21}$$

Examining the user achievable rate $R^{(i)}$ given by (4.9) as a function of W_i for $P_R^{(i)} \neq 0$ reveals that $R^{(i)}$ can have only one maximum value at W_i^* where $0 < W_i^* \leq W$. W_i^* can be obtained by solving $\frac{dR^{(i)}}{dW_i}|_{W_i^*} = 0$, where the derivative of $R^{(i)}$ with respect to W_i is given as:

$$\frac{dR^{(i)}}{dW_i} = \frac{1}{2}\log_2\Big(1 + \frac{P_S|h_{SD}^{(i)}|^2}{\Gamma N_0 W_i} + \frac{A_i P_R^{(i)}}{\Gamma W_i(B_i + P_R^{(i)} + C_i W_i)}\Big) - \log_2\Big(1 + \frac{P_S|h_{SD}^{(i)}|^2}{\Gamma N_0 (W - W_i)}\Big) + \frac{1}{2\ln(2)} \frac{\Big(\frac{-P_S|h_{SD}^{(i)}|^2}{\Gamma N_0 W_i} - \frac{A_i P_R^{(i)}(B_i + P_R^{(i)} + 2C_i W_i)}{\Gamma W_i (B_i + P_R^{(i)} + C_i W_i)^2}\Big)}{1 + \frac{P_S|h_{SD}^{(i)}|^2}{\Gamma N_0 W_i} + \frac{A_i P_R^{(i)}}{\Gamma W_i(B_i + P_R^{(i)} + C_i W_i)}} + \frac{1}{\Gamma N_0 \ln(2)} \frac{P_S|h_{SD}^{(i)}|^2}{(1 + \frac{P_S|h_{SD}^{(i)}|^2}{\Gamma N_0 (W - W_i)})(W - W_i)}. \tag{4.22}$$

If there exists no feasible solution that satisfies $\frac{dR^{(i)}}{dW_i} = 0$, then the maximum value of $R^{(i)}$ occurred at the boundaries; either at $W_i^* = 0$ or at

$W_i^* = W$. Hence, the optimal bandwidth W_i^* can be written as:

$$W_i^* = \begin{cases} \arg \frac{dR^{(i)}}{dW_i} = 0 & \text{Where } 0 < W_i^* < W. \\ 0 & P_R^{(i)} = 0 \text{ or, } \frac{dR^{(i)}}{dW_i} < 0, \ \forall W_i, \text{ where } 0 < W_i < W. \\ W & \text{If } \frac{dR^{(i)}}{dW_i} > 0, \ \forall W_i, \text{ where } 0 < W_i < W, \text{ and } R_{AF}^{(i)} > R_{SD0}^{(i)}. \end{cases} \tag{4.23}$$

The optimal bandwidth W_i^* can be obtained using an iterative algorithm as [103]:

$$W_i^{(t+1)} = W_i^{(t)} + \theta_{W_i} W_i^{(t)} \frac{dR^{t(i)}}{dW_i}. \tag{4.24}$$

where $W_i^{(t+1)}$ is the bandwidth update at iteration $t+1$, and θ_{W_i} is adjustment speed parameter. At optimal bandwidth $W_i^{(t+1)} = W_i^{(t)}$. The effect of θ_{W_i} on the convergence and the stability of the algorithm can be studied as in [1, 103]. The value of the derivative $\frac{dR^{t(i)}}{dW_i}$ can be estimated by user S_i using the central difference method. User S_i computes the date rate $R^{(i)}$ at iteration t by submitting the power $W_i^{(t)} \pm \epsilon_W$, where ϵ_W is a small number, then estimates $\frac{dR^{t(i)}}{dW_i} \approx \frac{R^{+(i)} - R^{-(i)}}{2\epsilon_W}$. The iterative distributed algorithm for joint power and bandwidth allocation is illustrated in **Algorithm 4.1**. Given the relay power constraints $P_{\max}^{(R)}$, the channel gains $h_{RD}^{(i)}$, $h_{SD}^{(i)}$, and $h_{SR}^{(i)}$ for $i \in \mathcal{I}$. The power and bandwidth profiles are allocated using equations (4.14) and (4.23), respectively. The convergence in the power is attained when $\sum_{i \in \mathcal{I}} P_R^{t(i)} = P_{\max}^{(R)}$. The The convergence in the bandwidth is attained when $W_i^{(t+1)} = W_i^{(t)}$. The convergence in the sum rate is attained when the sum rate could not be improved further by applying the power and bandwidth iterative steps $|\sum_{i \in \mathcal{I}} (R^{l+1(i)} - R^{l(i)})| < \delta$, where l denotes one procedure of one power allocation step plus one bandwidth allocation step.

Algorithm 4.1 Iterative Algorithm for Power and Bandwidth Allocation.

Require: $h_{SD}^{(i)}$, $h_{SR}^{(i)}$, $h_{RD}^{(i)}$, $\forall i \in \mathcal{I}$, $P_{\max}^{(R)}$, W, P_S, N_0, and Γ.
1: **Calculate**: A_i, B_i, and C_i.
2: **Initialize**: $W_i = W$, $\forall i \in \mathcal{I}$.
3: **Initialize**: $t = 0$, and $\lambda_R^{(0)} = \lambda_0$.
4: **while** convergence in $\boldsymbol{P}$ is not attained **do**
5: **Find** the power allocation $P_R^{t(i)}$, $\forall i \in \mathcal{I}$ using (4.14).
6: **Update** $\lambda_R^{(t+1)}$ using (4.19).
7: **Update** $t = t + 1$.
8: **end while**
9: **Return** $P_R^{*(i)}$, $\forall i \in \mathcal{I}$.
10: **Initialize**: $t = 0$.
11: **while** convergence in $\boldsymbol{W}$ is not attained **do**
12: **Compute** $\frac{dR^{t(i)}}{dW_i}$, $\forall i \in \mathcal{I}$.
13: **Update** $W_i^{(t+1)}$ using (4.24).
14: **Update** $t = t + 1$.
15: **end while**
16: **Return** W_i^*, $\forall i \in \mathcal{I}$.
17: **Compute** the sum rate $\sum_{i\in\mathcal{I}} R^{(i)}$ using $P_R^{*(i)}$ and W_i^*, $\forall i \in \mathcal{I}$.
18: **while** convergence in sum rate is not attained **do**
19: **Go to** 3
20: **end while**
21: **Return P**, **W**, and $\sum_{i\in\mathcal{I}} R^{(i)}$.

4.3 Frequency Selective Fading Improved AF Cooperative Communication

The capacity of single carrier frequency selective fading channels without relaying and with total source power constraint is addressed in [41, 44]. In this section, the sum rate of multi user single relay improved AF cooperative communication system is investigated under individual node power constraint at the source and relay nodes for single carrier frequency selective fading channels. Let $h_{SD}^{(i)}(f)$, $h_{SR}^{(i)}(f)$, and $h_{RD}^{(i)}(f)$ denote the ith instantaneous source-destination, source-relay and relay-destination channel gains as a function of frequency f, respectively. To simplify the forthcoming notations we define $\Gamma_{SD}^{(i)}(f) = \frac{|h_{SD}^{(i)}(f)|^2}{\Gamma N_0}$, $A^{(i)}(f) = \frac{|h_{SR}^{(i)}(f)|^2 |h_{RD}^{(i)}(f)|^2}{\Gamma N_0}$, $B^{(i)}(f) = |h_{SR}^{(i)}(f)|^2$ and $C^{(i)}(f) = |h_{RD}^{(i)}(f)|^2$.

The instantaneous data rate for user S_i for $i \in \mathcal{I}$ using (4.1)-(4.2) is obtained as:

$$R_{FS}^{(i)} = \frac{1}{2}\int_{f\in W_i^{(AF)}} \log_2\left(1 + P_{T_1}^{(i)}(f)\Gamma_{SD}^{(i)}(f) + \frac{P_{T_1}^{(i)}(f)P_R^{(i)}(f)A^{(i)}(f)}{N_0 + P_{T_1}^{(i)}(f)B^{(i)}(f) + P_R^{(i)}(f)C^{(i)}(f)}\right) df + \frac{1}{2}\int_{f\in W_i^{(DC)}} \log_2\left(1 + P_{T_1}^{(i)}(f)\Gamma_{SD}^{(i)}(f)\right) df + \frac{1}{2}\int_{f\in W_i^{(DC)}} \log_2\left(1 + P_{T_2}^{(i)}(f)\Gamma_{SD}^{(i)}(f)\right) df. \tag{4.25}$$

The equation inside the first integral can be thought of as the incremental data rate of user S_i for $i \in \mathcal{I}$ associated with a given frequency f over bandwidth df with power allocation profiles $P_{T_1}^{(i)}(f)$ and $P_R^{(i)}(f)$ at the source and relay nodes using AF relaying, respectively. The equation inside the second and third integrals can be interpreted as the incremental data rate of user S_i associated with a given frequency f over bandwidth df with power allocation profiles $P_{T_1}^{(i)}(f)$ and $P_{T_2}^{(i)}(f)$ at the source node in first and second time slots using direct transmission. The instantaneous sum rate optimization problem can be formulated as:

$$\max_{\boldsymbol{P}(f),\, \boldsymbol{W}} \sum_{i\in\mathcal{I}} R_{FS}^{(i)}, \tag{4.26a}$$

$$\text{s.t.} \sum_{i\in\mathcal{I}} \int_{f\in W_i^{(AF)}} P_R^{(i)}(f)df \le P_{\max}^{(R)}, \tag{4.26b}$$

$$\int_{f\in W} P_{T_1}^{(i)}(f)\, df \le P_{\max}^{(i)},\ \forall i \in \mathcal{I}, \tag{4.26c}$$

$$\int_{f\in W_i^{(DC)}} P_{T_2}^{(i)}(f)\, df \le P_{\max}^{(i)}, \forall i \in \mathcal{I}, \tag{4.26d}$$

$$P_R^{(i)}(f) \ge 0,\ P_{T_1}^{(i)}(f) \ge 0,\ P_{T_2}^{(i)}(f) \ge 0,\ \forall i \in \mathcal{I}, \tag{4.26e}$$

$$W_i^{(AF)} + W_i^{(DC)} = W,\ \forall i \in \mathcal{I}, \tag{4.26f}$$

$$W_i^{(AF)} \ge 0,\ W_i^{(DC)} \ge 0,\ \forall i \in \mathcal{I}. \tag{4.26g}$$

The optimization problem underlying variables are $\boldsymbol{P}(f)$, which includes $P_{T_1}^{(i)}(f)$, $P_{T_2}^{(i)}(f)$, and $P_R^{(i)}(f)$ for $f \in [0, W]$ and $\forall i \in \mathcal{I}$, and the bandwidth pro-

file $\boldsymbol{W}$, which includes $W_i^{(DC)}$, and $W_i^{(AF)}$, $\forall i \in \mathcal{I}$. Where $P_{T_1}^{(i)}(f)$ and $P_{T_2}^{(i)}(f)$, and $P_R^{(i)}(f)$ is the PSDs of user S_i in the first time slot T_1, and second time slot T_2 for direct transmission. $P_R^{(i)}(f)$ is the PSD of the relayed signal of user S_i in the second time slot T_2. $W_i^{(AF)}$, and $W_i^{(DC)}$ are frequency bands for cooperative and direct transmissions of user S_i, respectively. It is worth noting that in flat fading scenarios, each user transmits with constant power in all the bandwidth $[0, W]$ since the user faces one realization of the channel. Whereas, in frequency selective fading scenarios, the user can utilize one more degree of freedom by allocating the source power profiles $P_{T_1}^{(i)}(f)$ and $P_{T_2}^{(i)}(f)$ for $f \in [0, W]$.

Solving (4.26) is a complex task since the frequency is a continuous variable (infinite dimension) and the problem is not convex. To tackle this problem, we propose a four-step iterative recursive algorithm based on the algorithm proposed for the flat fading improved AF cooperative communication system.

1. **Relaying Power Allocation Step**: in this step for a given relaying bandwidth $\boldsymbol{W}$ and source power $\mathbf{P}_{T_1}(f)$ profiles, and by relaxing the relaying power constraint, the optimization problem using the Lagrangian multiplier λ_R can be written as:

$$\max_{\boldsymbol{P}_R(f)} \sum_{i\in\mathcal{I}} \frac{1}{2} \int_{f\in W_i^{(AF)}} \log_2\Big(1 + P_{T_1}^{(i)}(f)\Gamma_{SD}^{(i)}(f) + \frac{P_{T_1}^{(i)}(f)P_R^{(i)}(f)A^{(i)}(f)}{N_0 + P_{T_1}^{(i)}(f)B^{(i)}(f) + P_R^{(i)}(f)C^{(i)}(f)}\Big)\, df -$$
$$\lambda_R\Big(\sum_{i\in\mathcal{I}} \int_{f\in W_i^{(AF)}} P_R^{(i)}(f) df - P_{\max}^{(R)}\Big), \tag{4.27a}$$

$$\text{s.t. } (4.26e). \tag{4.27b}$$

Similar to (4.19), the optimal power solution can be obtained in an independent manner using the dual decomposition approach, where

each user S_i for $i \in \mathcal{I}$ maximizes her own rate as:

$$\max_{P_R^{(i)}(f)} \frac{1}{2} \int_{f \in W_i^{(AF)}} \log_2 \left(1 + P_{T_1}^{(i)}(f)\Gamma_{SD}^{(i)}(f) + \frac{P_{T_1}^{(i)}(f)P_R^{(i)}(f)A^{(i)}(f)}{N_0 + P_{T_1}^{(i)}(f)B^{(i)}(f) + P_R^{(i)}(f)C^{(i)}(f)}\right) df -$$
$$\lambda_R \int_{f \in W_i^{(AF)}} P_R^{(i)}(f)\, df, \tag{4.28a}$$
$$\text{s.t. (4.26e).} \tag{4.28b}$$

This is a convex optimization problem with respect to $P_R^{(i)}(f)$. To simplify the forthcoming notations, $\alpha_2^{(i)}(f)$, $\alpha_1^{(i)}(f)$, and $\alpha_0^{(i)}(f)$ are defined as:

$$\alpha_2^{(i)}(f) = \left(1 + \Gamma_{SD}^{(i)}(f)P_{T_1}^{(i)}(f)\right)C^{(i)2}(f) + A^{(i)}(f)C^{(i)}(f)P_{T_1}^{(i)}(f), \tag{4.29a}$$
$$\alpha_1^{(i)}(f) = 2C^{(i)}(f)\left(1 + \Gamma_{SD}^{(i)}(f)P_{T_1}^{(i)}(f)\right)\left(N_0 + P_{T_1}^{(i)}(f)B^{(i)}(f)\right) + \left(N_0 + P_{T_1}^{(i)}(f)B^{(i)}(f)\right)P_{T_1}^{(i)}(f)A^{(i)}(f), \tag{4.29b}$$
$$\alpha_0^{(i)}(f) = \left(1 + \Gamma_{SD}^{(i)}(f)P_{T_1}^{(i)}(f)\right)\left(N_0 + P_{T_1}^{(i)}(f)B^{(i)}(f)\right)^2 - \frac{\left(N_0 + P_{T_1}^{(i)}(f)B^{(i)}(f)\right)P_{T_1}^{(i)}(f)A^{(i)}(f)}{2\ln(2)\lambda_R}, \tag{4.29c}$$

then, the optimal solution $P_R^{*(i)}(f)$ can be obtained as:

$$P_R^{*(i)}(f) = \max\left(0, \frac{\sqrt{\alpha_1^{(i)2}(f) - 4\alpha_2^{(i)}(f)\alpha_0^{(i)}(f)} - \alpha_1^{(i)}(f)}{2\alpha_2^{(i)}(f)}\right), \tag{4.30}$$

and λ_R is chosen such that the total power constraint $\sum_{i \in \mathcal{I}} \int_{f \in W_i^{(AF)}} P_R^{*(i)}(f)df = P_{\max}^{(R)}$ is satisfied.

2. **Source Power Allocation Step**: in this step, for a given relaying bandwidth $\boldsymbol{W}$ and power $\boldsymbol{P_R}(f)$ profiles, the optimal source power alloca-

tion problem is formulated as follows:

$$\max_{\mathbf{P}_{T_1}(f),\,\mathbf{P}_{T_2}(f)} \frac{1}{2}\sum_{i\in\mathcal{I}}\int_{f\in W_i^{(AF)}} \log_2\Big(1+P_{T_1}^{(i)}(f)\Gamma_{SD}^{(i)}(f)+\frac{P_{T_1}^{(i)}(f)P_R^{(i)}(f)A^{(i)}(f)}{N_0+P_{T_1}^{(i)}(f)B^{(i)}(f)+P_R^{(i)}(f)C^{(i)}(f)}\Big)\,df+$$
$$\frac{1}{2}\sum_{i\in\mathcal{I}}\int_{f\in W_i^{(DC)}} \log_2\Big(1+P_{T_1}^{(i)}(f)\Gamma_{SD}^{(i)}(f)\Big)\,df+$$
$$\frac{1}{2}\sum_{i\in\mathcal{I}}\int_{f\in W_i^{(DC)}} \log_2\Big(1+P_{T_2}^{(i)}(f)\Gamma_{SD}^{(i)}(f)\Big)\,df, \tag{4.31a}$$

$$\text{s.t. (4.26c), (4.26d), and (4.26e).} \tag{4.31b}$$

Once again, the source power allocation problem can be separated into $2|\mathcal{I}|$ sub problems, each user S_i for $i \in \mathcal{I}$ solves two convex optimization problems; the first problem is the source power allocation in the first-time slot T_1 which is given as:

$$\max_{P_{T_1}^{(i)}(f)} \frac{1}{2}\int_{f\in W_i^{(AF)}} \log_2\Big(1+P_{T_1}^{(i)}(f)\Gamma_{SD}^{(i)}(f)+\frac{P_{T_1}^{(i)}(f)P_R^{(i)}(f)A^{(i)}(f)}{N_0+P_{T_1}^{(i)}(f)B^{(i)}(f)+P_R^{(i)}(f)C^{(i)}(f)}\Big)\,df$$
$$+\frac{1}{2}\int_{f\in W_i^{(DC)}} \log_2\Big(1+P_{T_1}^{(i)}(f)\Gamma_{SD}^{(i)}(f)\Big)\,df, \tag{4.32a}$$

$$\text{s.t. (4.26c) and (4.26e),} \tag{4.32b}$$

which is a convex optimization problem. However, the solution is difficult to find in closed form, but can be obtained using any convex optimization technique. The second problem is the allocation of the source power in the second time slot T_2 using direct transmission given as:

$$\max_{P_{T_2}^{(i)}(f)} \frac{1}{2}\int_{f\in W_i^{(DC)}} \log_2\Big(1+P_{T_2}^{(i)}(f)\Gamma_{SD}^{(i)}(f)\Big)\,df, \tag{4.33a}$$

$$\text{s.t. (4.26d) and (4.26e),} \tag{4.33b}$$

the solution of (4.33) is in the form of the well known water filling

solution given as [44]:

$$P_{T_2}^{*(i)}(f) = \left(\frac{1}{\lambda_S} - \Gamma_{SD}^{(i)}(f)\right)^+, \tag{4.34}$$

where λ_S is selected such that the source power constraint is satisfied $\int_{f \in W_i^{(DC)}} P_{T_2}^{*(i)}(f) = P_{\max}^{(i)}$ for $W_i^{(DC)} \neq 0$.

3. **Bandwidth Allocation Step**: in this step, first we compare the achievable data rate using direct transmission with the achievable rate using AF with $W_i = W$. If the achievable rate using direct link is larger than the achievable rate using AF with $W_i = W$, increasing the AF bandwidth W_i from zero to $W_i = W$ in a predetermined step size. Performing frequency scanning along side, source and relay power allocation steps for each change in the bandwidth is required. The bandwidth keeps increasing as long as the achievable data rate increases, otherwise it decreases until reaching the optimal bandwidth. On the other hand, if initially the achievable data rate using direct link is smaller than the achievable data rate using AF with $W_i = W$, decreasing AF relaying bandwidth from $W_i = W$ towards zero until reaching the optimal bandwidth. For each change in the bandwidth, performing frequency scanning along side with source and relay power allocation is required. Bandwidth allocation can be implemented by following a simple approach using a defined bandwidth increment for relaying, that is, $W_i \in \{0, \Delta W, 2\Delta W, ..., W\}$ and then finding the optimal bandwidth that maximizes the data rate over these bandwidth increments.

4. **Frequency Scanning Step**: the start and end frequencies for a given AF relaying bandwidth affect the power profiles at the source and relay nodes. In this sense, for each incremental bandwidth $W_i \in \{0, \Delta W, 2\Delta W, ..., W\}$, the start frequency for AF relaying in the range $[0, W]$ that maximizes the sum rate is sought. Note that the relaying bandwidth

Algorithm 4.2 Resource Allocation for Improved AF with Frequency Selective Channels.

Require: $h_{RD}^{(i)}(f)$, $h_{SD}^{(i)}(f)$, $h_{SR}^{(i)}(f)$, $P_{\max}^{(i)}$, $i \in \mathcal{I}$, $P_{\max}^{(R)}$, W, N_0, and Γ.

1: **Compute**: $\Gamma_{SD}^{(i)}(f)$, $A^{(i)}(f)$, $B^{(i)}(f)$, and $C^{(i)}(f)$.
2: **for** each relaying bandwidth $W_i \in \{\Delta W, 2\Delta W, \cdots, W\}$, $i \in \mathcal{I}$ **do**
3: **Scan** the whole bandwidth to find the relaying bandwidth $W_i^{(AF)}$ for a given W_i for $i \in \mathcal{I}$.
4: **Find** the power power profiles by **iterating** between solving (4.28), (4.32a) and (4.33a) for the relaying power profile $P_R^{(i)}(f)$ and the source power profiles $P_{T_1}^{(i)}(f)$ and $P_{T_2}^{(i)}(f)$.
5: **Compute** the sum rate $\sum_{i\in\mathcal{I}} R_{FS}^{(i)}$ for each W_i and $W_i^{(AF)}$ for $i \in \mathcal{I}$.
6: **end for**
7: **Find** the power profiles $P_R^{(i)}(f)$, $P_{T_1}^{(i)}(f)$, and $P_{T_2}^{(i)}(f)$, the relaying bandwidth $W_i^{(AF)}$ that maximize the sum rate.
8: Return **P**, **W**, and the maximum sum rate $\sum_{i\in\mathcal{I}} R_{FS}^{(i)}$.

$W_i^{(AF)}$ includes W_i and the start relaying frequency. For each change in the start point of the relaying bandwidth, source and relay power allocation steps are required to allocate the optimal start relaying frequency.

In our model where frequency is continuous, it is natural in wireless communications and digital subscriber lines to divide the available frequency bandwidth into N discrete channels each with bandwidth B_N and assume that the channel gain is constant in each discrete channel. This approximation makes the complexity of the resulting optimization problem scales with N as in [37]. This discretization is used in the simulations as described next. The iterative algorithm for joint power and bandwidth allocation for improved AF frequency with selective fading channels is illustrated in **Algorithm 4.2**. For given power constraints at the source and relay nodes $P_{\max}^{(R)}$, and $P_{\max}^{(i)}$, respectively, and channel gains $h_{RD}^{(i)}(f)$, $h_{SD}^{(i)}(f)$, $h_{SR}^{(i)}(f)$ for $i \in \mathcal{I}$, the power and bandwidth profiles can be determined using Steps 1-4. Furthermore, a distributed implementation for the resource allocation for the improved AF with frequency selective fading channels can be developed based on (4.28). The Lagrange multiplier $\lambda_R^{(t)}$ at $t = 0$ is initialized, then each

user S_i for $i \in \mathcal{I}$ determines the relaying bandwidth $W_i^{t(AF)}$, power profiles at the source and relay nodes $P_{T_1}^{t(i)}(f)$, $P_R^{t(i)}(f)$, and $P_{T_2}^{t(i)}(f)$, respectively, then the Lagrange multiplier $\lambda_R^{(t+1)}$ is updated as:

$$\lambda_R^{(t+1)} = \left(\lambda_R^{(t)} - \epsilon(P_{max}^{(R)} - \sum_{i\in\mathcal{I}} \int_{f\in W_i^{t(AF)}} P_R^{t(i)}(f)df)\right)^+, \tag{4.35}$$

the procedure is repeated until the relay total power constraint (4.26b) is satisfied.

4.4 Relay Selection and Joint Power and Bandwidth Allocation

In this section, we extend the resource allocation problem of flat fading channels using the improved AF transmission to multiple-relays. The system under consideration consists of I users, K relays, and a common destination D as depicted in **Figure 4.3**. In this setting, another degree of freedom is explored, where the relay assignment profile needs to be determined for each user with optimal relaying power and bandwidth profiles. Let $\mathcal{K} = \{1, ..., K\}$ be the set of active relays, each user S_i for $i \in \mathcal{I}$ can only use one relay from the set $\mathcal{K}$. The channel coefficients that are used for user S_i transmission, using relay R_k are denoted as $h_{SR}^{(ik)}$ and $h_{RD}^{(ik)}$. Following the lines of (4.1)-(4.10) in Section 4.2, the resource allocation problem can be

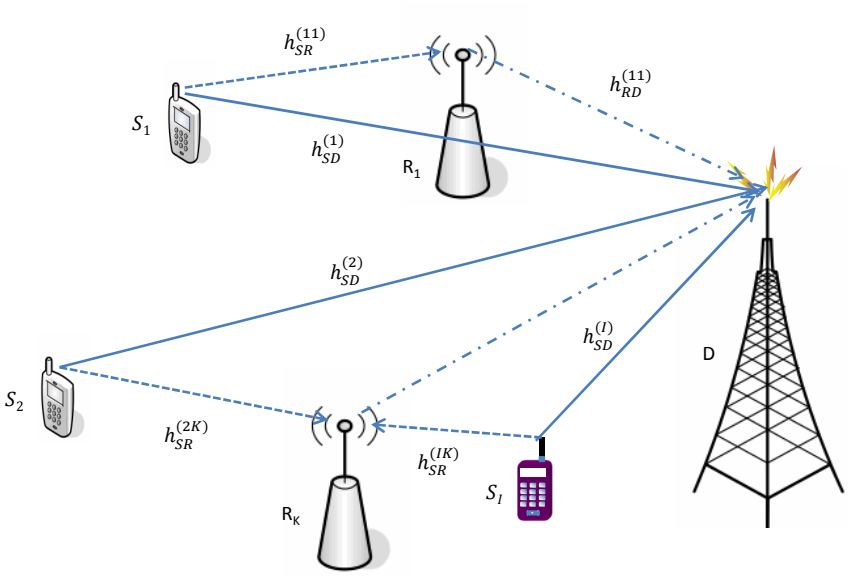

Figure 4.3 System Model: AF Multiple Users System.

formulated as:

$$\max_{\boldsymbol{Z},\boldsymbol{P},\boldsymbol{W}} \sum_{k\in\mathcal{K}}\sum_{i\in\mathcal{I}} Z_{ik}R^{(ik)}, \tag{4.36a}$$

$$\text{s.t.} \sum_{i\in\mathcal{I}} Z_{ik}P_R^{(ik)} \le P_{\max}^{(R_k)},\ \forall k\in\mathcal{K}, \tag{4.36b}$$

$$\sum_{k\in\mathcal{K}} Z_{ik} = 1,\ \forall i\in\mathcal{I}, \tag{4.36c}$$

$$W_{ik} \le W,\ \forall i\in\mathcal{I},\ \forall k\in\mathcal{K}, \tag{4.36d}$$

$$P_R^{(ik)} \ge 0,\ W_{ik}\ge 0,\ Z_{ik}\in\{0,1\},\ \forall i\in\mathcal{I},\ \forall k\in\mathcal{K}, \tag{4.36e}$$

where $\boldsymbol{Z}$ is the relay selection indicator profile with $Z_{ik} = 1$ indicates that relay R_k is assigned to user S_i. $\boldsymbol{P}$, and $\boldsymbol{W}$ are the relay power and bandwidth profiles respectively, for all users S_i for $i \in \mathcal{I}$, with $[\boldsymbol{P}]_{ik} = P_R^{(ik)}$, and $[\boldsymbol{W}]_{ik} = W_{ik}$ are the power and bandwidth profiles of user S_i by using relay R_k. The constraint (4.36b) means that the total power allocated to forward the data from all users assisted by relay R_k is limited to $P_{\max}^{(R_k)}$. Whereas, constraint (4.36d) indicates that the bandwidth allocated for user S_i is limited to W. Constraint (4.36c) means that only one relay is assigned to user S_i. The data

rate $R^{(ik)}$ for user S_i using relay R_k after using MRC is computed as:

$$R^{(ik)} = R_{SD}^{(ik)} + R_{AF}^{(ik)}, \tag{4.37}$$

where $R_{SD}^{(ik)}$ is the data rate using direct transmission, which is given as:

$$R_{SD}^{(ik)} = (W - W_{ik}) \log_2(1 + \frac{P_S |h_{SD}^{(i)}|^2}{\Gamma N_0 (W - W_{ik})}), \tag{4.38}$$

and $R_{AF}^{(ik)}$ is the achievable data rate of AF cooperative communication using relay R_k, with relaying bandwidth W_{ik} and power $P_R^{(ik)}$ given as:

$$R_{AF}^{(ik)} = \frac{W_{ik}}{2} \log_2(1 + \frac{\Gamma_{SD}^{(ik)} + \Gamma_{AF}^{(ik)}}{\Gamma}), \tag{4.39}$$

with $\Gamma_{SD}^{(ik)} = \frac{P_S |h_{SD}^{(i)}|^2}{N_0 W_{ik}}$, and $\Gamma_{AF}^{(ik)} = \frac{P_S P_R^{(ik)} |h_{SR}^{(ik)}|^2 |h_{RD}^{(ik)}|^2}{N_0 W_{ik} (N_0 W_{ik} + P_S |h_{SR}^{(ik)}|^2 + P_R^{(ik)} |h_{RD}^{(ik)}|^2)}$. Problem (4.36) is not only not jointly concave, but also a mixed integer (combinatorial problem), which is computationally intensive to solve using exhaustive search, where there are $|\mathcal{K}|^{|\mathcal{I}|}$ possible joint power and bandwidth profiles. Therefore, we resort to solving it using a PSO for mixed integer problems. We use a PSO algorithm for two fitness functions, the first is the objective function in (4.36a) and the second fitness function is formulated by adding the relay total power constraint as:

$$F = \sum_{k \in \mathcal{K}} \sum_{i \in \mathcal{I}} Z_{ik} R^{(ik)} + \sum_{k \in \mathcal{K}} \lambda_{R_k} (P_{\max}^{(R_k)} - \sum_{i \in \mathcal{I}} Z_{ik} P_R^{(ik)}), \tag{4.40}$$

where λ_{R_k} represent the sensitivity of the fitness function to the power constraint of relay R_k. This fitness function can be written as:

$$F = \sum_{i \in \mathcal{I}} F_i + \sum_{k \in \mathcal{K}} \lambda_{R_k} P_{\max}^{(R_k)} \tag{4.41}$$

where $F_i = \sum_{k\in\mathcal{K}}(Z_{ik}R^{(ik)} - \lambda_{R_k}Z_{ik}P_R^{(ik)})$. It is clear that maximizing F_i taking into consideration constraint (4.36b) for all $i \in \mathcal{I}$ leads to maximizing the system throughput. By this reordering and splinting of the fitness function we can apply a distributed PSO algorithm as explained next.

4.4.1 Distributed PSO

Capitalizing on the fitness function (4.41) and in order to have a flexible distributed resource allocation algorithm, we propose a distributed PSO algorithm that can be implemented at the users side with less information exchange between the users and the base station and without information exchange among the users. This entails the following: Initially, the base station announces the sensitivity parameter ($\lambda_{R_k}^{(0)}$, $\forall k \in \mathcal{K}$). Assuming all users use direct link only (initially no relay is assigned), set this allocation to $\mathbf{x}_{iGbest}^{(0)} = [\mathbf{P}_{iGbest}^{(0)}, \mathbf{W}_{iGbest}^{(0)}]$[2], $\mathbf{y}_{iGbest}^{(0)} = \mathbf{Z}_{iGbest}^{(0)}$ and $F_{iGbest}^{(0)} = R_{SD0}^{(i)}$ for all $i \in \mathcal{I}$. User S_i for $i \in \mathcal{I}$ at iteration t applies the PSO algorithm with her fitness function $F_i^{(t)}$; generating a swarm of size P and dimension $3|\mathcal{K}|$ and computing the new global best $F_{iGbest}^{(t)}$. Then, the base station collects all $F_{iGbest}^{(t)}$ and computes the value of the fitness function using (4.41) as ($\sum_{i\in\mathcal{I}} F_{iGbest}^{(t)}$) and compares it with the value of the fitness function of the previous iteration $\sum_{i\in\mathcal{I}} F_{iGbest}^{(t-1)}$, if the new value achieves a better performance, the base station informs the users to use the updated global bests $F_{iGbest}^{(t)}$, $\mathbf{x}_{iGbest}^{(t)}$, and $\mathbf{y}_{iGbest}^{(t)}$ in the next iteration. Otherwise, the users use the previous global bests $F_{iGbest}^{(t-1)}$, $\mathbf{x}_{iGbest}^{(t-1)}$, and $\mathbf{y}_{iGbest}^{(t-1)}$ in the next iteration using (2.76)-(2.78) to update the values of $\mathbf{x}_i^{(t)}$ and $\mathbf{y}_i^{(t)}$.

Using KKT condition we know that at a local or global optimal, the solutions must satisfy $\lambda_{R_k}(P_{max}^{(R_k)} - \sum_{i\in\mathcal{I}} Z_{ik}P_R^{(ik)}) = 0$, which means that $\lambda_{R_k} = 0$ or $(P_{max}^{(R_k)} - \sum_{i\in\mathcal{I}} Z_{ik}P_R^{(ik)}) = 0$. In this regard, the base station successively adjusts the sensitivity parameter $\lambda_{R_k}^{(t)}$ using gradient or sub-gradient methods as in

[2]The notations of PSO algorithm follow Subsection 2.4.6.

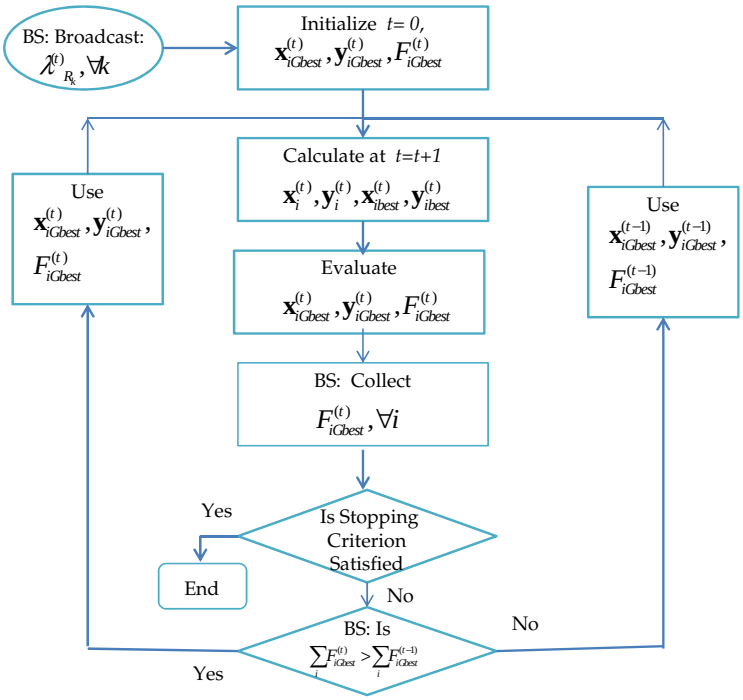

Figure 4.4 Flow Chart of the Distributed PSO Algorithm.

(2.63):

$$\lambda_{R_k}^{(t+1)} = \left(\lambda_{R_k}^{(t)} + \epsilon(P_{max}^{(R_k)} - \sum_{i\in\mathcal{I}} P_R^{t(ik)} Z_{ik}^{(t)})\right)^+ \tag{4.42}$$

where, $P_R^{t(ik)}$ and $Z_{ik}^{(t)}$ are obtained from $\mathbf{y}_{iGbest}^{(t)}$ and $\mathbf{x}_{iGbest}^{(t)}$, respectively. The distributed PSO algorithm is shown in **Figure 4.4**. Applying the distributed PSO algorithm and updating the sensitivity parameter $\lambda_{R_k}^{(t)}$ are repeated until convergence is achieved as illustrated in **Figure 4.5**. For the case of more than two relays, the binary variable **y** are updated as in [5] to satisfy constraint (4.36c). It is worth noting that, the user needs to know only her own information (the CSI between the source, the destination and all the relays in the system, can be measured at the user terminal, the CSI between the relay and the destination is feedbacked by the relay or base station to the user).

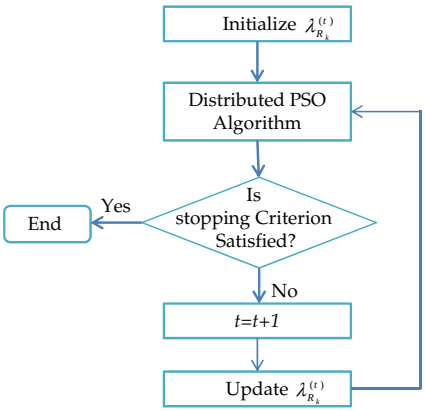

Figure 4.5 $\lambda_{R_k}^{(t)}$ Update Flowchart.

4.5 Simulation Results and Discussion

In the simulations for flat fading scenario, we consider a system of two users (S_1 and S_2), one relay and a common destination D as illustrated in **Figure 4.6**. The source S_1 is located at coordinate (−450m, 50m), S_2 is located at coordinate (400m, 0m), and the destination D is located at (0, 200m). The relay y-coordinate is fixed at 80m, and the x-coordinate varies from −1500m to 1500m to represent different channel gains. The channel gains are obtained using the simple path loss model [115] as κ/d^{α}, where α is the propagation loss factor $\alpha = 4$, d is the distance between the two transmission ends, and κ equals 0.097. The source transmitted power P_S is fixed for the two sources and set to 10mWatt. The two sources are assigned a bandwidth $W = 1$MHz each, and the capacity gap is set to $\Gamma = 1$. The noise PSD is selected as $N_0 = 1 \times 10^{-21}$Watt/Hz, unless otherwise specified [149].

Joint power and bandwidth resource allocation for the improved AF flat fading scheme is solved using various optimization methods; the exterior penalty method [12], PSO, and **Algorithm 4.1**. As clear from **Figure 4.7** the solution obtained using **Algorithm 4.1** coincides with negligible differences with the solutions obtained by PSO and exterior penalty methods. The external penalty method is difficult to tune in terms of the initial penalty factor

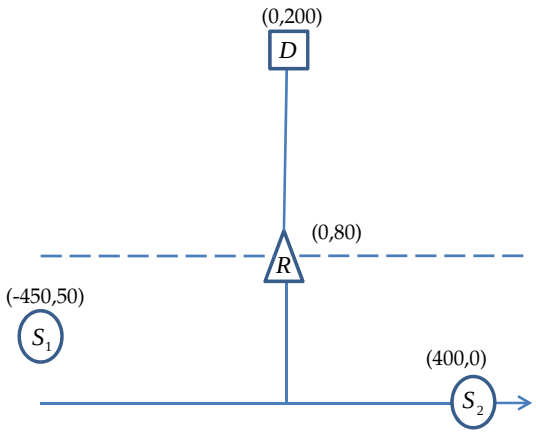

Figure 4.6 The Location of a System Consists of Two Users and a Relay.

[3] and the initial solutions. In addition, the initial penalty factor, the initial solutions and the number of iterations need to be adjusted for each relay x-coordinate. Simulation results show that obtaining the solution using the exterior penalty method becomes more difficult for low SNRs, i.e. when the problem could not be approximated by a convex function. The exterior penalty method is implemented using Powell's method for unconstrained nonlinear programming as in [12]. In contrast, PSO is not sensitive to initial solutions and no adjustment is needed for different relay x-coordinates and/or different SNR regimes but requires the evaluation and the updates for the whole population (the swarm) for number of iterations. On the other hand, simulation results show that **Algorithm 4.1** convergences to the solution in such few recursive steps. In **Figures 4.8 & 4.9**, the probability of the sum data rate of **Algorithm 4.1** to the optimal rate for l iterations with $l = 1, 2, 3, 4$ and $I = 2, 4$ users is shown. The users x,y-coordinates of the users are uniformly generated in $[-600, 600]$m for 1000 runs, the destination is set at $(0, 200)$m, and the relay is set at $(50, 80)$m. The optimal solution is obtained using the PSO method.

Figure 4.10 shows the convergence of the iterative bandwidth algorithm (4.24) for different values of θ_W and different initial values of $W_1^{(0)}$, $W_2^{(0)}$ for

[3]Modified versions of the penalty method can be used to handle some of these problems as in the augmented Lagrangian method [104]. However, the penalty method is only used to compare the result of **Algorithm 4.1**.

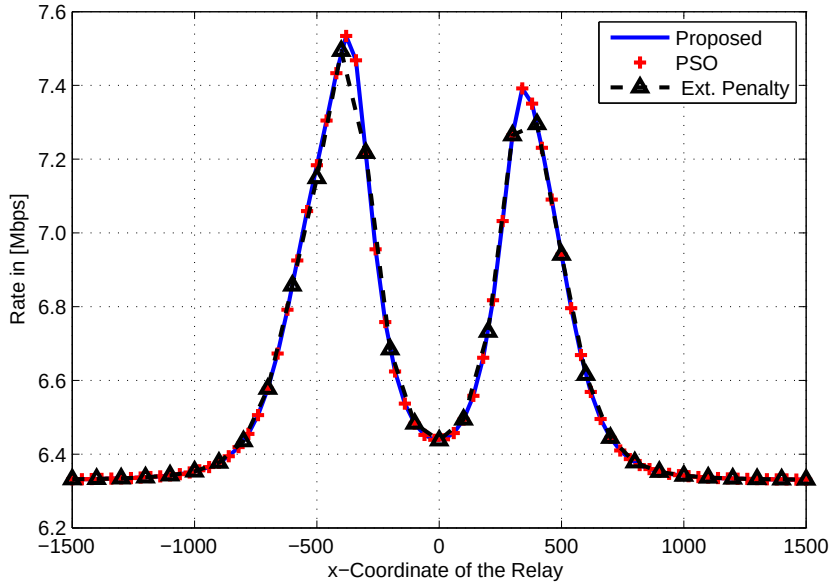

Figure 4.7 The Sum Rate Using Different Algorithms.

Table 4.1 Comparison Between Solution Methods

Algorithm	**Algorithm 4.1**	**PSO**	**Exterior Penalty**
Description	Iterative	Evolutionary	Conventional Non-Linear Program
Parameters	-	$c_1 = 2, c_2 = 2, \omega = 0.9$ Swarm Size 50, Particles: $P_R^{(1)}, P_R^{(2)}, W_1, W_2$	$\nu_t = 0.1, \beta = 2$
Convergence	3 – 5 Iterative Steps	< 50	< 50
Starting Point	Feasible Solution	Swarm of Feasible Solutions	Non-Feasible Solution
Stopping Point	The Rate is not Increasing for a Number of Iterations	All the Particles Reach a Global Solution Within a Certain Specified Tolerance	Reaching a Feasible Solution
Distributed Implementation	Possible	Possible	Not-Possible

$rx = 400$m and $P_R^{(1)} = P_R^{(2)} = 0.5$Watt.

Table 4.1, shows a comparison between different algorithms used to solve the joint resource allocation problem for the improved AF for flat fad-

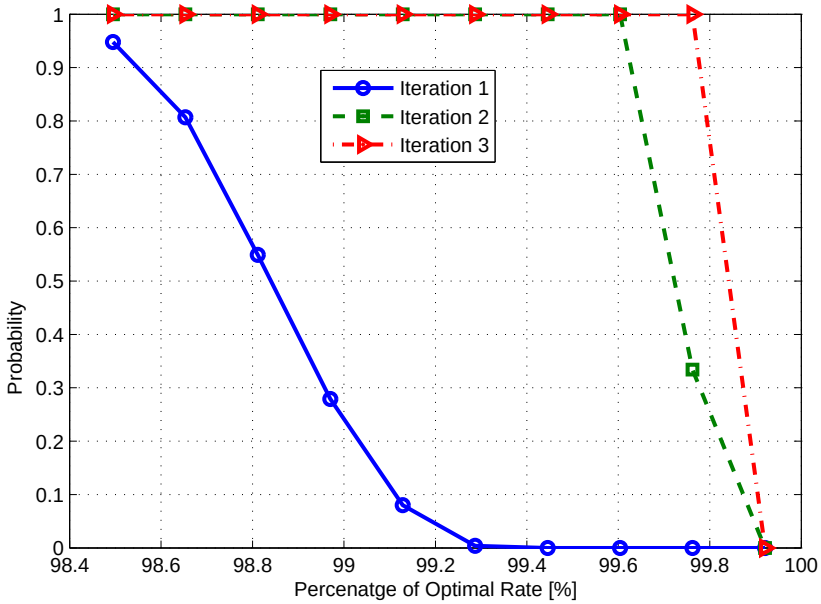

Figure 4.8 Convergence of **Algorithm 4.1** for Two Users.

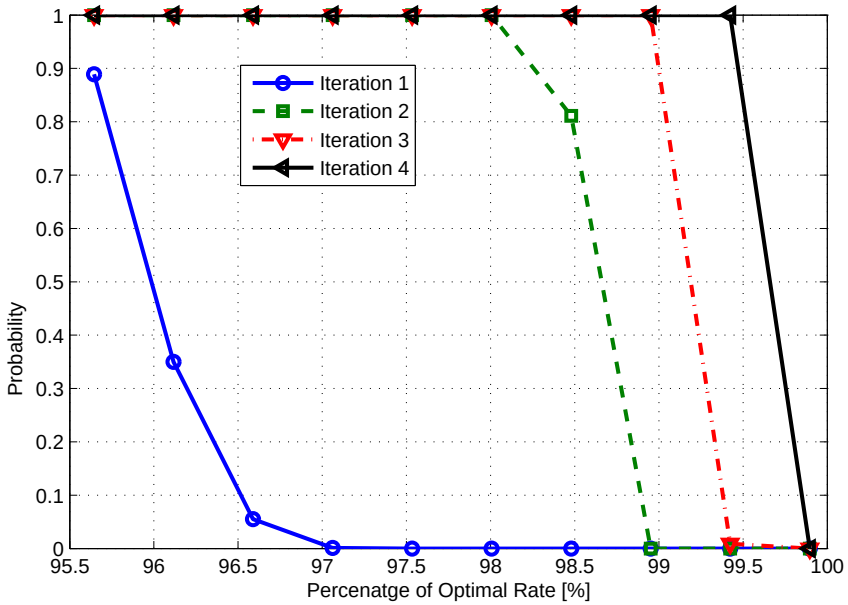

Figure 4.9 Convergence of **Algorithm 4.1** for Four Users.

ing scenario. It was noticed that **Algorithm 4.1** converges to the solution in $3-5$ iterations for any relay x-coordinate.

The convergence of the PSO algorithm for the improved AF scheme is tested for a swarm of size $P = 50$, and for different relay x-coordinates. PSO converges quickly in less than 50 iterations. The convergence for relay coordinate $x = 10$ is shown in **Figure 4.11**.

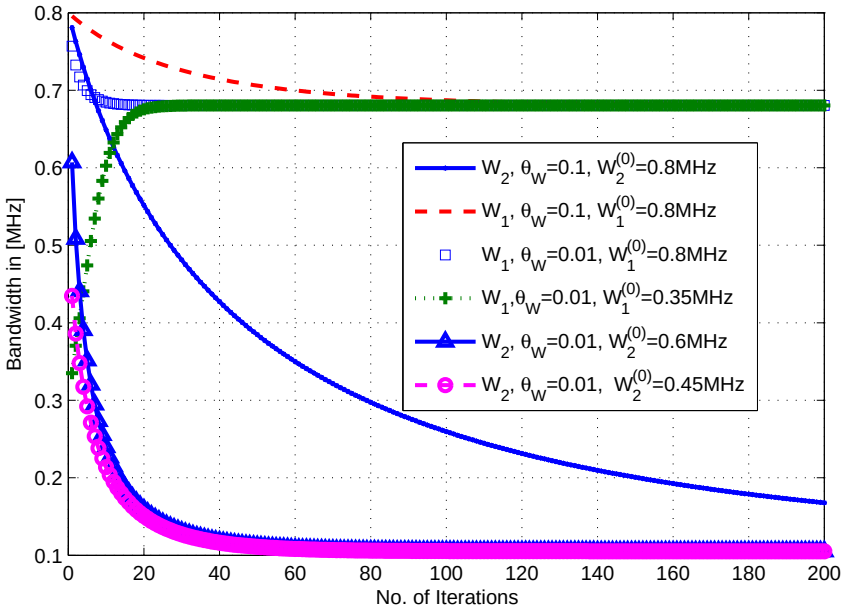

Figure 4.10 Convergence of Bandwidth Iterative Algorithm.

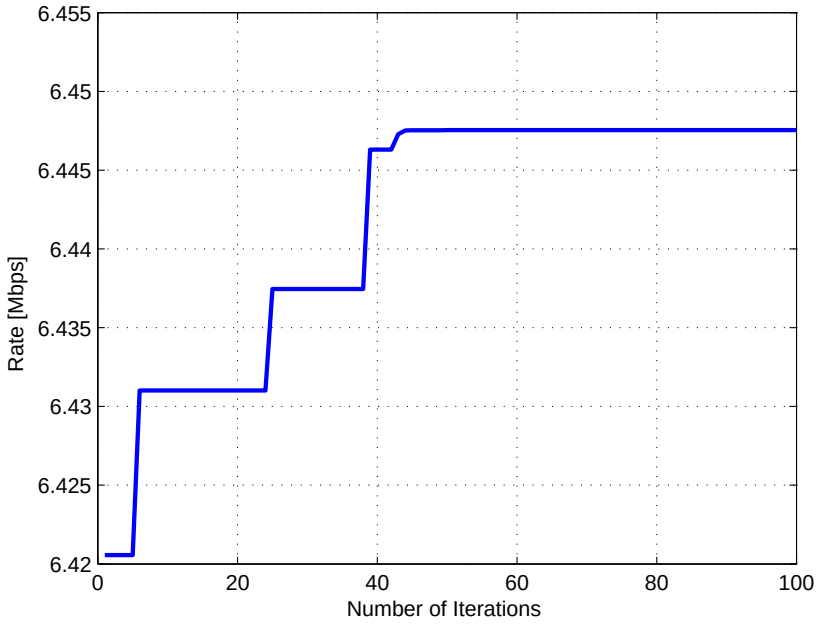

Figure 4.11 Convergence of PSO Algorithm.

Figure 4.12, shows the data rates for both users as a function of the relay x-coordinate using **Algorithm 4.1**. The region from −1500m to 0m represents a better channel gain for user S_1; the relay is much closer to source S_1 than to source S_2, so the achievable data rate for user S_1 is higher in this region than the data rate for user S_2. The same conclusion is drawn for user S_2 in the region from the 0m to 1500m.

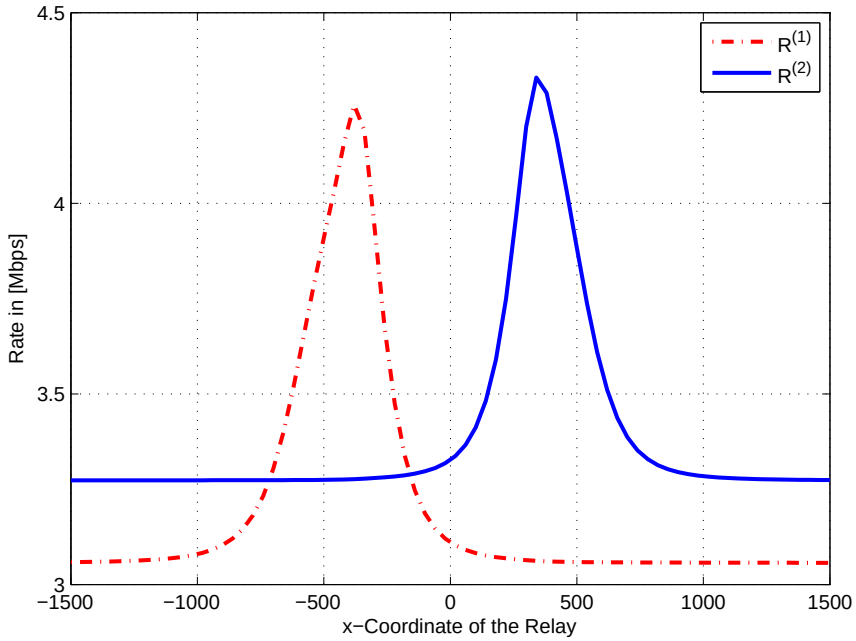

Figure 4.12 Data Rate as a Function of the Relay x-Coordinate.

Figure 4.13(a) and **Figure 4.13(b)** show the power and bandwidth allocation profiles as a function of the relay x-coordinate using **Algorithm 4.1**, which shows that the power constraint is always active, i.e. the sum of the relaying power equals $P_{max}^{(R)} = 1$Watt at all relay locations since at least one user is using the relay. Whereas, the bandwidth constraint is not active, i.e. the maximum allocated bandwidth for relaying is less than W at all relay locations; i.e. both users adapt a mixed strategy AF cooperative communication scheme.

Figure 4.14 compares the sum rate obtained using **Algorithm 4.1** with the solution of the dual problem (A.2). The dual problem was solved using a nested loop implementation as in [32]. Simulation results confirm the existence of a duality gap, so the joint resource allocation problem (4.10) could not be solved in the dual domain. The solution of the dual problem (some values of the power and bandwidth profiles) are not feasible solutions for (4.10).

Figure 4.15 shows the apparent sum rate using the approximated SNR

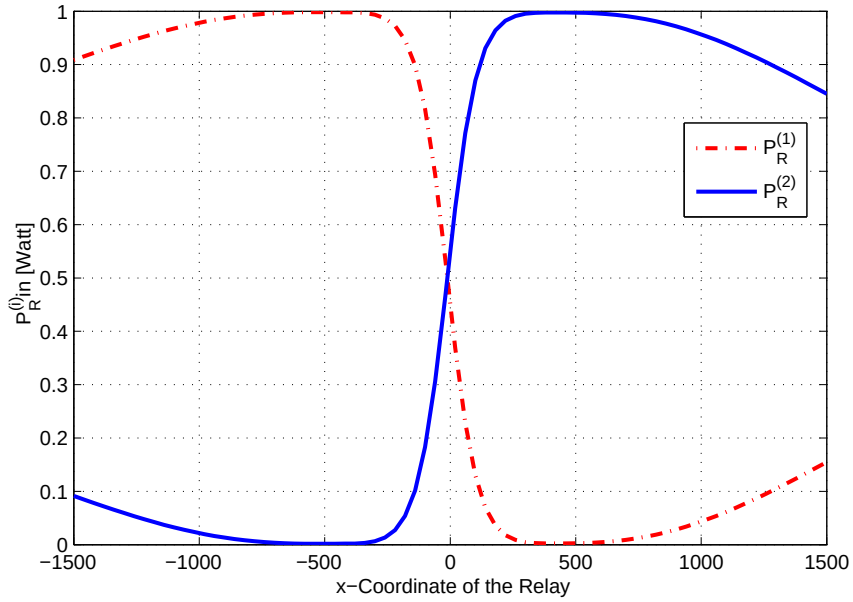

(a) Power Allocation as a Function of the Relay x-Coordinate.

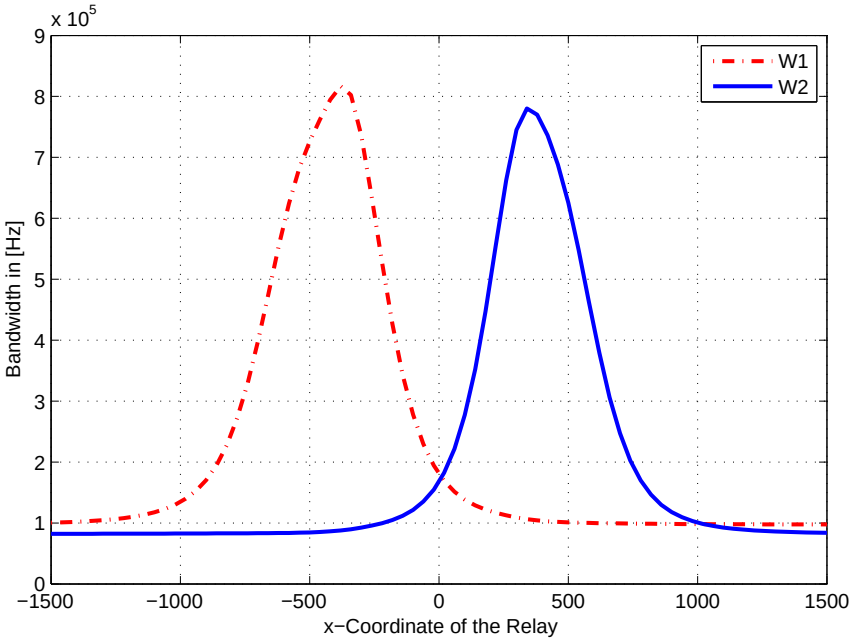

(b) Bandwidth Allocation as a Function of the Relay x-Coordinate.

Figure 4.13 Resource Allocation as a Function of the Relay x-Coordinate.

(by its upper bound) as in [56]:

$$\Gamma_{UB}^{(i)} = \frac{A_i P_R^{(i)}}{W_i(B_i + P_R^{(i)})}, \tag{4.43}$$

then, the achievable rate of user S_i using this approximation can be written

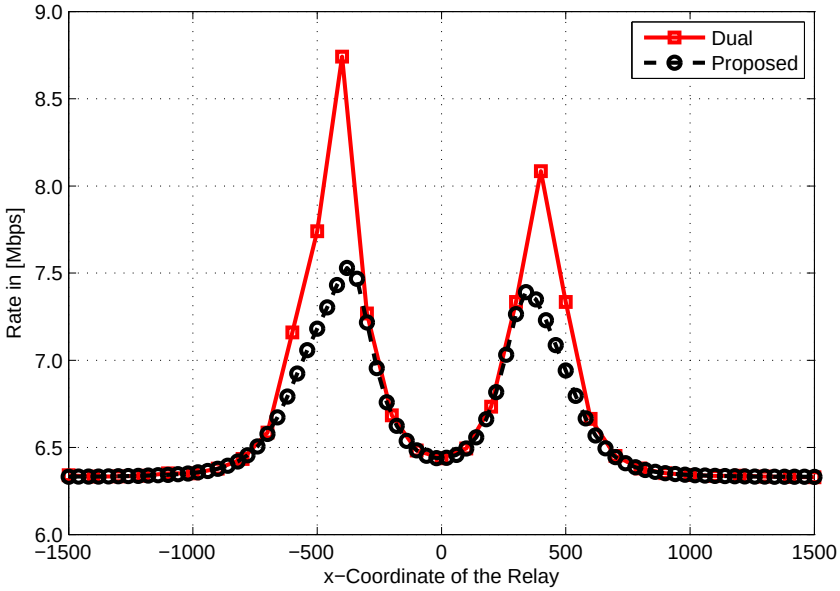

Figure 4.14 Comparison of the Sum Rate with the Solution of the Dual problem.

as:

$$R_{UB}^{(i)} = \frac{W_i}{2} \log_2(1 + \frac{\Gamma_{SD}^{(i)} + \Gamma_{UB}^{(i)}}{\Gamma}). \tag{4.44}$$

Using (4.44), the resource allocation problem is formulated as:

$$\max_{\boldsymbol{P},\boldsymbol{W}} \sum_{i \in \mathcal{I}} R_{UB}^{(i)} + R_{SD}^{(i)}, \tag{4.45a}$$

$$\text{s.t. (4.10b), (4.10c), and (4.10d).} \tag{4.45b}$$

with this approximation the sum rate becomes a jointly concave function in the power and bandwidth profiles, as can be proved by the second order derivative test (Hessian). Hence, it can be solved by any convex optimization technique. Here, the interior point method is used. The sum rate achieved by substituting the power and bandwidth profiles obtained from optimizing (4.45) in the user rate (4.9) is shown in **Figure 4.15**. Clearly, the difference between the two curves confirms that this approximation could not be used in low SNR regime, and this points out the need to solve the problem without the upper bound approximation, as is done in **Algo-**

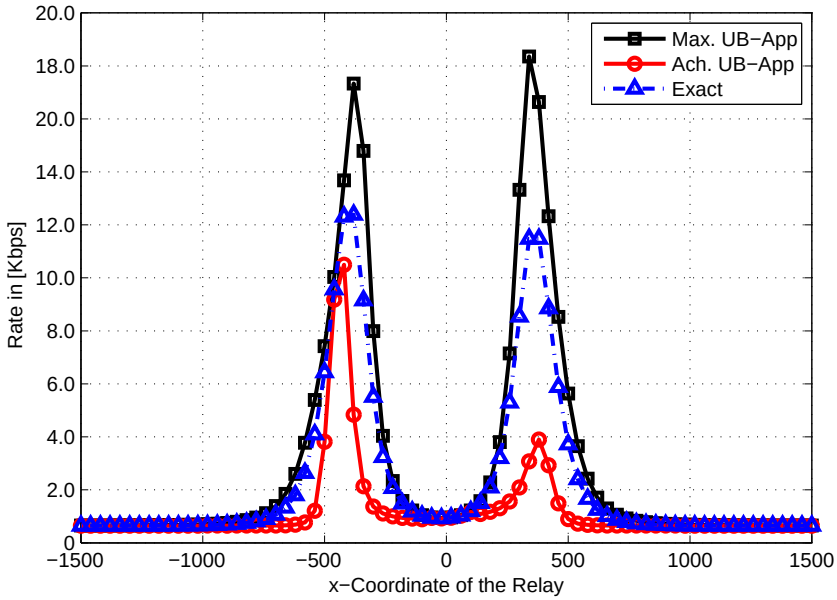

Figure 4.15 Comparison of The Sum Rate With The Solution of The Approximated Problem.

rithm 4.1. The dashed curve shows that the achievable sum rate based on the exact expression for the SNR using **Algorithm 4.1** is higher than the achievable sum rate using the approximation. To simulate a low SNR regime, the noise PSD is set at $N_0 = 1 \times 10^{-16}$Watt/Hz.

Figure 4.16 compares the sum date rate for different allocation criterion; optimum power and bandwidth FDM (improved AF), optimum power and fixed bandwidth $W_i = W$, and optimum bandwidth FDM and fixed power $P_R^{(i)} = P_{max}^{(R)}/2$, $i = 1, 2$ for the same power constraint $P_{max}^{(R)} = 1$Watt. Simulation results show that, optimal power and bandwidth allocation achieves maximum throughput compared to other allocation criterion.

Figure 4.17 shows the maximum sum rate as a function of the relay x-coordinate for different relay maximum power. Clearly, as $P_{\max}^{(R)}$ increases, the maximum sum rate increases, since AF data rate is a concave increasing function in the relay's power. Note that, the total power constraint is met with equality at the optimum solution if at least one user is using the relay. The bandwidth increase for AF relaying is beneficial until reaching a certain limit, after which the user does not benefit from the extra bandwidth as the

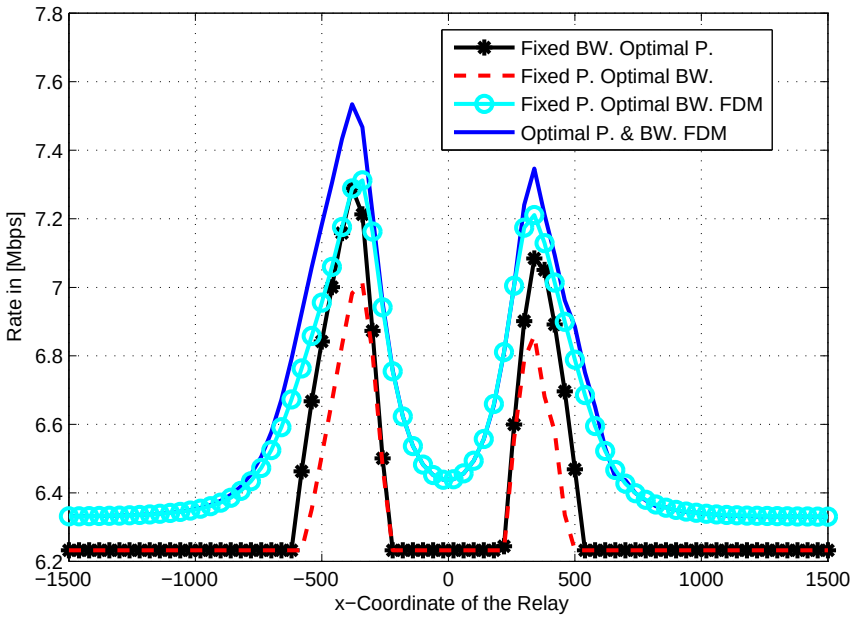

Figure 4.16 Sum Data Rate for Different Allocation Scenarios.

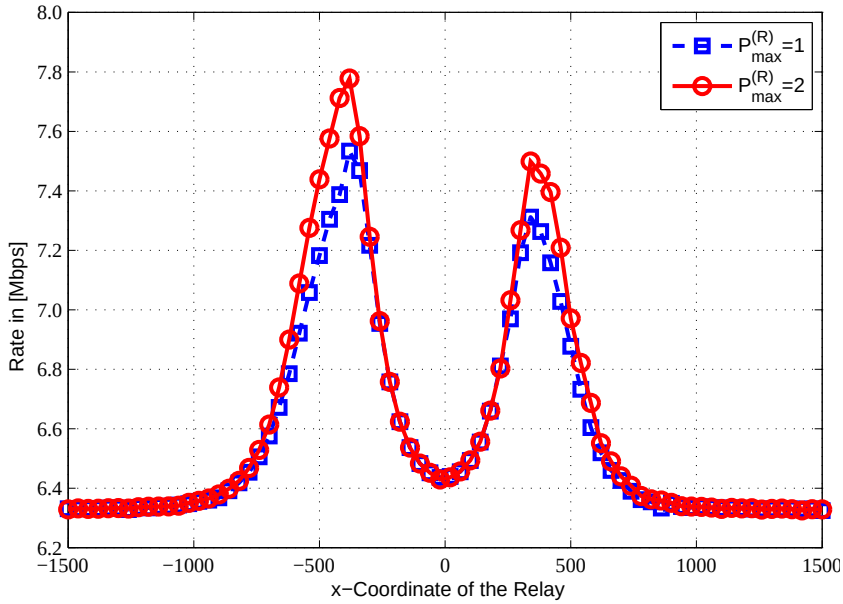

Figure 4.17 Data Rate for Different Maximum Relay Power Profiles.

noise power will increase. So the extra part of the bandwidth is used for direct transmission.

Figure 4.18 shows the sum rate as a function of the number of users. The solution obtained using **Algorithm 4.1** coincides with the solution obtained from PSO.

The effect of an additional relay bandwidth constraint $\sum_{i\in\mathcal{I}} W_i \leq W_{\max}$

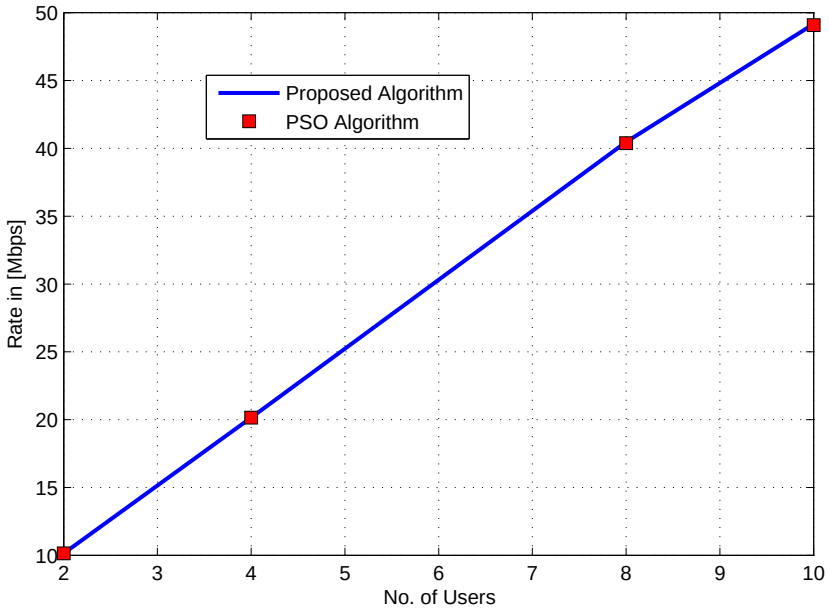

Figure 4.18 Sum Rate as a Function of the Number of Users.

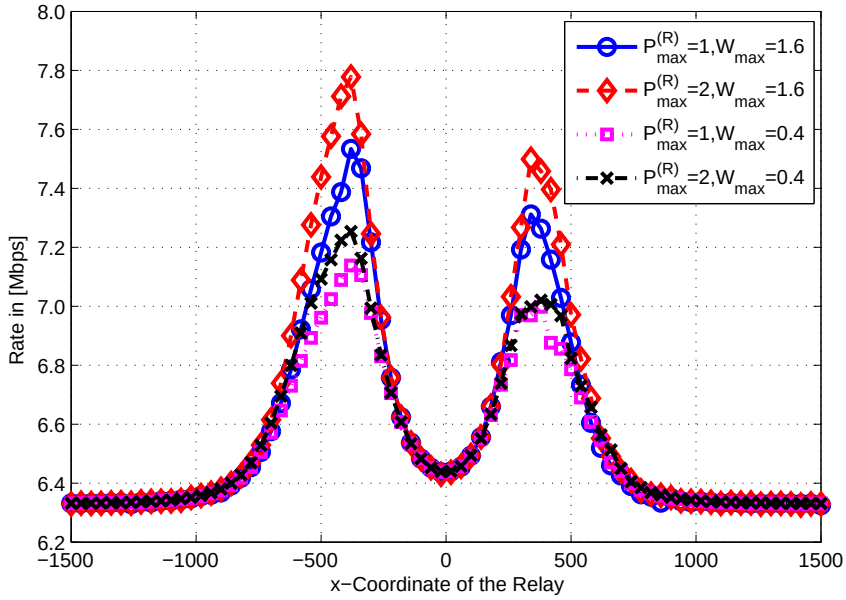

Figure 4.19 Data Rate for Different Maximum Relay Power and Bandwidth Profiles.

on the sum rate is investigated using PSO method; that is, the relay uses different frequency bands to forward the users information. The bandwidth increase is beneficial (that is, maximizes the sum rate) until reaching certain limit $W_{\max}$ = 1.6MHz, after that the user does not benefit from the extra bandwidth as the noise power will increase, the remaining bandwidth is used for direct transmission as shown in **Figure 4.19**.

Table 4.2 Achievable Data Rate for SFSC Scenario.

Scheme	Direct	AF	Improved AF
Sum Rate Using the Proposed Algorithm in [Mbps]	1.0743	1.4461	1.8520
Sum Rate Using PSO Algorithm in [Mbps]	1.0735	1.4315	1.7850

4.5.1 Frequency Selective Fading Channels Scenario

For the single carrier frequency selective channel (SCFSC) scenario, the channel gains are modeled using IEEE 802.11 channel model with 4 taps [26]. We assume an exponential power delay profile, where all taps are subject to Rayleigh fading. In our simulations, we set the relay at the origin $(0, 0)$m, the destination at $(-100, 0)$m, user S_1 at $(25, 25)$m, and user S_2 at $(25, -25)$m. For PSO, the particles are the sources' power profiles in the first and second time slots, the relaying power profile, and the start and end frequencies of AF relaying. The channel frequency response is divided into 64 sub-bands, where the channel gain is considered constant in each sub-band. The swarm size is set to 500, where each swarm consists of $64 * 3 + 4$ particles. To reduce the number of computations in **Algorithm 4.2**, we include a defined bandwidth increment for AF; i.e. AF is implemented in 0, 8, 16, $24, \cdots$, 64 adjacent sub-bands, and then we scan to find the best relaying range (the start and end frequencies). For example in the simulated scenario, we find that the relaying widths of 16, and 24 with starting frequencies of 49, and 1 for user S_1 and user S_2, respectively, achieve the maximum sum rate.

Table 4.2 compares the sum data rate for different allocation criteria. Clearly the improved AF scheme achieves the maximum sum date rate. Improved AF shows a 28.07% increase in the achievable data rate compared to full bandwidth AF. Simulation results show that **Algorithm 4.2** outperforms or achieves at least the same sum rate as the PSO algorithm. **Table 4.2** show

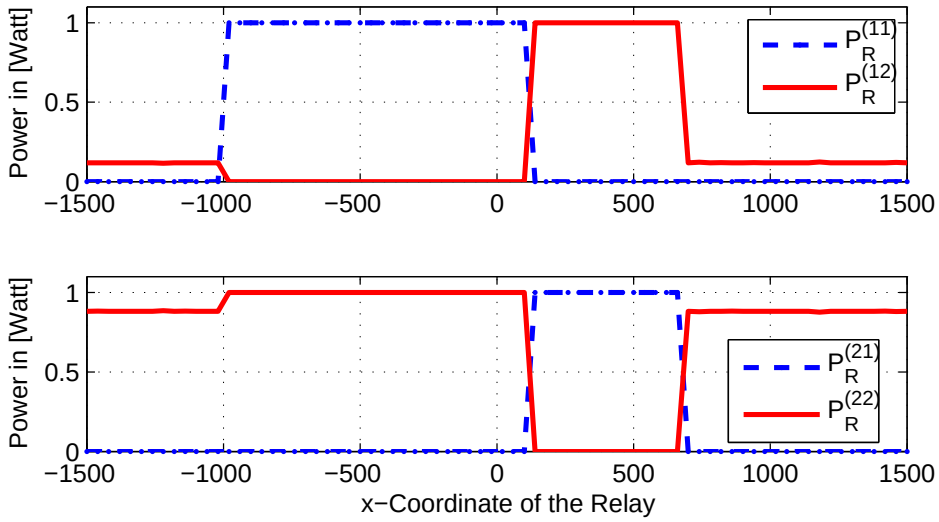

Figure 4.20 Power Allocation as a Function of Relay One x-Coordinate.

a case where **Algorithm 4.2** outperforms the PSO. Investigating this case, reveals that the PSO algorithm finds a local minimum. The implementation of the PSO does not scan all the frequency range to find the start and end points. PSO is based on generating start and end points randomly, and then updating until a stopping criterion is satisfied.

4.5.2 Relay Selection and Joint Power and Bandwidth Allocation

For multi-relay AF cooperative communication, we consider three scenarios. The first scenario consists of two sources, two relays, and a destination node; the position of the source and destination nodes are as shown in **Figure 4.6**, the x-coordinate of the first relay varies from -1500m to 1500m and the y-coordinate is fixed at 80m. The position of the second relay is fixed at x-coordinate of 100m and y-coordinate of 20m.

Figure 4.20 and **Figure 4.21** show the power and bandwidth allocation profiles, respectively as a function of the relay x-coordinate. It can be realized that the power constraint is always active, that is, the sum of the relaying power equals $P_{max}^{(R_k)} = 1$ for $k = 1, 2$ at all relay locations. Whereas,

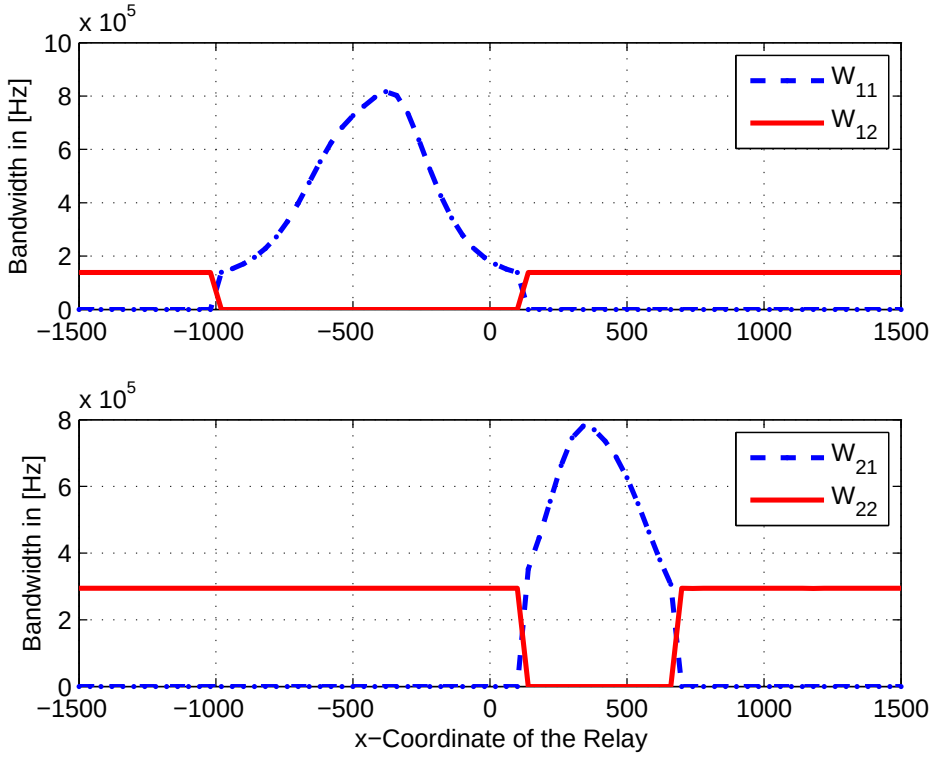

Figure 4.21 Bandwidth Allocation as a Function of Relay One x-Coordinate.

the bandwidth constraint is not active, that is, the maximum allocated bandwidth is less than W at many relay locations.

Table 4.3 shows the resource allocation for two scenarios: Scenario one consists of $I = 10$ users and $K = 2$ relays. Scenario two consists of $I = 10$ users and $K = 4$ relays. The position of the sources, relays and the destination are as shown in **Figure 4.22(a)** and **Figure 4.22(b)** for scenarios one and two, respectively. The position of the relays and destination nodes are fixed and the users are generated uniformly in the area.

Clearly, **Table 4.3** reveals that users S_6 and S_9 use only direct link for transmission in the two-relays scenario; they are not benefiting from the relays, users S_1, S_4, S_5, S_7 and S_8 use AF for all the bandwidth $W_i = W$, and the remaining users in this scenario use the mixed strategy; the bandwidth profile $W_{ik} < W$ for the selected relays. For the four relays scenario all users use mixed strategy profile $W_{ik} < W$ as shown in **Table 4.3**.

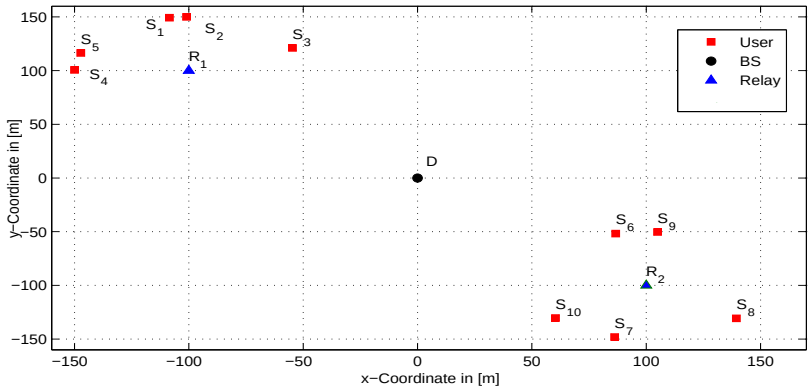

(a) Two-Relays Scenario.

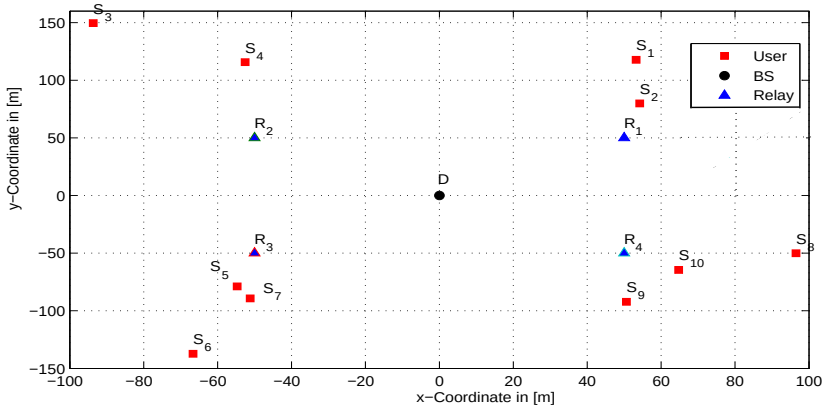

(b) Four-Relays Scenario.

Figure 4.22 Multi-Source Multi-Relay Scenario

4.5.3 Distributed PSO Algorithm

In this subsection, the sum rate of the distributed and centralized PSO algorithms is compared for one and two relay scenarios. **Figure 4.23**, compares the sum data rate for the centralized PSO and the distributed PSO algorithm for the scenario depicted in **Figure 4.6**. The relay power constraint is $P_{max}^{(R)} = 1Watt$. The initial fitness function (4.41) parameter is set as $\lambda_R^{(0)} = 0.4 \times 10^6$. The graph clearly demonstrates that the two curves coincide with negligible differences. The region from −1500m to 0m represents a better channel gain for user S_1; the relay is much closer to source S_1 than to source S_2, so the achievable data rate for user S_1 is higher in this region than the data rate of user S_2. The same conclusion is drawn for user S_2 in the region from 0m to 1500m.

Table 4.3 Resource Allocation

Two Relays Scenario										
Users	S_1	S_2	S_3	S_4	S_5	S_6	S_7	S_8	S_9	S_{10}
Relay	1	1	1	1	1	1	2	2	2	2
Power [Watt]	0.2226	0.1993	0.1469	0.2170	0.2141	0	0.3499	0.3503	0	0.2996
Bandwidth [MHz]	1	0.8965	0.6731	1	1	0	1	1	0	0.7988
Four Relays Scenario										
Users	S_1	S_2	S_3	S_4	S_5	S_6	S_7	S_8	S_9	S_{10}
Relay	1	1	2	2	3	3	3	4	4	4
Power [Watt]	0.1699	0.8300	0.2666	0.7334	0.5865	0.0706	0.3429	0.1779	0.2092	0.6128
Bandwidth [MHz]	0.6997	0.7878	0.7363	0.7044	0.7815	0.7118	0.7339	0.7040	0.7134	0.8085

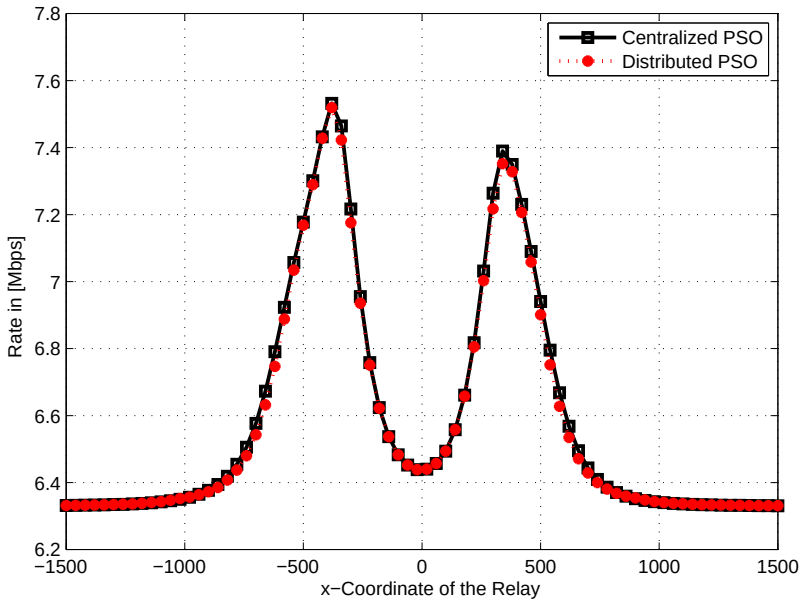

Figure 4.23 Comparison of the Sum Rate for the Distributed and the Centralized PSO Algorithms.

Figure 4.24(a), compares the data rate for the centralized PSO and the distributed PSO algorithm for joint relay selection and resource allocation for two users two relays scenario; the x-coordinate of the first relay varies from -1500m to 1500m and the y-coordinate is fixed at 80m. The position of the second relay is fixed at x-coordinate of 100m and y-coordinate of 20m. The coordinates of the two sources and the destination nodes are similar to

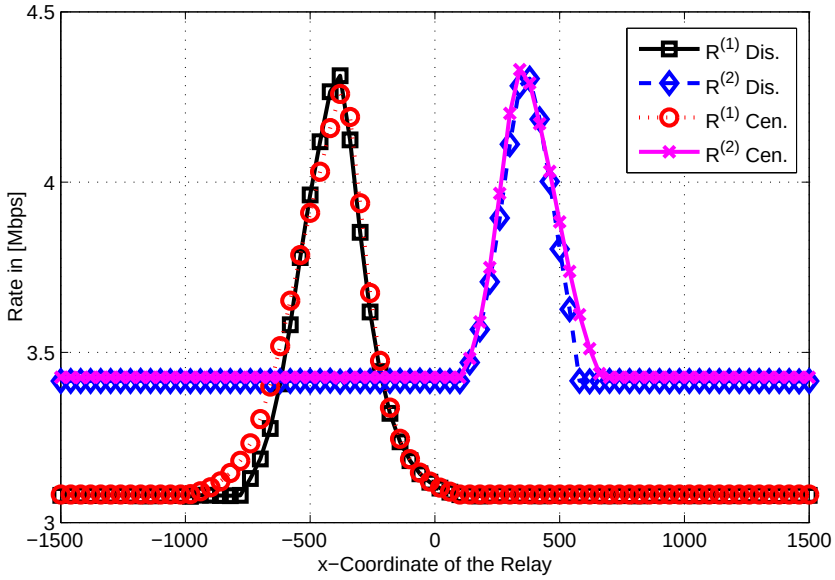

(a) Data Rates of User S_1 and User S_2.

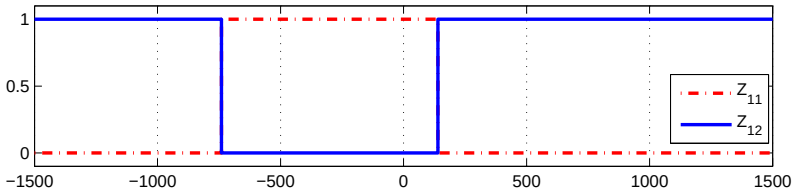

(b) Relay Selection for User S_1.

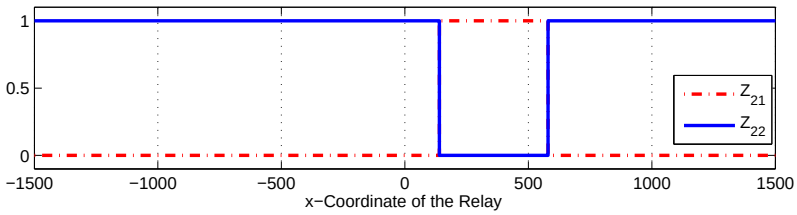

(c) Relay Selection for User S_2.

Figure 4.24 Resource Allocation as a Function of Relay One x-Coordinate Using the Distributed and Centralized PSO Algorithms.

those in scenario one.

Figure 4.24(b) and **Figure 4.24(c)** show the relay selection for user S_1 and user S_2 respectively. $Z_{11} = 1$, $Z_{12} = 1$, $Z_{21} = 1$, and $Z_{22} = 1$ is interpreted as selecting relay R_1 for user S_1, selecting relay R_2 for user S_1, selecting relay R_1 for user S_2, and selecting relay R_2 for user S_2, respectively.

4.6 Conclusions

In this chapter, we investigate joint power and bandwidth resource allocation for multiple users improved AF cooperative communication scheme for flat and frequency selective fading channels in the presence of a direct link between the source and destination nodes. In formulating the problem, we consider that the user may use an AF cooperative scheme with diversity for part of the bandwidth, and the remaining bandwidth is used for direct transmission without diversity in order to benefit from all available degrees of freedom. The optimization problem is formulated to maximize the sum rate. The problem is not jointly concave in the power and bandwidth profiles. A recursive algorithm is proposed to solve the problem which separates it into power and bandwidth subproblems. In addition, for the frequency selective fading scenario, the source power profile is to be optimized in the first and second time slots to utilize resources efficiently. The joint power and bandwidth allocation scenario outperforms both the power allocation for fixed bandwidth profile and the bandwidth allocation for fixed power profile scenarios. Joint relay selection and power and bandwidth allocation for multi source multi relay for flat fading using the improved AF cooperative communication scheme is addressed using PSO algorithm.

CHAPTER5

STACKELBERG GAME FOR JOINT POWER AND BANDWIDTH ALLOCATION FOR AF RELAYING

In this chapter, power and bandwidth pricing is proposed as incentives for cooperative communications, where a relay with limited resources is willing to sell its resources; power and bandwidth to multiple users, aiming to maximize its revenue. The users are competing for the relay resources. Stackelberg market framework is used to model a single relay multiple users AF cooperative communication system. The relay is the leader player in the Stackelberg game, the power and bandwidth prices are used to model the strategies of the leader, whereas, the users are the followers in the Stackelberg game. The power and bandwidth demands are used to model the follower strategies. No coordination or information exchange between the competing users is assumed in this model. The users determine the power and bandwidth demands according to Nash equilibrium; each user maximizes her own utility function.

The introduction and related research are presented in Section 5.1. AF Stackelberg game model and notations are introduced in Section 5.2. In Section 5.3, AF Stackelberg game is analyzed; the existence and uniqueness of Nash equilibrium (solution) are proven. Distributed algorithms for finding the power and bandwidth prices and the power and bandwidth profiles are also proposed. Numerical results are confirmed in Sections 5.4. Conclusions

are drawn in Section 5.5.

5.1 Introduction

In Chapter 4, we considered a system viewpoint by jointly allocating power and bandwidth profiles, aiming to maximize the sum rate for a multi user single relay modified AF cooperative communication system. An optimization approach was followed to find the solution. In this chapter, we want to capture the interactions between the users and the relay, aiming to maximize the relay revenue from selling its resources, power and bandwidth. The relay may not belong to the system or may support more than one system. In this sense, game theory is used to model the interactions between the users and the relay. The user determines the required power and bandwidth profiles based on power and bandwidth prices, her channel gains, and other users competing for the relay resources. The relay sets the prices aiming to maximize its revenue from selling its resources.

Game theory has been recently used for resource allocation in cooperative communications [28, 110, 127, 149, 156, 169]. In [110], the authors proposed a non-cooperative game framework for pricing a single relay AF multi-user system, aiming to maximize the relay revenue or the desirable system utility. The relay sets prices and correspondingly charges the users depending on the quality of the received signal. The user aims to maximize its utility through power allocation. An iterative algorithm is proposed to reach Nash equilibrium. In [169], the authors modeled the bandwidth sharing among the users in a single relay cooperative communication system using non-cooperative game, the utility function represents the achievable throughput in the presence of a pricing term. A distributed algorithm is proposed to find Nash equilibrium.

In [127], the authors studied Gaussian interference relay game (GIRG), where each user seeks an optimum power across a set of hops, and showed

that the GIRG for two users has a unique Nash equilibrium, which can be reached in a distributed manner. In addition, the conditions under which Nash equilibrium is Pareto optimal were studied. In [156], interference was considered as a detrimental factor for the performance of both AF and DF systems. The uniqueness and existence of Nash equilibrium are proven. Furthermore, a distributed algorithm to reach Nash equilibrium is implemented.

In [149], the authors proposed a Stackelberg game to perform power allocations in a multi-relay system. The relays announce the prices per unit of power to all active users in the system, this action can be modeled as the leader action in the Stackelberg game. The user determines her requirement of the power based on the prices and her channel gains between the source, relay and destination nodes. This action is modeled as the follower action in the Stackelberg game. The proposed model helps competing relays to maximize their own utility by asking optimal prices, and helps sources to find the relays with better locations and buys the optimal amount of power from them. In [28], the authors used Stackelberg game to model one relay and multi-users. The relay determines the price per unit bandwidth, and according to the price, each user determines the amount of bandwidth required for relaying her data.

In the aforementioned works, either power or bandwidth profiles are considered for allocation. However, in a relay network, both power and bandwidth allocation need to be accounted for. In this chapter, building on previous research in [28, 149, 163, 170], power and bandwidth allocation for AF single relay multi-user system is studied using Stackelberg game. In this sense, a utility function with pricing factors is formulated to represent the user demands for power and bandwidth. The pricing is used as a reimbursement for the relay as a compensation for using its resources. Relaying requirements are both power and bandwidth, which can be translated in

the language of game theory to the costs of power and bandwidth used for relaying. Because power and bandwidth are two different commodities, the cost of each depends on its availability and the competition between the users. Our goal in this chapter is to devise a revenue-maximizing pricing scheme for the relay for both power and bandwidth resources. Thus, a non-cooperative AF power and bandwidth game is played by the users (followers) in a Stackelberg game, where the goal of the leader (relay) is to set prices for the power and bandwidth to maximize its revenue.

Our model differs from previous research [28, 149, 163, 170] in several key aspects: First, in [149] the authors' main concern is to select the relays and determines the purchased power from each relay, i.e. the competition is between the relays to determine the prices, not between the users as in our work. The authors proposed a distributed algorithm to determine the relayed power price. Whereas in our research, the competition is between the users and the relay to determine Stackelberg Nash Equilibrium. In addition, we proposed a nested distributed algorithm; the inner algorithm is to determine the power and bandwidth allocation for the users for given power and bandwidth prices, and the outer algorithm is to determine the power and bandwidth prices. Second, we consider power and bandwidth as two commodities that the user wants to pay for, and the relay resources are limited and appeared in the user utility function. The case of joint power and bandwidth allocation is a generalized framework that can be used to study power allocation for unlimited bandwidth, and bandwidth allocation for unlimited power. The first case can be interpreted as bandwidth demand is less than the available bandwidth at the relay, i.e. there is no competition for bandwidth. The second case can be interpreted as power demand is less than the relay maximum power, i.e. there is no competition for power. The two cases can be investigated using our proposed framework as special cases. In our model, the relay by selling to the users the sub-bands of

its dedicated bandwidth and controlling the relaying power in each sub-band, aims to maximize its own revenue. The utility function of each user is formulated to be a jointly concave function in the power and bandwidth. None of the utility functions in [149] and [28] can be used to jointly allocate power and bandwidth, since the analysis of NE becomes untraceable. Third, the users and the relay in our model are assigned orthogonal frequency bands, whereas in [163, 170] two types of users are considered: a primary user who is assigned a specific time slot and secondary users who are not assigned any time slots. The secondary users relay the primary user information to access the channel, i.e. obtain a portion of the primary user time slot. Fourth, we investigate the uniqueness of the equilibrium using the concavity of the utility function and the theory of concave potential games. Whereas in [28, 149, 163, 170], there is no potential function associated with the utility function, and uniqueness is investigated using standard function theory.

5.2 AF Stackelberg Model

The system under consideration is depicted in **Figure 5.1**, where $\mathcal{I} = \{1, ..., I\}$ is the set of active users. Sender (Source) nodes S_i for $i \in \mathcal{I}$ are communicating with their destination terminals $D_1, D_2, \ldots, D_M$, where $M \leq I$ over stable channels with coefficients $h_{SD}^{(i)}$. The source-destination pair (S_i, D_m) is referred to as the ith user without loss of generality. In cellular systems we can consider all the destination nodes as one destination node, which is the common base station. The relay station R is used to improve the reliability of the communication between the source-destination pair using a simple AF cooperative scheme. In AF, the relay scales the received data or part of it and transmits it using a different frequency band in the relaying phase. Considering FDMA and assuming no interference between the users; each active user utilizes a different frequency band. In addition, the relay uses

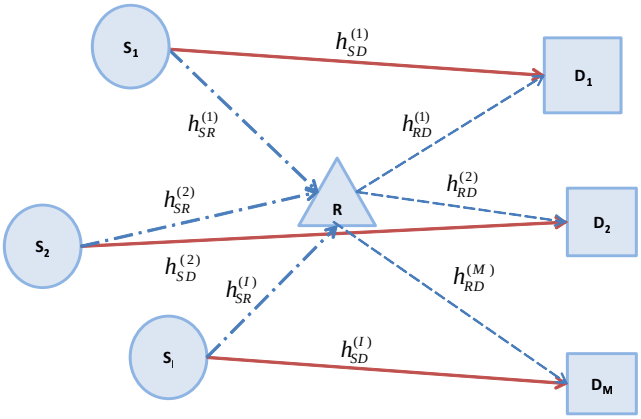

Figure 5.1 System Model: Multi-Source Destination Pairs and One Relay.

different frequency bands for relaying the user's information. Each user will use two time slots T_1 and T_2 in a TDM scenario. In the first time slot T_1, the source broadcasts its signal to the relay node and to its corresponding destination terminal. In the second time slot T_2, the relay amplifies the received signal without decoding and forwards it to the destination terminal. At the destination terminal the received messages are co-phased weighted and then combined using MRC. CSI from the source to the destination, from the source to the relay, and from the relay to the destination are assumed to be known at the destination node.

In order to explore the cooperative diversity, two fundamental questions need to be answered: First, what is the optimum power P_i for the AF cooperative scheme? Second, what is the optimum bandwidth W_i for the AF cooperative scheme? To answer these questions, we define users as buyers, relays as sellers, and power and bandwidth as commodities in a Stackelberg game framework as follows.

Definition 5.2.1 The Stackelberg Leadership Model [40]: *is a two-stage game in which the leader player (relay) moves first by announcing the prices of the power* Π_P *(per unit power) and bandwidth* Π_W *(per unit bandwidth), then the follower user moves sequentially by selecting the quantity of the power and bandwidth that maximizes her own utility function. The solution of the Stackelberg model is called* Stackelberg Nash Equilibrium (SNE). *SNE consists of* $(P_i^{(SE)}, W_i^{(SE)}, \Pi_P^{(SE)}\Pi_W^{(SE)}), \forall i \in$

$\mathcal{I}$, *where* $P_i^{(SE)}, W_i^{(SE)}$ *are the power and bandwidth strategies that maximize user i utility function to be defined later, and* $\Pi_P^{(SE)}$, $\Pi_W^{(SE)}$ *are the power and bandwidth prices respectively (the relay strategies) that maximize the relay utility function to be defined later.*

Users (Buyers): The users are represented by the buyers who seek to get the most benefits at the least possible expenses. The users are the followers in the Stackeberg game. In this context, we choose to define the utility function of user i as follows:

$$U_i = \sqrt{Z\, W_i \log\Big(\frac{1+\Gamma_{SD}^{(i)}+\Gamma_{SRD}^{(i)}}{1+\Gamma_{SD}^{(i)}}\Big)} - \Pi_P P_i - \Pi_W W_i - \frac{X}{P_{\max} - \sum_{j\in\mathcal{I}} P_j} - \frac{Y}{W_{\max} - \sum_{j\in\mathcal{I}} W_j}, \tag{5.1}$$

where X and Y are system constants that reflect the effect of the availability of the resources on the utility function. Z is related to the gain in the rate by using the relay. Non-identical Z_i can also be used for non-homogeneous systems (that is, different data rates or priorities) to reflect the ith user willingness to pay for the relay. Π_P and Π_W are the power and bandwidth selling prices per unit power and per unit bandwidth respectively.

The SNR for the ith user at the destination node without relaying $\Gamma_{SD}^{(i)}$ can be expressed as [149]:

$$\Gamma_{SD}^{(i)} = \frac{P_S |h_{SD}^{(i)}|^2}{\sigma^2}. \tag{5.2}$$

The end-to-end SNR utilizing the relay $\Gamma_{SRD}^{(i)}$ for AF scheme can be obtained as [174]:

$$\Gamma_{SRD}^{(i)} = \frac{P_S P_i |h_{SR}^{(i)}|^2 |h_{RD}^{(i)}|^2}{\sigma^2(\sigma^2 + P_S|h_{SR}^{(i)}|^2 + P_i|h_{RD}^{(i)}|^2)}, \tag{5.3}$$

where $\Gamma_{SRD}^{(i)}$ can be written in a simplified form as [149]:

$$\Gamma_{SRD}^{(i)} = \frac{A_i P_i}{B_i + P_i}, \tag{5.4}$$

with A_i and B_i are respectively computed as:

$$A_i = \frac{P_S|h_{SR}^{(i)}|^2}{\sigma^2}, \tag{5.5a}$$

$$B_i = \frac{P_S|h_{SR}^{(i)}|^2 + \sigma^2}{|h_{RD}^{(i)}|^2}. \tag{5.5b}$$

In formulating the utility function U_i, the following are considered:

1. Relate the utility function to a meaningful quantity in cooperative communication, which is in this case the square-root of the rate achieved using AF cooperation scheme. The square root, and the linear pricing are used to guarantee joint concavity of the utility function with respect to the power and bandwidth purchased from the relay, and to discourage the users from asking for high power and/or bandwidth demands.

2. The term $(1+\Gamma_{SD}^{(i)})$ is used in the denominator $\left(\frac{1+\Gamma_{SD}^{(i)}+\Gamma_{AF}^{(i)}}{1+\Gamma_{SD}^{(i)}}\right)$ to ensure zero AF data rate at zero relay power and/ or at zero relay bandwidth.

3. The available power and bandwidth of the relay are limited to $P_{\max}$ and $W_{\max}$.

4. The power and bandwidth purchased by the ith user depend on the relay prices Π_P and Π_W.

5. The linear pricing terms $-\Pi_P P_i - \Pi_W W_i$ are used to control power and bandwidth allocations separately.

6. The availability of power and (or) bandwidth encourage users to buy higher power and or higher bandwidth.

7. The competition for the resources between the users is captured by $\frac{X}{P_{\max}-\sum_{j\in\mathcal{I}} P_j}$ and $\frac{Y}{W_{\max}-\sum_{j\in\mathcal{I}} W_j}$ in the user utility function.

Relay (Seller): For the relay, the utility function is simply defined as:

$$U_R = (\Pi_P - C_P) \sum_{j \in \mathcal{I}} P_j + (\Pi_W - C_W) \sum_{j \in \mathcal{I}} W_j, \tag{5.6}$$

where C_P and C_W are the costs per unit power and per unit bandwidth respectively. The selected relay utility function, sums the benefit from selling the power and bandwidth resources separately to simplify the analysis of the equilibrium, but other functions can be used to achieve different objectives. Note that, $P_i = 0$ results in $W_i = 0$ and $W_i = 0$ results in $P_i = 0$ in the user utility function. So, the cases of selling power alone (with zero bandwidth) and bandwidth alone (with zero power) will not occur using this formulation. On the other hand, the cases of selling power with a fixed relaying bandwidth and selling bandwidth for a fixed relaying power can be investigated using this formulation. In addition, the relay utility sums monetary units (profits) not power and bandwidth profiles.

5.3 Stackelberg Game Analysis

Based on (5.1), the optimization problem for the *i*th user (buyer) can now be formulated as:

$$\max_{P_i, W_i} U_i \quad \text{s.t. } \{P_i \geq 0,\ 0 \leq W_i \leq W\}, \tag{5.7}$$

whereas, the optimization problem for the relay (seller) based on (5.6) can be formulated as:

$$\max_{\Pi_P, \Pi_W} U_R \quad \text{s.t. } \{\Pi_P \geq C_P,\ \Pi_W \geq C_W\}. \tag{5.8}$$

Since the Stackelberg game is a two stage game, two games are defined: the power bandwidth game (PWG) at the users' side, and the prices game (ΠG) at the relay side.

5.3.1 Users Side

The Power-Bandwidth Game (PWG) in a Stackelberg game model is defined as [115]:

Definition 5.3.1 *The PWG is defined as* $PWG = [\mathcal{I}, (\boldsymbol{P}_i, \boldsymbol{W}_i), U_i(.)]$, *which denotes the non-cooperative power and bandwidth purchases for a given power and bandwidth prices* Π_P *and* Π_W, *respectively.* $\boldsymbol{P}_i$ *and* $\mathbf{W}_i$ *are the power and bandwidth strategy sets of user i, and* $U_i(\cdot)$ *is the ith user utility function. Each user selects a power level* P_i *such that* $P_i \in \boldsymbol{P}_i$ *and a bandwidth share* W_i *such that* $W_i \in \boldsymbol{W}_i$. *Let the power vector* $\boldsymbol{P} = (P_1, \ldots, P_I) \in \vec{\boldsymbol{P}}$ *denotes the outcome of the game in terms of the selected power levels for all users, where* $\vec{\boldsymbol{P}}$ *is the set of all feasible power vectors. Furthermore, let the bandwidth vector* $\boldsymbol{W} = (W_1, \ldots, W_I) \in \vec{\boldsymbol{W}}$ *denotes the outcome of the game in terms of the selected bandwidth shares of all users, where* $\vec{\boldsymbol{W}}$ *is the set of all feasible bandwidth vectors. The resulting utility for the ith user is* $U_i\Big(\boldsymbol{P}, \boldsymbol{W}; (\Pi_P, \Pi_W)\Big)$. *An alternative notation* $U_i\Big(\boldsymbol{P}_i, \boldsymbol{W}_i, \boldsymbol{P}_{-i}, \boldsymbol{W}_{-i}; (\Pi_P, \Pi_W)\Big)$ *can also be used to emphasize that the ith user has control only over its own power and bandwidth strategies* $\boldsymbol{P}_i$ *and* $\boldsymbol{W}_i$ *respectively. In this sense,* $\boldsymbol{W}_{-i}$, *and* $\boldsymbol{P}_{-i}$ *denote a vector consisting of elements of the power* $\boldsymbol{P}$ *and bandwidth* $\boldsymbol{W}$ *excluding the ith element.*

Definition 5.3.2 *For a given* Π_P *and* Π_W, *the* Nash equilibrium *of the PWG is a two dimensional* $|\mathcal{I}|$ *tuples* $(W_i^* \geq 0,\ P_i^* \geq 0)$ *satisfying the following objective function* $\forall i \in \mathcal{I}$ *[40]:*

$$\max_{W_i,\, P_i} U_i\Big((W_i, P_i), (\boldsymbol{W}_{-i}^*, \boldsymbol{P}_{-i}^*); (\Pi_P, \Pi_W)\Big) = U_i\Big((W_i^*, P_i^*), (\boldsymbol{W}_{-i}^*, \boldsymbol{P}_{-i}^*); (\Pi_P, \Pi_W)\Big), \tag{5.9a}$$

$$s.t.\ 0 \leq W_i \leq W_{\max} - W_{-i}, \tag{5.9b}$$

$$0 \leq P_i \leq P_{\max} - P_{-i}, \tag{5.9c}$$

where $W_{-i} = \sum_{j \in \mathcal{I}, j \neq i} W_j$, *and* $P_{-i} = \sum_{j \in \mathcal{I}, j \neq i} P_j$. *At the Nash equilibria, given the*

power levels, bandwidth shares of the other users, no user can improve her utility level by making individual changes in its own power and/or bandwidth profiles, that is, no user has the incentive to unilaterally change her own strategy [105]. The power level and bandwidth share chosen by a rational self optimizing user constitute the best response to the power and bandwidth strategies chosen by the other users.

After defining the PWG and its Nash equilibrium, existence, uniqueness, analytical solution, adaptive algorithm, and the convergence of the adaptive algorithm are investigated as explained next.

(A) **Existence of a Nash Equilibrium**

The existence of the Nash equilibrium for the *PWG* is assured by **Theorem 2.5.3**. Anchored in **Theorem** (2.5.3), the *PWG* admits at least one Nash equilibrium, because the strategy space for each user is a convex and compact set ($0 \leq W_i \leq W_{\max} - W_{-i}$), ($0 \leq P_i \leq P_{\max} - P_{-i}$) and the payoff function of each user is continuous on **P** and **W**. Furthermore, the joint concavity of the utility function of user i in P_i and W_i can be proved by using the second derivative test as [149]:

$$\frac{\partial^2 U_i}{\partial W_i^2} = \frac{-1}{3\sqrt{W_i^3}} \sqrt{Z \log\left(\frac{1+\Gamma_{SD}^{(i)}+\Gamma_{SRD}^{(i)}}{1+\Gamma_{SD}^{(i)}}\right)} - \frac{2Y}{(W_{\max}-\sum_{j\in\mathcal{I}} W_j)^3}, \tag{5.10a}$$

$$\frac{\partial^2 U_i}{\partial P_i^2} = \frac{-\sqrt{ZW_i}}{2\sqrt{\log\left(\frac{1+\Gamma_{SD}^{(i)}+\Gamma_{SRD}^{(i)}}{1+\Gamma_{SD}^{(i)}}\right)}} \left(\frac{(\frac{A_iB_i}{P_i+B_i})^2}{(1+\Gamma_{SD}^{(i)}+\Gamma_{SRD}^{(i)})^2} + \frac{2A_iB_i}{(P_i+B_i)^3}(1+\Gamma_{SD}^{(i)}+\Gamma_{SRD}^{(i)}) \right) - \frac{\sqrt{W_i}(\frac{A_iB_i}{P_i+B_i})^2}{(1+\Gamma_{SD}^{(i)}+\Gamma_{SRD}^{(i)})^2 \sqrt{\left(Z\log\left(\frac{1+\Gamma_{SD}^{(i)}+\Gamma_{SRD}^{(i)}}{1+\Gamma_{SD}^{(i)}}\right)\right)^3}} - \frac{2X}{(P_{\max}-\sum_{j\in\mathcal{I}} P_j)^3}, \tag{5.10b}$$

$$\frac{\partial^2 U_i}{\partial W_i \partial P_i} = \frac{-A_iB_i\sqrt{Z}}{3\sqrt{W_i^3}\sqrt{\log\left(\frac{1+\Gamma_{SD}^{(i)}+\Gamma_{SRD}^{(i)}}{1+\Gamma_{SD}^{(i)}}\right)}(1+\Gamma_{SD}^{(i)}+\Gamma_{SRD}^{(i)})(P_i+B_i)^2}. \tag{5.10c}$$

It is straightforward to show that: $\frac{\partial^2 U_i}{\partial W_i^2} < 0$, $\frac{\partial^2 U_i}{\partial P_i^2} < 0$ and $\frac{\partial^2 U_i}{\partial W_i^2}\frac{\partial^2 U_i}{\partial P_i^2} - \left(\frac{\partial^2 U_i}{\partial W_i \partial P_i}\right)^2 \geq 0$. This completes the proof of the concavity. Hence quasi-

concavity is guaranteed for the proposed utility function U_i. Therefore, at least one Nash equilibrium exists.

(B) **Uniqueness of Nash Equilibrium**

The uniqueness of Nash equilibrium can be proved using the potential game theory. The *PWG* is an exact potential game as can be proved by (2.91), where $\frac{\partial U_i}{\partial W_i} = \frac{\partial V}{\partial W_i}$, and $\frac{\partial U_i}{\partial P_i} = \frac{\partial V}{\partial P_i}$ with a potential function $V(\cdot)$ defined as:

$$V(\mathbf{P},\mathbf{W}) = \sum_{i\in\mathcal{I}} \sqrt{Z\, W_i \log\Big(\frac{1+\Gamma_{SD}^{(i)}+\Gamma_{AF}^{(i)}}{1+\Gamma_{SD}^{(i)}}\Big)} - \Pi_P \sum_{i\in\mathcal{I}} P_i - \Pi_W \sum_{i\in\mathcal{I}} W_i - \frac{X}{P_{\max}-\sum_{i\in\mathcal{I}} P_i} - \frac{Y}{W_{\max}-\sum_{i\in\mathcal{I}} W_i}, \tag{5.11}$$

The potential function $V(\cdot)$, has many important properties. First, if user i is maximizing the potential function $V(\cdot)$ instead of his own utility function $U_i(\cdot)$, keeping the other users' strategies fixed, this will not affect the Nash equilibrium [8]. Second, the potential function $V(\cdot)$ is continuously differentiable, and *strictly concave* in the nonnegative-orthant bounded by the hyperplanes $P_{\max} = \sum_{j\in\mathcal{I}} P_j$ and $W_{\max} = \sum_{j\in\mathcal{I}} W_j$. It admits a unique solution (Nash equilibrium), which coincides with the only user by user Nash equilibrium. $U_i(\cdot)$ is a strictly concave function with respect to user i strategies as can be proved by the second derivative test (5.10). This proves the *uniqueness* of Nash equilibrium for the *PWG*.

(C) **Analytical Solution of Nash Equilibrium**

The derivative of the utility function of the ith user $U_i(\cdot)$ with respect to

W_i, and P_i, $\forall i \in \mathcal{I}$ are respectively obtained as:

$$\frac{\partial U_i}{\partial W_i} = \frac{\sqrt{Z \log\left(\frac{1+\Gamma_{SD}^{(i)}+\Gamma_{SRD}^{(i)}}{1+\Gamma_{SD}^{(i)}}\right)}}{2\sqrt{W_i}} - \Pi_W - \frac{\Upsilon}{(W_{\max} - \sum_{j\in\mathcal{I}} W_j)^2}, \tag{5.12a}$$

$$\frac{\partial U_i}{\partial P_i} = \frac{\sqrt{ZW_i}}{2\sqrt{\log\left(\frac{1+\Gamma_{SD}^{(i)}+\Gamma_{SRD}^{(i)}}{1+\Gamma_{SD}^{(i)}}\right)}} \frac{1}{1+\Gamma_{SD}^{(i)}+\Gamma_{SRD}^{(i)}} \frac{A_i B_i}{(P_i+B_i)^2} - \Pi_P - \frac{X}{(P_{\max} - \sum_{j\in\mathcal{I}} P_j)^2}. \tag{5.12b}$$

To obtain the Nash equilibrium (P_i^*, W_i^*) $\forall i \in \mathcal{I}$ the partial derivatives $\frac{\partial U_i}{\partial W_i}$ and $\frac{\partial U_i}{\partial P_i}$ are set as:

$$\frac{\partial U_i}{\partial W_i} = 0 \text{ and } \frac{\partial U_i}{\partial P_i} = 0 \text{ if } P_i^* \geq 0 \text{ and } W_i^* \geq 0. \tag{5.13}$$

Solving for the partial derivatives in (5.13), we arrive at:

$$\Pi_W + \frac{\Upsilon}{(W_{\max} - \sum_{j\in\mathcal{I}} W_j)^2} = \frac{\sqrt{Z \log\left(\frac{1+\Gamma_{SD}^{(i)}+\Gamma_{SRD}^{(i)}}{1+\Gamma_{SD}^{(i)}}\right)}}{2\sqrt{W_i}}, \tag{5.14}$$

and

$$\Pi_P + \frac{X}{(P_{\max} - \sum_{j\in\mathcal{I}} P_j)^2} = \frac{\sqrt{ZW_i}}{2\sqrt{\log\left(\frac{1+\Gamma_{SD}^{(i)}+\Gamma_{SRD}^{(i)}}{1+\Gamma_{SD}^{(i)}}\right)}} \frac{1}{(1+\Gamma_{SD}^{(i)}+\Gamma_{SRD}^{(i)})} \frac{A_i B_i}{(P_i+B_i)^2}. \tag{5.15}$$

The best response $BR_i(\mathbf{P}_{-i}, \mathbf{W}_{-i})$ of user i is described implicitly using (5.14) and (5.15). The solutions of (5.14) and (5.15) are the user's i power and bandwidth pair (P_i, W_i) as a function of $(\mathbf{P}_{-i}, \mathbf{W}_{-i})$, which are called the best response curves for user i. In order to find Nash equilibrium for all users, $2|\mathcal{I}|$ simultaneous equations must be solved. Since the left-hand-side (LHS) of (5.14)) and (5.15) are the same for all users on the right-hand-side (RHS), with some simplifications we obtain the follow-

ing solution:

$$\frac{A_i B_i}{\Big((1+\Gamma_{SD}^{(i)})(P_i+B_i)+A_i P_i\Big)(P_i+B_i)} = \frac{A_k B_k}{\Big((1+\Gamma_{SD}^{(k)})(P_k+B_k)+A_k P_k\Big)(P_k+B_k)}. \tag{5.16}$$

To solve for P_i in terms of P_k in (5.16), a second order algebraic equation is formulated. The non-negative solution is then derived as:

$$P_i = \frac{-\alpha_1^{(i)} + \sqrt{\alpha_1^{(i)2} - 4\alpha_2^{(i)}\alpha_0^{(i)}}}{2\alpha_2^{(i)}}, \tag{5.17}$$

where $\alpha_0^{(i)}$, $\alpha_1^{(i)}$, and $\alpha_2^{(i)}$ are respectively defined as follows:

$$\alpha_0^{(i)} = -\frac{A_i B_i}{A_k B_k}\Big((1+\Gamma_{SD}^{(k)}+A_k)P_k^2 + (2(1+\Gamma_{SD}^{(k)})+A_k B_k)P_k + (1+\Gamma_{SD}^{(k)})B_k^2\Big) + (1+\Gamma_{SD}^{(i)})B_i^2, \tag{5.18a}$$

$$\alpha_1^{(i)} = 2(1+\Gamma_{SD}^{(i)}) + A_i B_i, \tag{5.18b}$$

$$\alpha_2^{(i)} = 1+\Gamma_{SD}^{(i)} + A_i. \tag{5.18c}$$

It is worth noting that, only $\alpha_0^{(i)}$ depends on P_k. Using (5.18) the overall SNR $\Gamma_{SRD}^{(i)}$ of user i can be computed as a function of P_k as:

$$\Gamma_{SRD}^{(i)} = \frac{A_i\Big(-\alpha_1^{(i)} + \sqrt{\alpha_1^{(i)2} - 4\alpha_2^{(i)}\alpha_0^{(i)}}\Big)}{2\alpha_2^{(i)}B_i - \alpha_1^{(i)} + \sqrt{\alpha_1^{(i)2} - 4\alpha_2^{(i)}\alpha_0^{(i)}}}. \tag{5.19}$$

Similarly, the total sum power $\sum_{i\in\mathcal{I}} P_i$ can also be expressed in terms of P_k as:

$$\sum_{i\in\mathcal{I}} P_i = -\frac{1}{2}\sum_{i\in\mathcal{I}}\frac{\alpha_1^{(i)}}{\alpha_2^{(i)}} + \frac{1}{2}\sum_{i\in\mathcal{I}}\sqrt{\Big(\frac{\alpha_1^{(i)}}{\alpha_2^{(i)}}\Big)^2 - 4\Big(\frac{\alpha_0^{(i)}}{\alpha_2^{(i)}}\Big)}. \tag{5.20}$$

To simplify the forthcoming notations, we define $F_0^{(i)} = \alpha_0^{(i)}/\alpha_2^{(i)}$, $F_1^{(i)} =$

$\alpha_1^{(i)}/\alpha_2^{(i)}$, and define F_1 and F_2 as follows:

$$F_1 = -\frac{1}{2}\sum_{i\in\mathcal{I}} F_1^{(i)}, \tag{5.21a}$$

$$F_2 = \sum_{i\in\mathcal{I}} \frac{1}{2}\sqrt{F_1^{(i)2} - 4F_0^{(i)}}. \tag{5.21b}$$

The total sum power can now be simplified as:

$$\sum_{i\in\mathcal{I}} P_i = F_1 + F_2. \tag{5.22}$$

For the bandwidth, similar solutions can be sought as follows. The user i bandwidth W_i can be expressed in terms of W_k and P_k from (5.14) as:

$$W_i = W_k \frac{\log\left(\frac{1+\Gamma_{SD}^{(i)}+\Gamma_{SRD}^{(i)}}{1+\Gamma_{SD}^{(i)}}\right)}{\log\left(\frac{1+\Gamma_{SD}^{(k)}+\Gamma_{SRD}^{(k)}}{1+\Gamma_{SD}^{(k)}}\right)}. \tag{5.23}$$

Substituting (5.17), (5.19), (5.22) in (5.14) and (5.15), with some simplifications, the kth user power P_k is obtained as a solution of the following:

$$\frac{ZE}{4D} = \Pi_W + \frac{Y}{\left[W_{\max} - (4/Z)D^2E^{-2}\sum_{i\in\mathcal{I}}\log\left(\frac{1+\Gamma_{SD}^{(i)}+\Gamma_{SRD}^{(i)}}{1+\Gamma_{SD}^{(i)}}\right)\right]^2}, \tag{5.24}$$

where $D = \Pi_P + \frac{X}{(P_{\max}-F_1-F_2)^2}$, and $E = \frac{A_kB_k/(B_k+P_k)^2}{1+\Gamma_{SD}^{(k)}+\Gamma_{SRD}^{(k)}}$. Similarly, the kth user bandwidth W_k can be obtained as:

$$W_k = (4/Z)D^2E^{-2}\log\left(\frac{1+\Gamma_{SD}^{(k)}+\Gamma_{SRD}^{(k)}}{1+\Gamma_{SD}^{(k)}}\right). \tag{5.25}$$

The solutions of (5.24) and (5.25) are the Nash equilibrium P_k^*, W_k^*, $\forall k \in \mathcal{I}$. If the solutions are not feasible, i.e. if $P_k^* < 0$ and/or $W_k^* < 0$ or $W_k^* > W$, it is necessary to modify the solutions such that $\tilde{P}_k^* = \max(P_k^*, 0)$ for the power and $\tilde{W}_k^* = \min(\max(W_k^*, 0), W)$ for the bandwidth. It is clear from (5.24) that P_k^* depends on Π_W, Π_P, the channel gains of user

k, and all other users' channels gains. The solutions in (5.24) and (5.25) are obtained in a centralized fashion provided that exchange of information between users is possible. However, because exchange of information between users expends the system resources power and bandwidth; each user needs to know all other users channel gains which is impractical. The proposed non-cooperative game framework is used to represent the interactions among the users and the relay. The selfish behavior allows to reduce the signaling overheads; the users and the relay are trying to maximize their corresponding utility functions individually. So if a centralized solution is applied at the relay side, the problem is converted to an optimization problem and no-gain is obtained from using the game theory framework.

(D) **The Dynamic Adaptive PWG**

A solution that can be implemented at the user side not at the relay side with minimum information exchange between the users and the relay without coordination between the users (non-cooperative game) is recommended. This can be found using dynamic game algorithms. Based on the theorem of infinite potential game, the adopted algorithm to find the Nash equilibrium for the PWG can be formulated as [101, 103]:

$$P_i^{(t+1)} = P_i^{(t)} + \theta_{P_i} P_i^{(t)} \frac{\partial U_i}{\partial P_i}, \tag{5.26a}$$

$$W_i^{(t+1)} = W_i^{(t)} + \theta_{W_i} W_i^{(t)} \frac{\partial U_i}{\partial W_i}, \tag{5.26b}$$

where $P_i^{(t+1)}$ and $W_i^{(t+1)}$ are the power and bandwidth updates at iteration $t+1$, and θ_{W_i} and θ_{P_i} are adjustment speed parameters. At the Nash equilibrium $P_i^{(t+1)} = P_i^{(t)}$ and $W_i^{(t+1)} = W_i^{(t)}$. The effects of θ_{W_i} and θ_{P_i} on the convergence and the stability of the algorithm can be studied as in [1, 103]. The value of the partial derivative $\frac{\partial U_i}{\partial P_i}$ can be estimated

by the ith user using the central difference method. The ith user inquires the relay of the function $\frac{X}{P_{\max}-\sum_{j\in\mathcal{I}} P_j}$ at iteration t by submitting the power $P_i^{(t)} \pm \epsilon_P$, where ϵ_P is a small number, then the ith user observes the response of the relay and estimates $\frac{\partial U_i}{\partial P_i} \approx \frac{U_i^+(.)-U_i^-(.)}{2\epsilon_P}$. In a similar manner the ith user estimates $\frac{\partial U_i}{\partial W_i} = \frac{U_i^+(.)-U_i^-(.)}{2\epsilon_W}$, where ϵ_W is a small number represents the incremental change of the required bandwidth (the ith user inquires the relay of the function $\frac{Y}{W_{\max}-\sum_{j\in\mathcal{I}} W_j}$ at iteration t by submitting the bandwidth $W_i^{(t)} \pm \epsilon_W$). The ith user keeps updating its power and bandwidth until reaching Nash equilibrium $P_i^{(t+1)} = P_i^{(t)}$ and $W_i^{(t+1)} = W_i^{(t)}$, where $\frac{\partial U_i}{\partial P_i}$ and $\frac{\partial U_i}{\partial W_i}$ are equal to zero at Nash equilibrium.

Given the power and bandwidth update rules (5.26), two different approaches can be used to update the power and bandwidth profiles, namely, Gauss-Seidel and Jacobi based algorithms [117]. In Gauss-Seidel, the users update their strategies sequentially, whereas in Jacobi algorithms, the users update their strategies in parallel. In this research the Jacobi method is adopted and its stability is investigated next.

(E) **Stability Analysis of the *PWG* Distributed Algorithm**

Stability analysis of the distributed power and bandwidth update algorithm (5.26) can be investigated using the eigenvalues λ_l of the Jacobian matrix. The updated functions (5.26) will converge to the Nash equilibrium, if and only if, all the eigenvalues of the Jacobian matrix are inside the unit circle (i.e. $|\lambda_l| < 1 \ \forall, l \in 2I$) [103].

The Jacobian matrix J_{PW} for the distributed power and bandwidth up-

date algorithms (5.26) is as:

$$J_{PW} = \begin{pmatrix} \frac{\partial P_1^{(t+1)}}{\partial P_1^{(t)}} & \cdots & \frac{\partial P_1^{(t+1)}}{\partial P_I^{(t)}} & \frac{\partial P_1^{(t+1)}}{\partial W_1^{(t)}} & \cdots & \frac{\partial P_1^{(t+1)}}{\partial W_I^{(t)}} \\ \vdots & \vdots & \vdots & \vdots & \vdots & \vdots \\ \frac{\partial P_I^{(t+1)}}{\partial P_1^{(t)}} & \cdots & \frac{\partial P_I^{(t+1)}}{\partial P_I^{(t)}} & \frac{\partial P_I^{(t+1)}}{\partial W_1^{(t)}} & \cdots & \frac{\partial P_I^{(t+1)}}{\partial W_I^{(t)}} \\ \vdots & \vdots & \vdots & \vdots & \vdots & \vdots \\ \frac{\partial W_1^{(t+1)}}{\partial P_1^{(t)}} & \cdots & \frac{\partial W_1^{(t+1)}}{\partial P_I^{(t)}} & \frac{\partial W_1^{(t+1)}}{\partial W_1^{(t)}} & \cdots & \frac{\partial W_1^{(t+1)}}{\partial W_I^{(t)}} \\ \vdots & \vdots & \vdots & \vdots & \vdots & \vdots \\ \frac{\partial W_I^{(t+1)}}{\partial P_1^{(t)}} & \cdots & \frac{\partial W_I^{(t+1)}}{\partial P_I^{(t)}} & \frac{\partial W_I^{(t+1)}}{\partial W_1^{(t)}} & \cdots & \frac{\partial W_I^{(t+1)}}{\partial W_I^{(t)}} \end{pmatrix}. \tag{5.27}$$

Using the eigenvalues of the Jacobian matrix, θ_{W_i} and θ_{P_i} can be determined in a centralized way to ensure the stability of the adaptive algorithm, which are broadcasted to all users. In the simulations, we set $\theta_{W_i} = \theta_W$ and $\theta_{P_i} = \theta_P$, for $i \in \mathcal{I}$ to ensure synchronization of the convergence of the distributed algorithm among all users on the network [28].

5.3.2 Relay Side

The prices game (ΠG) in the the Stackelberg game model is defined as:

Definition 5.3.3 *Let* $\Pi G = [(\mathbf{\Pi_P}, \mathbf{\Pi_W}), (\boldsymbol{P}, \boldsymbol{W}), U_R(\cdot)]$ *denote the non-cooperative power and bandwidth prices for the given power and bandwidth demands* $\boldsymbol{P}$ *and* $\boldsymbol{W}$ *respectively.* $\mathbf{\Pi_P}$ *and* $\mathbf{\Pi_W}$ *are the power price and bandwidth price strategy sets, respectively. The relay selects a power price profile* $\Pi_P \in \mathbf{\Pi_P}$ *and a bandwidth price profile* $\Pi_W \in \mathbf{\Pi_W}$. *Finally,* $U_R(\cdot)$ *is the relay utility function as defined in* (5.6).

To complete the analysis of the Stackelberg game, the power and bandwidth prices Π_P and Π_W need to be selected to maximize the relay revenue (utility function of the relay). The revenue function (5.6) has the following properties: first, $U_R = 0$ when both $\Pi_W = C_W$, and $\Pi_P = C_P$. Second, U_R approaches

zero when both $\Pi_W \to \infty$, and $\Pi_P \to \infty$. Third, the feasible prices Π_W and Π_P are greater or equal to the costs ($\Pi_W \geq C_W, \Pi_P \geq C_P$). Fourth, for a finite number of users the revenue is finite.

Substituting the Nash equilibrium power and bandwidth (5.24) and (5.25) into (5.6), and differentiating U_R with respect to Π_W, Π_P, and setting to zero, we get:

$$\frac{\partial U_R}{\partial \Pi_P} = \sum_{j \in \mathcal{I}} P_j^* + (\Pi_P - C_P) \sum_{j \in \mathcal{I}} \frac{\partial P_j^*}{\partial \Pi_P} + (\Pi_W - C_W) \sum_{j \in \mathcal{I}} \frac{\partial W_j^*}{\partial \Pi_P} = 0, \tag{5.28a}$$

$$\frac{\partial U_R}{\partial \Pi_W} = \sum_{j \in \mathcal{I}} W_j^* + (\Pi_W - C_W) \sum_{j \in \mathcal{I}} \frac{\partial W_j^*}{\partial \Pi_W} + (\Pi_P - C_P) \sum_{j \in \mathcal{I}} \frac{\partial P_j^*}{\partial \Pi_W} = 0. \tag{5.28b}$$

After investigating the effect of changing the prices Π_P, and Π_W on the Nash equilibrium P_i^* on (5.24), using numerical simulations we found that P_i^* is a decreasing function of Π_P if Π_W is kept constant, and also P_i^* is a decreasing function of Π_W when Π_P is kept constant. In addition, investigating the concavity of the relay utility function U_R with respect to Π_P and Π_W at the users demands P_i^*, and W_i^* shows that U_R is a jointly concave function for the range of prices $\underline{\Pi}_P < \Pi_P < \overline{\Pi}_P$, and $\underline{\Pi}_W < \Pi_W < \overline{\Pi}_W$. It is difficult to obtain a closed form expressions for $\underline{\Pi}_P$, $\overline{\Pi}_P$, $\underline{\Pi}_W$, and $\overline{\Pi}_W$, but they can be computed numerically by satisfying the negative semi-definiteness of the Hessian matrix. The Hessian matrix H is defined as:

$$H = \begin{bmatrix} \frac{\partial^2 U_R}{\partial \Pi_P^2} & \frac{\partial^2 U_R}{\partial \Pi_P \partial \Pi_W} \\ \frac{\partial^2 U_R}{\partial \Pi_P \partial \Pi_W} & \frac{\partial^2 U_R}{\partial \Pi_W^2} \end{bmatrix}.$$

The solutions (5.28a), (5.28b), and (5.24) constitute the Stackelberg equilibrium $\Pi_P^{(SE)}$, $\Pi_W^{(SE)}$, $P_i^{(SE)}$. The Stackelberg equilibrium bandwidth $W_i^{(SE)}$ can be obtained using (5.25). In order to compute the Stackelberg equilibrium $[(\Pi_P^{(SE)}, \Pi_W^{(SE)}), (P_i^{(SE)}, W_i^{(SE)})]$ a centralized process is required, which may be impractical. A distributed algorithm can be used to search Nash equilib-

rium prices. The ΠG is treated as a dynamic game, the updates of this game, need to be slower than the updates in algorithm (5.26), to guarantee convergence. In this sense, the relay sets the initial prices $\Pi_P^{(0)}$ and $\Pi_W^{(0)}$ for the users, based on the power and bandwidth demands of the users, the relay adjusts its prices to achieve maximum revenue as follows:

$$\Pi_P^{(t+1)} = \Pi_P^{(t)} + \beta_P \Pi_P^{(t)} \frac{\partial U_R}{\partial \Pi_P}, \tag{5.29a}$$

$$\Pi_W^{(t+1)} = \Pi_W^{(t)} + \beta_W \Pi_W^{(t)} \frac{\partial U_R}{\partial \Pi_W}, \tag{5.29b}$$

where $\Pi_P^{(t+1)}$ and $\Pi_W^{(t+1)}$ are the power and bandwidth prices updates at iteration $t+1$, and β_P and β_W are adjustment speed parameters. At the Nash equilibrium $\Pi_P^{(t+1)} = \Pi_P^{(t)}$ and $\Pi_W^{(t+1)} = \Pi_W^{(t)}$. The value of the partial derivative $\frac{\partial U_R}{\partial \Pi_P}$ can be estimated at the relay using the central difference method; the relay inquires the users about their power and bandwidth demands by submitting the prices $(\Pi_P^{(t)} \pm \epsilon_{\Pi_P}, \Pi_W^{(t)})$, where ϵ_{Π_P} is a small number representing the incremental change in the power price. The relay then observes the response of the users and estimates $\frac{\partial U_R}{\partial \Pi_P} \approx \frac{U_R^+(.) - U_R^-(.)}{2\epsilon_{\Pi_P}}$. In a similar fashion, the relay estimates $\frac{\partial U_R}{\partial \Pi W}$ by submitting the prices $(\Pi_W^{(t)} \pm \epsilon_{\Pi_W}, \Pi_P^{(t)})$ and inquires about the users power and bandwidth demands, then estimates $\frac{\partial U_R}{\partial \Pi_W} \approx \frac{U_R^+(.) - U_R^-(.)}{2\epsilon_{\Pi_W}}$, where ϵ_{Π_W} is a small number that representing the incremental change in the bandwidth price. Stability analysis of the prices update algorithm can also be investigated in a similar fashion to the analysis followed in Subsection 5.3.1(E) using the eigenvalues of the prices' Jacobian matrix. The prices Jacobian matrix is defined as:

$$J_\Pi = \begin{pmatrix} \frac{\partial \Pi_P^{(t+1)}}{\partial \Pi_P^{(t)}} & \frac{\partial \Pi_P^{(t+1)}}{\partial \Pi_W^{(t)}} \\ \frac{\partial \Pi_W^{(t+1)}}{\partial \Pi_P^{(t)}} & \frac{\partial \Pi_W^{(t+1)}}{\partial \Pi_W^{(t)}} \end{pmatrix}. \tag{5.30}$$

The constants β_P and β_W are then selected to ensure that the absolute value of the eigenvalues of the prices' Jacobian matrix (5.30) are less than one. The stability of the price update algorithm is analyzed based on localization at the fixed points by considering the eigenvalues of the price Jacobian matrix and substituting equations (5.28a) and (5.28b) in (5.30). The fixed points are $(0,0)$, $(\Pi_{P_0},0)$, $(0,\Pi_{W_0})$, and $(\Pi_P^{(SNE)},\Pi_W^{(SNE)})$. A fixed point is stable if and only if the eigenvalues λ_i are inside the unit circle of the complex plane, i.e. $|\lambda_i|<1$. For any number of users we have two eigenvalues. Assuming that the power and bandwidth prices are higher than the costs C_P and C_W, the stability at the SNE fixed point $(\Pi_P^{(SNE)},\Pi_W^{(SNE)})$ can be investigated using the Jacobian matrix, which is given by:

$$J_\Pi(\Pi_P^{(SNE)},\Pi_W^{(SNE)})=\begin{bmatrix} J_{11}=1+\beta_P\Pi_P^{(SNE)}\frac{\partial^2 U_R}{\partial\Pi_P^2} & J_{12}=\beta_P\Pi_P^{(SNE)}\frac{\partial^2 U_R}{\partial\Pi_P\partial\Pi_W} \\ J_{21}=\beta_W\Pi_W^{(SNE)}\frac{\partial^2 U_R}{\partial\Pi_W\partial\Pi_P} & J_{22}=1+\beta_W\Pi_W^{(SNE)}\frac{\partial^2 U_R}{\partial\Pi_W^2} \end{bmatrix}. \quad (5.31)$$

The characteristic polynomial is then obtained as:

$$p(\lambda)=\lambda^2-(J_{11}+J_{22})\lambda+J_{11}J_{22}-J_{12}J_{21}. \quad (5.32)$$

The eigenvalues are given by the roots of the characteristic polynomial as:

$$\lambda_{1,2}=\frac{J_{11}+J_{22}\pm\sqrt{(J_{11}-J_{22})^2+4J_{12}J_{21}}}{2}. \quad (5.33)$$

The relationship between β_P and β_W can be obtained such that the SNE fixed point is stable for a given configuration and a given source-relay, relay-destination, and source-destination channel gains.

5.4 Simulation Results and Discussion

In order to evaluate the performance of the proposed algorithms, we consider a system of two users and one relay as illustrated in **Figure 5.2**. User 1

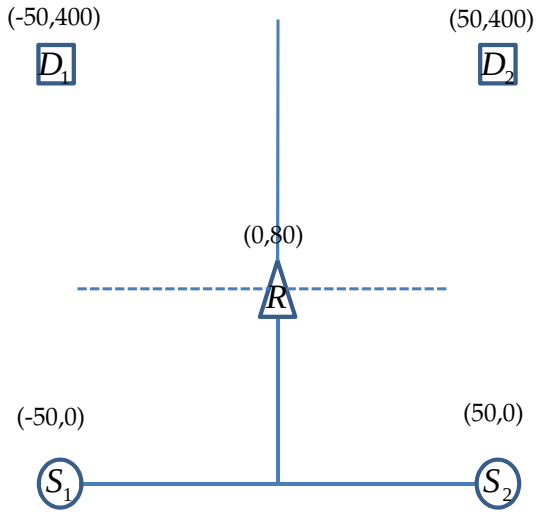

Figure 5.2 A System of Two Users and a Relay.

source-destination pair is (S_1, D_1), and user 2 source-destination pair is (S_2, D_2). The source S_1 is located at coordinate (-50m, 0m), and destination D_1 is located at (-50m, 400m). The source S_2 is located at coordinate (50m, 0m), and destination D_2 is located at (50m, 400m). The relay y-coordinate is kept fixed at (80m), and the x-coordinate varies from -800m to 800m to present different channel gains as in [28]. The available relay resources are $P_{\max}$ = 2Watt and $W_{\max}$ = 2MHz. We use the same channel gains as in [149], where, the propagation loss factor is set to 2. The source transmitted power P_S is fixed for the two sources and set at 10mWatt, and the capacity gap $\Gamma = 1$. The cost per unit power C_P = 1000unit price/Watt, and the cost per unit bandwidth $C_W = 1 \times 10^{-3}$ unit price/Hz. The users' utility function parameters are chosen as follows: $X = 1$, $Y = 1$ and $Z = \sqrt{\frac{0.5}{\log(2)}}$, and the noise power $\sigma^2 = 10^{-8}$Watt, unless otherwise specified.

Fixing the relay x-coordinate at 20m, SNE $\left(P_1^*, P_2^*, W_1^*, W_2^*, \Pi_P^*, \Pi_W^*\right)$ are computed as summarized in **Table 5.1**. As explained in this table, the users and the relay have no incentive to deviate from the SNE either by increasing or decreasing the users' power, the users' bandwidth, or their respective prices at the relay. The rows from 2 to 5 and from 10 to 13 illustrate that changing the power level, or the bandwidth share or both of user S_1 from

the SNE will not improve user's S_1 utility function U_1. In the same way, the rows from 6 to 9 illustrate that changing the power level, or the bandwidth share of user S_2 from the SNE will not improve user's S_2 utility function U_2. Finally, the rows from 14 to 21 illustrate that changing the power price, or the bandwidth price or both at the relay from the SNE will not improve the relay's utility function U_R. These examples prove that the obtained allocation and prices are a SNE strategy. The best response strategies of the relay to a deviation of user S_1 and user S_2 strategies from the SNE and vice verse is explained in **Table 5.2**. As shown in this table, the relay modifies its prices to any changes in the users' strategies as appears in rows 2 to 13. For example, row 2 shows that if user S_1 increases its demand from the SNE power strategy, this will increase its utility function U_1 but at the same time it will decrease the relay revenue U_R. Therefore, the relay will change the prices as a best-response to the change in users' demands until reaching the SNE strategies. Rows 3 to 13 can be explained in a similar way. In addition, **Table 5.2** shows that the users best-response to any deviation of the relay prices, where the users modify their demands as a response to changes in the relay's power and bandwidth prices, as illustrated in the rows from 14 to 21. For example, row 14 shows that if the relay increases its power price from the SNE strategy, this will decrease its utility function U_R, and in-return will decrease the users' utility functions U_1 and U_2. Hence, the relay will change the prices as a best-response to the change in users' demands until reaching the SNE strategies. Rows from 15 to 21 can be explained in a similar way where either the relay's power price or bandwidth price changes or the power and bandwidth prices change simultaneously. The optimum power and bandwidth allocation profiles of each user as a function of the $x-$coordinate of the relay are plotted in **Figure 5.3**. The region from -800m to 0m represents a better channel for user S_1, where the relay is much closer to S_1 than to S_2.

Table 5.1 Deviation from the Nash Equilibrium

	Strategy	Users Strategies				Relay Strategies		Utility Functions		
		P_1	P_2	W_1	W_2	Π_P	Π_W	U_1	U_2	U_R
		$\times 10^{-2}$	$\times 10^{-2}$	$\times 10^{5}$	$\times 10^{5}$	$\times 10^{3}$	$\times 10^{-3}$	$\times 10^{2}$	$\times 10^{2}$	$\times 10^{2}$
1	**SNE**	**4.4742**	**5.1000**	**2.0989**	**2.2181**	**1.3432**	**1.900**	**3.3790**	**3.5220**	**4.2139**
2	$P1 \uparrow$	5.4742						**3.3626** $\downarrow$		
3	$P1 \downarrow$	3.4742						**3.3570** $\downarrow$		
4	$W1 \uparrow$			2.1988				**3.3767** $\downarrow$		
5	$W1 \downarrow$			1.9989				**3.3767** $\downarrow$		
6	$P2 \uparrow$		6.1000						**3.5077** $\downarrow$	
7	$P2 \downarrow$		4.1000						**3.5034** $\downarrow$	
8	$W2 \uparrow$				2.3181				**3.5198** $\downarrow$	
9	$W2 \downarrow$				2.1181				**3.5198** $\downarrow$	
10	$P1 \uparrow, W1 \uparrow$	5.4742		2.1988				**3.3632** $\downarrow$		
11	$P1 \uparrow, W1 \downarrow$	5.4742		1.9989				**3.3575** $\downarrow$		
12	$P1 \downarrow, W1 \uparrow$	3.4742		2.1989				**3.3510** $\downarrow$		
13	$P1 \downarrow, W1 \downarrow$	3.4742		1.9989				**3.3584** $\downarrow$		
14	$\Pi_P \uparrow$					1.4432				**4.0998** $\downarrow$
15	$\Pi_P \downarrow$					1.2432				**4.1772** $\downarrow$
16	$\Pi_W \uparrow$						2.0000			**4.1867** $\downarrow$
17	$\Pi_W \downarrow$						1.7000			**4.1887** $\downarrow$
18	$\Pi_P \uparrow \Pi_W \uparrow$					1.4432	2.0000			**4.20343** $\downarrow$
19	$\Pi_P \uparrow \Pi_W \downarrow$					1.4432	1.8000			**3.9819** $\downarrow$
20	$\Pi_P \downarrow \Pi_W \uparrow$					1.24320	2.0000			**4.1514** $\downarrow$
21	$\Pi_P \downarrow \Pi_W \downarrow$					1.24320	1.8000			**4.1779** $\downarrow$

Note: empty cells are kept at SNE strategies

Table 5.2 Best Response

	Strategy	Users Strategies				Relay Strategies		Utility Functions		
		P_1	P_2	W_1	W_2	Π_P	Π_W	U_1	U_2	U_R
		$\times 10^{-2}$	$\times 10^{-2}$	$\times 10^{5}$	$\times 10^{5}$	$\times 10^{3}$	$\times 10^{-3}$	$\times 10^{2}$	$\times 10^{2}$	$\times 10^{2}$
1	**SNE**	**4.4742**	**5.1000**	**2.0989**	**2.2181**	**1.3432**	**1.900**	**3.3790**	**3.5220**	**4.2139**
2	$P1\uparrow$	5.4742				1.3135	1.8927	3.3951	3.5532	**4.1855** $\downarrow$
3	$P1\downarrow$	3.4742				1.3885	1.9090	**3.3208** $\downarrow$	**3.4789** $\downarrow$	4.2573
4	$W1\uparrow$			2.1988		1.2512	1.8801	3.4616	3.6130	**4.1279** $\downarrow$
5	$W1\downarrow$			1.9989		1.4395	1.9219	**3.2899** $\downarrow$	**3.4244** $\downarrow$	4.3082
6	$P2\uparrow$		6.1000			1.3135	1.8927	3.407	3.5420	**4.1855** $\downarrow$
7	$P2\downarrow$		4.1000			1.3885	1.9090	**3.3398** $\downarrow$	**3.4648** $\downarrow$	4.2573
8	$W2\uparrow$				2.3181	1.2513	1.8801	3.4619	3.6129	**4.1279** $\downarrow$
9	$W2\downarrow$				2.1181	1.4395	1.9219	**3.2900** $\downarrow$	**3.4244** $\downarrow$	4.3083
10	$P1\uparrow, W1\uparrow$	5.4742		2.1988		1.2380	1.8748	3.4771	3.6315	**4.1156** $\downarrow$
11	$P1\uparrow, W1\downarrow$	5.4742		1.9989		1.3924	1.91233	**3.3069** $\downarrow$	**3.4695** $\downarrow$	4.2621
12	$P1\downarrow, W1\uparrow$	3.4742		2.1989		1.2715	1.8861	3.4049	3.5894	**4.1466** $\downarrow$
13	$P1\downarrow, W1\downarrow$	3.4742		1.9989		1.5119	1.9343	**3.2298** $\downarrow$	**3.3599** $\downarrow$	4.3788
14	$\Pi_P\uparrow$	3.0261	4.7844	1.9757	2.1950	1.4432		**3.2999** $\downarrow$	**3.4726** $\downarrow$	**4.0998** $\downarrow$
15	$\Pi_P\downarrow$	4.8093	5.4575	2.1215	2.2424	1.2432		3.4255	3.5747	**4.1772** $\downarrow$
16	$\Pi_W\uparrow$	4.3145	4.8773	1.88379	1.9875		2.0000	**3.1802** $\downarrow$	**3.3120** $\downarrow$	**4.1867** $\downarrow$
17	$\Pi_W\downarrow$	4.8717	5.6180	2.6561	2.8135		1.7000	3.8516	4.0215	**4.1887** $\downarrow$
18	$\Pi_P\uparrow \Pi_W\uparrow$	3.9607	4.5737	1.8588	1.9664	1.4432	2.0000	**3.1382** $\downarrow$	**3.2649** $\downarrow$	**4.20343** $\downarrow$
19	$\Pi_P\uparrow \Pi_W\downarrow$	2.3637	4.8477	2.1247	2.4532	1.4432	1.8000	3.4378	3.7046	**3.9819** $\downarrow$
20	$\Pi_P\downarrow \Pi_W\uparrow$	4.6076	5.2205	1.9027	2.0097	1.24320	2.0000	**3.2247** $\downarrow$	**3.3625** $\downarrow$	**4.1514** $\downarrow$
21	$\Pi_P\downarrow \Pi_W\downarrow$	5.0289	5.7158	2.3791	2.5166	1.24320	1.8000	3.65004	3.8121	**4.1779** $\downarrow$

Note: empty cells are kept at SNE strategies

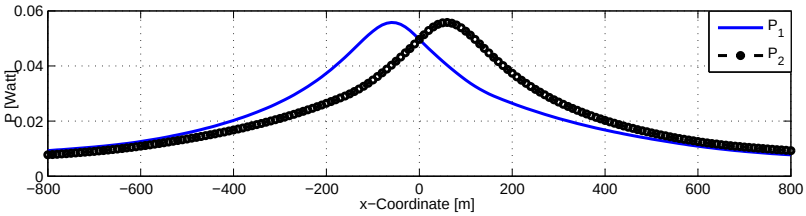

(a) Power Allocation Profiles

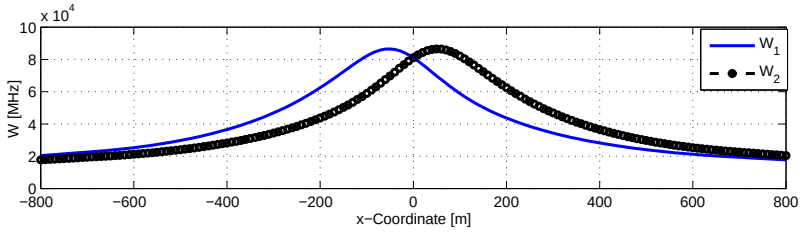

(b) Bandwidth Allocation Profiles

Figure 5.3 Power and Bandwidth Allocation as a Function of the Relay x-Coordinate.

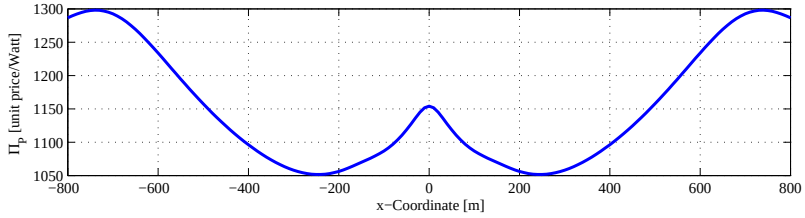

(a) Power Price.

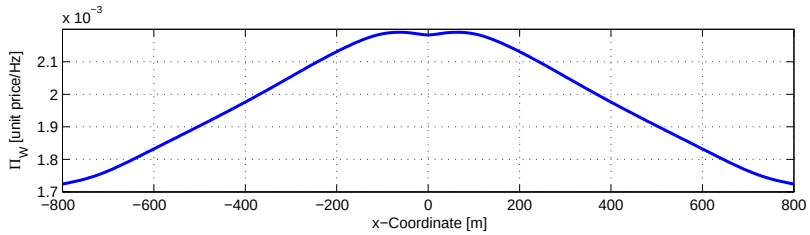

(b) Bandwidth Price.

Figure 5.4 Power and Bandwidth Prices as a Function of the Relay x-Coordinate.

The amount of power and bandwidth bought by user S_1 are more than the amount of power and bandwidth bought by user S_2 in the same region. On the other hand, the region from 0m to 800m represents a better channel condition for user S_2, so the power and bandwidth bought by user S_2 are larger. At the relay x-coordinate $rx = 0$, both users have similar channel conditions to the relay. Therefore, the two users bought the same amount of power and bandwidth. Note that at each rx the prices that maximize the relay revenue are computed as shown in **Figure 5.4**, where the power and

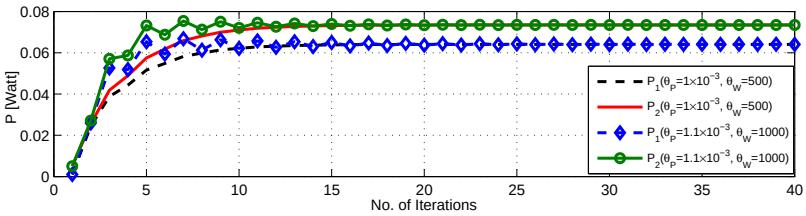

(a) Convergence of the Power Adaptive Algorithm.

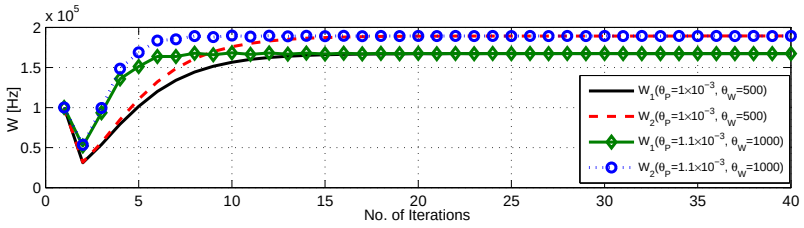

(b) Convergence of the Bandwidth Adaptive Algorithm.

Figure 5.5 Convergence of the Power and Bandwidth Adaptive Algorithm.

bandwidth profiles are computed using the adaptive prices algorithm as a function of the relay x-coordinate.

The convergence of the proposed adaptive power and bandwidth allocation algorithms for the two users scenario is shown in **Figure 5.5**. The prices are set at $\Pi_P = 1100$, and $\Pi_W = 1.1 \times 10^{-3}$ and the x-coordinate of the relay is set at 20m. Two cases are considered: in the first case $(\theta_P, \theta_W) = (1 \times 10^{-3}, 200)$ and in the second case $(\theta_P, \theta_W) = (1.1 \times 10^{-3}, 100)$. Both cases are selected to satisfy the convergence condition such that the absolute value of the eigenvalues of the Jacobian matrix are less than one. In case two, the power profiles go through oscillations before reaching Nash equilibrium.

Similar convergence behavior is shown in **Figure 5.6** for the proposed adaptive relay's power and bandwidth prices, where the x-coordinate of the relay is set at 50m. Two cases are also considered: in the first case, $(\beta_P, \beta_W) = (4 \times 10^{-6}, 4 \times 10^{-6})$, and in the second case $(\beta_P, \beta_W) = (6 \times 10^{-6}, 8 \times 10^{-6})$.

Figure 5.7 shows the convergence of the proposed adaptive power and bandwidth prices update algorithm for 2, 4, and 10 users. The locations of the relay and destination nodes are fixed at coordinate $(50, 80)$ for the relay and the destination at coordinate $(50, 400)$. The users' locations are randomly generated, where the (x, y)-coordinate is a uniform random vari-

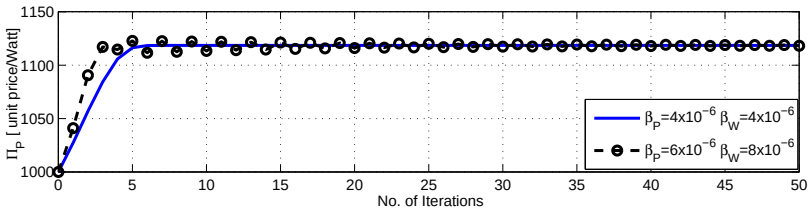

(a) Convergence of the Power Price Adaptive Algorithm.

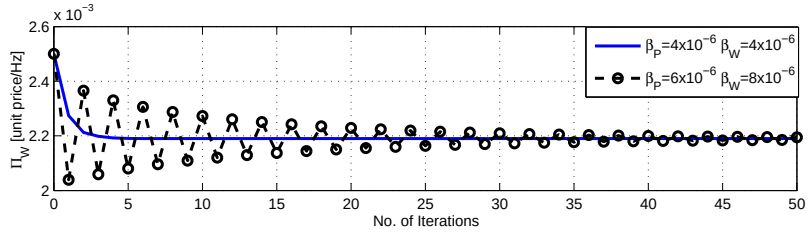

(b) Convergence of the Bandwidth Price Adaptive Algorithm.

Figure 5.6 Convergence of the Power and Bandwidth Prices Adaptive Algorithm.

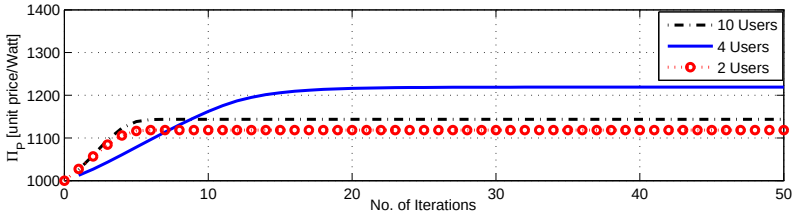

(a) Convergence of the Power Price Adaptive Algorithm.

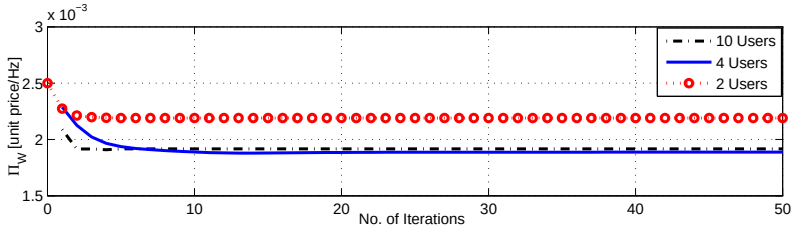

(b) Convergence of the Bandwidth Price Adaptive Algorithm.

Figure 5.7 The Convergence of the Prices Update Algorithm for Different Number of Users.

able over the interval $[0, 300]$. As shown in this figure the convergence time does not depend on the number of users. However, this does not imply that the prices for 2 users is lower or higher than the prices for 10 users because each curve realizes different users' locations.

The average relay utility as a function of the number of users is shown **Figure 5.8(a)**, and the users' locations are generated uniformly, where the (x, y) coordinate varies in the range from $[0, 300]$, for 200 runs. Clearly, the relay revenue increases as the number of users increase until a certain limit

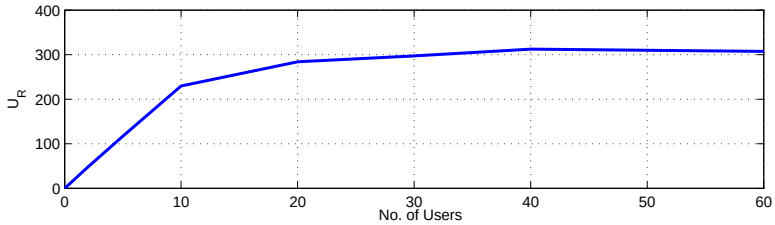

(a) The Average Relay Utility Function.

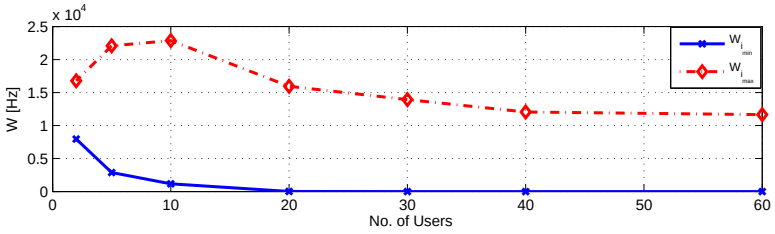

(b) Power Allocation Profiles.

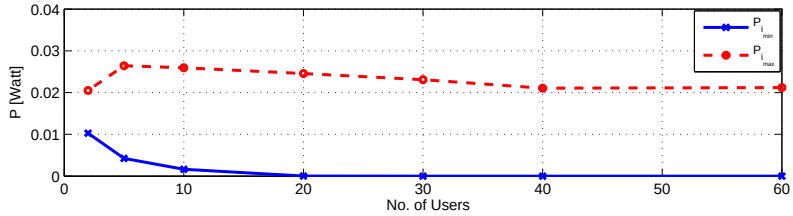

(c) Bandwidth Allocation Profiles.

Figure 5.8 The Average Relay Utility Function and Resource Allocation Profiles as a Function of the Number of Users.

after which there is no marginal increase in relay revenues, due to the fact that the relay resources are limited. As the number of users increases the number of users that are allocated zero power and bandwidth may also increase.

In **Figure 5.8(b)** and **Figure 5.8(c)**, we show the average minimum and average maximum power and bandwidth, respectively that are allocated to the users as a function of the number of users. Clearly, as the number of users increases, the allocated resources (power and bandwidth) to the users are reduced because of the increased competition among the users. In **Figure 5.9(a)**, we show the convergence of the prices' update algorithm from different initial prices $\Pi_P^{(0)}$, and $\Pi_W^{(0)}$ for two cases: relay x-coordinate equals 50 and relay x-coordinate 200. It is clear from this figure that the convergence range for the first case is larger than the convergence range of the second case. Whereas, in **Figure 5.9(b)** we show the convergence of the power

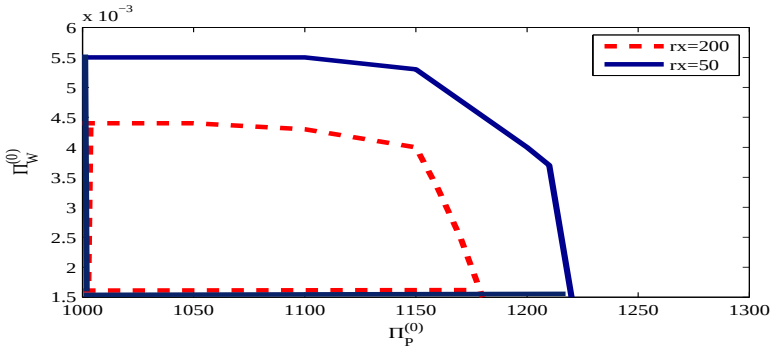

(a) Convergence of Prices.

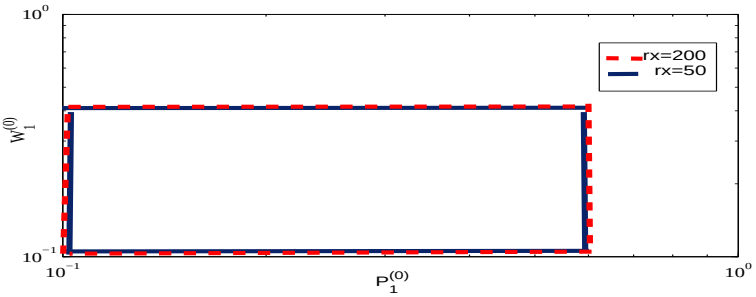

(b) Convergence Resource Allocation Profiles.

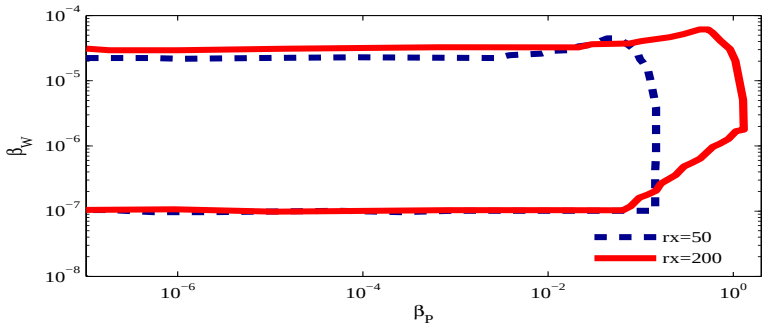

(c) Convergence of the Price Adaptive Algorithm as a Function of β_P and β_W

Figure 5.9 Convergence of Prices and Resource Allocation Profiles from Different Initial Values and β_P and β_W

and bandwidth allocation as a function of the initial allocations $P_1^{(0)}$, and $W_1^{(0)}$ of user S_1. The second user S_2 initial allocations are fixed at $P_2^{(0)} = 0.01$ and $W_2^{(0)} = 1 \times 10^5$. For the two cases, the convergence range is the same. **Figure 5.9(c)** shows the convergence of the prices update algorithm for different values of β_P and β_W. It is clear that the convergence range for relay x-coordinate 200 is larger than the convergence range of relay x-coordinate 50.

5.5 Conclusions

In this chapter, we propose a non-cooperative game theoretic framework for joint power and bandwidth resource allocation for the AF cooperative communication. The formulated user's utility function is related to the data rate achieved using the AF cooperation scheme, which depends on the power and bandwidth obtained from the relay. In addition, the utility function is associated with an exact potential function, which facilitates the analysis of the uniqueness of Nash equilibrium. A distributed algorithm is developed to find NE for given relay prices. Simulation results show the convergence of the proposed algorithm, and show how to allocate the resources between the selfish users without any coordination amongst them. Furthermore, a distributed price algorithm is developed to find the optimum price to maximize the relay revenue. The network is considered homogeneous, but the game formulation can be easily extended to a non-homogeneous network, by changing one of the parameters of the user's utility function.

Part II

Joint Power Allocation and Subchannel Assignment in OFDM and OFDMA Relay Networks

CHAPTER6

BASIC CONCEPTS OF OFDM AND OFDMA COMMUNICATION SYSTEMS

In this chapter, a brief overview of multi-carrier OFDM and OFDMA systems is presented. Resource allocation problems for OFDM and OFDMA systems are discussed. Resource allocation problems for OFDM and OFDMA systems with cooperative communication schemes are examined. Formulations and solutions of essential resource allocation problems are addressed. Fundamental principles that are used to solve resource allocation problems for OFDMA and OFDMA systems are highlighted, such as zero duality gap principle for non-convex problems, and two-bands partition principle for multicarrier systems.

Section 6.1 presents OFDM systems. In Section 6.2, OFDMA systems are introduced and basic principles of finding the solution of resource allocation problems are discussed. Conclusions are drawn in Section 6.3.

6.1 Basics of OFDM Systems

Frequency selective channels suffer from ISI, one way to mitigate this impairment is to use multicarrier modulation techniques, where the wide bandwidth signal to be transmitted is divided over multiple mutually orthogonal signals of a bandwidth small enough such that the channel appears to be non-frequency-selective. OFDM is a multicarrier modulation technique

that has been chosen as the modulation scheme for 4G mobile broadband standards and for high speed wireless networks. It implements multicarrier modulation using DFT and IDFT. Let $x(n)$ for $0 \leq n \leq N-1$, denote a discrete time sequence. The DFT of $x(n)$ is defined as [44]:

$$DFT\{x(n)\} = X(k) \triangleq \frac{1}{\sqrt{N}} \sum_{n=0}^{N-1} x(n) \mathrm{e}^{-j\frac{2\pi nk}{N}},\ k = 0, \cdots, N-1, \tag{6.1}$$

$X(k)$ characterizes the frequency content of the time samples $x(n)$ for $0 \leq n \leq N-1$. The sequence $x(n)$ can be recovered using the IDFT as:

$$IDFT\{X(k)\} = x(n) \triangleq \frac{1}{\sqrt{N}} \sum_{k=0}^{N-1} X(k) \mathrm{e}^{j\frac{2\pi nk}{N}},\ n = 0, \ldots, N-1. \tag{6.2}$$

The output sequence $y(n)$ when an input data $x(n)$ is sent through a linear time-invariant discrete-time channel with an impulse response $h(n)$, is given as:

$$y(n) = x(n) * h(n) = \sum_{m} h(m)x(n-m), \tag{6.3}$$

The *circular convolution* is defined as:

$$y(n) = x(n) \otimes h(n) = \sum_{m} h(m)x(n-m)_N, \tag{6.4}$$

where $x(n-m)_N$ is a periodic version of $x(n-m)$ with period N. From the properties of the DFT, circular convolution leads to multiplication in the frequency domain,

$$DFT\{y(n) = x(n) \otimes h(n)\} = Y(k) = X(k)H(k),\ k = 0, \cdots, N-1. \tag{6.5}$$

At the receiver, if the output of the channel is a circular convolution of the input sequence $x(n)$ and the channel impulse response $h(n)$, then the input data sequence $x(n)$ can be recovered by taking the IDFT of $Y(k)/H(k)$, $0 \leq k \leq N-1$. Unfortunately, the channel output is a linear convolution

not a circular convolution. However, linear convolution can be turned into circular convolution by adding a special prefix to the input sequence called a *cyclic prefix*. Consider a channel input sequence $x(n)$, $0 \leq n \leq N-1$ of length N and a discrete-time channel with FIR $h(n)$, $0 \leq n \leq L-1$ of length L. Let $\hat{\boldsymbol{x}} = \Big[\hat{x}(0) \cdots, \hat{x}(N+L-1)\Big]$ denote the input sequence after adding the cyclic prefix, such that:

$$\hat{\boldsymbol{x}} = \Big[x(N-L+1), \cdots, x(N-1), x(0), \cdots, x(N-1)\Big]. \tag{6.6}$$

The output sequence can be written as:

$$\hat{y}(n) = \sum_{l=0}^{L-1} h(l)\hat{x}(n-l) + v(n),\ n = 0, \cdots, N+L-1, \tag{6.7}$$

where $v(n)$ is AWGN. The multipath channel affects the first $L-1$ symbols. Therefore, the receiver ignores these symbols; the received sequence after removing the cyclic prefix is given as:

$$\boldsymbol{y} = \Big[y(0), \cdots, y(N-1)\Big]. \tag{6.8}$$

The input-output relation can be written in the frequency domain after removing the cyclic prefix in terms of the original sequence as:

$$Y(k) = H(k)X(k) + V(k),\ k = 0, \cdots, N-1, \tag{6.9}$$

where $V(k)$ is AWGN at the kth subcarrier. It is clear from (6.9) that the selective channel has been transformed into parallel flat channels using OFDM.

The block diagram of the OFDM transmitter is shown in **Figure 6.1(a)** where the input data is divided into blocks of size N referred to as OFDM symbols. Then a cyclic prefix is added to each OFDM symbol to induce circular convolution of the input sequence and the channel impulse response.

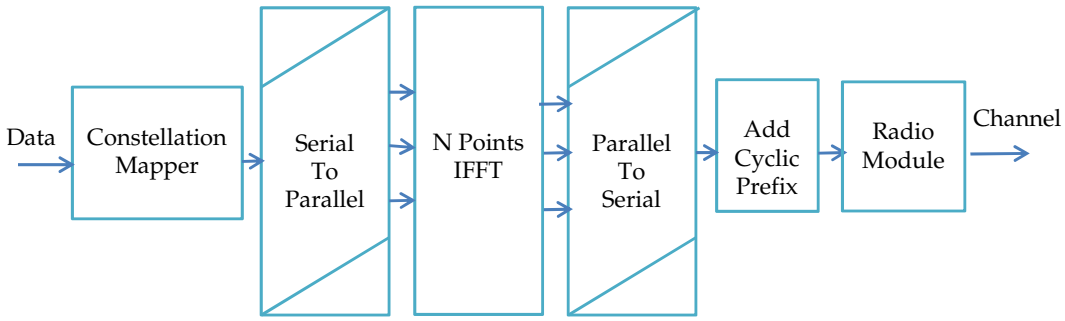

(a) Block Diagram of OFDM Transmitter.

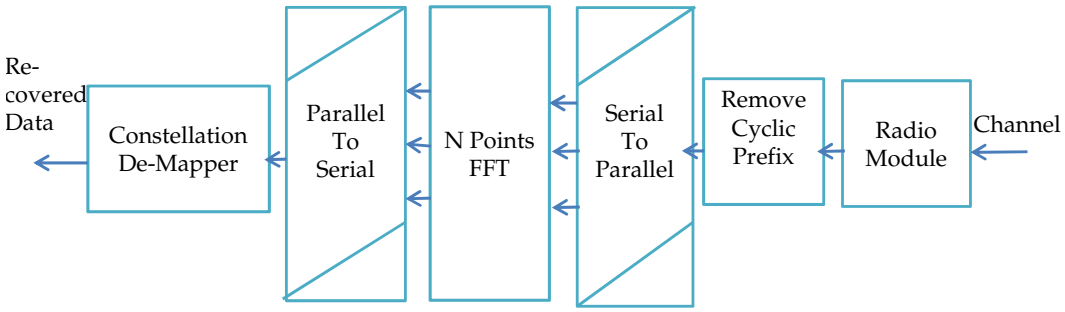

(b) Block Diagram of OFDM Receiver.

Figure 6.1 Block Diagram of OFDM System

At the receiver, as shown in **Figure 6.1(b)**, the output samples affected by ISI between OFDM symbols are removed by removing the cyclic prefix, then the DFT of the remaining samples are used to recover the original input sequence.

6.1.1 Capacity of OFDM Systems

In an OFDM system, the frequency-selective fading channel consists of a set of AWGN channels in parallel $H(j)$, as revealed from (6.9). Let $P(j)$ denote the power allocated to the jth subchannel (subcarrier), and $P^{\max}$ denote the total available power at the transmitter. The capacity of this parallel set of channels is the sum of rates associated with each subchannel with power optimally allocated over all subchannels. This can be formulated as:

$$C = \max_{\boldsymbol{P}} B_N \sum_{j \in \mathcal{J}} \log_2 \left(1 + \frac{|H(j)|^2 P(j)}{B_N N_0}\right), \tag{6.10a}$$

$$\text{s.t.} \sum_{j\in\mathcal{J}} P(j) \leq P^{\max}, \tag{6.10b}$$

$$P(j) \geq 0, \ \forall j \in \mathcal{J}, \tag{6.10c}$$

where B_N is the bandwidth of each subchannel, N_0 is the PSD of AWGN, $\mathcal{J} = \{1, \cdots, N\}$[1] is the set of subcarriers, and $\boldsymbol{P}$ is the vector of power allocation profile $\boldsymbol{P} = \Big[P(1), \cdots, P(N)\Big]$. The optimal power profile can be obtained using the Lagrangian approach[2] as[44]:

$$P(j) = \begin{cases} \frac{1}{\gamma_0} - \frac{1}{\gamma(j)} & \text{if } \gamma_j > \gamma_0, \\ 0 & \text{otherwise,} \end{cases} \tag{6.11}$$

where $\gamma(j) = \frac{|H(j)|^2}{B_N N_0}$, and γ_0 is some cutoff value that satisfies:

$$\sum_{j\in\mathcal{J}} \frac{1}{\gamma_0} - \frac{1}{\gamma(j)} = P^{\max}. \tag{6.12}$$

The optimal power allocation of OFDM system is known as *water-filling* allocation. The capacity then becomes:

$$C = B_N \sum_{j:\gamma(j)\geq\gamma_0} \log_2\Big(\frac{\gamma(j)}{\gamma_0}\Big). \tag{6.13}$$

This capacity is achieved by sending at different rates and powers over each subchannel. **Figure 6.2** shows a water-filling allocation for the OFDM scenario with $N = 16$ subcarriers; it is clear that subcarrier $j = 7$ is allocated zero power and subcarrier $j = 5$ is allocated the maximum power compared to the other subcarriers.

Adaptive loading can be used to maximize the total rate of the system using adaptive modulation such as variable-rate variable power M-QAM.

[1]The subcarrier index $j = 1, \cdots, N$ is used instead of $j = 0, \cdots, N-1$.
[2]Problem 6.10 is a convex optimization problem.

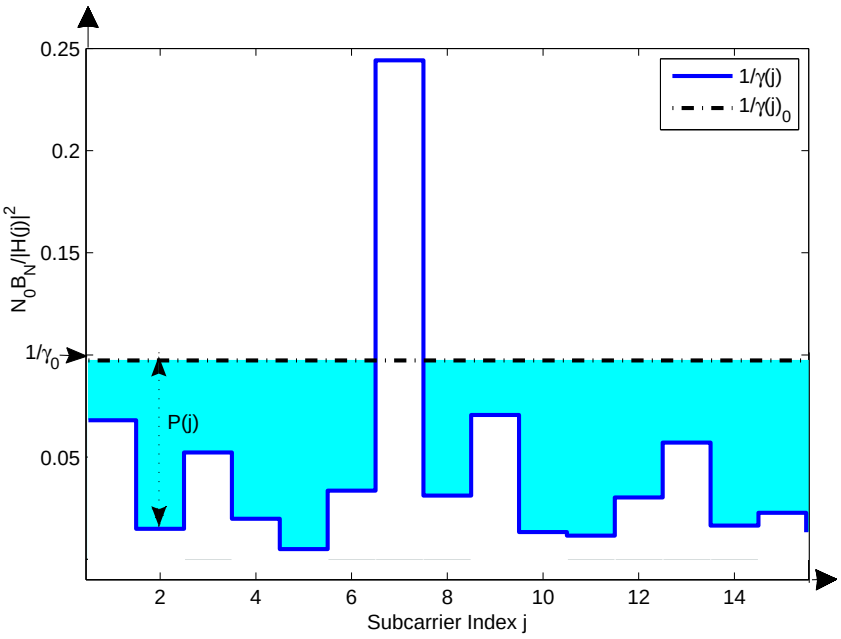

Figure 6.2 Optimal Power Allocation: Water-Filling.

The idea is to vary the data rate and the power assigned to each subchannel relative to that subchannel gain. The data rate for variable-rate variable-power M-QAM modulation scheme can be formulated as[3]:

$$R = \max_{\boldsymbol{P}} B_N \sum_{j \in \mathcal{J}} \log_2 \left(1 + \frac{\gamma(j)P(j)}{\Gamma}\right), \tag{6.14a}$$

$$\text{s.t.} \sum_{j \in \mathcal{J}} P(j) \leq P^{\max}, \tag{6.14b}$$

$$P(j) \geq 0, \ \forall j \in \mathcal{J}, \tag{6.14c}$$

where $\Gamma = -\frac{\ln(5P_e)}{1.5}$, and P_e is the desired target BER in each subchannel. The optimal power allocation is computed as:

$$P(j) = \begin{cases} \frac{1}{\gamma_0} - \frac{\Gamma}{\gamma(j)} & \text{if } \gamma_j > \Gamma\gamma_0, \\ 0 & \text{otherwise,} \end{cases} \tag{6.15}$$

where γ_0 is selected such that $\sum_{j \in \mathcal{J}} \frac{1}{\gamma_0} - \frac{\Gamma}{\gamma(j)} = P^{\max}$, and the corresponding

[3]This formulation only consider instantaneous rate; i.e. the temporal dimension is not being exploited when resource allocation is performed.

data rate can be computed as:

$$R = B_N \sum_{j:\, \gamma(j) \geq \Gamma\gamma_0} \log_2\Big(\frac{\gamma(j)}{\gamma_0}\Big). \tag{6.16}$$

6.1.2 OFDM with Cooperative Communications

Consider an OFDM system where the transmission between the source and destination nodes is facilitated by a relay node using AF cooperative communication scheme; the received signal using subcarrier j at the relay node is amplified and forwarded to the destination node at the same subcarrier[4] j. The received signals at the destination node from the direct-link and the relay node are combined using MRC. Let $H_{SD}(j)$, $H_{RD}(j)$, and $H_{SR}(j)$ denote the channel gains of the jth subcarrier between the source-destination, relay-destination, and source-relay nodes, respectively. The resource allocation problem for single relay AF-OFDM cooperative communication system with adaptive loading can be formulated using (2.28) as:

$$R = \max_{\boldsymbol{P}_S,\, \boldsymbol{P}_R} \frac{B_N}{2} \sum_{j\in\mathcal{J}} \log_2\Big(1 + \frac{\gamma_{SD}(j)P_S(j)}{\Gamma} + \frac{\gamma_{SR}(j)\gamma_{RD}(j)P_R(j)P_S(j)}{\Gamma(1+\gamma_{SR}(j)P_S(j)+\gamma_{RD}(j)P_R(j))}\Big), \tag{6.17a}$$

$$\text{s.t.} \sum_{j\in\mathcal{J}} P_S(j) \leq P_S^{\max}, \tag{6.17b}$$

$$\sum_{j\in\mathcal{J}} P_R(j) \leq P_R^{\max}, \tag{6.17c}$$

$$P_S(j) \geq 0, P_R(j) \geq 0,\ \forall j \in \mathcal{J}, \tag{6.17d}$$

where $\gamma_{SD}(j) = \frac{|H_{SD}(j)|^2}{B_N N_0}$, $\gamma_{RD}(j) = \frac{|H_{RD}(j)|^2}{B_N N_0}$, and $\gamma_{SR}(j) = \frac{|H_{SR}(j)|^2}{B_N N_0}$. $\boldsymbol{P}_R$ is the power profile vector at the relay node, with $\boldsymbol{P}_R = \Big[P_R(1), \cdots, P_R(N)\Big]$, and $\boldsymbol{P}_S$ is the power profile vector at the source node, with $\boldsymbol{P}_S = \Big[P_S(1), \cdots, P_S(N)\Big]$. The

[4]Forwarding the received signal at a different subcarrier is out of the scope of this dissertation.

resource allocation problem (6.17) is not a jointly concave function with respect to the source and relay power profiles $\boldsymbol{P}_S$ and $\boldsymbol{P}_R$, as can be proven by the second ordered derivative test given in (2.52). Before trying to solve (6.17), we will look at the solutions of two problems. The first problem is the achievable sum rate using fixed power profile at the source node and optimal power profile at the relay node. The second problem is the achievable sum rate using fixed power profile at the relay node and optimal power profile at the source node. The first problem; the resource allocation problem for a given source power profile can be formulated as [49][5]:

$$R = \max_{\boldsymbol{P}_R} \frac{B_N}{2} \sum_{j\in\mathcal{J}} \log_2\Big(1 + \frac{\gamma_{SD}(j)P_S(j)}{\Gamma} + \frac{\gamma_{SR}(j)\gamma_{RD}(j)P_R(j)P_S(j)}{\Gamma(1+\gamma_{SR}(j)P_S(j)+\gamma_{RD}(j)P_R(j))}\Big), \tag{6.18a}$$

$$\text{s.t.} \sum_{j\in\mathcal{J}} P_R(j) \le P_R^{\max}, \tag{6.18b}$$

$$P_R(j) \ge 0,\ \forall j \in \mathcal{J}. \tag{6.18c}$$

Problem (6.18) is a convex optimization problem, which can be solved by formulating the Lagrangian function, then equating to zero the derivative of the Lagrangian function with respect to $P_R(j)$, for $j = 1, \cdots, N$. The optimal power profile $P_R^*(j)$ can be obtained as:

$$P_R^*(j) = \Big(\frac{\sqrt{\alpha_1(j)^2 - 4\alpha_0(j)\alpha_2(j)}}{2\alpha_2(j)} - \alpha_1(j)\Big)^+, \tag{6.19}$$

where $\alpha_0(j)$, $\alpha_1(j)$, and $\alpha_2(j)$ are computed as:

$$\alpha_0(j) = [1 + P_S(j)\gamma_{SR}(j)]^2[\Gamma + P_S(j)\gamma_{SD}(j)] - K_R P_S(j)\gamma_{SR}(j)\gamma_{RD}(j)[1 + P_S(j)\gamma_{SR}(j)], \tag{6.20a}$$

$$\alpha_1(j) = [2(\Gamma + P_S(j)\gamma_{SD}(j)) + P_S(j)\gamma_{SR}(j)][1 + P_S(j)\gamma_{SR}(j)]\gamma_{RD}(j), \tag{6.20b}$$

[5]In [49], the formulated resource allocation problem was solved without considering diversity (no direct link between the source-destination nodes).

$$\alpha_2(j) = \Gamma + P_S(j)[\gamma_{SD}(j) + \gamma_{SD}(j)], \tag{6.20c}$$

where $K_R = \frac{B_N}{2\ln(2)\lambda_R}$, and λ_R is selected such that the relay power constraint is fulfilled (6.18b).

The second problem: the resource allocation for a given relay power profile can be formulated as:

$$R = \max_{P_S} \frac{B_N}{2} \sum_{j\in\mathcal{J}} \log_2\Big(1 + \frac{\gamma_{SD}(j)P_S(j)}{\Gamma} + \frac{\gamma_{SR}(j)\gamma_{RD}(j)P_R(j)P_S(j)}{\Gamma(1 + \gamma_{SR}(j)P_S(j) + \gamma_{RD}(j)P_R(j))}\Big), \tag{6.21a}$$

$$\text{s.t.} \sum_{j\in\mathcal{J}} P_S(j) \le P_S^{\max}, \tag{6.21b}$$

$$P_S(j) \ge 0, \ \forall j \in \mathcal{J}. \tag{6.21c}$$

Since (6.21) is a convex optimization problem, it can be solved using any convex optimization technique. However, it is difficult to obtain a closed form expression for the optimal source power profile $P_S^*(j)$, for $j = 1, \cdots, N$ since a cubic equation in $P_S^*(j)$ is obtained for each subcarrier $j \in \mathcal{J}$ by equating to zero the derivative of the Lagrangian function with respect to $P_S(j)$.

Optimal allocation of (6.17) can now be found by an alternate and separate optimization approach of the source and relay power profiles as given in (6.19) and the solution of (6.21). This approach will converge to a solution of the joint optimization problem (6.17) as can be proved using a similar approach to [49]. A simple iterative algorithm based on an approximated equivalent channel model was proposed in [126] to find the source and relay power profiles for (6.17).

For mathematical tractability, the data rate for the AF scheme under high SNR can be approximated as [57]:

$$R \approx \max_{P_R} \frac{B_N}{2} \sum_{j\in\mathcal{J}} \log_2\Big(1 + \frac{\gamma_{SD}(j)P_S(j)}{\Gamma} + \frac{\gamma_{SR}(j)\gamma_{RD}(j)P_R(j)P_S(j)}{\Gamma(\gamma_{SR}(j)P_S(j) + \gamma_{RD}(j)P_R(j))}\Big). \tag{6.22}$$

With this approximation, (6.17) becomes a convex optimization problem. The data rate in (6.22) is a jointly concave function with respect to the source and relay power profiles as proved in Appendix B.1, and the constraints are linear. Optimal source and relay power profiles can be obtained by formulating the Lagrangian function. Taking the derivative with respect to $P_R(j)$ and $P_S(j)$, and equating to zero, the source power profile is obtained as:

$$P_S^*(j) = \begin{cases} \left(\frac{K(\gamma_{SD}(j)+A(j))-\Gamma}{\gamma_{SD}(j)+B(j)}\right)^+ & \text{if } P_R^*(j) > 0, \\ \left(K - \frac{\Gamma}{\gamma_{SD}(j)}\right)^+ & \text{if } P_R^*(j) = 0, \end{cases} \tag{6.23}$$

where $A(j) = \frac{\gamma_{SR}(j)\gamma_{RD}^2(j)C^2(j)}{(\gamma_{SR}(j)+\gamma_{RD}(j)C(j))^2}$, $B(j) = \frac{\gamma_{SR}(j)\gamma_{RD}(j)C(j)}{\gamma_{SR}(j)+\gamma_{RD}(j)C(j)}$, $K = \frac{B_N}{2\ln(2)\lambda_S}$, and $C(j)$ is computed as:

$$C(j) = \frac{\gamma_{SR}(j)\Big(-1+\sqrt{1+(1+\frac{\gamma_{SR}(j)}{\gamma_{SD}(j)})(\frac{\lambda_S}{\lambda_R}\frac{\gamma_{RD}(j)}{\gamma_{SD}(j)}-1)}\Big)^+}{\gamma_{RD}(j)(1+\frac{\gamma_{SR}(j)}{\gamma_{SD}(j)})}, \tag{6.24}$$

where λ_S and λ_R are selected to satisfy the power constraints (6.17c), and (6.17b), respectively. The optimal relay power profile can be obtained as:

$$P_R^*(j) = C(j)P_S^*(j), \tag{6.25}$$

The resource allocation problem of AF-OFDM under total power constraint $P_R^{\max} + P_S^{\max} = P^{\max}$ and individual power constraints without direct link between the source and destination nodes were investigated and closed form expressions for the source and relay power profiles were found in [49]. Resource allocation with subcarrier pairing for multi-relay OFDM system was investigated using high SNR approximation in [30].

In order to compare the sum rate of the aforementioned power allocation criteria, we model the subcarrier channel coefficients between any two nodes with a separating distance d as $H(j) \sim \mathcal{CN}(0, \frac{1}{L(1+d)^\alpha})$, where $\mathcal{CN}(\mu_H, \sigma_H^2)$

Table 6.1 Uniform Resource Allocation for AF-OFDM.

Criterion	Unif. $P_S(j)$ No Relaying	Unif. $P_S(j)$ Unif. $P_R(j)$
Data Rate in [Kbps]	24.03	29.93

Table 6.2 Resource Allocation for AF-OFDM.

	Water-fill	Sub-Opt.	Sub-Opt.	Iterative	App. High SNR
Criterion	Opt. $P_S(j)$ No Relaying	Unif. $P_S(j)$ Opt. $P_R(j)$	Opt. P_S(j) Unif. $P_R(j)$	Opt. P_S(j) Opt. $P_R(j)$	Opt. $P_S(j)$ Opt. $P_R(j)$
Data Rate in [Kbps]	32.13	34.20	32.58	37.34	37.36

is the complex normal distribution with mean μ_H and variance σ_H^2, the propagation loss factor is $\alpha = 4$, and the number of channel taps is $L = 4$ as in [49]. The distance between the relay and destination nodes is $d_{RD} = 50$m, the distance between the source and destination nodes is $d_{SD} = 100$m, and the distance between the source and relay nodes is $d_{SR} = 50$m. The subcarrier noise power $\sigma^2 = N_0 B_N$ is set at 4×10^{-10}Watt. The source maximum transmit power is $P_S^{\max} = 1$Watt, and the relay maximum transmit power is $P_R^{\max} = 1$Watt. The subcarrier spacing is $B_N = 4$KHz, and the capacity gap is $\Gamma = 1$.

The achievable data rate using uniform power allocation at the source and relay nodes for AF-OFDM is compared with the achievable data rate using the direct link with uniform power allocation at the source node for $N = 16$, where the source and relay[6] power constraints are set to be equal to have a fair comparison between relaying and direct link transmissions. Clearly, the achievable data rate using AF is higher than the achievable rate using the direct link only as shown in **Table 6.1**.

Table 6.2, compares the achievable data rate for different AF relaying

[6]Typically, the relay power capability is higher than the source in the uplink scenario.

criteria; optimal source power allocation without relaying, optimal source and uniform relay power allocation, uniform source power allocation and optimal relay power allocation, optimal source and relay power allocation using the two steps iterative algorithm, and optimal source and relay power allocation using the high SNR approximation (6.22). Optimal source and relay power allocation achieves the highest data rate as expected, and the achievable data rates using the sub-optimal allocation criteria for AF-OFDM are higher than the achievable data rate using the direct link with optimal power allocation at the source node. The achievable data rate using the approximated high SNR is approximately similar to the achievable data rate using the iterative two steps algorithm with less computational complexity.

For DF-OFDM cooperative system, the resource allocation problem can be formulated as:

$$R = \max_{P_S, P_R} \frac{B_N}{2} \sum_{j \in \mathcal{J}} \min \left\{ \log_2 \left(1 + \frac{\gamma_{SD}(j) P_S(j)}{\Gamma} + \frac{\gamma_{RD}(j) P_R(j)}{\Gamma}\right), \log_2 \left(1 + \frac{\gamma_{SR}(j) P_S(j)}{\Gamma}\right)\right\}, \tag{6.26a}$$

$$\text{s.t. (6.17b), (6.17c), (6.17d).} \tag{6.26b}$$

Problem (6.26) is a convex optimization problem; the objective function is a concave function as can be proved using property 3 of concave functions introduced in Section 2.6, and the constraints are linear. Optimization problem (6.26) can be rewritten as:

$$R = \max_{P_S, P_R} \frac{B_N}{2} \sum_{j \in \mathcal{J}} \log_2 \left(1 + \frac{\gamma_{SD}(j) P_S(j)}{\Gamma} + \frac{\gamma_{RD}(j) P_R(j)}{\Gamma}\right), \tag{6.27a}$$

$$\text{s.t. } (\gamma_{SD}(j) - \gamma_{SD}(j)) P_S(j) + \gamma_{RD}(j) P_R(j) \leq 0, \ \forall j \in \mathcal{J}, \tag{6.27b}$$

$$\text{(6.17b), (6.17c), (6.17d).} \tag{6.27c}$$

Table 6.3 Resource Allocation for DF-OFDM.

	Water-fill	Unif.	Opt.
Criterion	Opt. $P_S(j)$ No Relaying	Unif. $P_S(j)$ Unif. $P_R(j)$	Opt. $P_S(j)$ Opt. $P_R(j)$
Data Rate in [Kbps]	32.13	32.72	46.93

The optimal power profile at the source node can be computed as:

$$P_S^*(j) = \begin{cases} \left(\frac{K\gamma_{SD}(j)}{\gamma_{SR}(j)} - \frac{\Gamma}{\gamma_{SR}(j)}\right)^+ & \text{if } P_R^*(j) > 0, \\ \left(K - \frac{\Gamma}{\gamma_{SD}(j)}\right)^+ & \text{if } P_R^*(j) = 0, \end{cases} \tag{6.28}$$

and the optimal power profile at the relay node can be obtained as:

$$P_R^*(j) = C(j)P_S^*(j), \tag{6.29}$$

with $C(j) = \frac{\left(\gamma_{SR}(j) - \gamma_{SD}(j)\right)^+}{\gamma_{RD}(j)}$ and $K = \frac{B_N}{2\ln(2)\lambda_S}$.

Resource allocation for DF scheme under total power constraint at the source and relay nodes was considered in [146]. Resource allocation for DF scheme with subcarrier pairing was investigated in [64].

Table 6.3, compares the achievable data rate for $N = 16$ subcarriers DF-OFDM system using the same setting as in **Tables 6.1 & 6.2**. Clearly, the achievable data rate of DF-OFDM with optimal power allocation at the source and relay nodes is higher than the achievable data rate of the direct link only with optimal power allocation at the source node, and higher than the achievable data rate of AF-OFDM with optimal power allocation at the source and relay nodes.

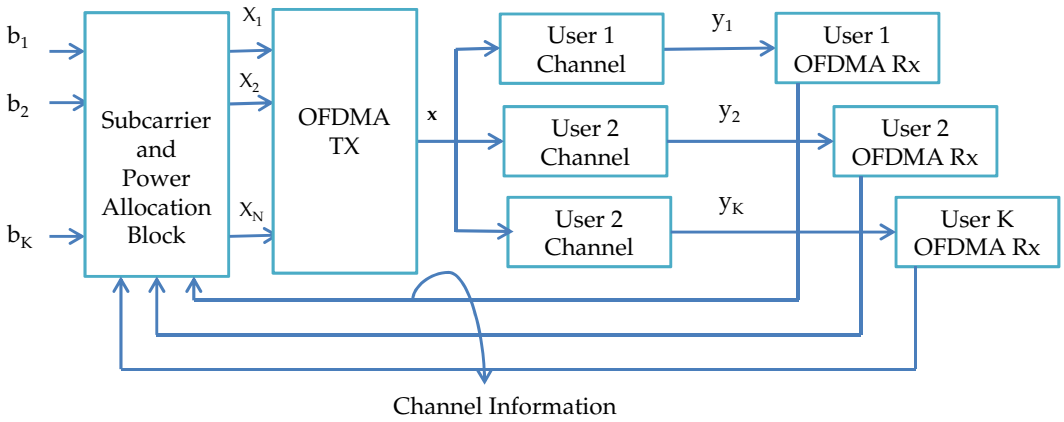

Figure 6.3 Block Diagram of OFDMA Transmitter.

6.2 Basics of OFDMA Systems

OFDMA is a method that allows multiple users to access the air interface at the same time by assigning different groups of subcarriers (in frequency) to different users. OFDM assigns all N subcarriers within a group to a single user, and only one user can transmit at a time. If multiple users want to transmit using OFDM, then those users have to take their turns in time (TDMA); i.e. in OFDM each user can be assigned one OFDM symbol in time, and OFDM symbols are assigned to their respective users. In OFDMA, instead of sequentially assigning OFDM symbols in time to different users, the subcarriers are directly assigned to different users. **Figure 6.3** shows the block diagram of OFDMA transmitter.

In general, there are many ways to assign users' data symbols to subcarriers. For example, distributed and contiguous assignments are common methods. In a distributed subcarrier assignment, subcarriers are assigned pseudorandomly to users. Whereas, in contiguous subcarrier assignments, subcarriers are assigned to users in continuous sets. The main advantages of OFDMA system are that it can benefit from frequency diversity and multiuser diversity. Frequency diversity can be utilized by assigning the subcarriers in a distributed way to the users; some of the users' subcarriers would likely experience good channel conditions, while other

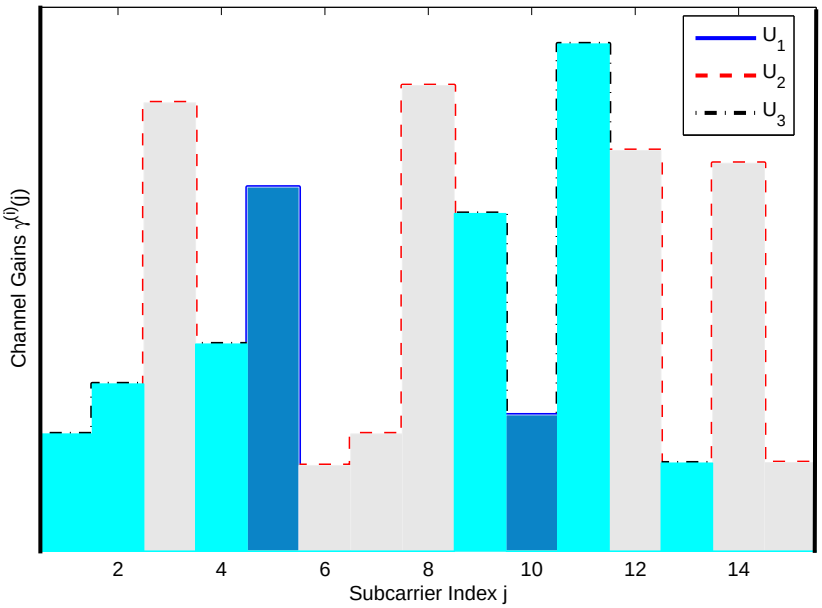

Figure 6.4 Subcarrier Assignment for OFDMA system.

user subcarriers would likely experience bad channel conditions. Multi-user diversity occurs because different users at different locations would likely experience different channel conditions. It can be utilized by assigning subcarriers that experience the best channel conditions to the best user [162]. **Figure 6.4** shows an example of three users OFDMA system, where the subcarrier is assigned to the user with the best channel gains. OFDM and OFDMA are used in many standards that include IEEE 802.11a/WiFi, IEEE 802.15/WiPAN, IEEE 802.16/ WiMAX, IEEE 802.20/MobileFi, IEEE 802.22/WiRAN, digital audio broadcasting (DAB), terrestrial broadcasting of digital television (DVB-T, DVB-H), Flash-OFDM, SDARS for satellite radio, G.DMT (ITU G.992.1) for ADSL, and ITU-T G.hn for power line communication [51].

6.2.1 Resource Allocation for OFDMA

The problem of assigning the subcarriers, rates, time slots, and power profiles to different users in an OFDMA system has been an area of active research over the past several years. The research in this area can be catego-

rized into two areas: margin-adaptive and rate-adaptive. In margin adaptation, the aim is to minimize the transmit power subject to minimum QoS parameters for each user, which could be a combination of data rate, bit error rates, delays, etc. In rate adaptation, the aim is to maximize the data rate subject to various QoS and/or resource constraints [154].

In the following formulations, two degrees of freedoms are utilized, namely frequency, and multi-user dimensions. The weighted-sum rate maximization subject to a single power constraint for down-link communication, as well as the weighted-sum rate maximization subject to individual power constraint for up-link communications are introduced, assuming perfect CSI is available at the transmitter(s). The weighted-sum rate maximization problem for up-link OFDMA system[7] can be formulated as:

$$\max_{\boldsymbol{P},\boldsymbol{Y}} B_N \sum_{i\in\mathcal{I}} \alpha_i \sum_{j\in\mathcal{J}} Y_i(j) \log_2\Big(1+\frac{\gamma^{(i)}(j)P^{(i)}(j)}{\Gamma}\Big), \tag{6.30a}$$

$$\text{s.t.} \sum_{i\in\mathcal{I}} Y_i(j)P^{(i)}(j) \le P_i^{\max},\ \forall i\in\mathcal{I} \tag{6.30b}$$

$$\sum_{i\in\mathcal{I}} Y_i(j) \le 1, \forall j\in\mathcal{J}, \tag{6.30c}$$

$$P^{(i)}(j)\ge 0, Y_i(j)\in\{0,1\},\ \forall j\in\mathcal{J},\ \forall i\in\mathcal{I}, \tag{6.30d}$$

where, the set of users is denoted as $\mathcal{I}=\{1,\cdots,I\}$. $\boldsymbol{P}$ contains the power profiles, where $[\boldsymbol{P}]_{i,j}=P^{(i)}(j)$ at the source nodes $\forall i\in\mathcal{I}$ and $\forall j\in\mathcal{J}$. The matrix $\boldsymbol{Y}$ is the subcarrier assignment profile $[\boldsymbol{Y}]_{i,j}=Y_i(j),\in\{0,1\}$, with $Y_i(j)=1$ indicates that subcarrier j is assigned to user i, and α_i's are the relative priority for each user.

The weighted-sum rate maximization problem for down-link OFDMA system can be formulated in a similar fashion to (6.30) by replacing the in-

[7] Assuming orthogonal transmission, i.e. no interference is considered between the users at the j subcarrier.

dividual power constraint (6.30b) by the total power constraint as:

$$\sum_{i\in\mathcal{I}}\sum_{j\in\mathcal{J}} Y_i(j)P^{(i)}(j) \leq P^{\max}, \tag{6.31}$$

where, $P^{\max}$ is the total available power at the base-station or the access-point. The resource allocation problem (6.30) for OFDMA is a MINLP problem, which is computationally complex for real-time implementation using exhaustive search algorithms. A popular approach to attain near-optimality is constraint relaxation. This approach performs a convex reformulation of the problem by relaxing the binary integer constraints $Y_i(j) \in \{0,1\}$ to interval constraints $0 \leq Y_i(j) \leq 1$, where $Y_i(j)$ is now a sharing factor. The solution to the reformulated convex problem is then projected back to the original constraint space using some criteria; for example, assigning each subcarrier to the user with the largest sharing factor. This approach is sub-optimal, and more importantly, it is also computationally prohibitive, because it involves solving a large constrained convex optimization problem with $2NI$ variables with $2NI + I + N + 1$, and $2IN + I + 1$ linear inequality constraints for up-link and down-link resource allocation problems, respectively. The number of operations per iteration when using Newton-type projected gradient methods is $O\left((2NI)^3\right)$ [154].

Another popular approach is based on Lagrangian relaxation of the power constraints, instead of the constraint relaxation. This relaxation incorporates the power constraints into the objective function, thereby allowing us to solve the dual problem instead and achieves relative optimality as discussed next.

6.2.2 Zero Duality Gap Principle

Problem (6.30) is one of a family of resource allocation problems for multicarrier communications, in which the optimization objective and the con-

straints consist of large number of individual functions, each corresponds to one of the $n \in \mathcal{J}$ frequency subcarriers, that is, the resource allocation problem can be written as [167]:

$$\max \sum_{n \in \mathcal{J}} f_n(\boldsymbol{x}_n), \tag{6.32a}$$

$$\text{s.t.} \sum_{n \in \mathcal{J}} \boldsymbol{h}_n(\boldsymbol{x}_n) \leq \boldsymbol{P}, \tag{6.32b}$$

where $\boldsymbol{x}_n \in \mathbb{R}^I$ are vectors of optimization variables, $f_n(\cdot)$ are $\mathbb{R}^I \mapsto \mathbb{R}$, and $\boldsymbol{h}_n$ are $\mathbb{R}^I \mapsto \mathbb{R}^L$ functions. Power constraints are denoted by the vector $\boldsymbol{P}$. Here, $\leq$ is used to denote a component-wise inequality. The time sharing condition is defined as:

Definition 6.2.1 *Let $\boldsymbol{x}_n^*$ and $\boldsymbol{y}_n^*$ be optimal solutions to the optimization problem* (6.32) *with $\boldsymbol{P} = \boldsymbol{P}_x$, and $\boldsymbol{P} = \boldsymbol{P}_y$, respectively. An optimization problem of the form* (6.32) *is said to satisfy the time sharing condition if for any $\boldsymbol{P}_x$ and $\boldsymbol{P}_y$ and for any $0 \leq \alpha \leq 1$, there always exists a feasible solution $\boldsymbol{z}_n$, such that $\sum_{n \in \mathcal{J}} f_n(\boldsymbol{z}) \geq \alpha \sum_{n \in \mathcal{J}} f_n(\boldsymbol{x}^*) + (1 - \alpha) \sum_{n \in \mathcal{J}} f_n(\boldsymbol{y}^*)$.*

The time sharing condition leads to the following theorem [167]:

Theorem 6.2.1 *For an optimization problem of the form* (6.32)*, if the optimization problem satisfies the time sharing property, then it has a zero duality gap regardless of the concavity of $f_n(\boldsymbol{x}_n)$ and the convexity of $h_n(\boldsymbol{x}_n)$. The time sharing condition for multi-carrier systems is satisfied in the limit as $N \to \infty$.*

The dual optimization framework for problem (6.30) is much less complex, with complexity order $O(IN)$ for non-orthogonal transmission as in [154]. The weighted-sum rate maximization problem for the down-link OFDMA system was solved using the dual approach as in [121]. Theorem 6.2.1 is used to solve many practical OFDMA resource allocation problems, since the problem can be solved in the dual domain by efficient numerical algorithms as in [30, 67, 68].

6.2.3 Two-Band Partition Principle

The two-band partition principle is an interesting approach that is used to allocate the subcarriers for two users up-link OFDMA system for high SNR scenarios, aiming to maximize the weighted sum rate. It can be stated by the following theorem [166].

Theorem 6.2.2 *For a two-user $i = 1, 2$ Gaussian mulitple-access channel for high SNR on each subcarrier, assume $S(m) = \frac{(\gamma^{(1)}(m))^{\alpha_1}}{(\gamma^{(2)}(m))^{\alpha_2}}$ is decreasing in m, then the optimal frequency partition that maximizes the weighted sum rate consists of two contiguous frequency bands with user 1 using subcarriers indexed from 1 to C_P in the ordered set, and user 2 using the subcarriers indexed from $C_p + 1$ to N in the ordered set. The ordering of the subcarriers is based on $\frac{(\gamma^{(1)}(j))^{\alpha_1}}{(\gamma^{(2)}(j))^{\alpha_2}}$ in a decreasing order, where $\gamma^{(i)}(j) = \frac{|H^{(i)}(j)|^2}{B_N N_0}$.*

Theorem 6.2.2 provides a less complex algorithm for a two user maximum weighted sum rate resource allocation problem; i.e. the maximum number of times required to solve the resource allocation problem (the power profile for a given subcarrier assignment profile) is $O(N)$ which can be reduced using binary search algorithms to $O\Big(\log_2(N)\Big)$. In addition, the sorting of the subcarriers in the proposed theorem requires $O\Big(N \log_2(N)\Big)$ computations for the worst case and $O(N)$ for the best case. Thus, using the two bands principle, avoids the need to solve the problem in the dual domain and find the optimal Lagrangian multipliers, which entails a large number of iterations using the gradient or subgradient methods [143]. The resource allocation for multiple users $I > 2$ uplink OFDM system aiming to maximize the weighted sum rate, was investigated based on the two bands principle (the two users case) using an iterative algorithm to exchange the subcarriers between the users as in [50].

6.2.4 OFDMA with Cooperative Communications

Power allocation and subcarrier pairing have attracted research attention in OFDMA cooperative communication systems. The weighted-sum rate maximization problem for a single relay OFDMA uplink cooperative communication system with subcarrier pairing can be formulated as:

$$\max_{\boldsymbol{P}_R, \boldsymbol{P}_S, \boldsymbol{Y}, \boldsymbol{X}} B_N \sum_{i\in\mathcal{I}} \alpha_i \sum_{j\in\mathcal{J}} \sum_{k\in\mathcal{J}} Y_i(j,k)X(j,k)R^{(i)}(j,k), \tag{6.33a}$$

$$\text{s.t.} \sum_{i\in\mathcal{I}} \sum_{k\in\mathcal{J}} \sum_{j\in\mathcal{J}} Y_i(j,k)X(j,k)P_R^{(i)}(k) \le P_R^{\max}, \tag{6.33b}$$

$$\sum_{k\in\mathcal{J}} \sum_{j\in\mathcal{J}} Y^{(i)}(j,k)X(j,k)P_S^{(i)}(j) \le P_i^{\max}, \forall i \in \mathcal{I}, \tag{6.33c}$$

$$\sum_{i\in\mathcal{I}} Y^{(i)}(j,k) \le 1, \forall j,k \in \mathcal{J}, \tag{6.33d}$$

$$\sum_{k\in\mathcal{J}} X(j,k) = 1, \ \forall j \in \mathcal{J}, \tag{6.33e}$$

$$\sum_{j\in\mathcal{J}} X(j,k) = 1, \ \forall k \in \mathcal{J}, \tag{6.33f}$$

$$P_S^{(i)}(j) \ge 0, \ P_R^{(i)}(k) \ge 0, \ \forall i \in \mathcal{I}, \ \forall j,k \in \mathcal{J}, \tag{6.33g}$$

$$Y^{(i)}(j,k) \in \{0,1\}, \ X(j,k) \in \{0,1\}, \ \forall i \in \mathcal{I}, \ \forall j,k \in \mathcal{J}, \tag{6.33h}$$

where $R^{(i)}(j,k)$ for AF cooperative communication is computed as:

$$R^{(i)}(j,k) = \frac{1}{2}\log_2\Big(1 + \frac{P_S^{(i)}(j)\gamma_{SD}^{(i)}(j)}{\Gamma} + \frac{\gamma_{SR}^{(i)}(j)\gamma_{RD}(k)P_S^{(i)}(j)P_R^{(i)}(k)}{\Gamma(1+\gamma_{SR}^{(i)}(j)P_S^{(i)}(j)+\gamma_{RD}(k)P_R^{(i)}(k))}\Big), \tag{6.34}$$

and $R^{(i)}(j,k)$ for DF cooperative communication is computed as:

$$R^{(i)}(j,k) = \frac{1}{2}\min\Big\{\log_2\Big(1 + \frac{P_S^{(i)}(j)\gamma_{SD}^{(i)}(j)}{\Gamma} + \frac{\gamma_{RD}(k)P_R^{(i)}(k)}{\Gamma}\Big), \log_2\Big(1 + \frac{P_S^{(i)}(\mathrm{j})\gamma_{SR}^{(i)}(\mathrm{j})}{\Gamma}\Big)\Big\}. \tag{6.35}$$

Subcarrier j is said to be paired to subcarrier k when $X(j,k) = 1$, i.e. subcarrier j is used for the first-hop transmission and subcarrier k is used for the second-hop transmission. $Y^{(i)}(j,k) = 1$ means that the pair of subcarriers (j,k) is assigned to user i. The constraint (6.33d) means that the pair of subcarriers (j,k), $\forall j,k \in \mathcal{J}$ can be assigned only to one user. The constraints (6.33e) and (6.33f) indicate that a subcarrier in the first-hop can be paired only to one subcarrier in the second-hop.

Problem (6.33) with some simplifications was solved in literature using the dual approach as in [128], where the maximum sum rate is found (i.e. $\alpha_i = 1$, $\forall i \in \mathcal{I}$) without direct-link communications between the sources and destination nodes for OFDMA-AF scheme, and using the high SNR approximation as given in (6.22). The weighted-sum rate maximization problem for single relay OFDMA-DF was solved using the dual approach and a polynomial time algorithm was proposed as in [48, 96]. The maximum sum rate down-link resource allocation for OFDM-DF under total power constraint at the source and relay nodes was solved with the assumption of no direct-link between the source and destination nodes, the subcarriers were ordered in the first and second hops and then paired as in [177]. Resource allocation for DF-OFDM with subcarrier pairing for two way relaying is addressed in [97]. Resource allocation in DF-OFDMA system with perfect and imperfect CSI is addressed in [18]. Resource allocation in multiple relay aided DF-OFDM system is addressed in [150].

6.3 Conclusions

In this chapter, fundamental concepts of OFDM and OFDMA systems are explained, some resource allocation problems are formulated. The achievable data rate of an OFDM system with AF/DF cooperative communication schemes for different resource allocation criteria are compared. Basic theorems for resource allocation for multicarrier systems are reviewed. Resource

allocation problems for OFDMA with cooperative communications are introduced. In the second part of this dissertation, the emphasis will be in designing resource allocation algorithms for OFDM and OFDMA systems with cooperative communications with reduced computational complexity.

CHAPTER7

RELAY MODE SELECTION FOR OFDM SYSTEMS

This chapter investigates resource allocation for a single user relay aided OFDM cooperative communication system. The objective is to allocate the resources to maximize the sum rate over one OFDM symbol subject to either individual power constraint on each node or total power constraint. Three scenarios are addressed in this chapter; in the first scenario, the relay uses AF to transmit messages on a set of available subcarriers with diversity, and the remaining subcarriers are used for direct transmission without diversity. In the second scenario, the relay uses DF to transmit messages on a set of available subcarriers with diversity and the remaining subcarriers are used for direct transmission without diversity. In the third scenario, the relay uses AF with diversity on a set of available subcarriers, and the remaining subcarriers are used for DF with diversity.

A low complexity algorithm is proposed based on high SNR approximation and optimal power profiles at the source and relay nodes for the three scenarios of $O(N)$ complexity, where N is the number of subcarriers. Simulation results demonstrate the merits of the proposed algorithm.

Introduction and related works are presented in Section 7.1. In Section 7.2, the formulation of the optimization problem for selective AF-OFDM, and the proposed subcarrier assignment algorithm are presented. In Section 7.3, the algorithm is extended for selective DF-OFDM. In Section 7.4, the algorithm is drawn out for the hybrid AF-DF-OFDM scheme. In Section 7.5,

AF/DF-OFDM and hybrid AF-DF-OFDM schemes are discussed under total power constraint. Numerical results are presented and discussed in Section 7.6. Finally, conclusions are drawn in Section 7.7.

7.1 Introduction

Efficient management of the relay and source resources becomes a critical issue for increasing transmission rate in relay-aided OFDM communication systems. As presented in Chapter 6, power allocation for OFDM cooperative communication can be studied under different criteria, for example, optimal power allocation at the source and relay nodes as in [49, 126]. In this chapter, another degree of freedom is explored to increase the transmission rate by selecting the mode of operation; for example, AF/DF cooperative scheme can be used for some subcarriers, and direct transmission will be used for the remaining subcarriers, this scheme is denoted as selective AF/DF-OFDM cooperative communication scheme.

Selective AF-OFDM can be considered as a special case of the improved AF cooperative communication scheme proposed in Chapter 4, where the subcarrier can be used either for AF with diversity or for direct transmission without diversity. In [36], resource allocation for selective AF-OFDM cooperative communication scheme under individual node power constraint is studied, and an iterative algorithm for subcarrier assignment based on the minimum required relaying power is proposed. In each iteration, the ordering of the subcarriers based on the relaying power is recomputed, and the subcarrier with the highest required relaying power is used for direct transmission. In [147] resource allocation for selective DF-OFDM cooperative communication scheme is investigated under individual node, and total power constraints based on the dual approach, and an iterative algorithm is developed to assign the subcarriers to the modes of transmission.

The main contribution of this chapter is to develop a low complexity

algorithm to allocate the resources; power profiles at the source and relay nodes and subcarrier assignment for selective AF-OFDM, selective DF-OFDM, and hybrid AF-DF-OFDM cooperative communication schemes in high SNR scenarios. Exploring the structure of each problem after relaxing the integer variables leads to the proposed algorithm. The idea is to search through a subset of frequency partitions and find the partition which is close to the global optimum. Such an approach was previously considered in [50, 166] to allocate the subcarriers in OFDMA system without cooperation. In this chapter, the algorithm is extended to cooperative communication scenarios. Although, it is based on the same idea, there is a major difference; the subcarriers in AF/DF-OFDM system after the assignment are constrained by the source power constraint, whereas in the OFDMA system after the subcarrier assignment step, each user water-fills its source power individually. In addition, the subcarriers in this research belong to a single user, but the subcarrier can be used in one transmission mode (i.e. either AF/DF relaying or direct transmission). Whereas, in the OFDMA system the subcarriers are allocated to multiple users.

In this chapter, the proposed algorithm is developed based on optimal source and relay power profiles; a simple function is used for sorting the subcarriers and splitting them into two partitions. In selective AF/DF-OFDM, the first partition is used for AF/DF cooperative communication with diversity, whereas the second partition is used for direct transmission without diversity. In hybrid AF-DF-OFDM, the first partition is used for AF cooperative communication with diversity, whereas the second partition is used for DF cooperative communication with diversity. The partition that maximizes the sum rate is searched. The proposed subcarrier assignment algorithm in this chapter is different from the algorithms proposed in [36, 147], since it is based on an ordering of the subcarriers according to a function defined in terms of the channel gains, and not on the minimum

required relaying power which is computed only once. Besides, the source and relay power profiles for selective AF-OFDM are found analytically in a closed form, using the upper bound of the end-to end SNR, without the need of the iterative two steps procedure to find the power profiles at the source and relay nodes.

7.2 Selective AF-OFDM Cooperative Communications

The system under consideration is depicted in **Figure 7.1**. Sender (Source) node S communicates with the destination terminal D. We consider a single relay two-hop multi carrier OFDM system, where the wide-band channel is divided into N narrow-band subcarriers, the bandwidth of each subcarrier is B_N and the set of subcarriers is defined as $\mathcal{J} = \{1, \cdots, N\}$. In selective AF-OFDM transmission, the jth subcarrier can be either used in AF two-hops transmission with diversity, referred to as mode one ($i = 1$), or it can be used for direct transmission without diversity referred to as mode two ($i = 2$). The received signals at the relay and destination nodes in the first-time slot T_1 at the jth subcarrier are defined as $Y_R(j)$ and $Y_{D_1}(j)$, respectively, and can be obtained as:

$$Y_R(j) = \sqrt{P_S^{(1)}(j)} H_{SR}(j) X_j + n_R(j), \tag{7.1a}$$

$$Y_{D_1}(j) = \sqrt{P_S^{(i)}(j)} H_{SD}(j) X_j + n_{D_1}(j), \tag{7.1b}$$

where $P_S^{(i)}(j)$ is the source transmit power on the jth subcarrier in the ith transmission mode for $i \in \{1, 2\}$ in the first-time slot. The transmitted symbol X_j at the jth subcarrier is drawn from a constellation with unit energy, $n_R(j)$ and $n_{D_1}(j)$ are AWGNs in the first-time slot with variance σ^2 received at the relay and destination nodes at the jth subcarrier, respectively. The SNR at

Subcarrier (j)	Strategy
1	AF
2	DC
...	...
N	AF

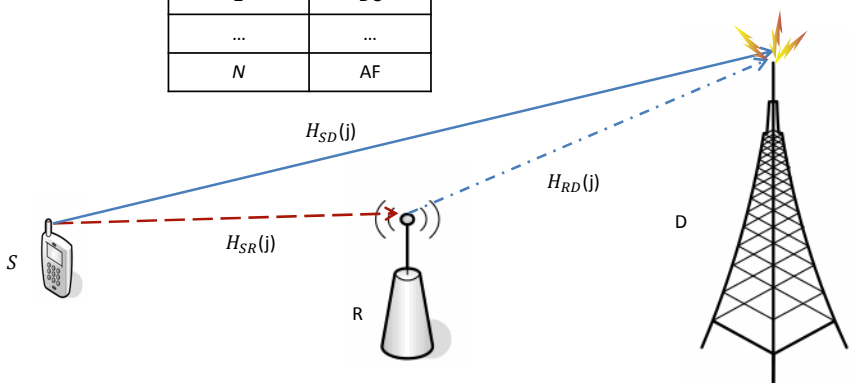

Figure 7.1 System Model

the jth subcarrier at the destination node is denoted as $\Gamma_{SD}^{(i)}(j)$, which results from direct transmission between the source-destination pair using the jth subcarrier, defined as:

$$\Gamma_{SD}^{(i)}(j) = \gamma_{SD}(j)P_S^{(i)}(j), \tag{7.2}$$

where $\gamma_{SD}(j) = \frac{|H_{SD}(j)|^2}{\sigma^2}$. During the second-time slot T_2, the relay amplifies and transmits the received signal at the same subcarrier. Hence, the received signal $Y_{D_2}(j)$ at the jth subcarrier at the destination node is obtained as:

$$Y_{D_2}(j) = G(j)\sqrt{P_R(j)}H_{RD}(j)Y_R(j) + n_{D_2}(j), \tag{7.3}$$

where $P_R(j)$ is the relay transmitted power at the jth subcarrier, $n_{D_2}(j)$ is the AWGN received at the destination node in the second-time slot. $G(j)$ is the normalization factor at the relay station given as $G(j) = \frac{1}{\sqrt{P_S^{(1)}(j)|H_{SR}(j)|^2+\sigma^2}}$. The end-to-end SNR of the jth subcarrier denoted as $\Gamma_{AF}(j)$ is given by [4]:

$$\Gamma_{AF}(j) = \frac{P_S^{(1)}(j)P_R(j)|H_{SR}(j)|^2|H_{RD}(j)|^2}{\sigma^2(\sigma^2 + P_S^{(1)}(j)|H_{SR}(j)|^2 + P_R(j)|H_{RD}(j)|^2)}, \tag{7.4}$$

which can be rewritten in a simplified form as:

$$\Gamma_{AF}(j) = \frac{\gamma_{SR}(j)\gamma_{RD}(j)P_S^{(1)}(j)P_R(j)}{1 + \gamma_{SR}(j)P_S^{(1)}(j) + \gamma_{RD}(j)P_R(j)}, \tag{7.5}$$

where $\gamma_{SR}(j) = \frac{|H_{SR}(j)|^2}{\sigma^2}$, and $\gamma_{RD}(j) = \frac{|H_{RD}(j)|^2}{\sigma^2}$. The data rate $R^{(1)}(j)$ of AF scheme at the destination node with the aid of the relay node in mode 1 and using the MRC technique can be computed as:

$$R^{(1)}(j) = \frac{B_N}{2} \log_2(1 + \frac{\Gamma_{SD}^{(1)}(j) + \Gamma_{AF}(j)}{\Gamma}), \tag{7.6}$$

The data rate $R^{(2)}(j)$ in mode 2 at the destination node is obtained as:

$$R^{(2)}(j) = B_N \log_2(1 + \frac{\Gamma_{SD}^{(2)}(j)}{\Gamma}). \tag{7.7}$$

The objective of the resource allocation problem is to maximize the achievable data rate over the entire OFDM symbol with N subcarriers, which can be formulated as:

$$R = \max_{\boldsymbol{P},\boldsymbol{Y}} \sum_{i=1}^{2} \sum_{j \in \mathcal{J}} \Upsilon_j^{(i)} R^{(i)}(j), \tag{7.8a}$$

$$\text{s.t.} \sum_{j \in \mathcal{J}} \Upsilon_j^{(1)} P_R(j) \leq P_R^{\max}, \tag{7.8b}$$

$$\sum_{i=1}^{2} \sum_{j \in \mathcal{J}} \Upsilon_j^{(i)} P_S^{(i)}(j) \leq P_S^{\max}, \tag{7.8c}$$

$$\sum_{i=1}^{2} \Upsilon_j^{(i)} \leq 1, \ \forall j \in \mathcal{J}, \tag{7.8d}$$

$$P_R(j) \geq 0, \ P_S^{(i)}(j) \geq 0, \ \Upsilon_j^{(i)} \in \{0,1\}, \ \forall j \in \mathcal{J}, \ i = 1,2, \tag{7.8e}$$

where $\boldsymbol{P}$, is the vector of the source and relay power profiles, which includes $P_S^{(i)}(j)$ and $P_R(j)$, $\forall j \in \mathcal{J}$ and $i = 1,2$. The vector $\boldsymbol{\Upsilon}$ is the carrier assignment profile with $\Upsilon_j^{(i)} = 1$ indicates that subcarrier j is used in the ith transmission mode ($i = 1,2$). Constraint (7.8b) means that the total power allocated to forward the data by the relay is constrained to $P_R^{\max}$. Whereas, constraint (7.8c) indicates that the source power is constrained to $P^{\max}$. Constraint (7.8d) means that the jth subcarrier can be assigned to maximally one mode of

transmission, either AF relaying (i.e. $i = 1$, with $(Y_j^{(1)}, Y_j^{(2)}) = (1, 0)$) or direct transmission (i.e. $i = 2$, with $(Y_j^{(1)}, Y_j^{(2)}) = (0, 1)$). Problem (7.8) is a mixed integer constraint optimization problem. First, we will solve the power allocation problem for a given subcarrier assignment profile, and then we will use the optimal power allocation profile to find the optimal subcarrier assignment profile. For high SNR $\Gamma_{AF}(j)$ can be approximated by its upper bound as in [56]:

$$\Gamma_{AF}(j) \approx \frac{\gamma_{SR}(j)\gamma_{RD}(j)P_S^{(1)}(j)P_R(j)}{\gamma_{SR}(j)P_S^{(1)}(j) + \gamma_{RD}(j)P_R(j)}, \tag{7.9}$$

which will be used from now on to derive the forthcoming results. With this approximation, the data rate (7.6) becomes a jointly concave function with respect to the source and relay power profiles as shown in Appendix B.1. Thus (7.8) for a given subcarrier assignment profile can be solved using any convex optimization technique. Here, we seek an analytical solution by relaxing the power constraints (7.8c) and (7.8e) and by formulating the Lagrangian function as:

$$\begin{aligned} L(\boldsymbol{P}, \boldsymbol{\lambda}) = &\sum_{j\in\mathcal{J}_1} R^{(1)}(j) + \sum_{j\in\mathcal{J}_2} R^{(2)}(j) - \lambda_R\Big(\sum_{j\in\mathcal{J}_1} P_R(j) - P_R^{\max}\Big) \\ &- \lambda_S\Big(\sum_{j\in\mathcal{J}_1} P_S^{(1)}(j) + \sum_{j\in\mathcal{J}_2} P_S^{(2)}(j) - P_S^{\max}\Big), \end{aligned} \tag{7.10}$$

$$\text{s.t. } \lambda_R \geq 0,\ \lambda_S \geq 0,\ P_S^{(i)}(j) \geq 0,\ P_R(j) \geq 0,\ \forall i = 1, 2,\ \forall j \in \mathcal{J}, \tag{7.11}$$

where $\mathcal{J}_i$ is the set of subcarriers that are assigned to mode i, for $i = 1, 2$. Assuming that subcarrier j is used in mode 1, differentiating (7.10) with respect to $P_S^{(1)}(j)$ and equating to zero, results in:

$$\frac{\Gamma + \Gamma_{SD}^{(1)}(j) + \Gamma_{AF}(j)}{B_N/2\ln(2)} = \frac{1}{\lambda_S}\Big(\gamma_{SD}(j) + \frac{\gamma_{SR}(j)\gamma_{RD}^2(j)P_R^2(j)}{(\gamma_{SR}(j)P_S^{(1)}(j) + \gamma_{RD}(j)P_R(j))^2}\Big). \tag{7.12}$$

Similarly, for the relay power, differentiating (7.10) with respect to $P_R(j)$ and equating to zero results in:

$$\frac{\Gamma + \Gamma_{SD}^{(1)}(j) + \Gamma_{AF}(j)}{B_N/2\ln(2)} = \frac{\gamma_{RD}(j)\gamma_{SR}^2(j)P_S^{(1)2}(j)}{\lambda_R\Big(\gamma_{SR}(j)P_S^{(1)}(j) + \gamma_{RD}(j)P_R(j)\Big)^2}. \tag{7.13}$$

Simultaneously, solving (7.12) and (7.13), the optimal source power profile for mode 1 can be obtained as:

$$P_S^{(1)}(j) = \frac{\Big(K(\gamma_{SD}(j) + A_j) - \Gamma\Big)^+}{\gamma_{SD}(j) + B_j}, \tag{7.14}$$

where $A_j = \frac{\gamma_{SR}(j)\gamma_{RD}^2(j)C_j^2}{(\gamma_{SR}(j)+\gamma_{RD}(j)C_j)^2}$, $B_j = \frac{\gamma_{SR}(j)\gamma_{RD}(j)C_j}{\gamma_{SR}(j)+\gamma_{RD}(j)C_j}$, $K = \frac{B_N}{2\ln(2)\lambda_S}$ and C_j is computed as:

$$C_j = \frac{\gamma_{SR}(j)\Big(-1 + \sqrt{1 + (1 + \frac{\gamma_{SR}(j)}{\gamma_{SD}(j)})(\frac{\lambda_S}{\lambda_R}\frac{\gamma_{RD}(j)}{\gamma_{SD}(j)} - 1)}\Big)^+}{\gamma_{RD}(j)(1 + \frac{\gamma_{SR}(j)}{\gamma_{SD}(j)})}. \tag{7.15}$$

The optimal relay power profile is obtained as:

$$P_R(j) = C_j P_S^{(1)}(j). \tag{7.16}$$

On the other hand, if subcarrier j is used in mode 2, differentiating (7.10) with respect to $P_S^{(2)}(j)$ and equating to zero results in:

$$P_S^{(2)}(j) = \Big(\frac{B_N}{\ln(2)\lambda_S} - \frac{\Gamma}{\gamma_{SD}(j)}\Big)^+. \tag{7.17}$$

The assumption here is that if subcarrier j is assigned to transmission mode $i = 1, 2$ then the power profiles at the source and relay nodes are as in (7.14) and (7.16) for mode 1 and the source power profile for mode 2 is as in (7.17) with λ_R, λ_S are selected to satisfy the power constraints (7.8b) and (7.8b), respectively. In order to decide on the subcarrier assignment profile, the problem is an integer problem that is difficult to solve unless an exhaustive

search is used over all possible $Y_j^{(i)}$. To simplify the analysis, the subcarrier assignment profile is relaxed as $0 \leq Y_j^{(i)} \leq 1$. Incorporating this into the Lagrangian function of (7.8), denoting it as $L(\boldsymbol{P}, \boldsymbol{Y}, \boldsymbol{\lambda})$[1], then equating the derivative of $L(\boldsymbol{P}, \boldsymbol{Y}, \boldsymbol{\lambda})$ with respect to the relaxed integer $Y_j^{(i)}$ to zero, results in:

$$\log_2\left(1 + \frac{\Gamma_{SD}^{(1)}(j) + \Gamma_{AF}(j)}{\Gamma Y_j^{(1)}}\right) - \frac{\Gamma_{SD}^{(1)}(j) + \Gamma_{AF}(j)}{\Gamma Y_j^{(1)} + \Gamma_{SD}^{(1)}(j) + \Gamma_{AF}(j)} = 2\log_2\left(1 + \frac{\Gamma_{SD}^{(2)}(j)}{\Gamma Y_j^{(2)}}\right) - \frac{2\Gamma_{SD}^{(2)}(j)}{\Gamma Y_j^{(2)} + \Gamma_{SD}^{(2)}(j)}. \quad (7.18)$$

The LHS and RHS of (7.18) can be interpreted as the marginal benefit for extra bandwidth for mode 1 and mode 2, respectively. If a subcarrier is shared between the two modes, the marginal benefits for the two modes should be equal [166]. If the LHS of (7.18) is strictly greater than the RHS of (7.18), the jth subcarrier should be used in mode 1, i.e. $Y_j^{(1)} = 1$, and $Y_j^{(2)} = 0$. Likewise, if the RHS of (7.18) is strictly greater than the LHS of (7.18), the jth subcarrier should be used in mode 2, i.e. $Y_j^{(2)} = 1$, and $Y_j^{(1)} = 0$. Based on this observation, the subcarrier should be assigned to the mode with the higher marginal benefit. At high SNR $\frac{\Gamma_{SD}^{(1)}(j)+\Gamma_{AF}(j)}{\Gamma Y_j^{(1)}+\Gamma_{SD}^{(1)}(j)+\Gamma_{AF}(j)} \approx 1$, and $\frac{\Gamma_{SD}^{(2)}(j)}{\Gamma Y_j^{(2)}+\Gamma_{SD}^{(2)}(j)} \approx 1$. Hence, substituting (7.12) in (7.18), the LHS of (7.18) can be approximated as:

$$\log_2\left(\gamma_{SD}(j) + \frac{\gamma_{SR}(j)\gamma_{RD}^2(j)P_R^2(j)}{(\gamma_{SR}(j)P_S^{(1)}(j) + \gamma_{RD}(j)P_R(j))^2}\right) + \log_2(B_N/2\ln(2)\Gamma\lambda_S) - 1. \quad (7.19)$$

Similarly, substituting (7.17) in (7.18), the RHS of (7.18) can be approximated as:

$$2\log_2\left(\gamma_{SD}(j)\right) + 2\log_2(B_N/\ln(2)\Gamma\lambda_S) - 2. \quad (7.20)$$

[1]The formulation of the $L(\boldsymbol{P}, \boldsymbol{Y}, \boldsymbol{\lambda})$ for OFDMA is explained in more details in Section 8.2.

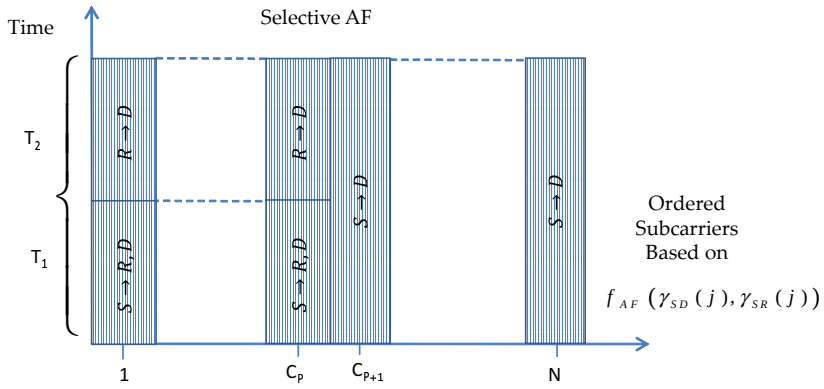

Figure 7.2 Two-Band Partition Assignment for Selective AF-OFDM

Substituting the optimal power profiles at the source and relay nodes given by (7.14) and (7.16) in (7.19) results in:

$$\log_2\left(\gamma_{SD}(j) + \frac{\gamma_{SR}(j)\gamma_{RD}^2(j)C_j^2}{(\gamma_{SR}(j) + \gamma_{RD}(j)C_j)^2}\right) + \log_2(B_N/2\ln(2)\Gamma\lambda_S) - 1. \tag{7.21}$$

This expression can be further simplified by using $0.5\min(\gamma_{SR}(j), \gamma_{RD}(j)C_j)$ as a lower bound for $\frac{\gamma_{SR}(j)\gamma_{RD}(j)C_j}{\gamma_{SR}(j)+\gamma_{RD}(j)C_j}$, and assuming $\frac{\gamma_{SR}(j)}{\gamma_{SD}(j)} > 1$ and $\frac{\gamma_{RD}(j)}{\gamma_{SD}(j)} > 1$, which are reasonable assumptions in cooperative communications. We take the difference between (7.21) and (7.20), and define the term that depends on the channel gains by the function $f_{AF}(\cdot)$ as:

$$f_{AF}\left(\gamma_{SD}(j), \gamma_{SR}(j)\right) = \log_2\left(\frac{\gamma_{SD}(j) + 0.25\gamma_{SR}(j)}{\gamma_{SD}^2(j)}\right). \tag{7.22}$$

The approach that we follow to assign subcarriers to the different modes of operation is accomplished by ordering the subcarriers based on (7.22) in descent ordering, then searching for the partition that maximizes the sum rate. We only need to find the boundary subcarrier C_P of the ordered set; i.e. the subcarriers $j \leq C_P$ of the ordered set are assigned to mode 1, and the subcarriers $j > C_P$ of the ordered set are assigned to mode 2 as shown in **Figure 7.2**.

Algorithm 7.1 Two-Band Assignment Algorithm for Selective AF-OFDM Scheme.

Require: $\gamma_{SD}(j)$, $\gamma_{SR}(j)$, $\gamma_{RD}(j)$, $j \in \mathcal{J}$, $P_R^{\max}$, and $P_S^{\max}$.

1: Set $\mathcal{J}_1 = \varnothing$, and $\mathcal{J}_2 = \varnothing$.
2: **for** $j \in \mathcal{J}$ **do**
3: $S_j \leftarrow \log_2\left(\frac{\gamma_{SD}(j)+0.25\gamma_{SR}(j)}{\gamma_{SD}^2(j)}\right)$.
4: **end for**
5: Find $\hat{S}$: The ordered set of $\boldsymbol{S} = \{S_1, \cdots, S_N\}$ from *largest* to *smallest* such as $\hat{S}_1 > \hat{S}_2 > \hat{S}_j > \cdots > \hat{S}_N$, where the first subcarrier is the subcarrier with the *largest*(S_j), and the Nth subcarrier is the subcarrier with the *smallest*(S_j), $\forall j \in \mathcal{J}$.
6: **for** $n = 0 : N$ **do**
7: Assign mode 1, the set of subcarriers $\mathcal{J}_1(n) \leftarrow 1 : n$.
8: Assign mode 2, the set of subcarriers $\mathcal{J}_2(n) \leftarrow n + 1 : N$.
9: Use (7.14), (7.16) and (7.17) to compute the power profiles at the source and relay nodes.
10: Compute the sum rate: $R(n) = \sum_{i=1}^{2} \sum_{j \in \mathcal{J}_i(n)} \Upsilon_j^{(i)} R^{(i)}(j)$, where $\Upsilon_j^{(1)} = 1$, $\forall j \in \mathcal{J}_1(n)$, and $\Upsilon_j^{(2)} = 1$, $\forall j \in \mathcal{J}_2(n)$.
11: **end for**
12: Find the partition C_P that maximizes the sum rate as: $C_P \leftarrow \arg\max_n R(n)$
13: Assign mode 1 the subcarriers : $\mathcal{J}_1 \leftarrow \{1 : C_P\}$.
14: Assign mode 2 the subcarriers: $\mathcal{J}_2 \leftarrow \{C_P + 1 : N\}$.
15: **return** $\mathcal{J}_1 \leftarrow \{1 : C_P\}$, $\mathcal{J}_2 \leftarrow \{C_P + 1 : N\}$, and $R(C_P)$.

7.2.1 Subcarrier Assignment Algorithm

The proposed subcarrier assignment algorithm is illustrated in **Algorithm 7.1**. Searching through a set of two-bands partitions, the subcarriers are sorted in descent ordering based on $S_j = \log_2\left(\frac{\gamma_{SD}(j)+0.25\gamma_{SR}(j)}{\gamma_{SD}^2(j)}\right)$, as $\hat{S}_1 > \hat{S}_2 > \cdots > \hat{S}_N$, where $\hat{S}_1 = \max(S_1, S_2, \cdots, S_N)$, and subcarrier 1 is the subcarrier with the largest S_j. Then the partition C_P that maximizes the sum rate is sought by assigning the subcarriers of the ordered set indices from 1 to C_P to mode 1, and the subcarriers of the ordered set indices from $C_P + 1$ to N to mode 2. The sum rate is computed by using the power profiles given in (7.14), (7.16), and (7.17).

7.3 Selective DF-OFDM Cooperative Communications

In this section, the algorithm is extended to the selective DF-OFDM cooperative scheme, where the jth subcarrier can be either used in DF transmission with diversity referred to as mode one ($i = 1$), or it can be used for direct transmission without diversity referred to as mode two ($i = 2$).

The data rate $R^{(1)}(j)$ for DF scheme at the destination node with the aid of the relay node in mode 1 and using the MRC technique can be computed as:

$$R^{(1)}(j) = \frac{B_N}{2} \min\left\{ \log_2(1 + \frac{\Gamma_{SD}^{(1)}(j) + \Gamma_{RD}(j)}{\Gamma}), \log_2(1 + \frac{\Gamma_{SR}^{(1)}(j)}{\Gamma})\right\}, \tag{7.23}$$

where $\Gamma_{RD}(j) = \gamma_{RD}(j)P_R(j)$, and $\Gamma_{SR}^{(1)}(j) = \gamma_{RS}(j)P_S^{(1)}(j)$. The Resource allocation problem aiming to maximize the achievable data rate over the entire OFDM symbol with N subcarriers for selective DF-OFDM cooperative schemes can be formulated as in (7.8) with $R^{(1)}(j)$ as given by (7.23).

Following the same lines of AF-OFDM scenario in Section 7.3; by relaxing the power constraints at the source and relay nodes and formulating the Lagrangian function for a given subcarrier assignment profile as in (7.10), then differentiating with respect to $P_S^{(1)}(j)$ and equating to zero, the optimal source power profile can be obtained as:

$$P_S^{(1)}(j) = \left(\frac{K\gamma_{SD}(j)}{\gamma_{SR}(j)} - \frac{\Gamma}{\gamma_{SR}(j)}\right)^+ \tag{7.24}$$

with $K = \frac{B_N}{2\ln(2)\lambda_S}$. The optimal relay power profile is obtained as:

$$P_R(j) = C_j P_S^{(1)}(j), \tag{7.25}$$

where C_j is computed as:

$$C_j = \frac{\left(\gamma_{SR}(j) - \gamma_{SD}(j)\right)^+}{\gamma_{RD}(j)}. \tag{7.26}$$

Similar to selective AF-OFDM scenario, the approach that we follow to assign subcarriers to the two different modes of operation is accomplished by ordering the subcarriers in descent ordering, based on $f^{DF}(\gamma_{SD}(j), \gamma_{SR}(j))$, which is defined as:

$$f_{DF}\Big(\gamma_{SD}(j), \gamma_{SR}(j)\Big) = \log_2\Big(\frac{\gamma_{SR}(j)}{\gamma^2_{SD}(j)}\Big), \tag{7.27}$$

then searching for the partition that maximizes the sum rate. We only need to find the boundary subcarrier C_P of the ordered set; i.e. the subcarriers $j \leq C_P$ of the ordered set are assigned to mode 1, and the subcarriers $j > C_P$ of the ordered set are assigned to mode 2.

Algorithm 7.1 can be used to find the mode of transmission for selective DF-OFDM by replacing $S_j = \log_2\Big(\frac{\gamma_{SD}(j)+0.25\gamma_{SR}(j)}{\gamma^2_{SD}(j)}\Big)$ by $S_j = \log_2\Big(\frac{\gamma_{SR}(j)}{\gamma^2_{SD}(j)}\Big)$, using (7.24) and (7.25) instead of (7.14) and (7.16) to compute the power profiles at the source and relay nodes, and using (7.23) instead of (7.6) to calculate the rate of subcarrier j using mode 1.

7.4 Hybrid OFDM Cooperative Communications

In this section, in order to save the energy of the source node, restrictions apply to the source transmission in the second time slot. In this regard, subcarrier j can be used either in AF cooperative transmission with diversity referred to as mode one ($i = 1$), or it can be used in DF transmission with diversity referred to as mode two ($i = 2$).

The data rate $R^{(1)}(j)$ for AF scheme at the destination node with the aid of the relay node in mode 1 and using the MRC technique can be computed

as:

$$R^{(1)}(j) = \frac{B_N}{2}\log_2(1 + \frac{\Gamma^{(1)}_{SD}(j) + \Gamma^{(1)}_{AF}(j)}{\Gamma}). \tag{7.28}$$

The data rate $R^{(2)}(j)$ for DF scheme at the destination node with the aid of the relay node in mode 2 and using the MRC technique can be computed as:

$$R^{(2)}(j) = \frac{B_N}{2}\min\Big\{\log_2(1 + \frac{\Gamma^{(2)}_{SD}(j) + \Gamma^{(2)}_{RD}(j)}{\Gamma}), \log_2(1 + \frac{\Gamma^{(2)}_{SR}(j)}{\Gamma})\Big\}. \tag{7.29}$$

Following the same lines as in selective AF/DF-OFDM, the power profile for mode 1 at the source and relay nodes can obtained as in (7.14) and (7.16), respectively. Whereas, the power profile for mode 2 at the source and relay nodes can be obtained as in (7.24) and (7.25), respectively. The approach that we follow to assign the subcarriers to the different modes of operation is accomplished by sorting the subcarriers in a descent ordering based on the function $f_H\Big(\gamma_{SD}(j), \gamma_{SR}(j)\Big)$ given as:

$$f_H\Big(\gamma_{SD}(j), \gamma_{SR}(j)\Big) = \log_2\Big(\frac{\gamma_{SD}(j) + 0.25\gamma_{SR}(j)}{\gamma_{SR}(j)}\Big), \tag{7.30}$$

Algorithm 7.1 can be used to find the mode of transmission for the hybrid OFDM Cooperative relaying by replacing the ordering function $S_j = \log_2\Big(\frac{\gamma_{SD}(j)+0.25\gamma_{SR}(j)}{\gamma^2_{SD}(j)}\Big)$ by $S_j = \log_2\Big(\frac{\gamma_{SD}(j)+0.25\gamma_{SR}(j)}{\gamma_{SR}(j)}\Big)$, using (7.25), (7.24), (7.16), and (7.14) to find the power allocation profiles, and using (7.28) and (7.29) to compute the data rate for mode 1 and mode 2, respectively.

7.5 OFDM Cooperative Communications with Total Power Constraint

Resource allocation for selective AF-OFDM, and selective DF-OFDM schemes under total power constraint, can be investigated by replacing (7.8b) and

(7.8c) in (7.8) by:

$$\sum_{j\in\mathcal{J}}(Y_j^{(1)}P_S^{(1)}(j) + 2Y_j^{(2)}P_S^{(2)}(j) + Y_j^{(1)}P_R(j)) \leq P_T. \tag{7.31}$$

and the resource allocation for hybrid cooperative OFDM scheme under total power constraint, can be studied by replacing constraints (7.8b) and (7.8c) in (7.8) by:

$$\sum_{i=1}^{2}\sum_{j\in\mathcal{J}}(Y_j^{(i)}P_S^{(i)}(j) + Y_j^{(i)}P_R^{(i)}(j)) \leq P_T. \tag{7.32}$$

The interesting result is that the proposed algorithms can be used also to select the mode of operation under total power constraint without changing the developed ordering functions. The only difference is that in the source and relay power profiles (7.17), (7.14), and (7.16) for selective AF-OFDM, and (7.17), (7.24), and (7.25) for selective DF-OFDM, λ_R, and λ_S are replaced by λ_T, which is selected to satisfy the total power constraint.

7.6 Simulation Results and Discussion

We model the subcarrier channel coefficient between any two nodes with a separating distance d as $H(j) \sim \mathcal{CN}(0, \frac{1}{L(1+d)^{\alpha}})$, $\alpha = 4$ is the propagation loss factor, and $L = 4$ is the number of channel taps as in [49]. The system consists of a source S, a relay R and a destination D. The distance between the source and destination d_{SD} is set to 100m and the relay is set at equal distance from the source and destination nodes, i.e. $d_{SR} = 50$, and $d_{RD} = 50$, this setting is selected since AF-OFDM scenario achieves maximum capacity when the relay is located midway between the source and distention nodes. However, it was noticed that selective AF/DF-OFDM relaying improves the capacity for all positions. The subcarrier noise power σ^2 is set at 4×10^{-11}Watt. The source maximum transmit power is $P_S^{\max} = 1$Watt.

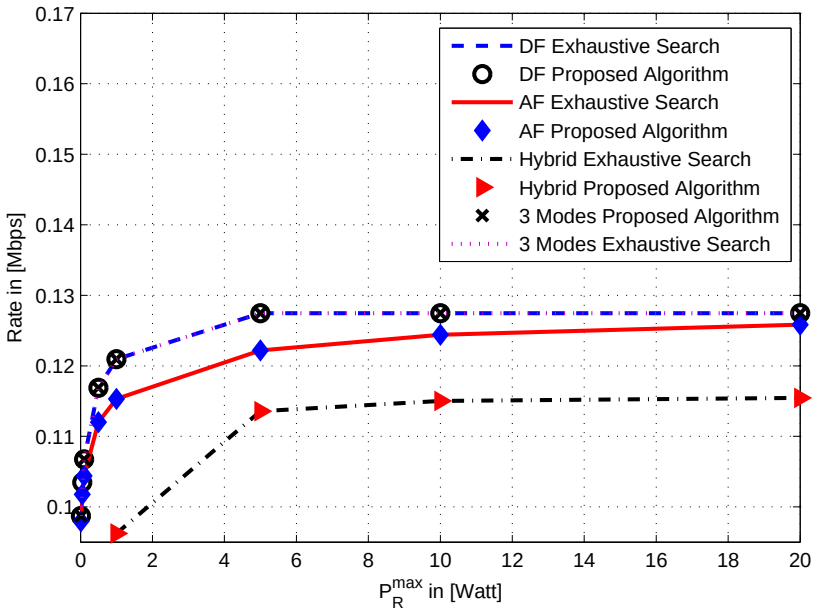

Figure 7.3 The Achievable Sum Rate for Different Scenarios and Algorithms as a Function of the Relay Maximum Transmit Power $P_R^{\max}$.

The subcarrier bandwidth B_N = 4KHz, the capacity gap is set to 1. The achievable sum rate and the subcarrier assignment of the proposed algorithm for selective AF-OFDM, selective DF-OFDM, hybrid-OFDM are compared with the achievable sum rate and the subcarrier assignment using exhaustive search algorithm for $N = 8$. The results of the two algorithms coincide as shown in **Figure 7.3**. The comparison was carried out for a large number of random channel realizations and for different maximum transmit power constraints. In all of these realizations, the proposed algorithm for subcarrier assignment coincides with that obtained by exhaustive search algorithm. However, the proposed subcarrier assignment algorithm is of much lower complexity than the exhaustive search algorithm. The maximum number of computations to find the optimal subcarrier assignment is $O(N)$ for the proposed algorithm, which can be further improved by using binary search algorithms to $O\left(\log_2(N)\right)$ compared to $O(2^N)$ for exhaustive search algorithms.

Further dimension is investigated by allowing the OFDM symbol to contain AF with diversity transmission, DF with diversity transmission and di-

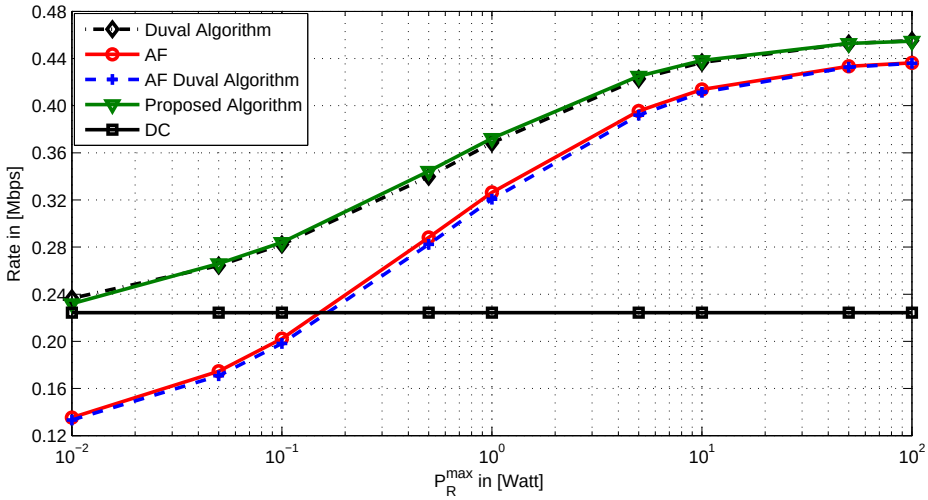

Figure 7.4 Comparison of the Achievable Sum Rate for Different Scenarios and Algorithms as a Function of the Relay Maximum Transmit Power $P_R^{\max}$.

rect transmission without diversity, known as the three modes ($3M$) scheme. This can be achieved by splitting the subcarriers between AF and DF using hybrid OFDM cooperative transmission, then splitting the first group of subcarriers, using selective AF-OFDM transmission between AF and direct transmission. Similarly, the second group of subcarriers can be split using selective DF-OFDM transmission between DF and direct transmission. **Algorithm 7.1** needs to be applied three times using the three different ordering functions (7.30), (7.27), and (7.22). It is clear from **Figure 7.3** that there is no gain from using the $3M$ scheme, the sum rate coincides with the sum rate of selective DF-OFDM scheme. This is because it is better to use DF transmission for the subcarriers with good channel gains, and to use direct transmission for the remaining subcarriers. The sum rate of the $3M$ scheme using the proposed algorithm coincides with the sum rate using exhaustive search as shown in **Figure 7.3**.

Figure 7.4 compares the sum rate of the proposed algorithm and the sum rate of AF, using all subcarriers as a function of the relay's maximum transmit power for a fixed source maximum transmit power $P_S^{\max} = 1$Watt with $N = 64$. Clearly, as the relay's maximum transmit power $P_R^{\max}$ increases, the achievable data rate increases. The achievable sum rate of the proposed

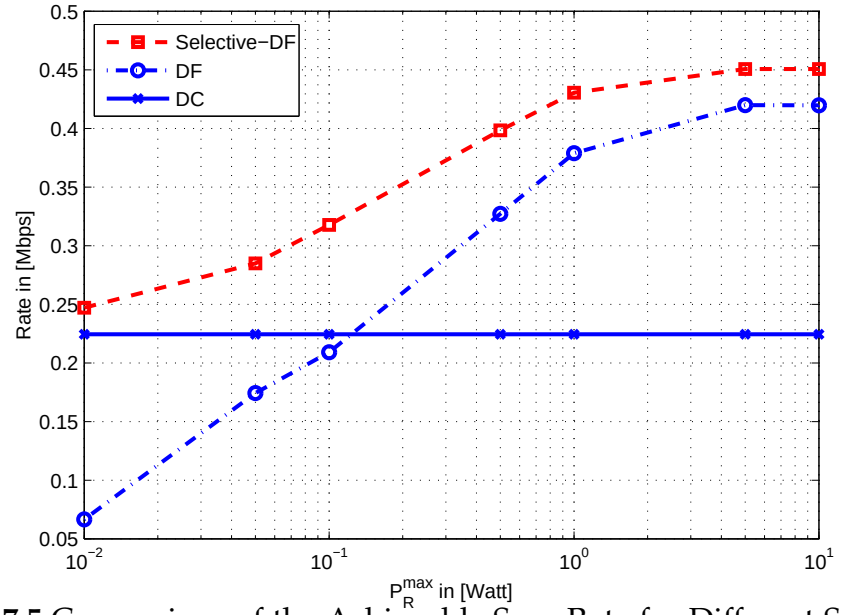

Figure 7.5 Comparison of the Achievable Sum Rate for Different Scenarios and Algorithms as a Function of the Relay Maximum Transmit Power $P_R^{\max}$.

algorithm is higher than the achievable sum rate of AF using all subcarriers and higher than the achievable sum rate of direct transmission using all subcarriers. In addition, **Figure 7.4** shows the achievable sum rate of AF using all subcarriers using (7.14), (7.16) and (7.17) and the achievable sum rate of AF using all subcarriers using the iterative algorithm proposed in [36]. Clearly, the two curves coincide with negligible difference for different relay's maximum transmit power. However, our proposed algorithm requires less computational complexity: In the proposed algorithm the ordering is done only once based on (7.22), whereas the ordering is done iteratively in [36] based on the minimum required relaying power. In addition, the power profiles are allocated using (7.14) and (7.16), no iterations are required to find the source and relay power profiles as in [36].

Figure 7.5 compares the sum rate of the proposed algorithm for selective DF-OFDM and the sum rate of DF-OFDM using all subcarriers as a function of the relay's maximum transmit power for a fixed source maximum transmit power $P_S^{\max} = 1$Watt with $N = 64$. It is clear that the sum rate of selective DF-OFDM scheme is higher than the sum rate of DF-OFDM.

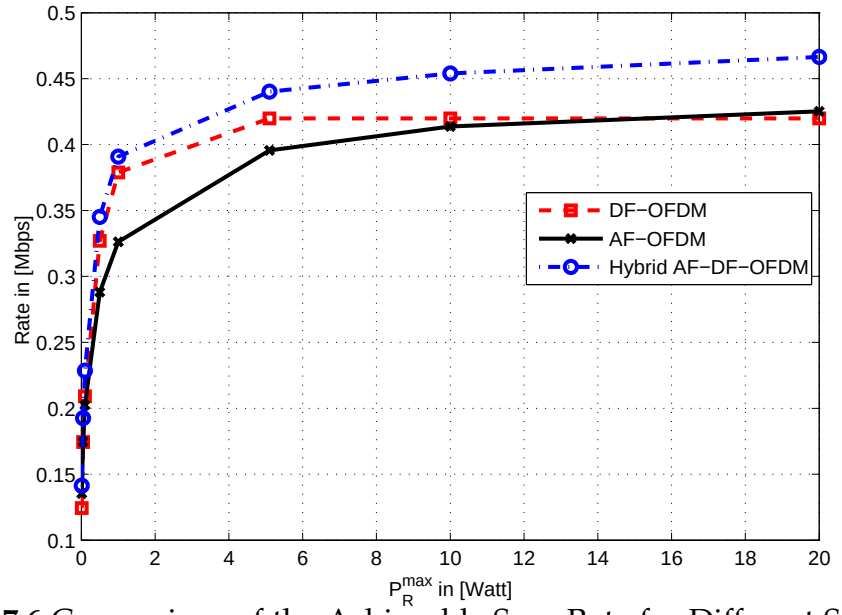

Figure 7.6 Comparison of the Achievable Sum Rate for Different Scenarios and Algorithms as a Function of the Relay Maximum Transmit Power $P_R^{\max}$.

Figure 7.6 compares the sum rate of the proposed algorithm for hybrid AF-DF-OFDM and the sum rate of AF-OFDM/DF-OFDM using all subcarriers as a function of the relay's maximum transmit power for a fixed source maximum transmit power $P_S^{\max} = 1$Watt with $N = 64$. It is clear that the sum rate of Hybrid AF-DF-OFDM scheme is higher than the sum rate of AF-OFDM and DF-OFDM cooperative schemes.

Figure 7.7 compares the sum rate of the proposed algorithms for AF/DF-OFDM and Hybrid-OFDM with exhaustive search under total power constraint. The sum rate of the proposed algorithms coincides with the sum rate of the exhaustive search algorithm.

Table 7.1 shows the number of subcarriers (N_{AF}/N_{DF}) used for AF/DF relaying as a function of the relay's maximum transmit power $P_R^{\max}$ under individual power constraint at the source and relay nodes. Clearly, the relation between increasing $P_R^{\max}$ and the number of subcarriers assigned to AF/DF is an increasing function until it goes to saturation for high relay maximum power, which confirms that selective DF/AF-OFDM achieves a higher data rate compared to DF/AF-OFDM, even with high maximum

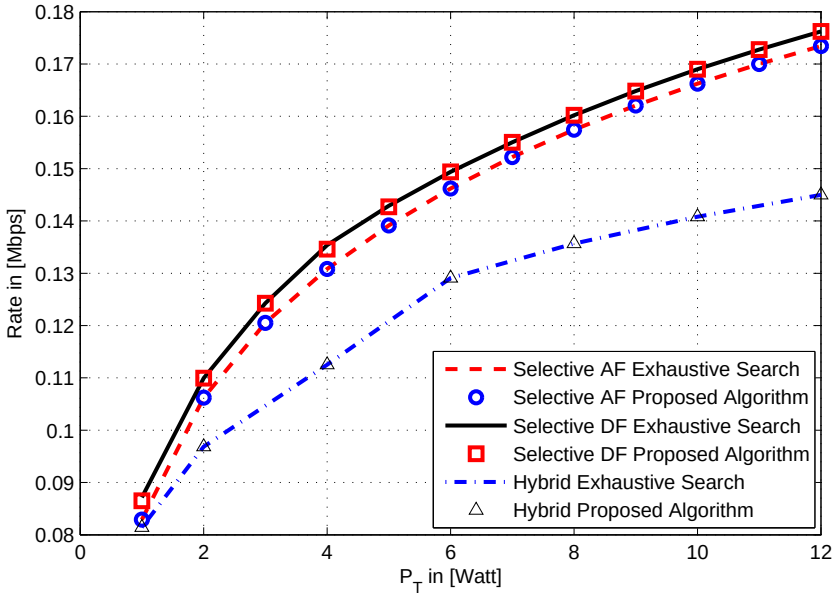

Figure 7.7 Comparison of the Achievable Sum Rate for Different Scenarios and Algorithms as a Function of the Total Power Constraint P_T.

Table 7.1 Number of Subcarriers Used for Relaying Using the Proposed Algorithm.

$P_R^{\max}$ [Watt]	0.01	0.05	0.1	1.0	5.0	10.0	50.0	100
N_{AF}	31	34	39	43	45	51	51	52
N_{DF}	25	33	41	44	51	52	53	53

transmit power at the relay node.

7.7 Conclusions

In this chapter, we investigate joint resource allocation for selective AF/DF-OFDM and hybrid AF-DF-OFDM cooperative communication systems, in the presence of a direct link between the source and destination nodes. The objective is to maximize the sum rate over one OFDM symbol under either individual node power constraint on each node or total power constraint. The subcarrier assignment is a combinatorial problem that can be solved by means of exhaustive search to get the optimal subcarrier assignment, and the source and relay power profiles. In this sense, we propose a suboptimal

low complexity algorithm for subcarrier assignment, and develop analytical expressions for both the source and relay power profiles for AF and DF cooperative schemes and direct transmission. The proposed algorithm is based on high SNR approximation, and optimal power profiles at the source and relay nodes. The maximum number of computations of the proposed algorithm is proportional to the number of subcarriers $O(N)$, which can be reduced using binary search algorithms to $O\left(\log_2(N)\right)$.

CHAPTER8

RESOURCE ALLOCATION FOR AF/DF-OFDMA RELAY NETWORKS

This chapter addresses joint subcarrier assignment and power allocation at the source and relay nodes for both relaying schemes AF and DF with multiple users using OFDMA. The resource allocation problem aims at maximizing the weighted sum rate subject to individual power constraint on each node. We formulate such a problem as subcarrier based resource allocation [1] that seeks joint optimization of subcarrier assignment and power profiles at the source and relay nodes. The formulated optimization problem is a MINLP, which is difficult to solve. In this sense, using high SNR approximation, two algorithms are proposed based on channel gains ordering. In the first algorithm, the first partition is assigned to one of the users, whereas, the second partition is assigned to the remaining users. The algorithm is applied repeatedly in a nested fashion by splitting each second partition into two partitions until the last partition is separated between the last two users. The optimal partitions that maximize the weighted sum rate are then sought. The computational complexity of finding the subcarrier assignment that maximizes the weighted sum rate for I users, and N subcarriers AF-OFDMA or DF-OFDMA scenarios is of $O\left(N^{I-1}\right)$. A second algorithm is proposed to further reduce the computational complexity, which consists

[1] Joint resource allocation with subcarrier pairing is a topic for further research.

of two stages: a basic stage, and a transfer stage. In the basic stage, each user is assigned a subset of the subcarriers based on an ordering function of the user channel gain to the other users channel gains. In the transfer stage, some boundary subcarriers are transferred among users to maximize the weighted sum rate.

This chapter is organized as follows. Introduction and related works are presented in Section 8.1. In Section 8.2, AF-OFDMA cooperative communication system model, formulation of the optimization problem, and the proposed algorithms for subcarrier assignment are described. The proposed algorithms are extended to DF-OFDMA as explained in Section 8.3. Numerical results are presented and discussed in Section 8.4. Conclusions are drawn in Section 8.5.

8.1 Introduction

Joint subcarrier assignment and power allocation in AF/DF-OFDMA cooperative communication systems is a MINLP and difficult to solve. Thanks to zero duality principle presented in **Theorem 6.2.1**, the resource allocation problem can be solved in the dual domain. However, using the dual domain requires a large number of iterations[2] to find the correct Lagrange multipliers, and even uses methods that exploit the structure of the problem, e.g., the ellipsoid method [19].

This chapter is motivated by the results of [50, 153, 166], where the subcarrier assignments for two users OFDMA system at high SNR is a two-band partition. In this chapter, we follow the same argument to prove that the subcarrier assignment is also a two-band partition for two users AF/DF-OFDMA cooperative communication system at high SNR in the presence of a direct link between the source and destination nodes. We develop an

[2]For uplink scenarios and under individual node constraints, where the number of Lagrange multipliers is $I + 1$. For downlink scenarios and total power constraint, it requires less number of iterations since there is only one Lagrange multiplier.

ordering function to split the subcarriers into a two-band partition based on optimal power profiles at the source and relay nodes, where the power profiles are allocated to maximize the weighted sum rate under individual power constraint at the source nodes, as well as at the relay node.

Resource allocation for uplink AF/DF-OFDMA differs from resource allocation for uplink OFDMA. Subcarriers in AF/DF-OFDMA systems after subcarrier assignment are connected by the relaying power constraint, whereas in OFDMA systems after the subcarrier assignment, each user water fills her source power individually. One more characteristic of the resource allocation for uplink AF/DF-OFDMA is that the two band partition applies either if all subcarriers are allocated non-zero relaying power, or all subcarriers are allocated zero relaying power. In case some subcarriers are allocated zero relaying power, four band partition is noticed, which requires reassignment of these subcarriers using a different ordering function.

For more than two users ($I > 2$), resource allocation for AF/DF-OFDMA cooperative communication systems can be studied based on the two users case, where the two band partition principle can be applied repeatedly between a user and the remaining users in the system. In addition, a simplified algorithm is proposed to reduce the computations that result from applying the algorithm repeatedly, which consists of two stages; basic and transfer. In the basic stage, each subcarrier is assigned to the user that achieves the maximum benefit using that subcarrier compared to all other users. In the transfer stage, subcarriers can be transferred from one user to another user in order to maximize the weighted sum rate.

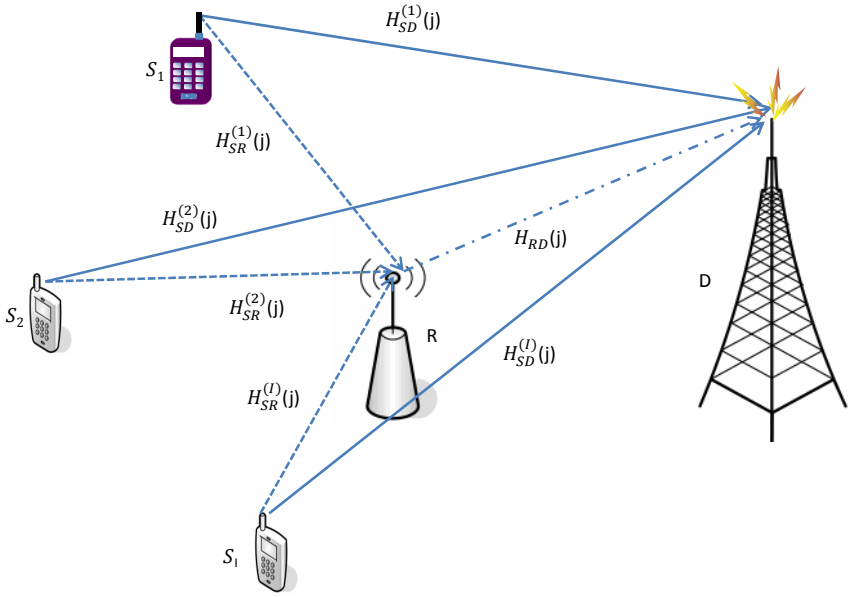

Figure 8.1 System Model.

8.2 AF-OFDMA Cooperative Communication Systems

The system under consideration is depicted in **Figure 8.1** which finds plenty of promising applications when it is difficult to install multiple antennas at the same radio equipment [86]. This system has been considered in the latest standards as IEEE 802.16j and long-term-evolution-advanced (LTE-A) standard [35]. Let $\mathcal{I} = \{1, 2, \cdots, I\}$ be the set of active users, sender (source) nodes S_i for $i \in \mathcal{I}$ communicate with a destination terminal D. We consider a single relay two-hop OFDMA system. The available bandwidth W is divided into N subcarriers, each subcarrier bandwidth is B_N, in which the channel coefficient is assumed to be frequency flat. In the first hop, the channel coefficients of the ith user between the source and destination nodes, and the source and relay nodes at the jth subcarrier are denoted by $H_{SD}^{(i)}(j)$, and $H_{SR}^{(i)}(j)$, respectively. In the second hop, the channel coefficient between the relay and the destination nodes at the jth subcarrier is denoted by $H_{RD}(j)$. The received signals at the destination and relay nodes in the first time slot T_1 for user i on the jth subcarrier are defined as $Y_{D_1}^{(i)}(j)$ and $Y_R^{(i)}(j)$ respectively,

and obtained as:

$$Y_{D_1}^{(i)}(j) = \sqrt{\hat{P}_S^{(i)}(j)} H_{SD}^{(i)}(j) X_j^{(i)} + n_{D_1}^{(i)}(j), \tag{8.1a}$$

$$Y_R^{(i)}(j) = \sqrt{\hat{P}_S^{(i)}(j)} H_{SR}^{(i)}(j) X_j^{(i)} + n_R^{(i)}(j), \tag{8.1b}$$

where $\hat{P}_S^{(i)}(j)$ is the ith user transmitted power on the jth subcarrier in the first time slot. The ith user transmitted symbol at the jth subcarrier is denoted as $X_j^{(i)}$, which is drawn from a constellation with unit energy, and $n_{D_1}^{(i)}(j)$ and $n_R^{(i)}(j)$ are AWGNs with variance σ^2 received at the destination and relay nodes on the jth subcarrier, respectively. Let $\hat{\Gamma}_{SD}^{(i)}(j)$ denote the SNR for the ith user at the jth subcarrier at the destination node, which results from direct transmission between the ith source-destination pair in the first time slot T_1, and can be expressed as $\hat{\Gamma}_{SD}^{(i)}(j) = \gamma_{SD}^{(i)}(j)\hat{P}_S^{(i)}(j)$, with $\gamma_{SD}^{(i)}(j) = \frac{|H_{SD}^{(i)}(j)|^2}{\sigma^2}$.

During the second time slot T_2, the relay amplifies and transmits the received signal at the same subcarrier. The received signal $Y_{D_2}^{(i)}(j)$ of the ith user at the jth subcarrier at the destination node is obtained as:

$$Y_{D_2}^{(i)}(j) = G^{(i)}(j) \sqrt{\hat{P}_R^{(i)}(j)} H_{RD}(j) Y_R^{(i)}(j) + n_{D_2}^{(i)}(j), \tag{8.2}$$

where $\hat{P}_R^{(i)}(j)$ is the relay transmitted power for the ith user at the jth subcarrier, $n_{D_2}^{(i)}(j)$ is the AWGN with variance σ^2 received at the destination node. $G^{(i)}(j)$ is the normalization factor at the relay node at the jth subcarrier given as $G^{(i)}(j) = \frac{1}{\sqrt{\hat{P}_S^{(i)}(j)|H_{SR}^{(i)}(j)|^2 + \sigma^2}}$. The noise variance is expressed as $\sigma^2 = N_0 B_N$, where N_0 is the PSD of AWGN. The end-to-end SNR of the ith user $\hat{\Gamma}_{AF}^{(i)}(j)$ using the relay link is given by [125]:

$$\hat{\Gamma}_{AF}^{(i)}(j) = \frac{\hat{P}_S^{(i)}(j)\hat{P}_R^{(i)}(j)|H_{SR}^{(i)}(j)|^2 |H_{RD}(j)|^2}{\sigma^2(\sigma^2 + \hat{P}_S^{(i)}(j)|H_{SR}^{(i)}(j)|^2 + \hat{P}_R^{(i)}(j)|H_{RD}(j)|^2)}, \tag{8.3}$$

which can be written in a simplified form as:

$$\hat{\Gamma}_{AF}^{(i)}(j) = \frac{\gamma_{SR}^{(i)}(j)\gamma_{RD}(j)\hat{P}_S^{(i)}(j)\hat{P}_R^{(i)}(j)}{1 + \gamma_{SR}^{(i)}(j)\hat{P}_S^{(i)}(j) + \gamma_{RD}(j)\hat{P}_R^{(i)}(j)}, \tag{8.4}$$

where $\gamma_{SR}^{(i)}(j) = \frac{|H_{SR}^{(i)}(j)|^2}{\sigma^2}$, and $\gamma_{RD}(j) = \frac{|H_{RD}(j)|^2}{\sigma^2}$.

The data rate $R_{AF}^{(i)}(j)$ at the destination node using subcarrier j for user i with the aid of the relay node and after using the MRC technique, is computed as:

$$R_{AF}^{(i)}(j) = \frac{B_N}{2}\log_2\Big(1 + \frac{\hat{\Gamma}_{SD}^{(i)}(j) + \hat{\Gamma}_{AF}^{(i)}(j)}{\Gamma}\Big). \tag{8.5}$$

The data rate $R_{AF}^{(i)}(j)$ is not a jointly concave function in $\hat{P}_S^{(i)}(j)$ and $\hat{P}_R^{(i)}(j)$ as can be proved by the second order derivative test introduced in Appendix B.1. To make the analysis more tractable, we use the approximation $\hat{\Gamma}_{AF}^{(i)}(j) \approx \frac{\gamma_{SR}^{(i)}(j)\gamma_{RD}(j)\hat{P}_S^{(i)}(j)\hat{P}_R^{(i)}(j)}{\gamma_{SR}^{(i)}(j)\hat{P}_S^{(i)}(j)+\gamma_{RD}(j)\hat{P}_R^{(i)}(j)}$, which is tight for high SNR. This approximation has been commonly used in literature [30, 56, 139]. It is proved that even in the low SNR regime, this approximation can reach optimal capacity very closely [139]. With this approximation the data rate is a jointly concave function in $\hat{P}_S^{(i)}(j)$ and $\hat{P}_R^{(i)}(j)$ as proved in Appendix B.1. From now on, $\hat{\Gamma}_{AF}^{(i)}(j)$ will be substituted for by its approximation.

One criterion for resource allocation is to maximize the weighted sum of the data rate. This criterion sometimes denoted as throughput preference maximizer, which appears in applications where users have different priorities. In addition, this criterion can be used to find the Pareto optimal boundary of a convex rate region by changing the weights. Therefore, the resource allocation problem can be formulated as follows:

$$\max_{\hat{\boldsymbol{P}}_R, \hat{\boldsymbol{P}}_S, \boldsymbol{Y}} \frac{B_N}{2}\sum_{i\in\mathcal{I}}\alpha_i\sum_{j\in\mathcal{J}}Y_j^{(i)}\log_2\Big(1 + \frac{\hat{\Gamma}_{SD}^{(i)}(j) + \hat{\Gamma}_{AF}^{(i)}(j)}{\Gamma}\Big), \tag{8.6a}$$

$$\text{s.t.} \sum_{i\in\mathcal{I}}\sum_{j\in\mathcal{J},\, i\in\mathcal{I}} Y_j^{(i)}\hat{P}_R^{(i)}(j) \le P_R^{\max}, \tag{8.6b}$$

$$\sum_{j\in\mathcal{J}} \Upsilon_j^{(i)} \hat{P}_S^{(i)}(j) \le P_i^{\max}, \forall i \in \mathcal{I}, \tag{8.6c}$$

$$\sum_{i\in\mathcal{I}} \Upsilon_j^{(i)} \le 1, \forall j \in \mathcal{J}, \tag{8.6d}$$

$$\hat{P}_S^{(i)}(j) \ge 0,\ \hat{P}_R^{(i)}(j) \ge 0,\ \Upsilon_j^{(i)} \in \{0,1\},\ \forall i \in \mathcal{I},\ \forall j \in \mathcal{J}, \tag{8.6e}$$

where the set $\mathcal{J} = \{1, 2, \cdots, N\}$ denotes the set of subcarriers, $\hat{\boldsymbol{P}}_S$ is the power profile matrix at the source node with $[\hat{\boldsymbol{P}}_S]_{i,j} = \hat{P}_S^{(i)}(j)$, $\forall i \in \mathcal{I}$ and $\forall j \in \mathcal{J}$. Similarly, $\hat{\boldsymbol{P}}_R$ is the power profile matrix at the relay node with $[\hat{\boldsymbol{P}}_R]_{i,j} = \hat{P}_R^{(i)}(j)$, $\forall i \in \mathcal{I}$ and $\forall j \in \mathcal{J}$. The matrix $\boldsymbol{\Upsilon}$ is the subcarrier assignment profile with $[\boldsymbol{\Upsilon}]_{i,j} = \Upsilon_j^{(i)} \in \{0,1\}$, $\forall i \in \mathcal{I}$, $\forall j \in \mathcal{J}$, $\Upsilon_j^{(i)} = 1$ indicates that subcarrier j is assigned to user i, and α_i's are the relative priority for each user. Constraint (8.6b) means that the total power allocated to forward the data from all users assisted by the relay is limited to $P_R^{\max}$, and constraint (8.6c) indicates that the source power for user i is limited to $P_i^{\max}$. Constraint (8.6d) means that the jth subcarrier can be assigned to only one user, i.e. if $\Upsilon_j^{(i)} = 1$, then $\Upsilon_j^{(k)} = 0$, $\forall k \in \mathcal{I}$, and $k \neq i$.

Problem (8.6) is a mixed integer constrained optimization problem. The traditional approach to solve such optimization problems is to perform an exhaustive search over the I users and N subcarriers. Hence, there are I^N possible subcarrier assignments. For each subcarrier assignment, the source and relay power profiles are allocated to maximize the weighted sum rate. In this sense, the optimal solution is the subcarrier assignment with its associated source and relay power profiles that maximize the objective function while satisfying all the constraints. However, this method is computationally intensive with complexity of $O(I^N)$.

Another approach is to solve (8.6) by relaxing the binary variables as $\Upsilon_j^{(i)} \in [0,1]$, $\forall i \in \mathcal{I}$ and $\forall j \in \mathcal{J}$. In this sense, $\Upsilon_j^{(i)}$ is a time sharing factor of the jth subcarrier that indicates the portion of time where subcarrier j is assigned to user i. Using the time sharing principle, (8.6) can be transformed

into a convex optimization problem as:

$$\max_{\boldsymbol{P}_R,\boldsymbol{P}_S,\boldsymbol{\Upsilon}} \frac{B_N}{2} \sum_{i\in\mathcal{I}} \alpha_i \sum_{j\in\mathcal{J}} \Upsilon_j^{(i)} \log_2\Big(1 + \frac{\Gamma_{SD}^{(i)}(j) + \Gamma_{AF}^{(i)}(j)}{\Gamma\Upsilon_j^{(i)}}\Big), \tag{8.7a}$$

$$\text{s.t.} \sum_{i\in\mathcal{I}} \sum_{j\in\mathcal{J}} P_R^{(i)}(j) \le P_R^{\max}, \tag{8.7b}$$

$$\sum_{j\in\mathcal{J}} P_S^{(i)}(j) \le P_i^{\max},\ \forall i \in \mathcal{I}, \tag{8.7c}$$

$$\sum_{i\in\mathcal{I}} \Upsilon_j^{(i)} \le 1,\ \forall j \in \mathcal{J}, \tag{8.7d}$$

$$P_S^{(i)}(j) \ge 0,\ P_R^{(i)}(j) \ge 0,\ 0 \le \Upsilon_j^{(i)} \le 1,\ \forall i \in \mathcal{I},\ \forall j \in \mathcal{J}, \tag{8.7e}$$

where $\boldsymbol{P}_S$ is the power profile matrix at the source node with $[\boldsymbol{P}_S]_{i,j} = P_S^{(i)}(j)$, $\forall i \in \mathcal{I}$ and $\forall j \in \mathcal{J}$, where $P_S^{(i)}(j) = \hat{P}_S^{(i)}(j)\Upsilon_j^{(i)}$. Similarly, $\boldsymbol{P}_R$ is the power profile matrix at the relay node with $[\boldsymbol{P}_R]_{i,j} = P_R^{(i)}(j)$, where $P_R^{(i)}(j) = \hat{P}_R^{(i)}(j)\Upsilon_j^{(i)}$. $\Gamma_{AF}^{(i)}(j)$, and $\Gamma_{SD}^{(i)}(j)$ are similar to $\hat{\Gamma}_{AF}^{(i)}(j)$, and $\hat{\Gamma}_{SD}^{(i)}(j)$, but are in terms of $P_S^{(i)}(j)$ and $P_R^{(i)}(j)$. This transformation leads to linear constraints as in [102]. It can be easily proved that (8.7) is a convex optimization problem; since the objective function is a jointly concave function in $\boldsymbol{P}_R$, $\boldsymbol{P}_S$, and $\boldsymbol{\Upsilon}$ as can be proved using the perspective property of concave functions given in (2.59), and the constraints are linear. Thus, (8.7) can be solved using any convex optimization technique. Although convex programming algorithms are numerically stable and can be solved with less complexity compared to exhaustive search algorithms, its computational complexity still depends on the number of optimization variables and the number of constraints, which are large if the number of users and subcarriers are large, e.g., in (8.7) the number of variables is $3NI$ and the number of constraints is $3NI + N + I + 1$. In addition, the optimal subcarrier assignment profile $\boldsymbol{\Upsilon}$ which is obtained using convex programing may contain real variables (not binary). In this sense, we will develop a subcarrier assignment algorithm that results in further reduction in the problem dimensionality and run-time complexity, which are impor-

tant if the subcarrier allocation is to be performed dynamically. In addition, our aim is to solve (8.6) not (8.7), but we use (8.7) as a tool to explore the solution. First we will solve the power allocation profiles at the source and relay nodes, and then we will use the optimal power allocation profiles to find the optimal subcarrier assignment profile. Here, we will find an analytical solution for (8.7) based on the KKT conditions which are sufficient and necessary optimality conditions. The Lagrangian function is formulated as:

$$L(\boldsymbol{P}_R, \boldsymbol{P}_S, \boldsymbol{\Upsilon}, \boldsymbol{\lambda}) = \frac{B_N}{2} \sum_{i \in \mathcal{I}} \alpha_i \sum_{j \in \mathcal{J}} \Upsilon_j^{(i)} \log_2 \Big(1 + \frac{\Gamma_{SD}^{(i)}(j) + \Gamma_{AF}^{(i)}(j)}{\Gamma \Upsilon_j^{(i)}}\Big) - \sum_{i \in \mathcal{I}} \lambda_i \Big(\sum_{j \in \mathcal{J}} P_S^{(i)}(j) - P_i^{\max}\Big) -$$
$$\lambda_R \Big(\sum_{i \in \mathcal{I}} \sum_{j \in \mathcal{J}} P_R^{(i)}(j) - P_R^{\max}\Big) - \sum_{j \in \mathcal{J}} \lambda_j^{\Upsilon} \Big(\sum_{i \in \mathcal{I}} \Upsilon_j^{(i)} - 1\Big), \tag{8.8a}$$

$$\text{s.t. } P_R^{(i)}(j) \geq 0, P_S^{(i)}(j) \geq 0, \ \Upsilon_j^{(i)} \geq 0, \ \lambda_R \geq 0, \ \lambda_i \geq 0, \ \lambda_j^{\Upsilon} \geq 0, \ \forall i \in \mathcal{I}, \ \forall j \in \mathcal{J}, \tag{8.8b}$$

where $\boldsymbol{\lambda}$ contains the Lagrange multipliers $[\lambda_R, \lambda_i, \cdots, \lambda_I, \lambda_1^{\Upsilon}, \cdots, \lambda_N^{\Upsilon}]$. Differentiating (8.8a) with respect to $P_S^{(i)}(j)$ and equating to zero results in:

$$\frac{\Upsilon_j^{(i)}\Gamma + \Gamma_{SD}^{(i)}(j) + \Gamma_{AF}^{(i)}(j)}{\Upsilon_j^{(i)} \alpha_i B_N / (2 \ln(2))} = \frac{1}{\lambda_i} \Big(\gamma_{SD}^{(i)}(j) + \frac{\gamma_{SR}^{(i)}(j) \gamma_{RD}^2(j) P_R^{(i)2}(j)}{(\gamma_{SR}^{(i)}(j) P_S^{(i)}(j) + \gamma_{RD}(j) P_R^{(i)}(j))^2}\Big). \tag{8.9}$$

Similarly, differentiating (8.8a) with respect to $P_R^{(i)}(j)$ and equating to zero results in:

$$\frac{\Upsilon_j^{(i)}\Gamma + \Gamma_{SD}^{(i)}(j) + \Gamma_{AF}^{(i)}(j)}{\Upsilon_j^{(i)} \alpha_i B_N / (2 \ln(2))} = \frac{\gamma_{RD}(j) \gamma_{SR}^{(i)2}(j) P_S^{(i)2}(j)}{\lambda_R (\gamma_{SR}^{(i)}(j) P_S^{(i)}(j) + \gamma_{RD}(j) P_R^{(i)}(j))^2}. \tag{8.10}$$

Differentiating the Lagrangian function (8.8a) with respect to the relaxed

integer $Y_j^{(i)}$[3] and equating to zero results in:

$$\alpha_i \log_2\Big(1+\frac{\Gamma_{SD}^{(i)}(j)+\Gamma_{AF}^{(i)}(j)}{\Gamma Y_j^{(i)}}\Big)-\frac{\alpha_i(\Gamma_{SD}^{(i)}(j)+\Gamma_{AF}^{(i)}(j))}{\Gamma Y_j^{(i)}+\Gamma_{SD}^{(i)}(j)+\Gamma_{AF}^{(i)}(j)}=\frac{\lambda_j^Y}{B_N/(2\ln(2))},\ \text{if } P_R^{(i)}(j)>0, \tag{8.11a}$$

and

$$\alpha_i \log_2\Big(1+\frac{\Gamma_{SD}^{(i)}(j)}{\Gamma Y_j^{(i)}}\Big)-\frac{\alpha_i(\Gamma_{SD}^{(i)}(j))}{\Gamma Y_j^{(i)}+\Gamma_{SD}^{(i)}(j)}=\frac{\lambda_j^Y}{B_N/(2\ln(2))},\qquad \text{if } P_R^{(i)}(j)=0. \tag{8.11b}$$

Simultaneously solving (8.9) and (8.10), the optimal source power profile can be obtained as:

$$P_S^{(i)}(j)=\begin{cases} Y_j^{(i)}\Big(\frac{K_i(\gamma_{SD}^{(i)}(j)+A_j^{(i)})-\Gamma}{\gamma_{SD}^{(i)}(j)+B_j^{(i)}}\Big)^+ & \text{if } P_R^{(i)}(j)>0,\\ Y_j^{(i)}\Big(K_i-\frac{\Gamma}{\gamma_{SD}^{(i)}(j)}\Big)^+ & \text{if } P_R^{(i)}(j)=0,\end{cases} \tag{8.12}$$

where $(x)^+=\max\{x,0\}$, $A_j^{(i)}=\frac{\gamma_{SR}^{(i)}(j)\gamma_{RD}^2(j)C_j^{(i)2}}{(\gamma_{SR}^{(i)}(j)+\gamma_{RD}(j)C_j^{(i)})^2}$, $B_j^{(i)}=\frac{\gamma_{SR}^{(i)}(j)\gamma_{RD}(j)C_j^{(i)}}{\gamma_{SR}^{(i)}(j)+\gamma_{RD}(j)C_j^{(i)}}$, $K_i=\frac{\alpha_i B_N}{2\ln(2)\lambda_i}$, and $C_j^{(i)}$ is computed as:

$$C_j^{(i)}=\frac{\gamma_{SR}^{(i)}(j)\Big(-1+\sqrt{1+(1+\frac{\gamma_{SR}^{(i)}(j)}{\gamma_{SD}^{(i)}(j)})(\frac{\lambda_i}{\lambda_R}\frac{\gamma_{RD}(j)}{\gamma_{SD}^{(i)}(j)}-1)}\Big)^+}{\gamma_{RD}(j)(1+\frac{\gamma_{SR}^{(i)}(j)}{\gamma_{SD}^{(i)}(j)})}, \tag{8.13}$$

where λ_R and λ_is are selected to satisfy the total power constraints (8.7b) and (8.7c). The optimal relay power profile can be obtained as:

$$P_R^{(i)}(j)=C_j^{(i)}P_S^{(i)}(j). \tag{8.14}$$

It is worth noting that our aim is not to find the solution of (8.9)-(8.11)

[3]There is a singularity when $Y_j^{(i)}=0$, the condition should be interpreted in the limiting sense. Note that $Y_j^{(i)}=0$ implies that $P_S^{(i)}(j)=0$ and $P_R^{(i)}(j)=0$. A rigorous condition can be obtained by replacing the constraints $Y_j^{(i)}\geq 0$ with $Y_j^{(i)}\geq\epsilon$, and letting ϵ goes to zero [166].

using convex optimization techniques; the optimal solutions require a lot of computations and may lead to sharing some of the subcarriers, that is, $\exists\, \Upsilon_j^{(i)} \notin \{0,1\}$. We aim to use the characteristics of the solution of (8.7) without the need to solve (8.9)-(8.11) to find the subcarrier allocation such as $\Upsilon_j^{(i)} \in \{0,1\}, \forall i \in \mathcal{I}, \forall j \in \mathcal{J}$.

8.2.1 Two Users Scenario

In order to select the subcarrier assignment profile $\boldsymbol{\Upsilon}$ and particularly for the two users case, we first need to characterize the subcarrier(s) that are shared between the two users, that is, for some subcarriers $\Upsilon_j^{(1)} > 0$, and $\Upsilon_j^{(2)} > 0$. In this regards, (8.11) can be written as:

$$\alpha_1 \log_2\Big(1 + \frac{\Gamma_{SD}^{(1)}(j) + \Gamma_{AF}^{(1)}(j)}{\Gamma\Upsilon_j^{(1)}}\Big) - \frac{\alpha_1(\Gamma_{SD}^{(1)}(j) + \Gamma_{AF}^{(1)}(j))}{\Gamma\Upsilon_j^{(1)} + \Gamma_{SD}^{(1)}(j) + \Gamma_{AF}^{(1)}(j)} =$$
$$\alpha_2 \log_2\Big(1 + \frac{\Gamma_{SD}^{(2)}(j) + \Gamma_{AF}^{(2)}(j)}{\Gamma\Upsilon_j^{(2)}}\Big) - \frac{\alpha_2(\Gamma_{SD}^{(2)}(j) + \Gamma_{AF}^{(2)}(j))}{\Gamma\Upsilon_j^{(2)} + \Gamma_{SD}^{(2)}(j) + \Gamma_{AF}^{(2)}(j)}, \text{ if } P_R^{(i)}(j) > 0, \quad (8.15a)$$

and

$$\alpha_1 \log_2\Big(1 + \frac{\Gamma_{SD}^{(1)}(j)}{\Gamma\Upsilon_j^{(1)}}\Big) - \frac{\alpha_1\Gamma_{SD}^{(1)}(j)}{\Gamma\Upsilon_j^{(1)} + \Gamma_{SD}^{(1)}(j)} = \alpha_2 \log_2\Big(1 + \frac{\Gamma_{SD}^{(2)}(j)}{\Gamma\Upsilon_j^{(2)}}\Big) - \frac{\alpha_2\Gamma_{SD}^{(2)}(j)}{\Gamma\Upsilon_j^{(2)} + \Gamma_{SD}^{(2)}(j)},$$
$$\text{if } P_R^{(i)}(j) = 0. \quad (8.15b)$$

This equation can be used to describe three cases for subcarrier allocation: Case one, which is characterized by adequate relaying power for all subcarriers i.e. $C_j^{(i)} > 0, \forall j \in \mathcal{J}$. In this case, (8.15a) is used to determine the subcarrier assignment profile between the two users as follows. The subcarriers which make the LHS of (8.15a) greater than the RHS, are allocated to user 1. Whereas, the subcarriers that make the LHS of (8.15a) smaller than the RHS are assigned to user 2, and the subcarrier that makes the two sides equal is shared between the two users.

Case two, which is characterized by zero relaying power, (8.15b) is then used to determine the subcarrier assignment profile between the two users as follows. The subcarriers which make the LHS of (8.15b) greater than the RHS, are allocated to user 1. Whereas, the subcarriers that make the LHS of (8.15b) smaller than the RHS are assigned to user 2, and the subcarrier that makes the two sides equal is shared between the two users.

Case three, where some subcarriers are used with AF relaying and the remaining subcarriers are used without relaying, both equations (8.15a) and (8.15b) are used to assign the subcarriers between the two users by splitting the subcarriers into two sets; one set is treated as in case one, and the other set is treated as in case two.

In conclusion, the subcarrier assignment profile in (8.6) can be obtained by finding the subcarriers that make the LHS of (8.15) greater than the RHS, those subcarriers are allocated to user 1. Whereas, the subcarriers that make the LHS of (8.15) smaller than the RHS are assigned to user 2, and the subcarrier that makes the two sides of (8.15) equal is assigned to the user with the highest data rate using that subcarrier, this can be formulated by the following theorem.

Theorem 8.2.1 *The optimal subcarrier assignment maximizer of the weighted sum rate for a two users AF-OFDMA system at high SNR at each subcarrier (using the approximated SNR) consists of two contiguous frequency bands where each user is allocated exclusively one frequency band if all subcarriers are allocated non-zero relaying power. And it consists of four frequency bands if some of the subcarriers are allocated zero relaying power. The contiguous frequency bands are determined based on the ordering of the subcarriers' channel gains as explained next.*

Ordering the subcarriers using the difference between the LHS and the RHS of (8.15) can be used to determine the subcarrier allocation. Substituting for the source and relay power profiles using the optimal power profiles $P_S^{(i)}(j)$

and $P_R^{(i)}(j)$ obtained in (8.12) and (8.14) respectively, reduces (8.15) to:

$$\alpha_1 \log_2(K_1 g_{1,j}) + \frac{\alpha_1}{K_1 g_{1,j}} - \alpha_1 = \alpha_2 \log_2(K_2 g_{2,j}) + \frac{\alpha_2}{K_2 g_{2,j}} - \alpha_2, \tag{8.16}$$

where

$$g_{i,j} = \begin{cases} \gamma_{SD}^{(i)}(j) + A_j^{(i)}, & \text{if } P_R^{(i)}(j) > 0 \\ \gamma_{SD}^{(i)}(j), & \text{if } P_R^{(i)}(j) = 0 \end{cases} \tag{8.17}$$

Then (8.16) is similar to the weighted sum maximization in [166], with $g_{i,j}$ is replaced by $\gamma_{SD}^{(i)}(j) + A_j^{(i)}$ if $P_R^{(i)}(j) > 0$ and $g_{i,j}$ is replaced by $\gamma_{SD}^{(i)}(j)$ if $P_R^{(i)}(j) = 0$, for $i \in \{1, 2\}$, and $j \in \mathcal{J}$. With simple algebraic manipulation, the source power profile (8.12) can be written in the form of a (modified) water filling as:

$$\frac{P_S^{(i)}(j)}{\Upsilon_j^{(i)}} \Big(\frac{\gamma_{SD}^{(i)}(j) + B_j^{(i)}}{\gamma_{SD}^{(i)}(j) + A_j^{(i)}} \Big) + \frac{\Gamma}{\gamma_{SD}^{(i)}(j) + A_j^{(i)}} = K_i, \text{ if } P_R^{(i)}(j) > 0, \tag{8.18a}$$

$$\frac{P_S^{(i)}(j)}{\Upsilon_j^{(i)}} + \frac{\Gamma}{\gamma_{SD}^{(i)}(j)} = K_i, \text{ if } P_R^{(i)}(j) = 0. \tag{8.18b}$$

We follow a similar argument as in [166] to prove **Theorem 8.2.1**.

Starting with the case of enough relaying power for all subcarriers, we consider the following.

1. Assume that the two users have the same channel gains $g_{1,j} = g_{2,j} = g_j$, $\Gamma = 1$, and $\alpha_1 \neq \alpha_2$. The difference between the LHS and RHS can be written as a function of $x = \frac{1}{g_j}$ as:

$$f(x) = (\alpha_2 - \alpha_1) \log_2(x) + x\left(\frac{\alpha_1}{K_1} - \frac{\alpha_2}{K_2}\right) + \alpha_1 \log_2(K_1) - \alpha_2 \log_2(K_2) - \alpha_1 + \alpha_2, \tag{8.19}$$

   - The subcarriers are sorted based on $x = 1/g_j$ and the set S is defined as the set of the ordered subcarriers, where 1 is the index

of the subcarrier with the smallest $1/g_j$ and N is the index of the subcarrier with the largest $1/g_j$.

- There exists a subcarrier with index L_1 in the ordered set such that $f(1/g_j) < 0$ for $j < L_1$ and $f(1/g_j) > 0$ for $j > L_1$. Hence, the subcarriers $1 < j < L_1$ in the ordered set are used exclusively by user 2. Subcarrier L_1 is shared by both users, and user 1 will use the subcarriers with indices from $L_1 + 1$ to N in the ordered set.
- The value x is upper bounded by K_2 as can be inferred from (8.18), because user 2 can only use subcarrier j with $1/g_j$ is less than K_2.
- To show that $f(x)$ can have only one root in the range $0 < x < K_2$, we differentiate $f(x)$ with respect to x. The sign of the derivative in the range $0 < x < K_2$ shows that it is an increasing function and can have only one root when $\frac{\alpha_1}{K_1} - \frac{\alpha_2}{K_2} > 0$ and $\alpha_2 - \alpha_1 > 0$. For the case when $\frac{\alpha_1}{K_1} - \frac{\alpha_2}{K_2} < 0$ and $\alpha_2 - \alpha_1 > 0$, the function is increasing in the first segment, and decreasing in the second segment, in which it could not reach zero. Once again, the function can have only one root. Hence, the subcarriers $j = 1, \cdots, L_1 - 1$ in the ordered set are assigned to user 2, and the subcarriers $j = L_1 + 1, \cdots, N$ in the ordered set are assigned to user 1. Subcarrier L_1 in the ordered set is shared by both users.

2. For the case of different channel gains $g_{1,j} \neq g_{2,j}$.
   - At high SNR, the fraction $\frac{\Gamma_{SD}^{(i)}(j)+\Gamma_{AF}^{(i)}(j)}{\Gamma+\Gamma_{SD}^{(i)}(j)+\Gamma_{AF}^{(i)}(j)}$ on either side of (8.15) can be approximated by 1.
   - The difference between the LHS and RHS of (8.16) can be defined by the function $f(g_{1,j}^{\alpha_1}/g_{2,j}^{\alpha_2})$ as:

$$f\Big(\frac{g_{1,j}^{\alpha_1}}{g_{2,j}^{\alpha_2}}\Big) \approx \log_2\Big(\frac{g_{1,j}^{\alpha_1}}{g_{2,j}^{\alpha_2}}\Big) + \log_2\Big(\frac{K_1^{\alpha_1}}{K_2^{\alpha_2}}\Big) + \alpha_2 - \alpha_1. \tag{8.20}$$

- By sorting the subcarriers based on $g_{1,j}^{\alpha_1}/g_{2,j}^{\alpha_2}$ and defining S as the set of ordered subcarriers, where 1 is the index of the subcarrier with the largest $g_{1,j}^{\alpha_1}/g_{2,j}^{\alpha_2}$, and N is the index of the subcarrier with the smallest $g_{1,j}^{\alpha_1}/g_{2,j}^{\alpha_2}$, there exists a subcarrier with index L_1 such that $f(g_{1,j}^{\alpha_1}/g_{2,j}^{\alpha_2}) > 0$ for $j < L_1$ and $f(g_{1,j}^{\alpha_1}/g_{2,j}^{\alpha_2}) < 0$ for $j > L_1$. The subcarriers in the ordered set $j < L_1$ are used by user 1, and the subcarriers in the ordered set $j > L_1$ are used by user 2. This implies that the optimal subcarrier assignment is a two-band solution.

The case of inadequate relaying power for all subcarriers may appear in some scenarios. In this situation, the subcarriers with zero relaying power are removed from the allocation and reordered again based on $f\Big(\frac{(\gamma_{SD}^{(1)}(j))^{\alpha_1}}{(\gamma_{SD}^{(2)}(j))^{\alpha_2}}\Big) = \log_2\Big(\frac{(\gamma_{SD}^{(1)}(j))^{\alpha_1}}{(\gamma_{SD}^{(2)}(j))^{\alpha_2}}\Big)$ and the partition boundary that maximizes the weighted sum rate is sought. Once again, this is a two-band partition as proved in [166].

8.2.2 Multiple Users $I > 2$ Scenario

In order to allocate the subcarriers $\forall j \in \mathcal{J}$ among multiple users $I > 2$, we extend the two users case to multiple users by partitioning the subcarriers between user i and the group of users $\mathcal{I}_{-\{i\}}$, with $\mathcal{I}_{-\{S\}}$ defined as $\mathcal{I}_{-\{S\}} = \mathcal{I} \backslash S$.

With some algebraic manipulation and assuming enough relaying power for all subcarriers, (8.11a) can be written as:

$$\alpha_1 \log_2\Big(1 + \frac{\Gamma_{SD}^{(1)}(j) + \Gamma_{AF}^{(1)}(j)}{\Gamma \Upsilon_j^{(1)}}\Big) - \frac{\alpha_1(\Gamma_{SD}^{(1)}(j) + \Gamma_{AF}^{(1)}(j))}{\Gamma \Upsilon_j^{(1)} + \Gamma_{SD}^{(1)}(j) + \Gamma_{AF}^{(1)}(j)} =$$
$$\frac{1}{(I-1)}\Big(\sum_{i \in \mathcal{I}_{-\{1\}}} \alpha_i \log_2\Big(1 + \frac{\Gamma_{SD}^{(i)}(j) + \Gamma_{AF}^{(i)}(j)}{\Gamma \Upsilon_j^{(i)}}\Big) - \frac{\alpha_i(\Gamma_{SD}^{(i)}(j) + \Gamma_{AF}^{(i)}(j))}{\Gamma \Upsilon_j^{(i)} + \Gamma_{SD}^{(i)}(j) + \Gamma_{AF}^{(i)}(j)}\Big). \quad (8.21)$$

The LHS and RHS of (8.21) can be interpreted as the marginal benefit for extra bandwidth for user 1 and the average marginal benefit for extra bandwidth for the group of users $\mathcal{I}_{-\{1\}}$, respectively. If a subcarrier is shared

between user 1 and the group of users $\mathcal{I}_{-\{1\}}$, the marginal benefits should be equal. If a subcarrier is solely used by user 1, that is, $\Upsilon_j^{(1)} = 1$, and $\Upsilon_j^{(i)} = 0$, $\forall i \in \mathcal{I}_{-\{1\}}$ the LHS of (8.21) should be strictly greater than the RHS. Likewise, if a subcarrier is used by $\mathcal{I}_{-\{1\}}$, that is, $\exists i \in \mathcal{I}_{-\{1\}}$, such that $\Upsilon_j^{(i)} = 1$, and $\Upsilon_j^{(k)} = 0$, $k \neq i$ where the RHS of (8.21) is strictly greater than the LHS. Based on these observations, the carrier should be assigned to either user 1 or to $\mathcal{I}_{-\{1\}}$ whichever has higher marginal benefit (LHS or RHS of (8.21)). By using the high SNR approximation, that is, $\frac{\Gamma_{SD}^{(i)}(j)+\Gamma_{AF}^{(i)}(j)}{\Gamma\Upsilon_j^{(i)}+\Gamma_{SD}^{(i)}(j)+\Gamma_{AF}^{(i)}(j)} \approx 1$, $\forall i \in \mathcal{I}$, the ith user terms in (8.21) can be simplified as:

$$\alpha_i \log_2\left(1+\frac{\Gamma_{SD}^{(i)}(j)+\Gamma_{AF}^{(i)}(j)}{\Gamma\Upsilon_j^{(i)}}\right)-\frac{\alpha_i(\Gamma_{SD}^{(i)}(j)+\Gamma_{AF}^{(i)}(j))}{\Gamma\Upsilon_j^{(i)}+\Gamma_{SD}^{(i)}(j)+\Gamma_{AF}^{(i)}(j)} \cong \alpha_i \log_2\left(1+\frac{\Gamma_{SD}^{(i)}(j)+\Gamma_{AF}^{(i)}(j)}{\Gamma\Upsilon_j^{(i)}}\right)-\alpha_i. \tag{8.22}$$

Substituting the optimal source and relay power profiles obtained in (8.12) and (8.14) in (8.22) results in:

$$\alpha_i \log_2\left(1+\frac{\Gamma_{SD}^{(i)}(j)+\Gamma_{AF}^{(i)}(j)}{\Gamma\Upsilon_j^{(i)}}\right)-\alpha_i = \alpha_i \log_2\left(\gamma_{SD}^{(i)}(j)+A_j^{(i)}\right)+\alpha_i \log_2(K_i)-\alpha_i. \tag{8.23}$$

The expression can be further simplified by using the approximation:

$$A_j^{(i)} \approx \frac{\min^2(\gamma_{SR}^{(i)}(j), \gamma_{RD}(j)C_j^{(i)})}{4\gamma_{SR}^{(i)}(j)} \approx \frac{\gamma_{SR}^{(i)}(j)}{4}, \tag{8.24}$$

where $\frac{1}{2}\min(\gamma_{SR}^{(i)}(j), \gamma_{RD}(j)C_j^{(i)})$ can be used as a lower bound for $\frac{\gamma_{SR}^{(i)}(j)\gamma_{RD}(j)C_j^{(i)}}{\gamma_{SR}^{(i)}(j)+\gamma_{RD}(j)C_j^{(i)}}$. The assumptions that $\frac{\gamma_{SR}^{(i)}(j)}{\gamma_{SD}^{(i)}(j)} > 1$ and $\frac{\gamma_{RD}(j)}{\gamma_{SD}^{(i)}(j)} > 1$, which are reasonable assumptions in cooperative communications are used to set $\gamma_{SR}^{(i)}(j)$ as a lower bound for $\gamma_{RD}(j)C_j^{(i)}$ in $A_j^{(i)}$ i.e. $\gamma_{SR}^{(i)}(j) < \gamma_{RD}(j)C_j^{(i)}$.

This leads us to assign the subcarriers for multiple users by ordering the subcarriers from largest to smallest based on the difference between the

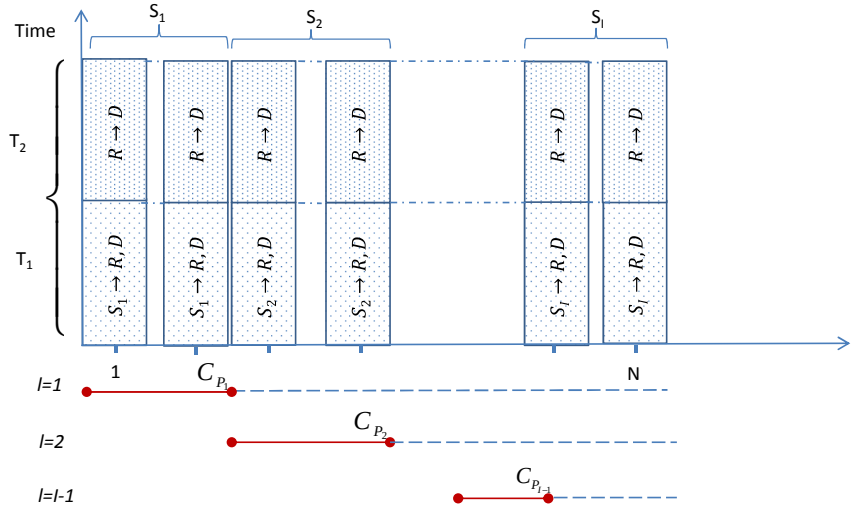

Figure 8.2 Multi-Users Two-Bands Subcarriers' Assignment Approach.

LHS and RHS of (8.21) using $I-1$ ordering levels. The ordering function at level l, for $l=1,\cdots,I-1$ denoted as $f_{AF}^{(l)}(\boldsymbol{\gamma}_{SD}^{(l)}(j),\boldsymbol{\gamma}_{SR}^{(l)}(j))$ is defined as:

$$f_{AF}^{(l)}\left(\boldsymbol{\gamma}_{SD}^{(l)}(j),\boldsymbol{\gamma}_{SR}^{(l)}(j)\right)=\log_2\left(\frac{\left(\gamma_{SD}^{(l)}(j)+0.25\gamma_{SR}^{(l)}(j)\right)^{\alpha_l}}{\prod_{k\in\mathcal{I}_{-\{1,\cdots,l\}}}\left(\gamma_{SD}^{(k)}(j)+0.25\gamma_{SR}^{(k)}(j)\right)^{\frac{\alpha_k}{I-l}}}\right). \tag{8.25}$$

where $\boldsymbol{\gamma}_{SD}^{(l)}(j)=[\gamma_{SD}^{(l)}(j),\cdots,\gamma_{SD}^{(I)}(j)]$, and $\boldsymbol{\gamma}_{SR}^{(l)}(j)=[\gamma_{SR}^{(l)}(j),\cdots,\gamma_{SR}^{(I)}(j)]$ are vectors of all users source-destination channel gains and source-relay channel gains, respectively.

The boundary profile $\boldsymbol{C}_P=[C_{P_1},C_{P_2},\cdots,C_{P_{I-1}}]$ that maximizes the weighted sum rate is sought in a nested hierarchical fashion. Then the subcarriers $C_{P_{l-1}}<j\leq C_{P_l}$, for $l=1,\cdots,I-1$ are assigned to user l, subcarriers $j\leq C_{P_1}$ are assigned to user 1, and the subcarriers $j>C_{P_{I-1}}$ are assigned to user I. The procedure of reordering and searching for the partition boundaries is shown in **Figure 8.2**. The proposed subcarrier assignment algorithm is illustrated in **Algorithm 8.1**. It is based on searching the partition boundaries $C_{P_1},C_{P_2},\cdots,C_{P_{I-1}}$ that maximize the weighted sum rate. $I-1$ levels are required to split the subcarriers between the users and search the partition boundaries. *ORD-DES($\mathcal{M}$,l)* is used to order the subcarriers in the set $\mathcal{M}$, where l is the ordering level $l=1,\cdots,I-1$, and $S(j)=$

$\log_2\left(\frac{(\gamma_{SD}^{(l)}(j)+0.25\gamma_{SR}^{(l)}(j))^{\alpha_l}}{\prod_{k\in\mathcal{I}_{-\{1,\cdots,l\}}}(\gamma_{SD}^{(k)}(j)+0.25\gamma_{SR}^{(k)}(j))^{\frac{\alpha_k}{I-l}}}\right)$ is used to order the subcarriers in descent ordering. The function *ORD-DES($\mathcal{M}$,l)* returns the index vector $\boldsymbol{O}_S = \left[O_S(1), \cdots, O_S(|\mathcal{M}|)\right]$ of the ordered set $\mathcal{M}$ such that $S(O_S(1)) > S(O_S(2)) > S(j) > \cdots > S(O_S(|\mathcal{M}|))$, where $|\mathcal{M}|$ is the cardinality of the set $\mathcal{M}$. The set of subcarriers that is assigned to user l at level l for $l = 1, \cdots, I-1$ is denoted as $\mathcal{J}_l$. At level l, the set of subcarriers $G_{l-1} = \mathcal{J} - \cup_{k=1}^{l-1}\mathcal{J}_k$ which is assigned to $\mathcal{I}_{-\{1,\cdots,l-1\}}$ is reordered using $\boldsymbol{O}_l$ =*ORD-DES(G_{l-1},l)*, and then sliding the subcarrier index $0 \leq j_l \leq |\boldsymbol{O}_l|$ and using the function *TWO-PAR*($\boldsymbol{O}_l$, j_l) to assign the subcarriers with index $j \leq j_l$ of the ordered set $\boldsymbol{O}_l$ to user l as $\mathcal{J}_l$, and the subcarriers with index $j > j_l$ of the ordered set $\boldsymbol{O}_l$ are assigned to $\mathcal{I}_{-\{1,\cdots,l\}}$ as G_l. The algorithm, then proceeds in a similar fashion until level $I-1$. The weighted sum rate $R(j_1, j_2, \cdots, j_{I-1}) = \sum_{i\in\mathcal{I}}\alpha_i\sum_{j\in\mathcal{J}_i}R_{AF}^{(i)}(j)$ is computed with the subcarrier assignment profiles $\mathcal{J}_i$, $\forall i \in \mathcal{I}$. The optimal power profiles at the source and relay nodes are computed as in (8.12) and (8.14). The partition vector $\boldsymbol{C}_P$ is determined as $\boldsymbol{C}_P = \arg\max_{j_1,j_2,\cdots,j_{I-1}} R(j_1, j_2, \cdots, j_{I-1})$.

For all subcarriers that are allocated zero relaying power, a second phase is required. In this phase, these subcarriers are removed from the users' assignment profile and added to a set $\mathcal{L}$ with cardinality $|\mathcal{L}|$. Similar to **Algorithm 8.1**, $I-1$ levels are performed for searching the partitions. The differences between the two phases are (1) the use of the function *ORD-DES-M($\mathcal{M}$,l)* instead of *ORD-DES($\mathcal{M}$,l)* to order the subcarriers in the second phase. In *ORD-DES-M($\mathcal{M}$,l)*, the subcarriers in $\mathcal{M}$ at level l are ordered from largest to smallest based on $S^M(j) = \log_2\left(\frac{(\gamma_{SD}^{(l)}(j))^{\alpha_l}}{\prod_{k\in\mathcal{I}_{-\{1,\cdots,l\}}}(\gamma_{SD}^{(k)}(j))^{\frac{\alpha_k}{I-k}}}\right)$. (2) The subcarrier assignment in **Algorithm 8.1** is for the set $\mathcal{J}$, whereas the subcarrier assignment in **Algorithm 8.2** is only for the subcarriers with zero relaying power grouped in the set $\mathcal{L}$. The computational complexity[4] of **Algorithm 8.1** is of $O(N^{I-1})$ compared to $O(I^N)$ for the exhaustive search algorithm. The proposed algorithm is suitable for large number of subcarri-

[4]For **Algorithm 8.2**, the computational complexity is of $O(|\mathcal{L}|^{I-1})$.

Algorithm 8.1 Subcarrier Assignment Algorithm for I Users AF-OFDMA.

Require: $P_R^{\max}$, α_i, $\gamma_{SD}^{(i)}(j)$, $\gamma_{SR}^{(i)}(j)$, $\gamma_{RD}(j)$, $P_i^{\max}$, $\forall i \in \mathcal{I}$, and $\forall j \in \mathcal{J}$.
1: Set $\mathcal{J}_i = \varnothing$, $\forall i \in \mathcal{I}$.
2: $\boldsymbol{O}_l \leftarrow$ ORD-DES(G_{l-1}, l), for $l = 1, \cdots, I-1$.
3: $\mathcal{J}_l, G_l \leftarrow$ TWO-PAR($\boldsymbol{O}_l$, j_l), for $j_l = 0, \cdots, |\boldsymbol{O}_l|$, and $l = 1, \cdots, I-1$.
4: $R(j_1, j_2, \cdots, j_{I-1}) = \sum_{i \in \mathcal{I}} \alpha_i \sum_{j \in \mathcal{J}_i} R_{AF}^{(i)}(j)$, for $j_l = 0, \cdots, |\boldsymbol{O}_l|$, and $l = 1, \cdots, I-1$.
5: $\boldsymbol{C}_P \leftarrow \arg \max_{j_1, j_2, \cdots, j_{I-1}} R(j_1, j_2, \cdots, j_{I-1})$.
6: Find $\mathcal{J}_i$, $\forall i \in \mathcal{I}$ corresponding to $\boldsymbol{C}_P$.
7: **Return** $\mathcal{J}_i$, $\forall i \in \mathcal{I}$.
8: **function** ORD-DES($\mathcal{M}$, l)
9: $S(j) \leftarrow \log_2\Big(\frac{(\gamma_{SD}^{(l)}(j)+0.25\gamma_{SR}^{(l)}(j))^{\alpha_l}}{\prod_{k=l+1}^{I}(\gamma_{SD}^{(k)}(j)+0.25\gamma_{SR}^{(k)}(j))^{\frac{\alpha_k}{I-l}}}\Big)$, $\forall j \in \mathcal{M}$.
10: $Sort(S(j), \forall j \in \mathcal{M}, Descent)$.
11: Find the index vector $\boldsymbol{O}_S = [O_S(1), \cdots, O_S(|\mathcal{M}|)]$, where $S(O_S(1)) > S(O_S(2)) > S(j) > \cdots > S(O_S(|\mathcal{M}|))$.
12: **Return** $\boldsymbol{O}_S$.
13: **end function**
14: **function** TWO-PAR($\boldsymbol{O}_l$, j_l)
15: $\mathcal{J}_l \leftarrow \boldsymbol{O}_l(0 : j_l)$.
16: $G_l \leftarrow \boldsymbol{O}_l(j_1 + 1 : |\boldsymbol{O}_l|)$.
17: **Return** $\mathcal{J}_l$, G_l.
18: **end function**

ers and small number of users. The computational complexity comes from searching the boundaries in a nested fashion. To reduce further the computational complexity, we develop a simplified heuristic algorithm to assign the subcarriers to the users aiming to maximize the weighted sum rate without the need to search the boundaries in a nested fashion. The main idea is to assign each subcarrier to the user with the maximum marginal benefits (based on the channel gains) and construct a frequency partition for each user. Based on the weighted sum rate, the boundaries of the partition are then tuned to improve the weighted sum rate. The simplified algorithm contains two stages; basic assignment stage and subcarrier transfer stage. The basic assignment stage is based on assigning each subcarrier to the user with the maximum marginal benefit. User i marginal benefit of subcarrier j

Algorithm 8.2 The Second Phase of the Subcarrier Assignment Algorithm for I Users AF-OFDMA.

Require: $P_R^{\max}$, $P_i^{\max}$, α_i, $\gamma_{SD}^{(i)}(j)$, $\gamma_{SR}^{(i)}(j)$, $\gamma_{RD}(j)$, $P_R^{(i)}(j)$, $\forall i \in \mathcal{I}$, $j \in \mathcal{J}$, $\mathcal{J}_i$, $\forall i \in \mathcal{I}$ and $\mathcal{L} = \varnothing$.

1: **if** $P_R^{(i)}(j) = 0,\ j \in \mathcal{J}$ **then**
2: $\quad \mathcal{L} \leftarrow \{\mathcal{L}, j\}$.
3: **end if**
4: $\mathcal{J}_i \leftarrow \mathcal{J}_i - \mathcal{L}, \forall i \in \mathcal{I}$.
5: $\boldsymbol{O}_l^M \leftarrow$ ORD-DES-M(G_{l-1}^M, l), $l = 1 : I-1$.
6: $\mathcal{J}_l^M, \mathcal{J}_{-\{1,\cdots,l\}}^M \leftarrow$ TWO-PAR$(\boldsymbol{O}_l^M, j_l)$, $j_l = 0 : |\boldsymbol{O}_l^M|$, $l = 1 : I-1$, $\forall i \in \mathcal{I}$.
7: $\mathcal{J}_i^M \leftarrow \mathcal{J}_i \cup \mathcal{J}_i^M$.
8: $R(j_1, j_2, \cdots, j_{I-1}) = \sum_{i\in\mathcal{I}} \alpha_i \sum_{j\in\mathcal{J}_i^M} R_{AF}^{(i)}(j)$, $j_l = 0 : |\boldsymbol{O}_l^M|$, $l = 1 : I-1$.
9: $\boldsymbol{C}_P \leftarrow \arg \max_{j_1, j_2, \cdots, j_{I-1}} R(j_1, j_2, \cdots, j_{I-1})$
10: Find $\mathcal{J}_1^M, \mathcal{J}_2^M, \cdots, \mathcal{J}_I^M$ corresponding to $\boldsymbol{C}_P$.
11: **Return** $\mathcal{J}_1^M, \mathcal{J}_2^M, \cdots, \mathcal{J}_I^M$.
12: **function** ORD-DES-M$(\mathcal{M}, l)$
13: $\quad S(j) \leftarrow \log_2\Big(\frac{(\gamma_{SD}^{(l)}(j))^{\alpha_i}}{\prod_{k=l+1}^{I}(\gamma_{SD}^{(k)}(j))^{\frac{\alpha_k}{I-l}}}\Big), \forall j \in \mathcal{M}$.
14: $\quad Sort(S(j), \forall j \in \mathcal{M}, Descent)$.
15: $\quad$ Find the index vector $\boldsymbol{O}_S = [O_S(1), \cdots, O_S(|\mathcal{M}|)]$, where $S(O_S(1)) > S(O_S(2)) > S(j) > \cdots > S(O_S(|\mathcal{M}|))$.
16: $\quad$ **Return** $\boldsymbol{O}_S$.
17: **end function**

can be defined based on (8.21) as:

$$f_{i,\mathcal{I}_{-\{i\}}}^{AF}\Big(\boldsymbol{\gamma}_{SD}^{(1)}(j), \boldsymbol{\gamma}_{SR}^{(1)}(j)\Big) = \log_2\Big(\frac{(\gamma_{SD}^{(i)}(j) + 0.25\gamma_{SR}^{(i)}(j))^{\alpha_i}}{\prod_{k\in\mathcal{I}_{-\{i\}}}(\gamma_{SD}^{(k)}(j) + 0.25\gamma_{SR}^{(k)}(j))^{\frac{\alpha_k}{I-1}}}\Big). \tag{8.26}$$

Subcarrier $j \in \mathcal{J}$ is assigned to user i^* such that $i^* = \arg\max_i f_{i,\mathcal{I}_{-\{i\}}}^{AF}\Big(\boldsymbol{\gamma}_{SD}^{(1)}(j), \boldsymbol{\gamma}_{SR}^{(1)}(j)\Big)$. The set of subcarriers assigned to user i based on the marginal benefit is defined as $\mathcal{J}_i$. The initial weighted sum rate R_0 is computed as $R_0 = \sum_{i\in\mathcal{I}} \alpha_i \sum_{j\in\mathcal{J}_i} R_{AF}^{(i)}(j)$, where the optimal power profiles at the source and relay nodes are computed as in (8.12) and (8.14).

In the transfer stage, users in turns are allowed to transfer subcarriers aiming to maximize the weighted sum rate R_0; user i in her turn is allowed to transfer subcarrier(s) starting with the subcarrier that has the minimum marginal benefit in the set $\mathcal{J}_i$ obtained as $j^* = \arg\min_{j\in\mathcal{J}_i} f_{i,\mathcal{I}_{-\{i\}}}^{AF}\Big(\boldsymbol{\gamma}_{SD}^{(1)}(j), \boldsymbol{\gamma}_{SR}^{(1)}(j)\Big)$ to user i^* as $i^* = \arg\max_{k\in\mathcal{I}, k\neq i} f_{k,\mathcal{I}_{-\{k\}}}^{AF}\Big(\boldsymbol{\gamma}_{SD}^{(1)}(j^*), \boldsymbol{\gamma}_{SR}^{(1)}(j^*)\Big)$ with the next highest benefit

Algorithm 8.3 Basic Stage of The Simplified Subcarrier Assignment Algorithm for I Users AF-OFDMA.

Require: $P_R^{\max}$, α_i, $\gamma_{SD}^{(i)}(j)$, $\gamma_{SR}^{(i)}(j)$, $P_i^{\max}$ $\forall i \in \mathcal{I}$, and $\forall j \in \mathcal{J}$.
1: Set $\mathcal{J}_i = \varnothing$, $\forall i \in \mathcal{I}$.
2: Compute $f_{i,\mathcal{I}_{-\{i\}}}^{AF}(\boldsymbol{\gamma}_{SD}^{(1)}(j), \boldsymbol{\gamma}_{SR}^{(1)}(j)) = \log_2\Big(\frac{(\gamma_{SD}^{(i)}(j)+0.25\gamma_{SR}^{(i)}(j))^{\alpha_i}}{\prod_{k\in\mathcal{I}_{-\{i\}}}(\gamma_{SD}^{(k)}(j)+0.25\gamma_{SR}^{(k)}(j))^{\frac{\alpha_k}{I-1}}}\Big)$, $\forall i \in \mathcal{I}$, $\forall j \in \mathcal{J}$.
3: **for** $j \in \mathcal{J}$ **do**
4: Find $i^* = \arg\max_i f_{i,\mathcal{I}_{-\{i\}}}^{AF}(\boldsymbol{\gamma}_{SD}^{(1)}(j), \boldsymbol{\gamma}_{SR}^{(1)}(j))$.
5: Update $\mathcal{J}_{i^*} \leftarrow \mathcal{J}_{i^*} \cup j$.
6: **end for**
7: Compute $R_0 = \sum_{i\in\mathcal{I}} \alpha_i \sum_{j\in\mathcal{J}_i} R_{AF}^{(i)}(j)$.

conditioned on increasing the weighted sum rate. The algorithm then proceeds to the next subcarrier in the set $\mathcal{J}_i$ until the weighted sum rate could not be increased further. The algorithm proceeds to the next user in the same way. The algorithm can be applied for a number of iterations to ensure no further improvement in the weighted sum rate can be gained. This basic stage of the simplified algorithm is illustrated in **Algorithm 8.3**.

8.3 DF-OFDMA Cooperative Communications

In this section, we extend the subcarrier assignment algorithms to DF-OFDMA cooperative communication scheme. The achievable data rate of the ith user at the jth subcarrier $R_{DF}^{(i)}(j)$ for DF-OFDMA scheme at the destination node with the aid of the relay node and after using MRC technique is computed as [86]:

$$R_{DF}^{(i)}(j) = \frac{B_N}{2}\min\Big\{\log_2\Big(1+\frac{\gamma_{SR}^{(i)}(j)\hat{P}_S^{(i)}(j)}{\Gamma}\Big), \log_2\Big(1+\frac{\gamma_{SD}^{(i)}(j)\hat{P}_S^{(i)}(j)+\gamma_{RD}(j)\hat{P}_R^{(i)}(j)}{\Gamma}\Big)\Big\}. \tag{8.27}$$

The weighted sum rate resource allocation problem can be formulated as:

$$\max_{\hat{\boldsymbol{P}}_R, \hat{\boldsymbol{P}}_S, \boldsymbol{\Upsilon}} \frac{B_N}{2}\sum_{i\in\mathcal{I}}\alpha_i\sum_{j\in\mathcal{J}}\Upsilon_j^{(i)}\log_2\Big(1+\frac{\gamma_{SD}^{(i)}(j)\hat{P}_S^{(i)}(j)+\gamma_{RD}(j)\hat{P}_R^{(i)}(j)}{\Gamma}\Big), \tag{8.28a}$$

$$\text{s.t. } \log_2\Big(1+\frac{\gamma_{SD}^{(i)}(j)\hat{P}_S^{(i)}(j)+\gamma_{RD}(j)\hat{P}_R^{(i)}(j)}{\Gamma}\Big) \le \log_2\Big(1+\frac{\gamma_{SR}^{(i)}(j)\hat{P}_S^{(i)}(j)}{\Gamma}\Big),$$

$$\forall j \in \mathcal{J}, \forall i \in \mathcal{I}, \tag{8.28b}$$

$$\sum_{i\in\mathcal{I}}\sum_{j\in\mathcal{J}} \Upsilon_j^{(i)} \hat{P}_R^{(i)}(j) \le P_R^{\max}, \tag{8.28c}$$

$$\sum_{j\in\mathcal{J}} \Upsilon_j^{(i)} \hat{P}_S^{(i)}(j) \le P_i^{\max}, \forall i \in \mathcal{I}, \tag{8.28d}$$

$$\sum_{i\in\mathcal{I}} \Upsilon_j^{(i)} \le 1, \ \forall j \in \mathcal{J}, \tag{8.28e}$$

$$\hat{P}_S^{(i)}(j) \ge 0, \ \hat{P}_R^{(i)}(j) \ge 0, \ \Upsilon_j^{(i)} \in \{0,1\}, \ \forall i \in \mathcal{I}, \ \forall j \in \mathcal{J}, \tag{8.28f}$$

constraints (8.28c)-(8.28e) can be interpreted as (8.6b)-(8.6d) in Section 8.2, respectively.

Problem (8.28) is similar to (8.6) in that it is a mixed integer constrained optimization problem. The same approach used to solve (8.6) can also be followed here. The problem can be transformed into a convex optimization problem by relaxing the binary variables as $\Upsilon_j^{(i)} \in [0,1]$, $\forall i \in \mathcal{I}$, and $\forall j \in \mathcal{J}$. Using the time sharing principle, problem (8.28) is transformed into:

$$\max_{\boldsymbol{P}_R, \boldsymbol{P}_S, \boldsymbol{\Upsilon}} \frac{B_N}{2} \sum_{i\in\mathcal{I}} \alpha_i \sum_{j\in\mathcal{J}} \Upsilon_j^{(i)} \log_2\Big(1 + \frac{\gamma_{SD}^{(i)}(j) P_S^{(i)}(j) + \gamma_{RD}(j) P_R^{(i)}(j)}{\Gamma \Upsilon_j^{(i)}}\Big), \tag{8.29a}$$

$$\text{s.t.} \sum_{i\in\mathcal{I}}\sum_{j\in\mathcal{J}} P_R^{(i)}(j) \le P_R^{\max}, \tag{8.29b}$$

$$\sum_{j\in\mathcal{J}} P_S^{(i)}(j) \le P_i^{\max}, \forall i \in \mathcal{I}, \tag{8.29c}$$

$$\sum_{i\in\mathcal{I}} \Upsilon_j^{(i)} \le 1, \forall j \in \mathcal{J}, \tag{8.29d}$$

$$\Big(\gamma_{SD}^{(i)}(j) - \gamma_{SR}^{(i)}(j)\Big) P_S^{(i)}(j) + \gamma_{RD}(j) P_R^{(i)}(j) \le 0, \ \forall j \in \mathcal{J}, \ \forall i \in \mathcal{I}, \tag{8.29e}$$

$$P_S^{(i)}(j) \ge 0, \ P_R^{(i)}(j) \ge 0, \ \Upsilon_j^{(i)} \in \{0,1\}, \ \forall i \in \mathcal{I}, \ \forall j \in \mathcal{J}. \tag{8.29f}$$

It can be proved easily that (8.29) is a convex optimization problem. The objective function is a jointly concave function with respect to $\boldsymbol{P}_R$, $\boldsymbol{P}_S$, and $\boldsymbol{\Upsilon}$ as can be proved by the second order derivative test and the constraints are linear. Similar to AF-OFDMA, we will find an analytical solution based on

the KKT conditions which are sufficient and necessary optimality conditions for this problem. The Lagrangian function can be formulated as:

$$L(\boldsymbol{P}_S, \boldsymbol{P}_R, \boldsymbol{\Upsilon}, \boldsymbol{\lambda}) = \frac{B_N}{2} \sum_{i\in\mathcal{I}} \alpha_i \sum_{j\in\mathcal{J}} \Upsilon_j^{(i)} \log_2 \Big(1 + \frac{\gamma_{SD}^{(i)}(j) P_S^{(i)}(j) + \gamma_{RD}(j) P_R^{(i)}(j)}{\Gamma \Upsilon_j^{(i)}}\Big) -$$
$$\sum_{i\in\mathcal{I}} \lambda_i \Big(\sum_{j\in\mathcal{J}} P_S^{(i)}(j) - P_i^{\max}\Big) - \lambda_R \Big(\sum_{i\in\mathcal{I}} \sum_{j\in\mathcal{J}} P_R^{(i)}(j) - P_R^{\max}\Big) - \sum_{j\in\mathcal{J}} \lambda_j^{\Upsilon} \Big(\sum_{i\in\mathcal{I}} \Upsilon_j^{(i)} - 1\Big), \tag{8.30a}$$

$$\text{s.t. } P_R^{(i)}(j) \geq 0,\ P_S^{(i)}(j) \geq 0,\ \Upsilon_j^{(i)} \geq 0,\ \lambda_R \geq 0,\ \lambda_i \geq 0, \lambda_j^{\Upsilon} \geq 0,\ \forall j \in \mathcal{J},\ \forall i \in \mathcal{I}, \tag{8.30b}$$

where λ_R, λ_is, for $i \in \mathcal{I}$ and λ_j^{Υ}, for $j \in \mathcal{J}$ are Lagrange multipliers. The achievable weighted sum rate for DF-OFDMA is maximized when constraint (8.29e) is satisfied with equality, that is

$$\gamma_{SR}^{(i)}(j) P_S^{(i)}(j) = \gamma_{SD}^{(i)}(j) P_S^{(i)}(j) + \gamma_{RD}(j) P_R^{(i)}(j),\ \forall j \in \mathcal{J}, \forall i \in \mathcal{I}. \tag{8.31}$$

Hence, the relaying power $P_R^{(i)}(j)$ can be obtained as:

$$P_R^{(i)}(j) = C_j^{(i)} P_S^{(i)}(j), \tag{8.32}$$

with $C_j^{(i)} = \frac{\left(\gamma_{SR}^{(i)}(j) - \gamma_{SD}^{(i)}(j)\right)^+}{\gamma_{RD}(j)}$.

Differentiating (8.30a) with respect to $P_S^{(i)}(j)$ and equating to zero results in:

$$1 + \frac{\gamma_{SD}^{(i)}(j) P_S^{(i)}(j) + \gamma_{RD}(j) P_R^{(i)}(j)}{\Upsilon_j^{(i)} \Gamma} = \begin{cases} \frac{\alpha_i \gamma_{SD}^{(i)}(j) B_N / (2\ln(2))}{\Gamma \lambda_i}, & \text{if } P_R^{(i)}(j) = 0, \\ \frac{\alpha_i \gamma_{SR}^{(i)}(j) B_N / (2\ln(2))}{\Gamma \lambda_i}, & \text{if } P_R^{(i)}(j) > 0. \end{cases} \tag{8.33}$$

Substituting (8.32) in (8.33) results in:

$$P_S^{(i)}(j) = \begin{cases} \Upsilon_j^{(i)}\left(\frac{K_i\gamma_{SD}^{(i)}(j)}{\gamma_{SR}^{(i)}(j)} - \frac{\Gamma}{\gamma_{SR}^{(i)}(j)}\right)^+ & \text{if } P_R^{(i)}(j) > 0, \\ \Upsilon_j^{(i)}\left(K_i - \frac{\Gamma}{\gamma_{SD}^{(i)}(j)}\right)^+, & \text{if } P_R^{(i)}(j) = 0, \end{cases} \tag{8.34}$$

where $K_i = \frac{\alpha_i B_N}{2\ln(2)\lambda_i}$. Following the same approach adapted for AF-OFDMA scenario in Section 8.2, differentiating the Lagrangian function (8.30a) with respect to the relaxed integer $\Upsilon_j^{(i)}$ and equating to zero results in:

$$\alpha_i \log_2\left(1 + \frac{\gamma_{SD}^{(i)}(j)P_S^{(i)}(j) + \gamma_{RD}(j)P_R^{(i)}(j)}{\Gamma\Upsilon_j^{(i)}}\right) - \frac{\alpha_i(\gamma_{SD}^{(i)}(j)P_S^{(i)}(j) + \gamma_{RD}(j)P_R^{(i)}(j))}{\Gamma\Upsilon_j^{(i)} + \gamma_{SD}^{(i)}(j)P_S^{(i)}(j) + \gamma_{RD}(j)P_R^{(i)}(j)} = \frac{\lambda_j^{\Upsilon}}{B_N/(2\ln(2))}. \tag{8.35}$$

In a two users case, if $\Upsilon_j^{(1)} > 0$ and $\Upsilon_j^{(2)} > 0$, using high SNR approximation, i.e. $\frac{\gamma_{SD}^{(i)}(j)P_S^{(i)}(j)+\gamma_{RD}(j)P_R^{(i)}(j)}{\Gamma+\gamma_{SD}^{(i)}(j)P_S^{(i)}(j)+\gamma_{RD}(j)P_R^{(i)}(j)} \approx 1$, and using (8.33) results in:

$$\alpha_1 \log_2(K_1 g_{1,j}) + \frac{\alpha_1}{K_1 g_{1,j}} - \alpha_1 = \alpha_2 \log_2(K_2 g_{2,j}) + \frac{\alpha_2}{K_2 g_{2,j}} - \alpha_2, \tag{8.36}$$

where

$$g_{i,j} = \begin{cases} \gamma_{SR}^{(i)}(j), & \text{if } P_R^{(i)}(j) > 0, \\ \gamma_{SD}^{(i)}(j), & \text{if } P_R^{(i)}(j) = 0. \end{cases} \tag{8.37}$$

This shows that the frequency partitions principle for the two user subcarrier allocation introduced in **Theorem 8.2.1** is also applicable for DF-OFDMA cooperative scheme. The only difference between OFDMA-AF and OFDMA-DF is in the ordering function. Extending the resource allocation to multiple users scenario can be done in a similar fashion to the AF-OFDMA scenario, by partitioning the subcarriers between user i and the group of users $\mathcal{I}_{-\{1,\cdots,i\}}$ for $1 \leq i \leq I-1$ in a nested fashion, and searching for the

partitions that maximize the weighted sum rate.

With some algebraic manipulation and using the high SNR approximation in (8.35), the lth level ordering function for DF-OFDMA cooperative communications $f_l^{DF}(\cdot)$ can be computed as:

$$f_{DF}^{(l)}\left(\boldsymbol{\gamma}_{SR}^{(l)}(j)\right) = \log_2\left(\frac{(\gamma_{SR}^{(l)}(j))^{\alpha_l}}{\prod_{k\in\mathcal{I}_{-\{1,\cdots,l\}}}(\gamma_{SR}^{(k)}(j))^{\frac{\alpha_k}{(I-l)}}}\right). \tag{8.38}$$

Hence, **Algorithm 8.1** can be used for DF-OFDMA subcarrier assignment, by replacing $f_{AF}^{(l)}(\boldsymbol{\gamma}_{SD}^{(l)}(j), \boldsymbol{\gamma}_{SR}^{(l)}(j))$ by $f_{DF}^{(l)}(\boldsymbol{\gamma}_{SR}(j))$ in *ORD-DES*$(\mathcal{M}, i)$. The weighted sum data rate is now computed as: $R(j_1, j_2, \cdots, j_{I-1}) = \sum_{i\in\mathcal{I}} \alpha_i \sum_{j\in\mathcal{J}_i} R_{DF}^{(i)}(j)$. Similar to the AF-OFDMA scenario, a second phase might be required if some of the subcarriers are allocated zero relaying power. In the second phase, **Algorithm 8.2** can be used to allocate the subcarriers of zero relaying power grouped in the set $\mathcal{L}$.

The simplified assignment **Algorithm 8.3** can also be used for DF-OFDMA subcarrier assignment, by replacing $f_{i,\mathcal{I}_{-\{i\}}}^{(AF)}\left(\boldsymbol{\gamma}_{SD}^{(l)}(j), \boldsymbol{\gamma}_{SR}^{(l)}(j)\right)$ by $f_{i,\mathcal{I}_{-\{i\}}}^{DF}\left(\boldsymbol{\gamma}_{SR}^{(l)}(j)\right)$ computed as:

$$f_{i,\mathcal{I}_{-\{i\}}}^{DF}\left(\boldsymbol{\gamma}_{SR}^{(1)}(j)\right) = \log_2\left(\frac{(\gamma_{SR}^{(i)}(j))^{\alpha_i}}{\prod_{k\in\mathcal{I}_{-\{i\}}}(\gamma_{SR}^{(k)}(j))^{\frac{\alpha_k}{K-1}}}\right). \tag{8.39}$$

8.4 Simulation Results and Discussion

The same setup used in Chapters 6 and 7 is replicated here, where the subcarrier channel coefficients between any two nodes with a separating distance d are modeled as $H(j) \sim \mathcal{CN}(0, \frac{1}{L(1+d)^{\alpha}})$, the propagation loss factor $\alpha = 4$, and the number of channel taps $L = 4$ as in [49].

The scenario under consideration consists of I users (sources) ($S_1, S_2, \cdots, S_I$), one relay and a common destination node D as shown in **Figure 8.3**. The distance between the relay and the destination nodes is $d_{RD} = 50$m.

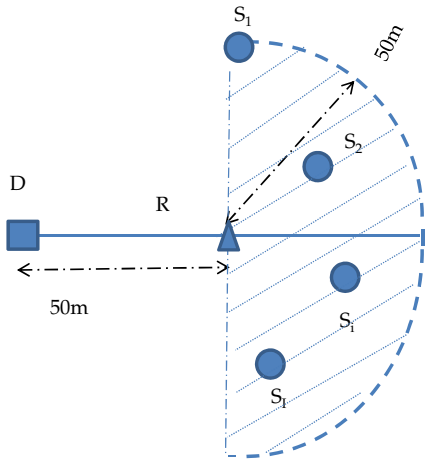

Figure 8.3 Sources, Relay and Destination Nodes Positions.

The sources are uniformly distributed in the shaded area. This scenario is considered to obtain source-relay and relay-destination channel gains better than the source-destination channel gains (i.e. $d_{S_iD} > d_{S_iR}$ and $d_{S_iD} > d_{RD}$) as in [131].

The subcarrier noise power σ^2 is set at 4×10^{-11}Watt. The source maximum transmit power is $P_i^{\max} = 1$Watt, and the relay maximum transmit power is $P_R^{\max} = 10$Watt, unless otherwise specified. The subcarrier spacing is $B_N = 4$KHz, and the capacity gap is $\Gamma = 1$.

The achievable weighted sum rate and the subcarrier assignment of **Algorithm 8.1** / **Algorithm 8.2** for AF/DF-OFDMA are compared with the achievable weighted sum rate and the subcarrier assignment of the exhaustive search algorithm for $N = 8$ subcarriers[5] and $I = 2$ and 3 users, respectively. The comparison was carried out for a large number of random channel realizations and for different maximum transmit source and relay power constraints. The computational complexity of the proposed algorithm for the two users case is $O(N)$ compared to $O(2^N)$ for the exhaustive search algorithm. The complexity of the proposed algorithm can be further reduced to $O(\log_2 N)$ for the two users case using binary search algorithms. In addition, sorting the subcarriers in the proposed algorithm requires $O(N \log N)$

[5]Note that the complexity of the exhaustive search becomes prohibitive for large number of subcarriers or large number of users.

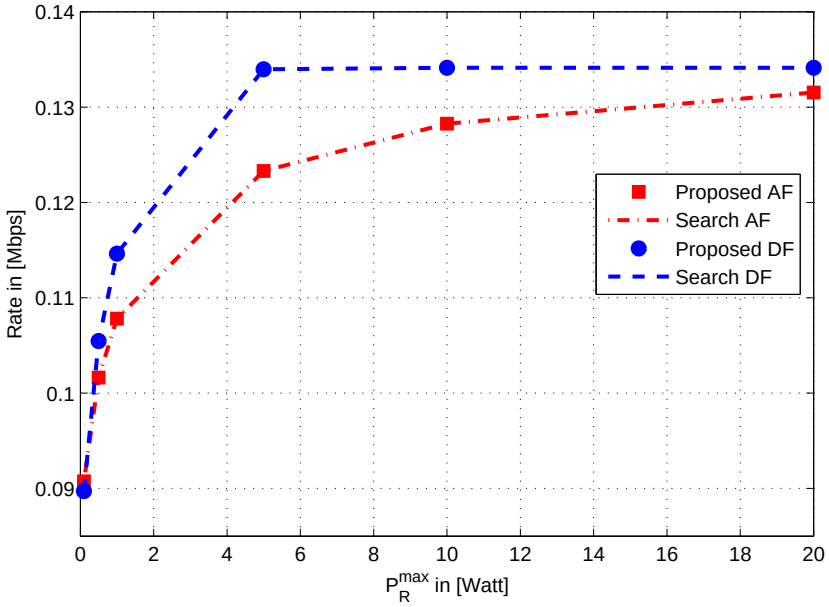

(a) The Sum Rate for I=2

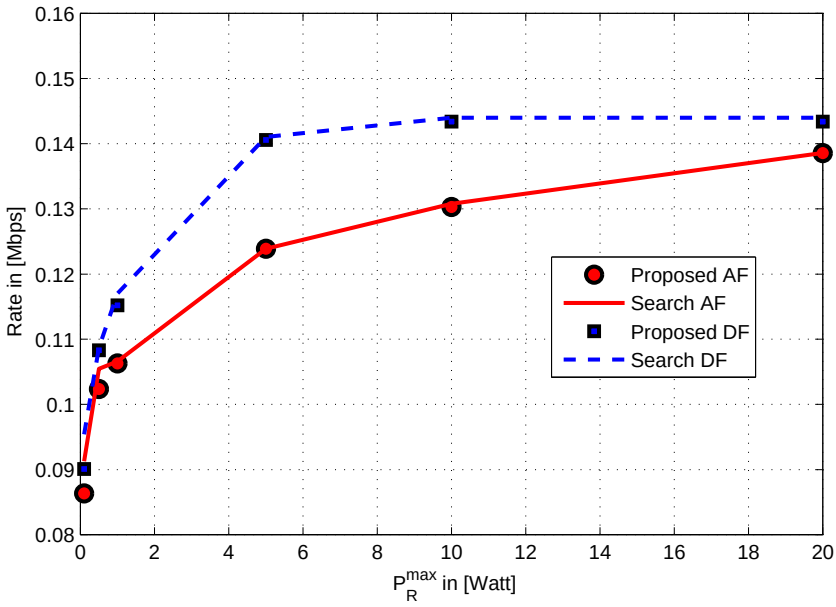

(b) The Sum Rate for I=3

Figure 8.4 The Sum Rate for **Algorithm 8.1** / **Algorithm 8.2** and the Exhaustive Search Algorithm

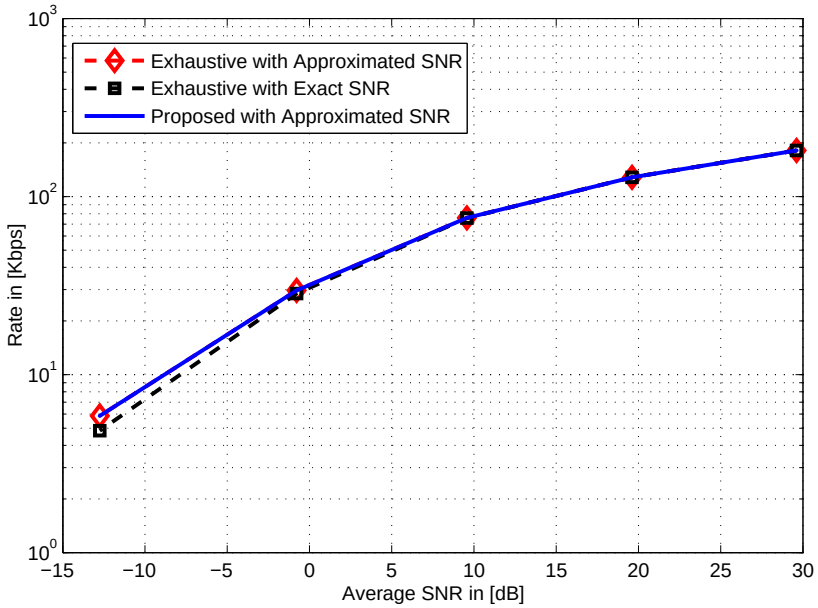

Figure 8.5 The Sum Rate for **Algorithm 8.1** and the Exhaustive Search Algorithm.

computations for the worst case and $\mathcal{O}(N)$ for the best case. **Figure 8.4(a)** and **Figure 8.4(b)** compare the achievable sum rate using **Algorithm 8.1** / **Algorithm 8.2** and the achievable sum rate using exhaustive search for AF/DF-OFDMA as a function of the relay's maximum power $P_R^{\max}$. Clearly, the achievable sum rate for $I = 2, 3$ of the proposed algorithm coincides with the achievable sum rate of the exhaustive search algorithm with negligible difference.

Figure 8.5 shows the sum data rate for a two users AF-OFDMA scenario as a function of the SNR (by varying the noise power) for three algorithms: **Algorithm 8.1** / **Algorithm 8.2**, exhaustive search algorithm using the high SNR approximation, and exhaustive search algorithm based on exact SNR. The power allocation profiles for the exhaustive search algorithm based on the exact SNR are obtained for a given subcarrier assignment profile by an iterative algorithm; alternating between two steps. In step I, the relay power profile is computed for a given source power profile. In step II, the source power profile is computed for a given relay power profile. The algorithm is repeated until convergence. The average SNR is computed as $\mathrm{E}[\frac{P_S^c|H_{SD}|^2}{\sigma^2} +$

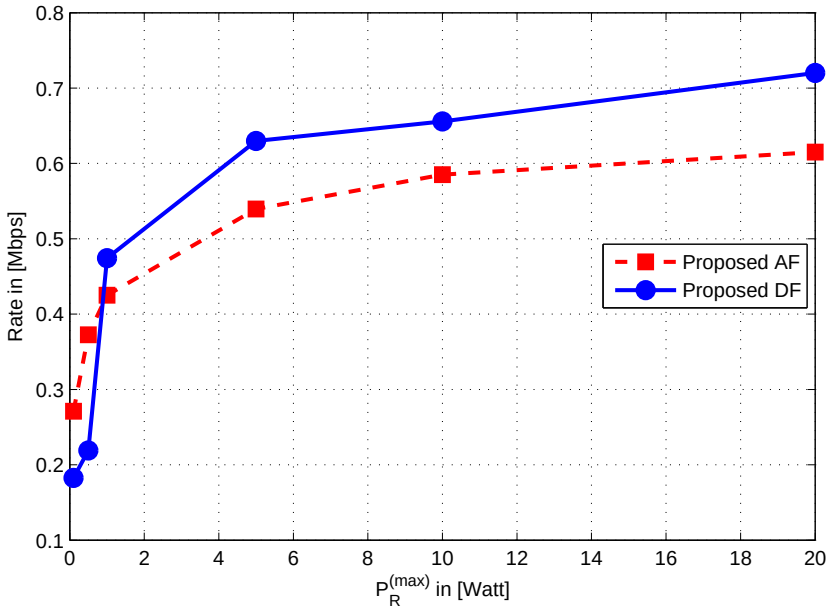

Figure 8.6 The Sum Rate of **Algorithm 8.1** / **Algorithm 8.2** as a Function of the Relay Maximum Transmit Power.

$\frac{P_S^c|H_{SR}|^2 P_R^c|H_{RD}|^2}{\sigma^2(\sigma^2+P_S^c|H_{SR}|^2+P_R^c|H_{RD}|^2)}$]. The average subcarrier source and relay power profiles are defined as $P_S^c = \frac{P_i^{max}}{N}$, and $P_R^c = \frac{P_R^{max}}{N}$, respectively. The channel gains $H_{SR}^{(i)}(j)$, $H_{RD}^{(i)}(j)$ and $H_{SD}^{(i)}(j)$, for $i = 1,2$ and $j \in \mathcal{J}$ are generated with $H(j) \sim \mathcal{CN}(0, \frac{1}{L(1+d)^n})$ with the following separation distances $d_{S_iR} = 50$m, $d_{RD} = 50$m and $d_{S_iD} = 100$m, for $i = 1,2$ respectively. It is clear that the difference in the sum rate using the high SNR approximation $\Gamma_{AF}^{(i)}(j) \approx \frac{\gamma_{SR}^{(i)}(j)\gamma_{RD}(j)P_S^{(i)}(j)P_R^{(i)}(j)}{\gamma_{SR}^{(i)}(j)P_S^{(i)}(j)+\gamma_{RD}(j)P_R^{(i)}(j)}$ and using the exact SNR, $\Gamma_{AF}^{(i)}(j) = \frac{\gamma_{SR}^{(i)}(j)\gamma_{RD}(j)P_S^{(i)}(j)P_R^{(i)}(j)}{1+\gamma_{SR}^{(i)}(j)P_S^{(i)}(j)+\gamma_{RD}(j)P_R^{(i)}(j)}$ is negligible. The sum rate of the three algorithms is the same for SNR> 0dB.

Figure 8.6 shows the sum rate using **Algorithm 8.1** / **Algorithm 8.2** as a function of the relay's maximum transmit power for fixed sources maximum transmit power for AF/DF-OFDMA with $I = 2$ users and $N = 64$ subcarriers. As the relay's maximum transmit power $P_R^{\max}$ increases, the achievable data rate increases. In addition, by increasing $P_R^{\max}$ for AF/DF-OFDMA scenario we could identify three regions based on the maximum relaying power. In the first-region where $P_R^{\max}$ is small, there is no-relaying and the subcarriers are assigned to the users based on descent ordering of $\log_2\left(\frac{\gamma_{SD}^{(1)}(j)}{\gamma_{SD}^{(2)}(j)}\right)$. In the second-region when $P_R^{\max}$ is less than some threshold

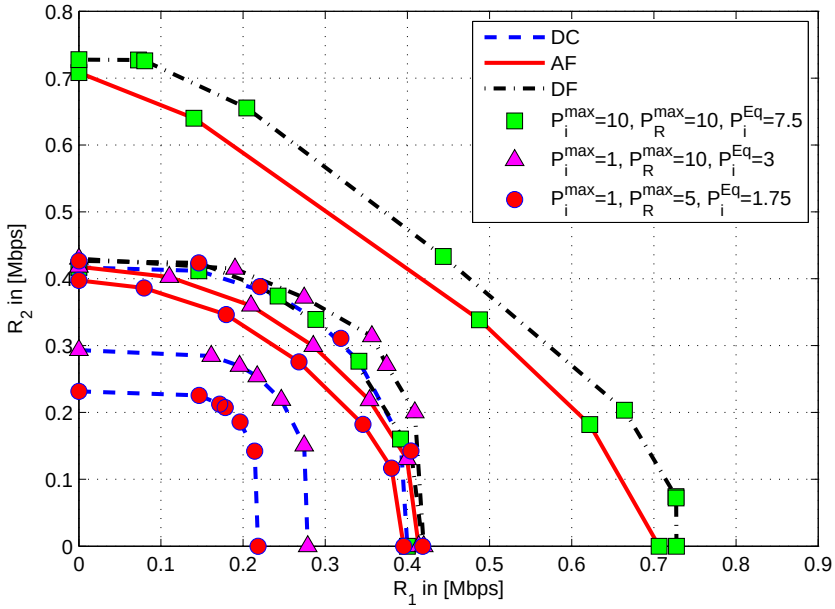

Figure 8.7 Rate Region.

value P_{th}, part of the subcarriers are assigned based on descent ordering of $\log_2\left(\frac{(\gamma_{SD}^{(1)}(j)+0.25\gamma_{SR}^{(1)}(j))}{(\gamma_{SD}^{(2)}(j)+0.25\gamma_{SR}^{(2)}(j))}\right)$ for AF-OFDMA and $\log_2\left(\frac{\gamma_{SR}^{(1)}(j)}{\gamma_{SR}^{(2)}(j)}\right)$ for DF-OFDMA, and the other part of the subcarriers are assigned based on descent ordering of $\log_2\left(\frac{\gamma_{SD}^{(1)}(j)}{\gamma_{SD}^{(2)}(j)}\right)$. In the third-region where is $P_R^{\max} > P_{th}$, the subcarriers are assigned based on descent ordering of $\log_2\left(\frac{(\gamma_{SD}^{(1)}(j)+0.25\gamma_{SR}^{(1)}(j))}{(\gamma_{SD}^{(2)}(j)+0.25\gamma_{SR}^{(2)}(j))}\right)$ for AF-OFDMA and $\log_2\left(\frac{\gamma_{SR}^{(1)}(j)}{\gamma_{SR}^{(2)}(j)}\right)$ for DF-OFDMA.

Figure 8.7 compares the achievable rate region of AF/DF-OFDMA scenarios with the achievable rate region of OFDMA without relaying for $N = 64$ subcarriers for $I = 2$ users using **Algorithm 8.1** / **Algorithm 8.2**. Both curves are obtained by varying α_1 from 0 to 1, and setting $\alpha_2 = 1 - \alpha_1$. The source and relay powers are set $P_i^{\max} = 1$ and 10Watt, $P_R^{\max} = 1, 5$ and 10Watt, respectively. For OFDMA without relaying scenario the source power is set to obtain an overall equivalent average power computed as $P_i^{Eq} = \frac{2P_i^{\max}+P_R^{\max}}{4}$. The corresponding equivalent average power constraints are $P_i^{Eq} = 1.75$, 3, and 7.5Watt. Clearly, AF/DF-OFDMA cooperative communication expands the achievable rate region beyond that of the achievable rate region for OFDMA under the equivalent average power constraint.

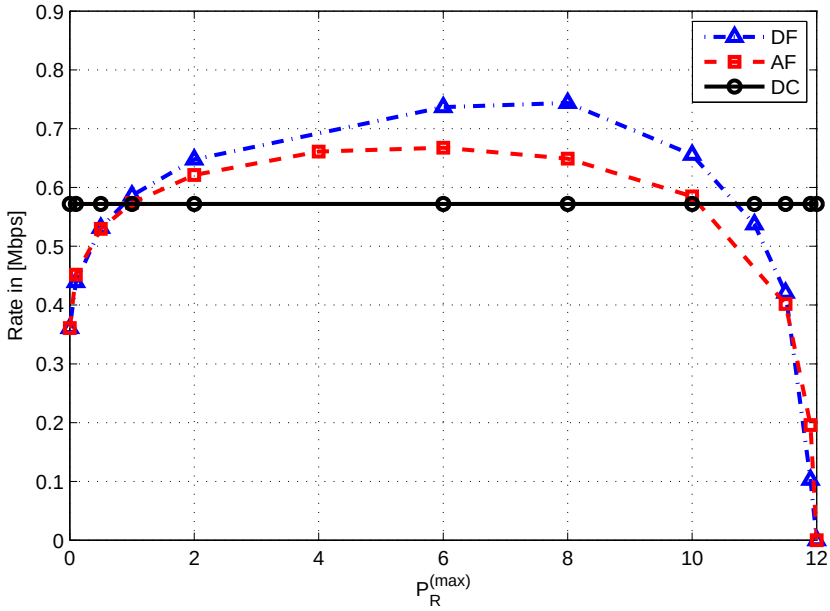

Figure 8.8 The Sum Rate as a Function of the Relay Maximum Transmit Power for P_i^{Eq} = 3Watt.

The sum rate for AF/DF-OFDMA scenarios using **Algorithm 8.1** / **Algorithm 8.2** as a function of the maximum relay power $P_R^{\max}$ with a fixed average power constraint P_i^{Eq} = 3Watt are shown in **Figure 8.8**. AF/DF-OFDMA cooperative communications are beneficial only for certain ranges of $P_R^{\max}$ and $P_i^{\max}$ for a fixed average power constraint, e.g., $1 < P_R^{\max} < 10$ for AF-OFDMA, and $1 < P_R^{\max} < 11$ for DF-OFDM, since as shown in (8.14) and (8.32) the relation between the optimal source and relay power profile is $P_R^{(i)}(j) = C_j^{(i)} P_S^{(i)}(j)$ with $P_S^{(i)}(j)$ is in the form of a water-filling profile or a modified-water-filling profile. Hence, decreasing $P_i^{\max}$ affects the water level, which consequently affects the optimal relaying power profile. Therefore, for a fixed average power constraint, there is an optimal power division between the source and relay nodes.

Problem (8.7) for $I = 3$ users, and $N = 16$ subcarriers is studied for three cases. In case 1, the integer variables $\Upsilon_j^{(i)} \in [0,1]$, $\forall i \in \mathcal{I}$, $\forall j \in \mathcal{J}$ are relaxed. The problem is solved then using convex optimization (interior point) method. In case 2, the problem is relaxed and constraints on the subcarriers that are assigned to S_1 are added. $m \in \{0,1,2,\cdots,16\}$ means only

Table 8.1 Sum Data Rate for AF-OFDMA for $I = 3$ Users and $N = 16$ Subcarriers.

	Added Constraints on the Subcarrier Assignment of S_1						
	$m = 0$	$m = 1$	$m = 2$	$m = 3$	$m = 4$	$m = 5$	$m > 5$
Sum Rate in [*kbps*]	202.35	205.33	207.63	209.29	211.36	209.86	< 209.44
Comments	May Exist Some Subcarriers that are Shared Between Users S_2&S_3.						
	Problem (8.7)				**Algorithm 8.1**		
Sum Rate in [*kbps*]	212.92				211.36		
Comments	Shared Subcarriers.				No Sharing.		

the first mth subcarriers of the ordered set $\boldsymbol{O}_1$ are assigned to S_1. The subcarriers in $\boldsymbol{O}_1$ are ordered based on $\log_2\left(\frac{(\gamma_{SD}^{(1)}(j)+0.25\gamma_{SR}^{(1)}(j))^2}{(\gamma_{SD}^{(2)}(j)+0.25\gamma_{SR}^{(2)}(j))(\gamma_{SD}^{(3)}(j)+0.25\gamma_{SR}^{(3)}(j))}\right)$ in descent order, where $m = 0$ means no subcarrier is assigned to S_1. Problem (8.7) with the added constraints is solved using the interior point method. In case 3, **Algorithm 8.1** is used to obtain the subcarrier assignment profile and the power profiles at the source and relay nodes. The results for the three cases are shown in **Table 8.1**. The difference in the sum rate between case 1 and case 3 is due to the sharing of some subcarriers in case 1. For case 2, the sum rate increases by adding subcarriers $m = 0, 1, \cdots, 4$ from the ordered set $\boldsymbol{O}_1$ to the assignment of user S_1, until reaching the optimal assignment $m = 4$. Adding more subcarriers $m > 4$ from the ordered set $\boldsymbol{O}_1$ decreases the sum rate, which coincides with the trends and the assignment of **Algorithm 8.1**.

The computational complexity of **Algorithm 8.3** for AF-OFDMA for the optimal subcarrier allocation is compared to the computational complexity of the optimal subcarrier allocation of **Algorithm 8.1**, for a different number of users I with $P_i^{\max} = 1$, $P_R^{\max} = 10$, and $N = 64$ subcarriers. The number of computations are shown in **Table 8.2**. Computational complexity means here the number of times required to solve the optimal power profiles at the source and relay nodes for a given subcarrier assignment profile. Clearly,

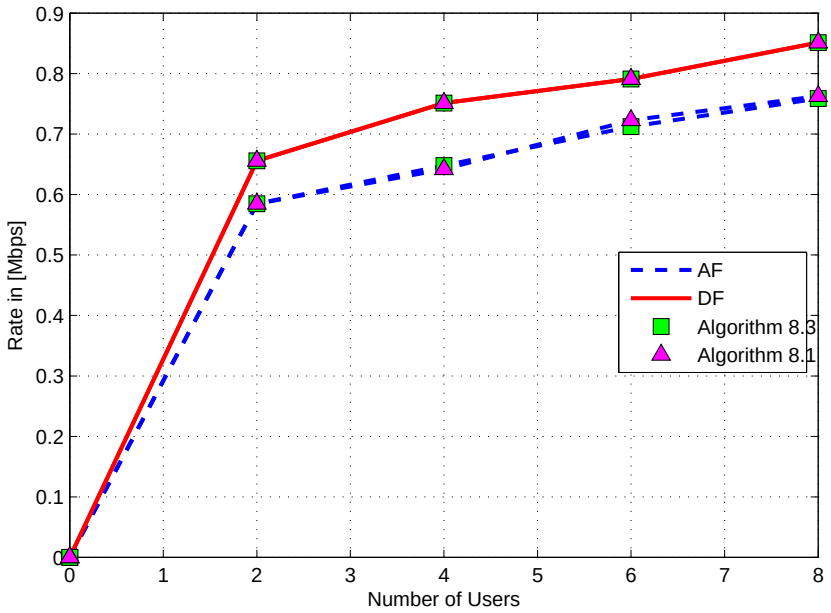

Figure 8.9 The Sum Rate as a Function of the Number of Users for the Proposed Algorithms

Table 8.2 Computational Complexity.

	Number of Users I			
	2	4	6	8
Algorithm 8.1	64	4225	8385	12545
Algorithm 8.3	7	10	24	25

the computational complexity of **Algorithm 8.3** is $O(N)$ compared to $O(N^{I-1})$ for **Algorithm 8.1**.

The sum rate using **Algorithm 8.1** and **Algorithm 8.3** for AF/DF-OFDMA cooperative schemes is shown in **Figure 8.9**. It was noted that **Algorithm 8.1** may require a tuning stage to adjust some of the subcarriers, especially if the number of users is large. In this tuning stage, the boundary between any two users $i,k \in \mathcal{I}$, $i \neq k$ can be adjusted by transferring subcarrier $j^* = \arg\min_{j\in\mathcal{J}_i} \log_2\left(\frac{(\gamma_{SD}^{(i)}(j)+0.25\gamma_{SR}^{(i)}(j))^{\alpha_i}}{(\gamma_{SD}^{(k)}(j)+0.25\gamma_{SR}^{(k)}(j))^{\alpha_k}}\right)$ for AF-OFDMA scheme, and for DF-OFDMA scheme as $j^* = \arg\min_{j\in\mathcal{J}_i} \log_2\left(\frac{(\gamma_{SR}^{(i)}(j))^{\alpha_i}}{(\gamma_{SR}^{(k)}(j))^{\alpha_k}}\right)$ to the assignment of user k as $\mathcal{J}_k = \mathcal{J}_k \cup j^*$ if the weighted sum rate increases.

Figure 8.10 compares the sum rate using **Algorithm 8.3** for AF/DF-OFDMA

scenarios as a function of the number of users with $P_R^{\max} = 10$Watt, $P_i^{\max} = 1$Watt and $N = 64$ subcarriers with the achievable sum rate obtained by solving the dual problem based on the assumption of zero duality gap as in [30]. The dual approach transforms the problem into I distinct single-user problems, and each per user problem can be separated into N subcarrier problems, as explained in Appendix B.2. Clearly, the proposed algorithm asymptotically achieves the sum rate of the dual approach, with less computational complexity, since solving the dual problem requires a large number of iterations to find the correct Lagrange multipliers. In general, the computational complexity of the subgradient method is not known [48]. We use the subgradient method to solve the dual problem with a diminishing step size policy as $\epsilon = \frac{0.01}{\sqrt{t}}$, about $100,000$ λ-evaluations are required. We notice that as the number of subcarriers or users increases, the number of evaluations required to find the optimal Lagrange multipliers increases. In addition, we use the elliptical method to solve the dual problem, but the difficulty lies in finding the initial ellipsoid. Besides using the dual approach at each iteration, we need to assign each subcarrier to the user who achieves the maximum rate on that subcarrier before updating the Lagrange multipliers, as shown in Appendix (B.6).

An alternative approach can be followed to assign the subcarriers for I users AF/DF-OFDMA scenarios aiming to maximize the weighted sum rate based on an iterative subcarrier exchange between a pair of users. At the first step, the subcarriers are assigned randomly to the users, then each user achievable data rate is calculated. A pair-assignment problem is then formulated to find the pairs of users that maximize the weighted sum rate. Each pair of users will perform subcarrier exchange based on (8.25)/(8.38) for $I = 2$; the two users pool their initial assigned subcarriers and relaying power, then this group of subcarriers are exchanged between the two users to maximize the weighted sum rate based on **Algorithm 8.1** / **Algorithm 8.2**

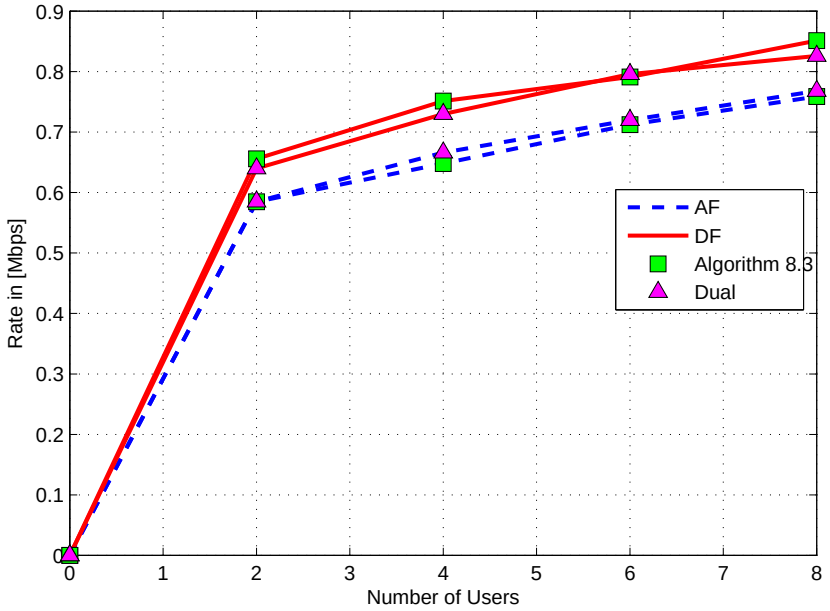

Figure 8.10 The Sum Rate as a Function of the Number of Users for the proposed and the Dual-Based Algorithms

for the special case of two users. The cost function for the assignment problem is calculated as $b_{n,m} = \max\{(\alpha_n \hat{R}_n + \alpha_m \hat{R}_m) - (\alpha_n R_n + \alpha_m R_m), 0\}$, where $\hat{R}_i$, and R_i for $i \in n, m$ are the user data rate after and before the subcarrier exchange.

The pair assignment problem can be formulated as:

$$\max_{X} \sum_{n=1}^{I} \sum_{n=1}^{I} X_{nm} b_{nm}, \tag{8.40a}$$

$$\text{s.t.} \sum_{n=1}^{I} X_{nm} = 1, \; m = 1, \cdots, I, \tag{8.40b}$$

$$\sum_{m=1}^{I} X_{nm} = 1, \; n = 1, \cdots, I, \tag{8.40c}$$

$$X_{nm} \in \{0, 1\}, \; \forall n, m, \tag{8.40d}$$

where $\boldsymbol{X}$ is a matrix of the assignment profile with $[\boldsymbol{X}]_{n,m} = X_{nm}$ and $X_{nm} = 1$ if user n is paired with user m. Problem (8.40) can be solved using the Hungarian method as in [50]. The procedure is repeated until no further improvement can be achieved in the weighted sum rate. We notice that, the

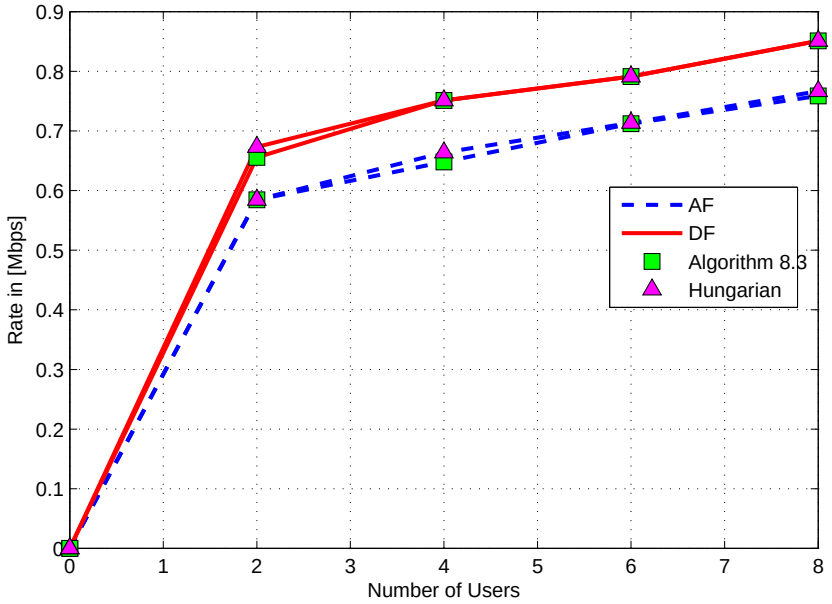

Figure 8.11 The Sum Rate as a Function of the Number of Users for the Proposed and the Hungarian Based Algorithms.

performance of the algorithm depends on the initial subcarrier assignment in contrast to the proposed algorithms. Each step, requires finding the cost matrix and applying the Hungarian method, which entails $\mathcal{O}(I^3)$ computations. The cost matrix is a symmetric zero diagonal matrix. Each entry (from the $\frac{I^2}{2} - I$ entries) requires applying the two users subcarrier assignment algorithm. We notice that the algorithm converges in less than 8 iterations, but the algorithm may fall into a local minimum. To have a fair comparison with **Algorithm 8.3**, we apply the iterative pairs based algorithm with an initial assignment obtained from the basic phase of the simplified algorithm as in **Algorithm 8.3**. We notice that the algorithm converges in less than three iterations. **Figure 8.11** shows the sum rate for AF/DF-OFDMA scenarios based on iterative subcarrier exchange between a pair of users as a function of the number of users for $P_R^{\max} = 10$Watt, $P_i^{\max} = 1$Watt and $N = 64$ subcarriers.

The proposed algorithm can be extended to the case of M-relays assisting the sources in orthogonal fashion as in the scenario described in [86]. The subcarriers for AF-OFDMA for the two users case will be ordered based on

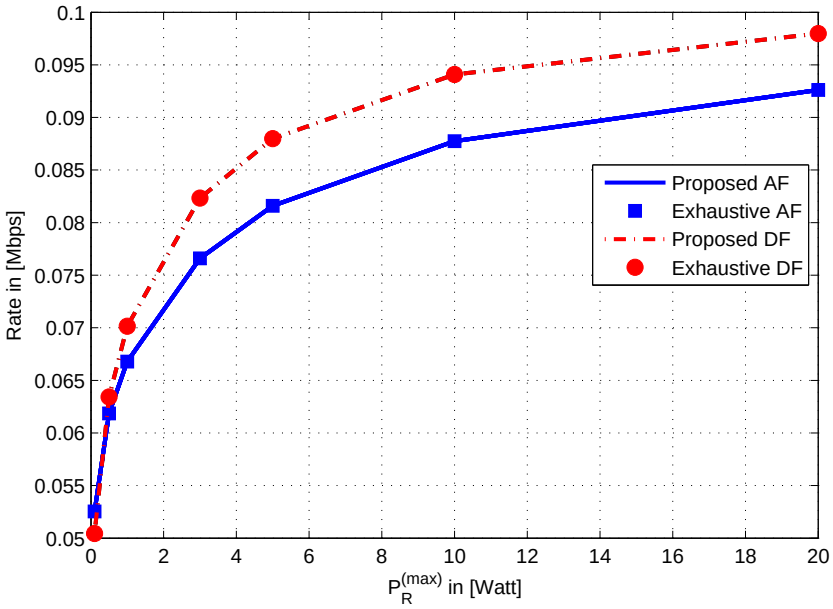

Figure 8.12 The Sum Rate as a Function of $P_R^{\max}$ for Two Relays Two Sources Scenario.

$\log_2\left(\frac{\gamma_{SD}^{(1)}(j)+\sum_{m=1}^{M}0.25\gamma_{SR_m}^{(1)}(j)}{\gamma_{SD}^{(2)}(j)+\sum_{m=1}^{M}0.25\gamma_{SR_m}^{(2)}(j)}\right)$, and the subcarriers for DF-OFDMA for two users case will be ordered based on $\log_2\left(\frac{\sum_{m=1}^{M}\gamma_{SR_m}^{(1)}(j)-(M-1)\gamma_{SD}^{(1)}(j)}{\sum_{m=1}^{M}\gamma_{SR_m}^{(2)}(j)-(M-1)\gamma_{SD}^{(2)}(j)}\right)$ to maximize the sum rate. **Figure 8.12** compares the sum rate of AF/DF-OFDMA of the proposed algorithm with the sum rate of AF/DF-OFDMA using the exhaustive search algorithm for the case of two-relays assisting two sources in an orthogonal fashion for $N = 8$ subcarriers. The sum rate of the proposed algorithm for AF/DF-OFDMA coincides with the sum rate of the exhaustive search.

8.5 Conclusions

In this chapter, we investigate joint resource allocation for multiple users single relay AF/DF-OFDMA cooperative communication systems, in the presence of a direct link between the source and destination nodes. The objective is to maximize the weighted sum rate. The subcarrier assignment is a combinatorial problem that can be solved by means of an exhaustive search to get the optimal subcarrier assignment, and the sources and relay power profiles. In this sense, we propose suboptimal low complexity algorithms

for subcarrier assignment, and develop analytical expressions for both the source and relay power profiles. The proposed algorithms are based on high SNR approximation. The sum rate of the proposed algorithms for $I = 2, 3$ users coincides with the sum rate of the exhaustive search algorithm. The sum rate of the proposed algorithms are asymptotically similar to the sum data rate using the dual approach, without the need to solve the dual problem iteratively. In addition, using the dual approach at each iteration requires the determination of the user who achieves the maximum data rate in that subcarrier before updating the Lagrange multipliers.

CHAPTER9

AUCTION FRAMEWORK FOR RESOURCE ALLOCATION IN AF-OFDMA RELAY NETWORKS

In this chapter, competition based resource allocation is proposed to allocate the subcarriers in AF-OFDMA system based on optimal power profiles at the source and relay nodes. Two auction algorithms are developed. The first algorithm is based on sequential single item auction, where each user submits a bid based on either the marginal increase or the relative marginal increase of the data rate, after using that subcarrier. The first bidding strategy aims to maximize the sum data rate, whereas the second bidding strategy aims to maximize the fairness index. In both cases, the subcarrier is assigned to the user who submits the highest bid. The algorithm proceeds in a sequential fashion until all subcarriers are assigned. Both bidding strategies require synchronized interactions between the base-station and the users for each subcarrier. To reduce the interactions between the base-station and the users, we propose a one-shot auction algorithm, where each user submits bids for all subcarriers at once based on the Shapley value, a well-known cooperative-game theoretic concept. The user evaluates each subcarrier based on an estimate of the Shapley value. The subcarriers are then allocated based on the submitted bids using an iterative algorithm that maximizes the fairness index.

The ntroduction and related research are presented in Section 9.1. In

Section 9.2, the AF-OFDMA single relay cooperative communication system model, the formulation of the optimization problems and the proposed resource allocation algorithms are presented. The proposed algorithms are extended to multiple relays scenario, as explained in Section 9.3. The performance measures are defined in Section 9.4. Numerical results are presented and discussed in Section 9.5. Finally, conclusions are drawn in Section 9.6.

9.1 Introduction

In Chapter 8, joint resource allocation for AF-OFDMA is considered based on a centralized approach, where an optimization problem is formulated and a low complexity algorithm is proposed to assign the subcarriers and allocate the power profiles at the source and relay nodes. In this chapter, user competition is utilized to devise distributed algorithms to allocate the subcarriers based on auction theory.

Recently, auction theory has been considered for resource allocation for wireless communication systems to handle the problem of resource competition among selfish users as in [33, 83, 137, 148, 173]. In [137], the authors proposed a channel allocation algorithm based on the second-price auction mechanism to allow users to compete for a wireless fading channel, but they did not consider multi-carrier systems. In [148], an auction algorithm for sub-channel allocation is proposed, using the difference of the throughput among sub-channels to allow users to compete through bidding. In [83], the authors proposed an auction-based scheduling algorithm for OFDMA communication system, to achieve proportional fair resource allocation. In [33], an auction algorithm is proposed for the subcarrier allocation to balance efficiency and fairness with service differentiation in AF-OFDMA relay networks. The bidding strategy considers the users' minimum rate requirements and their different willingness to pay for heterogeneous services. Using an auction framework for resource allocation for

wireless communications is reviewed in [173]. Optimal power allocation at the source and relay nodes was not considered in determining the bidding strategy in [33, 83, 148].

In this chapter, subcarrier assignment algorithms are developed based on either sequential or one-shot auctions. For sequential-auction based algorithms, at each step the user evaluates the worth of the subcarrier as either the difference or the relative difference between the achievable data rate before and after using the subcarrier with optimal power allocation at the source and relay nodes. This evaluation is used as the bidding strategy, and sequentially one subcarrier is assigned to the user with the highest bid. The base-station collects the bids from all users at each iteration for a given subcarrier and then assigns it to the user with the highest bid and informs her before proceeding to the next iteration (subcarrier assignment step). This, however, requires a lot of synchronized interactions between the base-station and the users. To proceed, the user needs to know if the subcarrier is assigned to her or not to determine the bid for the next subcarrier. As a result, we propose the one-shot auction algorithm, where the user evaluates the worth of all subcarriers based on the Shapley value at once. The worth of the subcarrier using the Shapley value represents the average marginal contribution of that subcarrier for all coalitions of subcarriers that can be assigned to the user with optimal power profiles at the source and relay nodes. The Shapley value allows the users to determine the most influential subcarriers and to bid on them, i.e. the Shapley value allows the users to quantify accurately the contribution of each subcarrier towards the full achievable data rate (using all subcarriers). The computational complexity of calculating the Shapley value is avoided by using a sampling method to approximate it with reasonable accuracy.

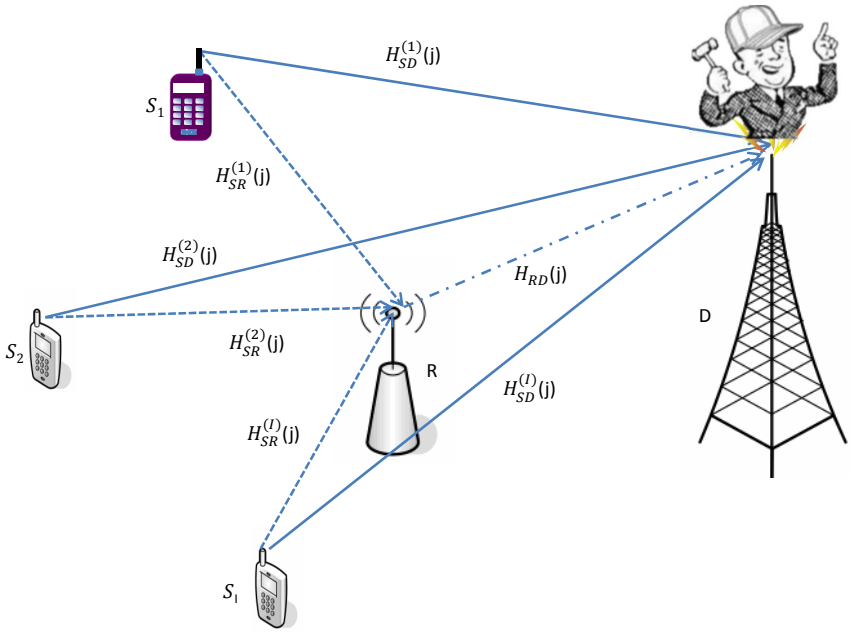

Figure 9.1 System Model.

9.2 Problem Formulation for Single Relay Scenario

The system under consideration is depicted in **Figure 9.1**. Let $\mathcal{I} = \{1, 2, \cdots, I\}$ be the set of active users, sender (source) nodes S_i for $i \in \mathcal{I}$ communicate with a destination terminal D (that is, base-station, or access-point). We consider a single relay two-hop multi-carrier OFDMA system, for multiple relays see Section 9.3. The available bandwidth W is divided into N subcarriers, the bandwidth of each subcarrier is B_N, in which the channel coefficients is assumed to be frequency flat. The set of subcarriers in the system is denoted as $\mathcal{J} = \{1, 2, \cdots, N\}$. The first-hop channel coefficients of the ith user between the source and destination nodes, and the source and relay nodes at the jth subcarrier are denoted by $H_{SD}^{(i)}(j)$, and $H_{SR}^{(i)}(j)$, respectively. The second-hop channel coefficient between the relay and the destination nodes at the jth subcarrier is denoted by $H_{RD}(j)$.

The achievable data rate $R_{AF}^{(i)}(j)$ of user i using subcarrier j at the destination node with the aid of the relay node and after using the MRC technique

is computed using (8.1)-(8.4) as:

$$R_{AF}^{(i)}(j) = \frac{B_N}{2}\log\Big(1 + \frac{\Gamma_{SD}^{(i)}(j) + \Gamma_{AF}^{(i)}(j)}{\Gamma}\Big), \tag{9.1}$$

where $\Gamma_{SD}^{(i)}(j) = \gamma_{SD}^{(i)}(j)P_S^{(i)}(j)$, $\Gamma_{AF}^{(i)}(j) = \frac{\gamma_{SR}^{(i)}(j)\gamma_{RD}(j)P_S^{(i)}(j)P_R^{(i)}(j)}{1+\gamma_{SR}^{(i)}(j)P_S^{(i)}(j)+\gamma_{RD}(j)P_R^{(i)}(j)}$, and $P_S^{(i)}(j)$, and $P_R^{(i)}(j)$ are the ith user transmit power profiles on the jth subcarrier at the source and relay nodes, respectively. In this chapter, we consider the problem of uplink resource allocation for AF-OFDMA wireless access system[1]. During each OFDM symbol, the scheduler at the base station needs to make the following resource allocation decision: how to allocate the subcarriers to the users and the corresponding power profiles at the source and relay nodes to achieve a certain objective (for example, maximum sum data rate, or maximum rate fairness).

The maximum sum rate resource allocation problem can be formulated as:

$$\max_{\boldsymbol{P},\boldsymbol{Y}} \sum_{i\in\mathcal{I}}\sum_{j\in\mathcal{J}} Y_j^{(i)} R_{AF}^{(i)}(j), \tag{9.2a}$$

$$\text{s.t.} \sum_{i\in\mathcal{I}}\sum_{j\in\mathcal{J}} Y_j^{(i)} P_R^{(i)}(j) \le P_R^{\max}, \tag{9.2b}$$

$$\sum_{j\in\mathcal{J}} Y_j^{(i)} P_S^{(i)}(j) \le P_i^{\max}, \forall i \in \mathcal{I}, \tag{9.2c}$$

$$\sum_{i\in\mathcal{I}} Y_j^{(i)} \le 1, \forall j \in \mathcal{J}, \tag{9.2d}$$

$$P_S^{(i)}(j) \ge 0,\ P_R^{(i)}(j) \ge 0, Y_j^{(i)} \in \{0,1\}, \forall j \in \mathcal{J}, \forall i \in \mathcal{I}, \tag{9.2e}$$

where $\boldsymbol{P} = (\boldsymbol{P}_S, \boldsymbol{P}_R)$ is the vector of the source and relay power profiles, with $[\boldsymbol{P}_S]_{i,j} = P_S^{(i)}(j)$ and $[\boldsymbol{P}_R]_{i,j} = P_R^{(i)}(j)$, $\forall i \in \mathcal{I}$ and $\forall j \in \mathcal{J}$. $\boldsymbol{Y}$ is the subcarrier assignment profile with $[\boldsymbol{Y}]_{i,j} = Y_j^{(i)} \in \{0,1\}$, and $Y_j^{(i)} = 1$ indicates that subcarrier j is assigned to user i. Constraint (9.2b) means that the total power allocated to forward the data from all users assisted by the relay is limited

[1]Resource allocation for uplink DF-OFDMA scheme can be treated in a similar fashion.

to $P_R^{\max}$, whereas, constraint (9.2c) indicates that the source power for user i is limited to $P_i^{\max}$. Constraint (9.2d) means that the jth subcarrier can be assigned to maximally one user.

The resource allocation that aims at maximizing the rate fairness[2] using the max-min fairness criteria, can be formulated as:

$$\max_{\boldsymbol{P},\boldsymbol{Y}} R_{min}, \tag{9.3a}$$

$$\text{s.t.} \sum_{j\in\mathcal{J}} Y_j^{(i)} R_{AF}^{(i)}(j) \geq R_{min}, \forall i \in \mathcal{I}, \tag{9.3b}$$

$$\sum_{i\in\mathcal{I}} \sum_{j\in\mathcal{J}} Y_j^{(i)} P_R^{(i)}(j) \leq P_R^{\max}, \tag{9.3c}$$

$$\sum_{j\in\mathcal{J}} Y_j^{(i)} P_S^{(i)}(j) \leq P_i^{\max}, \forall i \in \mathcal{I}, \tag{9.3d}$$

$$\sum_{i\in\mathcal{I}} Y_j^{(i)} \leq 1, \forall j \in \mathcal{J}, \tag{9.3e}$$

$$P_S^{(i)}(j) \geq 0,\ P_R^{(i)}(j) \geq 0, Y_j^{(i)} \in \{0,1\}, \forall j \in \mathcal{J}, \forall i \in \mathcal{I}. \tag{9.3f}$$

Constraint (9.3b) means that the minimum achievable data rate for any user is R_{min} needs to be maximized, and constraints (9.3c)-(9.3f) can be interpreted similar to (9.2b)-(9.2e).

Jain's fairness index can be used to measure the rate fairness of the resource allocation problem, which is defined as:

$$F_I = \frac{(\sum_{i\in\mathcal{I}} R_i)^2}{|\mathcal{I}| \sum_{i\in\mathcal{I}} R_i^2}, \tag{9.4}$$

where $R_i = \sum_{j\in\mathcal{J}} Y_j^{(i)} R_{AF}^{(i)}(j)$ is the achievable data rate of user i, a value of fairness index F_I closer to 1 means a better rate fairness.

Problem (9.2) and (9.3) can be solved using a centralized approach, which has two disadvantages: (1) users are forced to reveal all local information; such as channel gains and power capabilities to the scheduler at the des-

[2]Other rate fairness criterion such as proportional fairness and Nash bargaining fairness can be considered in formulating the optimization problem as in [50].

tination (base-station), which may not be desirable due to overheads and privacy, (2) the centralized scheduler needs to have sophisticated computational capabilities to solve a complicated MINLP problem in a short time[3]. One of the key factors to a successful subcarrier allocation in the forthcoming wireless communication systems is the possibility of a distributed implementation. In this chapter, we use the auction framework to devise distributed solutions to the resource allocation problem which reduces the computation complexity at the scheduler. In addition, an auction framework can capture the users' competition. Users bid for the subcarrier based on its worth; the worth of the subcarrier is not the same for all users, since the channel gains are different. The subcarrier is then assigned to the user with the highest bid. The main point towards a distributed allocation of the resources in an AF-OFDMA system is to construct a utility function that can be used to evaluate the worth of the subcarrier(s) per user. This utility function should depend only on the user's information, such as channel gains, maximum total power, etc. A common value broadcasted from the base-station to the users can also be included in the design of the utility function to disclose information regarding the availability of the relay resources, that is, the maximum transmit relay power. Furthermore, the utility function needs to reflect a physical meaning quantity to the user; for example, the achievable data rate, and the utility function needs to allow the user to utilize all degrees of freedom available to her by allocating optimally the power profiles at the source and relay nodes.

A utility function of the ith user for a given subset of subcarriers $\mathcal{J}_i \subseteq \mathcal{J}$ and a common value λ_R denoted as $U_i(\boldsymbol{P}_i, \lambda_R)$ is designed to include the abovementioned rationales for AF-OFDMA system as:

$$U_i(\boldsymbol{P}_i, \lambda_R) = \sum_{j \in \mathcal{J}_i} R_{AF}^{(i)}(j) - \lambda_R \Big(\sum_{j \in \mathcal{J}_i} P_R^{(i)}(j) \Big), \tag{9.5}$$

[3] **Algorithm 8.1**/ **Algorithm 8.2** and **Algorithm 8.3** proposed in Chapter 8 can be used to solve the problem in a centralized fashion.

where $\boldsymbol{P}_i = (\boldsymbol{P}_S^i, \boldsymbol{P}_R^i)$ is the vector of the source and relay power profiles for user i, with $[\boldsymbol{P}_S^i]_j = P_S^{(i)}(j)$ and $[\boldsymbol{P}_R^i]_j = P_R^{(i)}(j)$, $\forall j \in \mathcal{J}_i$. The first summation in (9.5) represents the achievable data rate using the set of subcarriers $\mathcal{J}_i$, whereas the second summation limits the requests for excess relay power demands. Note that: the utility function $U_i(\boldsymbol{P}_i, \lambda_R)$ depends only on users i channel gains and does not depend on other users channel gains, since the worth of the subcarrier to the user depends only on her own channel gains and the allocated power profiles. The relay-destination channel gain $H_{RD}(j)$, $\forall j \in \mathcal{J}$ and λ_R are common information broadcasted from the base-station (or relay) node to all users. λ_R is used as a control parameter for the relaying power profiles, since the relay node has a limited power. We expect a higher value of λ_R if the number of users is large, or the available $P_R^{(\max)}$ is small. Updating λ_R by the base-station or relay node is explained in detail in Section 9.4.

The data rate $R_{AF}^{(i)}(j)$ given in (9.1) is not jointly concave function in $P_S^{(i)}(j)$ and $P_R^{(i)}(j)$, as can be proved by the second-order derivative test. To make the analysis more tractable, we use the approximation $\Gamma_{AF}^{(i)}(j) \approx \frac{\gamma_{SR}^{(i)}(j)\gamma_{RD}(j)P_S^{(i)}(j)P_R^{(i)}(j)}{\gamma_{SR}^{(i)}(j)P_S^{(i)}(j)+\gamma_{RD}(j)P_R^{(i)}(j)}$, which is tight for high SNR. This approximation has been used commonly in literature [30, 56, 139]. Using this approximation, the data rate is jointly concave in $P_S^{(i)}(j)$ and $P_R^{(i)}(j)$ as can be proved by the second-order derivative test. Henceforth, we will use this approximation value for computing $R_{AF}^{(i)}(j)$.

For a given $\lambda_R > 0$ and $\mathcal{J}_i$, user i aims to maximize her utility function $U_i(\boldsymbol{P}_i, \lambda_R)$ by allocating the power profiles at the source and relay nodes by

solving:

$$\max_{\boldsymbol{P}_i} U_i(\boldsymbol{P}_i, \lambda_R), \tag{9.6a}$$

$$\text{s.t.} \sum_{j\in\mathcal{J}_i} P_S^{(i)}(j) \le P_i^{\max}, \tag{9.6b}$$

$$P_S^{(i)}(j) \ge 0,\ P_R^{(i)}(j) \ge 0, \forall j \in \mathcal{J}_i. \tag{9.6c}$$

Problem (9.6) is now convex optimization problem which can be solved analytically by relaxing the source power constraint (9.6b) and formulating the Lagrangian function as:

$$L_i(\boldsymbol{P}_i, \lambda_R, \lambda_i) = U_i(\boldsymbol{P}_i, \lambda_R) - \lambda_i\Big(\sum_{j\in\mathcal{J}_i} P_S^{(i)}(j) - P_i^{\max}\Big). \tag{9.7}$$

Differentiating (9.7) with respect to $P_S^{(i)}(j)$ and equating to zero results in:

$$\frac{\Gamma + \Gamma_{SD}^{(i)}(j) + \Gamma_{AF}^{(i)}(j)}{B_N/(2\ln(2))} = \frac{1}{\lambda_i}(\gamma_{SD}^{(i)}(j) + \frac{\gamma_{SR}^{(i)}(j)\gamma_{RD}^2(j)P_R^{(i)2}(j)}{(\gamma_{SR}^{(i)}(j)P_S^{(i)}(j) + \gamma_{RD}(j)P_R^{(i)}(j))^2}). \tag{9.8}$$

Similarly, differentiating (9.7) with respect to $P_R^{(i)}(j)$ and equating to zero results in:

$$\Gamma + \frac{\Gamma_{SD}^{(i)}(j) + \Gamma_{AF}^{(i)}(j)}{B_N/(2\ln(2))} = \frac{\gamma_{RD}(j)\gamma_{SR}^{(i)2}(j)P_S^{(i)2}(j)}{\Gamma\lambda_R(\gamma_{SR}^{(i)}(j)P_S^{(i)}(j) + \gamma_{RD}(j)P_R^{(i)}(j))^2}. \tag{9.9}$$

Simultaneously solving (9.8) and (9.9), optimal source power profile for $j \in \mathcal{J}_i$ can be obtained as:

$$P_S^{(i)}(j) = \begin{cases} \frac{\left(K_i(\gamma_{SD}^{(i)}(j)+A_j^{(i)})-\Gamma\right)^+}{\gamma_{SD}^{(i)}(j)+B_j^{(i)}} & \text{if } P_R^{(i)}(j) > 0, \\ \left(K_i - \frac{\Gamma}{\gamma_{SD}^{(i)}(j)}\right)^+ & \text{if } P_R^{(i)}(j) = 0, \end{cases} \tag{9.10}$$

where $A_j^{(i)} = \frac{\gamma_{SR}^{(i)}(j)\gamma_{RD}^2(j)C_j^{(i)2}}{(\gamma_{SR}^{(i)}(j)+\gamma_{RD}(j)C_j^{(i)})^2}$, $B_j^{(i)} = \frac{\gamma_{SR}^{(i)}(j)\gamma_{RD}(j)C_j^{(i)}}{\gamma_{SR}^{(i)}(j)+\gamma_{RD}(j)C_j^{(i)}}$, $K_i = \frac{B_N}{2\lambda_i\ln(2))}$, and $C_j^{(i)}$ is com-

puted as:

$$C_j^{(i)} = \frac{\gamma_{SR}^{(i)}(j)\Big(-1+\sqrt{1+(1+\frac{\gamma_{SR}^{(i)}(j)}{\gamma_{SD}^{(i)}(j)})(\frac{\lambda_i}{\lambda_R}\frac{\gamma_{RD}(j)}{\gamma_{SD}^{(i)}(j)}-1)}\Big)^+}{\gamma_{RD}(j)\Big(1+\frac{\gamma_{SR}^{(i)}(j)}{\gamma_{SD}^{(i)}(j)}\Big)}, \tag{9.11}$$

with the per user Lagrangian multiplier λ_i is selected to satisfy the source power constraint $\sum_{j\in\mathcal{J}_i} P_S^{(i)}(j) = P_i^{\max}$. The user i optimal relay power profile for $j \in \mathcal{J}_i$ can be obtained as:

$$P_R^{(i)}(j) = C_j^{(i)} P_S^{(i)}(j). \tag{9.12}$$

The achievable data rate for user i for a given $\lambda_R > 0$ and $\mathcal{J}_i \neq \varnothing$ denoted as $v_i(\mathcal{J}_i, \lambda_R)$, is computed using (9.10) and (9.12) as:

$$v_i(\mathcal{J}_i, \lambda_R) = \sum_{j\in\mathcal{J}_i} R_{AF}^{(i)*}(j). \tag{9.13}$$

The overall system throughput can be computed as $\sum_{i\in\mathcal{I}} v_i(\mathcal{J}_i, \lambda_R)$, with $\cup_{i\in\mathcal{I}}\mathcal{J}_i = \mathcal{J}$ and $\mathcal{J}_{\hat{i}} \cap \mathcal{J}_i = \varnothing$ for $\hat{i} \neq i$, $\forall i, \hat{i} \in \mathcal{I}$.

In order to select the per user subcarrier assignment profile $\mathcal{J}_i$, the competition and the intelligent of the users can be exploited using the proposed utility function and the auction framework. In this regard, we propose two auction based subcarrier assignment algorithms: a sequential based subcarrier assignment, and a one-shot subcarrier assignment.

9.2.1 Sequential Subcarrier Assignment

In sequential assignment, the subcarriers are assigned in a sequential fashion based on the bids submitted by the users. At each step, the user submits a bid for the current subcarrier, that depends on the previous allocations; the user needs to know her allocated subcarriers before bidding on the next subcarriers. The bid of the current subcarrier equals the worth of that sub-

carrier to the user. Bidding strategies based on higher or lower than the worth of the subcarrier is out of the scope of this work and a topic of future work. The worth of subcarrier j for user i is constructed based on the objective of the resource allocation problem. If the objective is to maximize the overall system throughput (sum data rate), the worth of subcarrier j for user i is based on the marginal contribution of subcarrier j denoted as $M_c^{(i)}(j, \lambda_R)$. It is computed as $M_c^{(i)}(j, \lambda_R) = v_i(\mathcal{J}_i \cup j, \lambda_R) - v_i(\mathcal{J}_i, \lambda_R)$, with $j \cap \mathcal{J}_i = \varnothing$, and $v_i(\cdot, \cdot)$ is computed as in (9.13) based on maximizing the ith user utility function (9.6) with optimal source and relay power profiles. It can be proven that the bidding strategy based on the marginal contribution of the data rate using the subcarrier for the sequential auction, maximizes the system throughput. Adding the sum data rate of the previous allocation to each user current bid and allocating the subcarrier to the user with the highest bid, results in maximizing the new sum data rate. Hence, the the sum data rate is maximized at each step.

On the other hand, if the objective is to maximize the fairness index, the worth of subcarrier j for user i is based on the relative increase of the data rate (relative marginal contribution) using subcarrier j which is computed as $\frac{M_c^{(i)}(j,\lambda_R)}{v_i(\mathcal{J}_i \cup j, \lambda_R)}$. The user submits a bid equal to the worth of the subcarrier, and the subcarrier is allocated to the user with the highest bid. Clearly, this bidding strategy achieves a proportional fair rate allocation, as was proven in [22].

Algorithm 9.1, illustrates the sequential subcarrier assignment auction. In this algorithm, the objective (obj) of the resource allocation problem can be selected either as $obj = s$ or $obj = f$ to maximize either the sum data rate or the fairness index, respectively. The base-station or the relay announces the relay destination channel gain $H_{RD}(j)$, $\forall j \in \mathcal{J}$ and the common value λ_R, which allows the user to compute the optimal power profiles at the source and relay nodes as in (9.10) and (9.12). The rule of the common value λ_R is

Algorithm 9.1 AF-OFDMA Sequential Subcarrier Assignment Auction.

Require: $\gamma_{SD}^{(i)}(j)$, $\gamma_{SR}^{(i)}(j)$, $\gamma_{RD}(j)$, $P_i^{\max}$, $\forall j \in \mathcal{J}, \forall i \in \mathcal{I}$, λ_R, and the objective $obj \in \{f, s\}$.

$\mathcal{J}_i \leftarrow \varnothing$, and $v_i(\mathcal{J}_i, \lambda_R) \leftarrow 0$, $\forall i \in \mathcal{I}$.
for $l = 1 : N$ **do**
  Calculate $M_c^{(i)}(l, \lambda_R) = v_i(\mathcal{J}_i \cup l, \lambda_R) - v_i(\mathcal{J}_i, \lambda_R)$, $\forall i \in \mathcal{I}$.
  if $obj = s$ **then**
    $b_{obj}^{(i)}(l) \leftarrow M_c^{(i)}(l, \lambda_R)$, $\forall i \in \mathcal{I}$.
  else
    $b_{obj}^{(i)}(l) \leftarrow \frac{M_c^{(i)}(l,\lambda_R)}{v_i(\mathcal{J}_i \cup l, \lambda_R)}$, $\forall i \in \mathcal{I}$.
  end if
  Find $i^* = \arg \max_i b_{obj}^{(i)}(l)$.
  $\mathcal{J}_{i^*} \leftarrow \mathcal{J}_{i^*} \cup l$.
end for
return $\mathcal{J}_i$, $\forall i \in \mathcal{I}$.

discussed in Section 9.4.

Initially, all subcarriers are not assigned to any user, i.e. $\mathcal{J}_i = \varnothing$, and the corresponding achievable data rate is set to $v_i(\mathcal{J}_i, \lambda_R) = 0$, $\forall i \in \mathcal{I}$. At the lth stage for $l = 1, \cdots, N$, each user $i \in \mathcal{I}$ determines the worth of subcarrier l based on the objective function $obj \in \{f, s\}$ and the previously allocated subcarriers $\mathcal{J}_i$ and submits its bid $b_{obj}^{(i)}(l)$, which is computed either as $b_s^{(i)}(l) = v_i(\mathcal{J}_i \cup l, \lambda_R) - v_i(\mathcal{J}_i, \lambda_R)$, or $b_f^{(i)}(l) = \frac{v_i(\mathcal{J}_i \cup l, \lambda_R) - v_i(\mathcal{J}_i, \lambda_R)}{v_i(\mathcal{J}_i \cup l, \lambda_R)}$. The winner user i^* of subcarrier l is determined as: $i^* = \arg \max_i b_{obj}^{(i)}(l)$ and the set $\mathcal{J}_{i^*}$ is updated as $\mathcal{J}_{i^*} = \mathcal{J}_{i^*} \cup l$. The algorithm proceeds iteratively until all subcarriers are allocated.

9.2.2 One-Shot Subcarrier Assignment

Sequential auction requires synchronized interactions between the users and the scheduler at the base-station. The user needs to know the subcarriers allocated to her before bidding for the current subcarrier and the scheduler needs to receive the bids for the current subcarrier from all users in the same time window to allocate the subcarrier properly. To reduce these interactions, a one-shot multiple-item auction can be used, in which each user

submits bids for all subcarriers at once. To evaluate the worth of the subcarrier for each user in a one-shot auction, it is important to be aware of the following: (1) The worth of the subcarrier depends on all possible subsets that contain the subcarrier with optimal power profiles at the source and relay nodes. Evaluating the worth of the subcarrier based on its achievable rate assuming that $\mathcal{J}_i = \mathcal{J}$ and using optimal power profiles at the source and relay nodes will not reveal the actual valuation, (2) bidding based on the channel gains without optimal power profiles at the source and relay nodes, disregards one degree of freedom that can be utilized. In addition, it is difficult to find a function to order the subcarriers[4] (evaluate the worth) based on the channel gains, since the data rate depends on the source destination, source relay, and relay destination channel gains, and the power profiles at the source and relay nodes[5], (3) the shortage of feedback information to adjust the worth of the subcarrier in contrast to a sequential auction where feedback information (history of the allocated subcarriers) is used to evaluate the worth of the current subcarrier. Towards this end, the Shapley value can be used to evaluate the worth of the subcarriers. The Shapley value of a subcarrier represents the average marginal contribution of that subcarrier using all possible combinations (subsets) of subcarriers that can be assigned to the user with optimal power profiles at the source and relay nodes. Hence, the possibility of gaining a subset of the subcarriers without feedback is captured by the Shapley value and the optimal power profiles at the source and relay nodes. Note that, the average marginal contribution of the subcarrier using the Shapley value encompasses the possibility of gaining more than one subcarrier by taking the average over all possible combinations, whereas the marginal contribution in the sequential auction is with respect to the previous allocation of subcarriers only. Before defining

[4]The ordering functions that are developed in Chapter 8 represent base-station preference not user's preference.

[5]Here, we assume that the worth of subcarrier j for user i is independent of the worth of subcarrier j for user k, $\forall k \in \mathcal{I}, i \neq k$.

the bidding strategy for the one-shot auction, we will define AF-OFDMA co-operative game based on terminologies from cooperative game as follows.

Definition 9.2.1 *An AF-OFDMA cooperative game for the ith user (*AF-OFDMA-CG-i*) with transferable utility (TU) is defined by the pair ($\mathcal{J}$,v_i), where the set of subcarriers $\mathcal{J} = \{1, \cdots, N\}$ is called the grand coalition, and $v_i : \mathcal{J}_i \rightarrow \mathcal{R}$ is a real valued mapping of $\mathcal{J}_i$ which is called the ith user characteristic function or the ith user value function. The subset $\mathcal{J}_i$ represents one of the 2^N possible subsets of $\mathcal{J}$.*

For *AF-OFDMA-CG-i*, the value function $v_i(\mathcal{J}_i, \lambda_R)$ represents the achievable data rate using the set $\mathcal{J}_i$ of subcarriers and a common value λ_R. It is defined as in (9.13), with $v_i(\varnothing, \lambda_R) = 0$. The achievable data rate of user i by using all subcarriers $\mathcal{J}$ with optimal power profiles at the source and relay nodes denoted as $v_i(\mathcal{J}, \lambda_R)$ is called the value of the grand coalition for user i.

There are many solution concepts for TU games such as; the core, kernel, nucleolus, and the Shapley value that can be used to evaluate the worth of the subcarrier to the user. We choose the Shapley value, since as discussed in Subsection 2.5.5, it always uniquely exists and can be obtained using a closed form expression.

The Shapley value Φ_j^i of a subcarrier j for user i can be interpreted in terms of the average marginal contribution of subcarrier j that makes to any coalition (subset) of $\mathcal{J}$ subcarriers, assuming all orderings are equally likely. The Shapley value of a subcarrier accurately reflects the bargaining power of that subcarrier and the marginal contribution that the subcarrier brings to the ith user. Let $\mathbf{\Phi}^{(i)} = \left(\Phi_1^{(i)}, \Phi_2^{(i)}, \cdots, \Phi_N^{(i)}\right)$ denote the Shapley value vector for user i. The Shapley value $\Phi_j^{(i)}$ of subcarrier j for user i is computed as:

$$\Phi_j^{(i)} = \frac{1}{N!} \sum_{\pi \in \Omega} v_i(C_j(\pi) \cup j, \lambda_R) - v_i(C_j(\pi), \lambda_R), \tag{9.14}$$

where Ω is the set of all possible $N!$ permutations on $\mathcal{J}$, π is a permutation in Ω, and $C_j(\pi)$ is the set of subcarriers that precede subcarrier j in the permutation π. $v_i(C_j(\pi) \cup j, \lambda_R) - v_i(C_j(\pi), \lambda_R)$ represents the ith user marginal contribution $M_c^{(i)}(\pi, j; \lambda_R)$ of subcarrier j to the set $C_j(\pi) \cup j$ of subcarriers.

It is clear that (9.14) requires $N!$ permutations on $\mathcal{J}$ to compute the average marginal contribution of the subcarriers which is computationally complex especially for a large N. Hence, the direct approach for computing the Shapley value of a subcarrier is not tractable. The Shapley value can be computed approximately using a sampling-based approach that works in polynomial time [23].

The estimation of the Shapley value is illustrated in **Algorithm 9.2**. The population Ω of the sampling process P will be the set of $N!$ permutations of $\mathcal{J}$, i.e. $P \in \Omega$. The sampling process P contains M samples (permutations), each is obtained from Ω with replacement, i.e. each with $\frac{1}{N!}$ probability. A sample of the process P is denoted as π_m for $m = 1, \cdots, M$. The marginal contribution of subcarrier j for user i using permutation π_m denoted as $M_c^{(i)}(\pi_m, j; \lambda_R)$ is computed as $M_c^{(i)}(\pi_m, j; \lambda_R) = v_i(C_j(\pi_m) \cup j, \lambda_R) - v_i(C_j(\pi_m), \lambda_R)$. The estimate of the Shapley value vector for user i is denoted as $\hat{\mathbf{\Phi}}^{(i)} = (\hat{\Phi}_1^{(i)}, \hat{\Phi}_2^{(i)}, \cdots, \hat{\Phi}_N^{(i)})$, where Shapley value of subcarrier j for user i is estimated as $\hat{\Phi}_j^{(i)} = \frac{1}{M} \sum_{m=1}^{M} M_c^{(i)}(\pi_m, j; \lambda_R)$.

In the one-shot auction scenario, the requirement of multiple interactions between the users and the base-station is minimized. Each user submits bids on all subcarriers at once, that equal the worth of the subcarriers. Similar to the sequential auction, the user requires the knowledge of the relay-destination channel gain $H_{RD}(j)$, $\forall j \in \mathcal{J}$ and the common value λ_R which is discussed in more detail in Section 9.4.

Let $\boldsymbol{b}_{Sh}^{(i)} = (b_{Sh}^{(i)}(1), b_{Sh}^{(i)}(2), \cdots, b_{Sh}^{(i)}(N))$ denote the bidding strategy of user i on the set $\mathcal{J}$. The bidding strategy of user i on subcarrier $j \in \mathcal{J}$ is computed based on the approximated Shapley value as $b_{Sh}^{(i)}(j) = \frac{\hat{\Phi}_j^{(i)}}{\sum_{j \in \mathcal{J}} \hat{\Phi}_j^{(i)}}$, $\forall j \in \mathcal{J}$. By

Algorithm 9.2 Estimation of the Shapley Value $\hat{\mathbf{\Phi}}^{(i)}$ Using the Sampling Approach.

Require: M, $\gamma_{SD}^{(i)}(j)$, $\gamma_{SR}^{(i)}(j)$, $\gamma_{RD}(j)$, $\forall j \in \mathcal{J}$, λ_R, $P_i^{\max}$.

$\hat{\Phi}_j^{(i)} \leftarrow 0, \forall j \in \mathcal{J}$.
for $m = 1 : M$ **do**
  Generate a sample $\pi_m \in \Omega$ with probability $\frac{1}{N!}$.
  for $j = 1 : N$ **do**
    Find the set $C_j(\pi_m)$.
    Compute $v_i(C_j(\pi_m) \cup j, \lambda_R)$ and $v_i(C_j(\pi_m), \lambda_R)$ using (9.13).
    Compute $M_c^{(i)}(\pi_m, j; \lambda_R) = v_i(C_j(\pi_m) \cup j, \lambda_R) - v_i(C_j(\pi_m), \lambda_R)$.
    Compute $\hat{\Phi}_j^{(i)} = \hat{\Phi}_j^{(i)} + M_c^{(i)}(\pi_m, j; \lambda_R)$.
  end for
end for
$\hat{\Phi}_j^{(i)} = \frac{\hat{\Phi}_j^{(i)}}{M}, \forall j \in \mathcal{J}$.
return $\hat{\mathbf{\Phi}}^{(i)}$.

using this bidding strategy, we ensure that the users submit bids based on the relative worth rather than the actual worth. Hence, all users will abide to a common scale, which in a way will ensure fairness. The bid $b_{Sh}^{(i)}(j)$ represents the relative importance (worth) of subcarrier j to user i. $b_{Sh}^{(i)}(j) = \frac{\Phi_j^{(i)}}{\sum_{j \in \mathcal{J}} \Phi_j^{(i)}}$ After all users submit their bids, the base-station formulates a mixed integer programing problem to assign the subcarriers to the users aiming at maximizing the rate fairness as:

$$\max_{\boldsymbol{\Upsilon}} C, \tag{9.15a}$$

$$\text{s.t.} \sum_{j \in \mathcal{J}} \Upsilon_j^{(i)} b_{Sh}^{(i)}(j) \geq C, \forall i \in \mathcal{I}, \tag{9.15b}$$

$$\sum_{i \in \mathcal{I}} \Upsilon_j^{(i)} = 1, \forall j \in \mathcal{J}, \tag{9.15c}$$

$$\Upsilon_j^{(i)} \in \{0, 1\}, \forall j \in \mathcal{J}, \forall i \in \mathcal{I}, \tag{9.15d}$$

where $\Upsilon_j^{(i)}$ is the subcarrier assignment indicator; $\Upsilon_j^{(i)} = 1$ means that subcarrier j is assigned to user i. Constraint (9.15b) represents the fairness criterion for the base-station subcarrier assignment. Each user is assigned at least a worth of C, whereas constraint (9.15c) means that each subcarrier is

assigned to exactly one user. The optimization problem (9.15) can be solved by using linear integer programing algorithms [129].

The cost value C is initialized to some C_0, and the optimal subcarrier assignment is obtained. The value C is increased gradually until no feasible solution can be found. The highest value of C and its corresponding subcarrier assignment with a feasible solution is considered as the solution to the subcarrier assignment problem. Problem (9.15) differs from (9.3) in that (9.15) requires only the bids to find the solution and it is a MILP, whereas (9.3) requires all the users information; such as channel gains and maximum source power. Even though (9.15) is a MILP, and there are many methods to solve it, it entails high computational complexity. To assign the subcarriers to the users with less computational complexity, we propose an iterative algorithm, where one subcarrier is assigned at each iteration based on the difference between the submitted bid and the accumulated worth of previous iterations. The algorithm proceeds until all subcarriers are assigned.

Initially all subcarriers are not assigned to any user; i.e. $\mathcal{J}_i \leftarrow \varnothing, \forall i \in \mathcal{I}$ and the accumulative worth of the subcarriers for user i is set to $V_{AC}^{(i)} = 0$, $\forall i \in \mathcal{I}$. At stage l for $l = 1, \cdots, N$ the difference between the bidding $b_{Sh}^{(i)}(l)$ and the accumulative worth $V_{AC}^{(i)}$ denoted as $V_D^{(i)}(l)$ is computed as $V_D^{(i)}(l) = b_{Sh}^{(i)}(l) - V_{AC}^{(i)}$ for $\forall i \in \mathcal{I}$. The winner user of subcarrier l is determined as $i^* = \arg\max_i V_D^{(i)}(l)$ and the accumulative worth for user i^* is updated as $V_{AC}^{(i^*)} = V_{AC}^{(i^*)} + b_{Sh}^{(i^*)}(l)$ and the set $\mathcal{J}_{i^*}$ is updated as $\mathcal{J}_{i^*} = \mathcal{J}_{i^*} \cup l$. The algorithm proceeds until all subcarriers are allocated as shown in **Algorithm 9.3**. The source and relay power profiles with the assignment profile $\mathcal{J}_i, \forall i \in \mathcal{I}$ are determined using (9.10) and (9.12).

Algorithm 9.1 and **Algorithm 9.3** differ in that, in **Algorithm 9.3** the user bid depends only on $b_{sh}^{(i)}(l)$, $\forall i \in \mathcal{I}$ and there is no need to calculate the rate based on the updated assignment at each iteration. The data rate and optimal source and relay power profiles are calculated once after all the

Algorithm 9.3 AF-OFDMA Iterative Subcarrier Assignment Algorithm for the One-Shot Auction.

Require: $b_{Sh}^{(i)}, \forall i \in \mathcal{I}$.
1: $\mathcal{J}_i \leftarrow \varnothing$, and $V_{AC}^{(i)} \leftarrow 0, \forall i \in \mathcal{I}$.
2: **for** $l = 1 : N$ **do**
3: Calculate $V_D^{(i)}(l) = b_{Sh}^{(i)}(l) - V_{AC}^{(i)}, \forall i \in \mathcal{I}$.
4: Find $i^* = \arg \max_i V_D^{(i)}(l)$.
5: Update $\mathcal{J}_{i^*} \leftarrow \mathcal{J}_{i^*} \cup l$.
6: Update $V_{AC}^{(i^*)} \leftarrow V_{AC}^{(i^*)} + b_{Sh}^{(i^*)}(l)$
7: **end for**
8: **return** $\mathcal{J}_i, \forall i \in \mathcal{I}$.

subcarriers are assigned, whereas in **Algorithm 9.1**, the bid of the subcarrier depends on the marginal contribution or the relative marginal contribution of the data rate before and after using that subcarrier and needs to be calculated after each subcarrier assignment step which requires synchronized interactions at each step between the base station and the users.

9.3 Resource Allocation for Multiple Relays

In this section, we extend the resource allocation solution using the auction framework to multiple-relays AF-OFDMA cooperative communication systems. The system under consideration consists of I users, K relays, and a common destination D. In this setting, another degree of freedom is explored, where the relay assignment profile needs to be determined for each subcarrier as well as the user assignment profile (subcarrier assignment) with optimal power profiles at the source and relay nodes. A subcarrier $j \in \mathcal{J}$ is allowed to be used maximally by one user $i \in \mathcal{I}$ using one relay $k \in \mathcal{K}$, where $\mathcal{K} = \{1, 2, \cdots, K\}$ is the set of relays in the AF-OFDMA cooperative communication system. Following the lines of the single relay scenario and using the notations summarized in **Table 9.1**, the utility function $U_i(\boldsymbol{P}_i, \boldsymbol{\lambda_R})$ of user i for a given subset of subcarriers $\mathcal{J}_{i,k} \in \boldsymbol{\mathcal{J}}_i$ per relay k, and a given common value $\lambda_{R_k} \in \boldsymbol{\lambda_R}$ per relay k, $\forall k \in \mathcal{K}$ can be formulated

Table 9.1 Multiple Relay Scenario Summary of Parameters

Symbol	Description/ Value	Symbol	Description/Value
$H_{SR}^{(i,k)}(j)$	The channel gain between source i and relay k at subcarrier j.	$\gamma_{SR}^{(i,k)}(j)$	$\frac{\lvert H_{SR}^{(i,k)}(j)\rvert^2}{\sigma^2}$
$H_{RD}^{(k)}(j)$	The channel gain between relay k and the destination at subcarrier j.	$\gamma_{RD}^{(k)}(j)$	$\frac{\lvert H_{RD}^{(k)}(j)\rvert^2}{\sigma^2}$
$P_{R_k}^{\max}$	The maximum transmitted power of relay k.	$P_R^{(i,k)}(j)$	The power transmitted by relay k for user i at subcarrier j.
$P_s^{(i,k)}(j)$	The power transmitted by user i at subcarrier j and amplified and forwarded by relay k.	$\Gamma_{SD}^{(i,k)}(j)$	$\gamma_{SD}^{(i)}(j)P_s^{(i,k)}(j)$
$\Gamma_{AF}^{(i,k)}(j)$	$\frac{\gamma_{SR}^{(i,k)}(j)\gamma_{RD}^{(k)}(j)P_S^{(i,k)}(j)P_R^{(i,k)}(j)}{\gamma_{SR}^{(i,k)}(j)P_S^{(i,k)}(j)+\gamma_{RD}^{(k)}(j)P_R^{(i,k)}(j)}$	$R_{AF}^{(i,k)}(j)$	$\frac{B_N}{2}\log\left(1+\frac{\Gamma_{SD}^{(i,k)}(j)+\Gamma_{AF}^{(i,k)}(j)}{\Gamma}\right)$
$\mathcal{J}_{i,k}$	The set of subcarriers assigned to user i using relay k	λ_{R_k}	The common value of relay k
$\boldsymbol{\mathcal{J}}_i$	$[\mathcal{J}_{i,1},\cdots,\mathcal{J}_{i,K}]$	$\boldsymbol{\lambda}_R$	$[\lambda_{R_1},\cdots,\lambda_{R_K}]$
$\boldsymbol{P}_i$	$(\boldsymbol{P}_S^i,\boldsymbol{P}_R^i)$	$[\boldsymbol{P}_S^i]_{j,k}$	$P_S^{(i,k)}(j)$
$\boldsymbol{H}_{RD}(j)$	$[H_{RD}^{(1)}(j),\cdots,H_{RD}^{(K)}(j)]$	$[\boldsymbol{P}_R^i]_{j,k}$	$P_R^{(i,k)}(j)$

as:

$$U_i(\boldsymbol{P}_i, \boldsymbol{\lambda_R}) = \sum_{k\in\mathcal{K}} \sum_{j\in\mathcal{J}_{i,k}} R_{AF}^{(i,k)}(j) - \sum_{k\in\mathcal{K}} \lambda_{R_k} \sum_{j\in\mathcal{J}_{i,k}} P_R^{(i,k)}(j). \tag{9.16}$$

The optimal source and relay power profiles for $j \in \mathcal{J}_{i,k}$ can be obtained by maximizing the utility function $U_i(\boldsymbol{P}_i, \boldsymbol{\lambda_R})$ with a maximum source power constraint expressed as $\sum_{k\in\mathcal{K}} \sum_{j\in\mathcal{J}_{i,k}} P_S^{(i,k)}(j) \leq P_i^{\max}$. Similar to (9.6)-(9.9), the source power profile can be obtained as:

$$P_S^{(i,k)}(j) = \begin{cases} \frac{\left(K_i(\gamma_{SD}^{(i)}(j)+A_j^{(i,k)})-\Gamma\right)^+}{\gamma_{SD}^{(i)}(j)+B_j^{(i,k)}} & \text{if } P_R^{(i,k)}(j) > 0, \\ \left(K_i - \frac{\Gamma}{\gamma_{SD}^{(i)}(j)}\right)^+ & \text{if } P_R^{(i,k)}(j) = 0, \end{cases} \tag{9.17}$$

where $A_j^{(i,k)} = \frac{\gamma_{SR}^{(i,k)}(j)\gamma_{RD}^{(k)2}(j)C_j^{(i,k)2}}{(\gamma_{SR}^{(i,k)}(j)+\gamma_{RD}^{(k)}(j)C_j^{(i,k)})^2}$, $B_j^{(i,k)} = \frac{\gamma_{SR}^{(i,k)}(j)\gamma_{RD}^{(k)}(j)C_j^{(i,k)}}{\gamma_{SR}^{(i,k)}(j)+\gamma_{RD}^{(k)}(j)C_j^{(i,k)}}$, $K_i = \frac{B_N}{2\ln(2)\lambda_i}$ and $C_j^{(i,k)}$ is computed as:

$$C_j^{(i,k)} = \frac{\gamma_{SR}^{(i,k)}(j)\Big(-1+\sqrt{1+(1+\frac{\gamma_{SR}^{(i,k)}(j)}{\gamma_{SD}^{(i)}(j)})(\frac{\lambda_i}{\lambda_{R_k}}\frac{\gamma_{RD}^{(k)}(j)}{\gamma_{SD}^{(i)}(j)}-1)}\Big)^+}{\gamma_{RD}^{(k)}(j)(1+\frac{\gamma_{SR}^{(i,k)}(j)}{\gamma_{SD}^{(i)}(j)})}, \tag{9.18}$$

with the per user Lagrangian multiplier λ_i is selected to satisfy the source power constraint $\sum_{k\in\mathcal{K}} \sum_{j\in\mathcal{J}_{i,k}} P_S^{(i,k)}(j) = P_i^{\max}$. The optimal relay power profile for $j \in \mathcal{J}_{i,k}$ can be obtained as:

$$P_R^{(i,k)}(j) = C_j^{(i,k)} P_S^{(i,k)}(j). \tag{9.19}$$

The achievable data rate for the ith user for a given $\lambda_{R_k} > 0$ and $\mathcal{J}_{i,k}$, $\forall k \in \mathcal{K}$ is computed as:

$$v_i(\boldsymbol{\mathcal{J}}_i, \boldsymbol{\lambda}_R) = \sum_{k\in\mathcal{K}} v_i^{(k)}(\mathcal{J}_{i,k}, \lambda_{R_k}), \tag{9.20}$$

where $v_i^{(k)}(\mathcal{J}_{i,k}, \lambda_{R_k})$ is obtained as:

$$v_i^{(k)}(\mathcal{J}_{i,k}, \lambda_{R_k}) = \sum_{j\in\mathcal{J}_{i,k}} R_{AF}^{(i,k)*}(j), \tag{9.21}$$

with $R_{AF}^{(i,k)*}(j)$ is the data rate obtained by using the optimal power profiles $P_S^{(i,k)}(j)$ and $P_R^{(i,k)}(j)$ computed as in (9.17) and (9.19), respectively. The overall system throughput of the multiple relays scenario can be obtained as $\sum_{i\in\mathcal{I}} v_i(\boldsymbol{\mathcal{J}}_i, \boldsymbol{\lambda}_R)$. Similar to the one relay AF-OFDMA scenario, the auction framework is used to find the subcarrier assignment profiles $\boldsymbol{\mathcal{J}}_i$, $\forall i \in \mathcal{I}$ based on the sequential subcarrier assignment algorithm as well as on the one-shot subcarrier assignment algorithm.

9.3.1 Sequential Subcarrier Assignment

The subcarriers and the corresponding relays are assigned in a sequential fashion based on the bids submitted by the users. At each step, the user submits a bid for the current subcarrier and selects the corresponding relay. If the objective is to maximize the system throughput (sum rate), the worth of subcarrier j is the maximum marginal increase of the data rate using subcarrier j assisted by relay k computed as $M_c^{(i)}(j_k, \boldsymbol{\lambda}_R) = v_i(\boldsymbol{\mathcal{J}}_i \cup j_k, \boldsymbol{\lambda}_R) - v_i(\boldsymbol{\mathcal{J}}_i, \boldsymbol{\lambda}_R)$, with $j_k \cap \boldsymbol{\mathcal{J}}_i = \varnothing$, where j_k means that subcarrier j is assisted by relay k. $v_i(\cdot,\cdot)$ is computed as in (9.20) based on maximizing the utility function defined in (9.16).

If the objective is to maximize the fairness index, the worth of subcarrier j is the maximum relative marginal increase of the data rate using subcarrier j assisted by relay k computed as $\frac{M_c^{(i)}(j_k,\boldsymbol{\lambda}_R)}{v_i(\boldsymbol{\mathcal{J}}_i \cup j_k,\boldsymbol{\lambda}_R)}$.

Algorithm 9.4, illustrates the sequential subcarrier assignment for multiple relays AF-OFDMA cooperative communications system. The base-station announces the common value vector $\boldsymbol{\lambda}_R$, and relay destination channel gain vector $\boldsymbol{H}_{RD}(j)$ which allows the users to compute the optimal power profiles at the source and relay nodes as in (9.17) and (9.19). The value and the update of $\boldsymbol{\lambda}_R$ are discussed in Section 9.4.

Initially, all subcarriers are not assigned to any user, $\mathcal{J}_{i,k} = \varnothing$, and the corresponding achievable data rate is set to $v_i(\mathcal{J}_{i,k}, \lambda_{R_k}) = 0$, $\forall i \in \mathcal{I}$ and $\forall k \in$

Algorithm 9.4 AF-OFDMA Multiple Relays Sequential Subcarrier Assignment Auction.

Require: $\gamma_{SD}^{(i)}(j)$, $\gamma_{SR}^{(i,k)}(j)$, $\gamma_{RD}^{(k)}(j)$, $\boldsymbol{\lambda}_R$, $P_i^{\max}$, $\forall j \in \mathcal{J}$, $\forall i \in \mathcal{I}$, $\forall k \in \mathcal{K}$, and $obj \in \{s, f\}$.
1: $\mathcal{J}_{i,k} \leftarrow \varnothing$, and $v_i(\mathcal{J}_{i,k}, \boldsymbol{\lambda}_R) \leftarrow 0$, $\forall k \in \mathcal{K}$, and $\forall i \in \mathcal{I}$.
2: $\boldsymbol{\mathcal{J}}_i = \{\mathcal{J}_{i,1}, \cdots, \mathcal{J}_{i,K}\}$, $\forall i \in \mathcal{I}$.
3: **for** $l = 1 : N$ **do**
4: Calculate $M_c^{(i)}(l_k, \boldsymbol{\lambda}_R) = v_i(\boldsymbol{\mathcal{J}}_i \cup l_k, \boldsymbol{\lambda}_R) - v_i(\boldsymbol{\mathcal{J}}_i, \boldsymbol{\lambda}_R)$, $\forall i \in \mathcal{I}$, $\forall k \in \mathcal{K}$.
5: **if** $obj = s$ **then**
6: Find $k_i^* = \arg\max_k M_c^{(i)}(l_k, \boldsymbol{\lambda}_R)$, $\forall i \in \mathcal{I}$.
7: $b_{obj}^{(i)}(l_{k_i^*}) \leftarrow M_c^{(i)}(l_{k_i^*}, \boldsymbol{\lambda}_R)$, $\forall i \in \mathcal{I}$.
8: **else**
9: Find $k_i^* = \arg\max_k \frac{M_c^{(i)}(l_k, \boldsymbol{\lambda}_R)}{v_i(\boldsymbol{\mathcal{J}}_i \cup l_k, \boldsymbol{\lambda}_R)}$, $\forall i \in \mathcal{I}$.
10: $b_{obj}^{(i)}(l_{k_i^*}) \leftarrow \frac{M_c^{(i)}(l_{k_i^*}, \boldsymbol{\lambda}_R)}{v_i(\boldsymbol{\mathcal{J}}_i \cup l_{k_i^*}, \boldsymbol{\lambda}_R)}$, $\forall i \in \mathcal{I}$.
11: **end if**
12: Find $i^* = \arg\max_i b_{obj}^{(i)}(l_{k_i^*})$.
13: $\mathcal{J}_{i^*,k^*} \leftarrow \mathcal{J}_{i^*,k^*} \cup l_{k_{i^*}^*}$.
14: $\boldsymbol{\mathcal{J}}_{i^*} = \{\mathcal{J}_{i^*,1}, \cdots, \mathcal{J}_{i^*,K}\}$.
15: **end for**
16: **return** $\boldsymbol{\mathcal{J}}_i$, $\forall i \in \mathcal{I}$.

$\mathcal{K}$. At the lth stage for $l = 1, \cdots, N$, each user $i \in \mathcal{I}$ determines the worth of subcarrier l using relay k based on the objective function $obj \in \{f, s\}$ and the previously allocated subcarriers and their corresponding relays $\boldsymbol{\mathcal{J}}_i$ and submits its bid either as $b_s^{(i)}(l) = M_c^{(i)}(l_{k_i^*}, \boldsymbol{\lambda}_R)$, or $b_f^{(i)}(l) = \frac{M_c^{(i)}(l_{k_i^*}, \boldsymbol{\lambda}_R)}{v_i(\boldsymbol{\mathcal{J}}_i \cup l_{k_i^*}, \boldsymbol{\lambda}_R)}$ for $obj = s$ and $obj = f$, respectively. k_i^* is the relay that achieves either the maximum marginal contribution or maximum relative marginal contribution for user i using subcarrier l, and is determined as $k_i^* = \arg\max_k M_c^{(i)}(l_k, \boldsymbol{\lambda}_R)$ for $obj = s$, and as $k_i^* = \arg\max_k \frac{M_c^{(i)}(l_k, \boldsymbol{\lambda}_R)}{v_i(\boldsymbol{\mathcal{J}}_i \cup l_k, \boldsymbol{\lambda}_R)}$ for $obj = s$. The winner user i^* of subcarrier l using relay $k_{i^*}^*$ is determined as: $i^* = \arg\max_i b_{obj}^{(i)}(l)$. The set $\mathcal{J}_{i^*,k^*}$ is updated as $\mathcal{J}_{i^*,k^*} = \mathcal{J}_{i^*,k^*} \cup l_{k_{i^*}^*}$. The algorithm proceeds iteratively until all subcarriers are allocated.

9.3.2 One-Shot Subcarrier Assignment

In AF-OFDMA multiple relays one-shot auction, each user submits bids for all subcarriers and the corresponding relays based on an estimate of

the Shapley value, where **Algorithm 9.3** can be used to assign the subcarriers to the users. To capture the possibility of different relay assignments to each subcarrier, a random relay assignment approach is adopted, in which ς_m represents a random assignment of the relays to the subcarriers, e.g., ς_m = [1 2 1 2] means that subcarriers $\{1,3\}$ are assigned to relay 1 and subcarriers $\{2,4\}$ are assigned to relay 2 and so forth. The elements in the random assignment ς_m are generated from independent and identically distributed random variables. The value of each element is an integer $k \in \{1,\cdots,K\}$ occurs with equal probability $\frac{1}{K}$. The set of subcarriers precedes subcarrier j in the permutation π_m and their corresponding relay assignment in ς_m is denoted by $C_j(\pi_m,\varsigma_m)$. The relay assigned to subcarrier j in permutation π_m and assignment ς_m is represented by r_j. The marginal contribution $M_c^{(i)}(\pi_m,\varsigma_m;j,k;\boldsymbol{\lambda}_R)$ of subcarrier j assisted by relay k of user i in the permutation π_m and assignment ς_m is computed as $M_c^{(i)}(\pi_m,\varsigma_m;j,k;\boldsymbol{\lambda}_R) = v_i(C_j(\pi_m,\varsigma_m)\cup(j,k),\boldsymbol{\lambda}_R) - v_i(C_j(\pi_m,\varsigma_m),\boldsymbol{\lambda}_R)$. The estimate of the Shapley value for user i is denoted as $\hat{\boldsymbol{\Phi}}^{(i)} = (\hat{\Phi}_{1,1}^{(i)},\cdots,\hat{\Phi}_{J,K}^{(i)})$, where $\hat{\Phi}_{j,k}^{(i)}$ is computed as $\frac{1}{M}\sum_{m=1}^{M} M_c^{(i)}(\pi_m,\varsigma_m;j,k;\boldsymbol{\lambda}_R)$, where M is number of samples.

Algorithm 9.5 illustrates the estimation of the Shapley value for AF-OFDMA multiple relays scenario based on a sampling approach.

Let $\boldsymbol{b}_{Sh}^{(i)} = (b_{Sh}^{(i)}(1), b_{Sh}^{(i)}(2),\cdots, b_{Sh}^{(i)}(N))$ denote the bidding strategy of user i on the set $\mathcal{J}$. The bidding strategy of user i on subcarrier $j \in \mathcal{J}$ is computed as: $b_{Sh}^{(i)}(j) = \frac{\max\limits_k \hat{\Phi}_{j,k}^{(i)}}{\sum_{j\in\mathcal{J}} \max\limits_k \hat{\Phi}_{j,k}^{(i)}}$. The corresponding relay assignment profile of user i defined as $\boldsymbol{R}_s^{(i)} = (R_s^{(i)}(1),\cdots,R_s^{(i)}(N))$ is obtained as $R_s^{(i)}(j) = \arg\max\limits_k \hat{\Phi}_{j,k}^{(i)}$, where $R_s^{(i)}(j) \in \{1,\cdots,K\}$. $b_{Sh}^{(i)}(j) = \frac{\max\limits_k \Phi_{j,k}^{(i)}}{\sum_{j\in\mathcal{J}} \max\limits_k \Phi_{j,k}^{(i)}}$.

Similar to the single relay scenario; after all users submit their bids, the base-station assigns the subcarriers and their corresponding relays to the users using **Algorithm 9.3**. Then the source and relay power profiles are computed using (9.17) and (9.19).

Algorithm 9.5 Estimation of the Shapley Value $\hat{\mathbf{\Phi}}^{(i)}$ for Multiple Relays Scenario.

Require: M, $\gamma_{SD}^{(i)}(j)$, $\gamma_{SR}^{(i,k)}(j)$, $\gamma_{RD}^{(k)}(j)$, $\boldsymbol{\lambda}_R$, $P_i^{\max}$, $\forall j \in \mathcal{J}$, $\forall k \in \mathcal{K}$.

$\hat{\Phi}_{j,k}^{(i)} \leftarrow 0$, $\forall j \in \mathcal{J}$ and $\forall k \in \mathcal{K}$.
for $m = 1 : M$ **do**
  Generate a sample $\pi_m \in \Omega$ with probability $\frac{1}{N!}$.
  Generate a sample ς_m of N elements; each element is a random integer from $\{1, \cdots, K\}$ with probability $\frac{1}{K}$.
  for $j \in \mathcal{J}$ **do**
    for $k \in \mathcal{K}$ **do**
      Find the set $C_j(\pi_m, \varsigma_m)$.
      Find the relay r_j which is assigned to subcarrier j in ς_m.
      Find $v_i(C_j(\pi_m, \varsigma_m) \cup (j, r_j), \boldsymbol{\lambda}_R)$ and $v_i(C_j(\pi_m, \varsigma_m), \boldsymbol{\lambda}_R)$ using (9.20).
      if $k = r_j$ **then**
        $M_c^{(i)}(\pi_m, \varsigma_m; j, k; \boldsymbol{\lambda}_R) = v_i(C_j(\pi_m, \varsigma_m) \cup (j, k), \boldsymbol{\lambda}_R) - v_i(C_j(\pi_m, \varsigma_m), \boldsymbol{\lambda}_R)$.
      else
        $M_c^{(i)}(\pi_m, \varsigma_m; j, k; \boldsymbol{\lambda}_R) = 0$.
      end if
      Calculate $\hat{\Phi}_{j,k}^{(i)} = \hat{\Phi}_{j,k}^{(i)} + M_c^{(i)}(\pi_m, \varsigma_m; j, k; \boldsymbol{\lambda}_R)$.
    end for
  end for
end for
$\hat{\Phi}_{j,k}^{(i)} = \frac{\hat{\Phi}_{j,k}^{(i)}}{M}$, $\forall j \in \mathcal{J}$, $\forall k \in \mathcal{K}$.
return $\hat{\mathbf{\Phi}}^{(i)}$.

9.4 Performance Comparison

A key factor in determining the subcarrier assignment profiles of the proposed auction algorithms is the common value λ_R for the one relay scenario and the common value vector $\boldsymbol{\lambda}_R$ for multiple relays scenario. Changing the value of λ_R, or $\lambda_{R_k} \in \boldsymbol{\lambda}_R$ has a direct impact on the power profiles as clear from (9.10), (9.12), (9.17), and (9.19). Hence, it has an indirect impact on the submitted bids. In this chapter, we prefer to use the term common value instead of the pricing. Pricing is a commonly used concept in game theory framework as in [115, 149], to emphasize that this value is common to all users and it is announced by the base-station or relay to control the relaying power demands, and it is not used to charge the users. The common value is used to disclose information about the relay resources. It used in

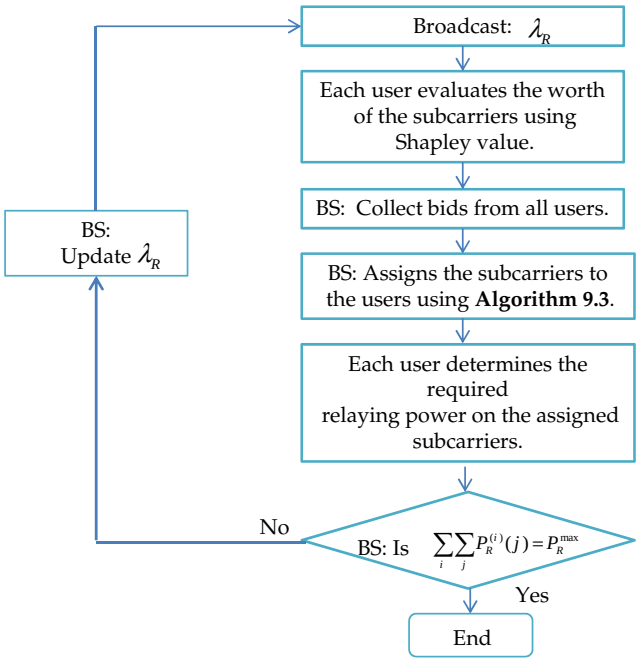

Figure 9.2 Flowchart of the One-Shot Auction Algorithm.

the design of the ith user utility function (9.5) to allow the user to determine her relaying power profiles. In this regard, if the total relaying power which results from the auction assignment differs from $P_R^{\max}$, the base-station announces an updated value of λ_R to the users. The common value [6] λ_R can be adjusted iteratively until the relay power constraint is satisfied using the gradient or sub-gradient methods as in [21]:

$$\lambda_R^{(t+1)} = \left(\lambda_R^{(t)} - \epsilon\left(P_R^{max} - \sum_{i\in\mathcal{I}} \sum_{j\in\mathcal{J}_i} P_R^{(i)}(j)\right)\right)^+, \tag{9.22}$$

where ϵ is a small step size, t is the iteration index, $P_R^{(i)}(j)$ is the optimal power profile computed as in (9.12) using $\lambda_R = \lambda_R^{(t)}$, and $\mathcal{J}_i$ is determined by using one of the proposed auction algorithms. The auction algorithm is applied repeatedly until the total power constraint is satisfied as shown in **Figure 9.3** and **Figure 9.2** for the sequential and one-shot auctions, respectively.

Let λ_R^* be the relay common value that satisfies the power constraint

[6] For multiple relays scenario a similar approach can be followed to update λ_R.

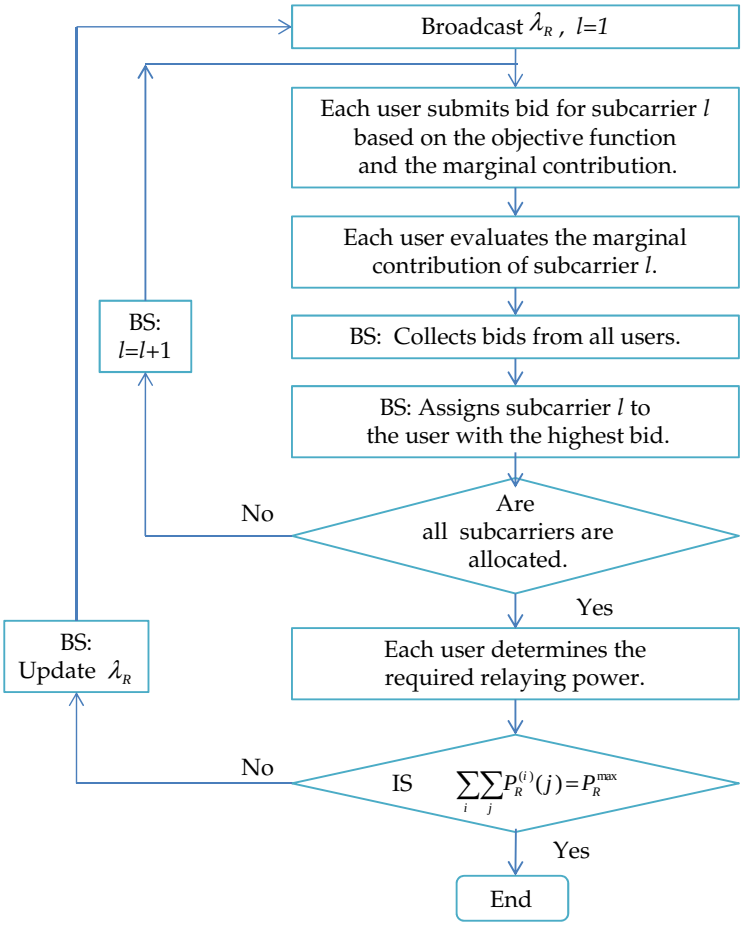

Figure 9.3 Flowchart of the Sequential Auction Algorithm.

$\sum_{i\in\mathcal{I}} \sum_{j\in\mathcal{J}_i^*} P_R^{(i)}(j) = P_R^{max}$, and $\mathcal{J}_i^*$ be the corresponding subcarrier assignment using the selected auction algorithm for $i \in \mathcal{I}$. Then, the system throughput index T_I is defined using λ_R^* and $\mathcal{J}_i^*$ as:

$$T_I = \frac{\sum_{i\in\mathcal{I}} v_i(\mathcal{J}_i^*, \lambda_R^*)}{\sum_{i\in\mathcal{I}} \hat{v}_i}, \tag{9.23}$$

where $\sum_{i\in\mathcal{I}} \hat{v}_i$ is the allocation of subcarriers, source and relay power profiles that maximizes the sum rate in (9.2). In order to find $\sum_{i\in\mathcal{I}} \hat{v}_i$, we solve the dual problem based on the assumption of zero duality gap, since OFDMA systems satisfy the time sharing property for a large number of subcarriers, as was proven in [30]. The dual approach transforms the problem into I distinct single-user problems, then a per user problem can be separated into N subcarrier problems as explained, in Appendix B.2.

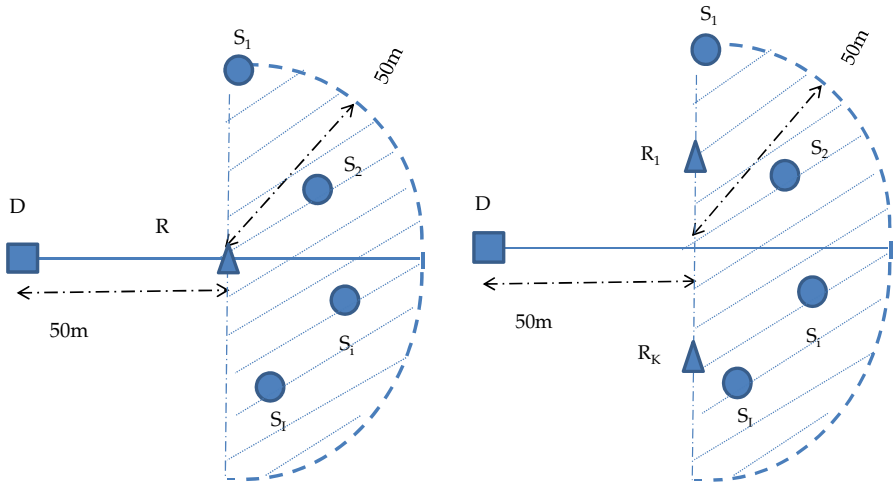

(a) Scenario One. **(b)** Scenario Two.

Figure 9.4 Sources, Relays and Destination Nodes Positions.

For the purpose of comparison, Jain's fairness index F_I is used with the optimal λ_R^* and $\mathcal{J}_i^*$.

9.5 Simulation Results and Discussion

We model the subcarrier channel coefficient between any two nodes with a separating distance d as $H(j) \sim \mathcal{CN}(0, \frac{1}{L(1+d)^\alpha})$, where, $\alpha = 4$ is the propagation loss factor, and $L = 4$ is the number of channel taps as in [49]. The subcarrier noise power σ^2 is set at 4×10^{-11}Watt. The source maximum transmit power $P_i^{\max} = 1$Watt, and the relay maximum transmit power $P_R^{\max} = 10$Watt, unless otherwise specified. The number of subcarriers $N = 32$, the subcarrier bandwidth $B_N = 4$KHz, and the capacity gap $\Gamma = 1$.

9.5.1 Single Relay Scenario

The scenario under consideration consists of I users (S_1, S_2, $\cdots$, S_I), one relay and a common destination D as shown in **Figure 9.4(a)**. The distance between the relay and the destination nodes is $d_{RD} = 50$m. The users are uniformly distributed in the shaded area.

Figure 9.5 shows the sum data rate, the throughput, and the fairness

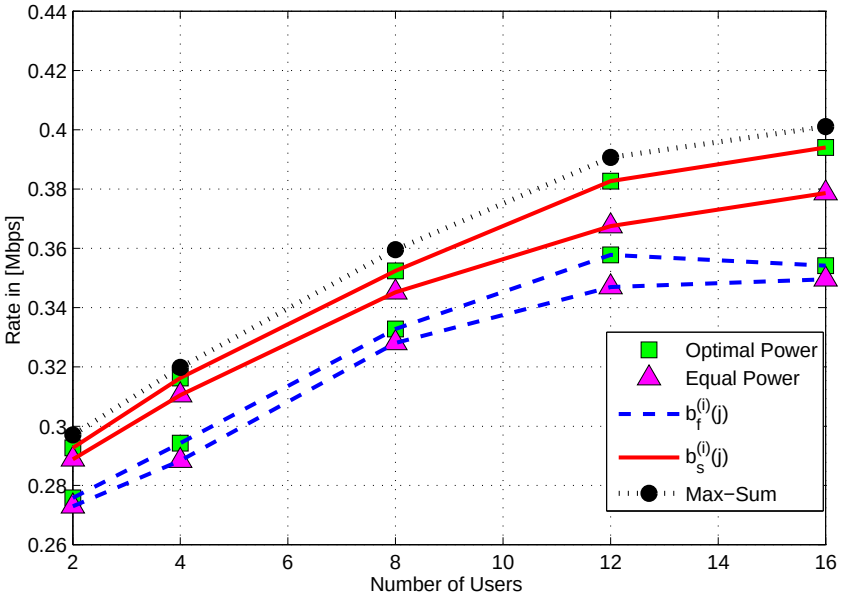

(a) Sum Data Rate

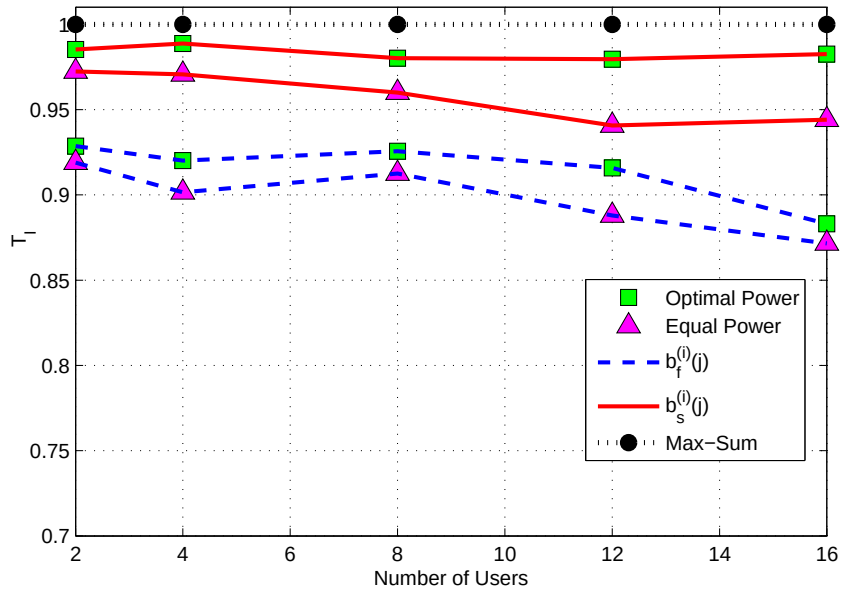

(b) Throughput Index T_1

indices as a function of the number of users for a single relay scenario for the sequential subcarrier assignment auction for the two bidding strategies (aiming either to maximize the sum data rate, or to maximize the fairness index) with optimal and uniform power allocation profiles at the source and relay nodes for P_R^{max} = 10Watt. Uniform (equal) power allocation profile means that the relaying power for each subcarrier is set at P_R^{max}/N and the user's maximum transmitted power P_i^{max} is allocated equally between the

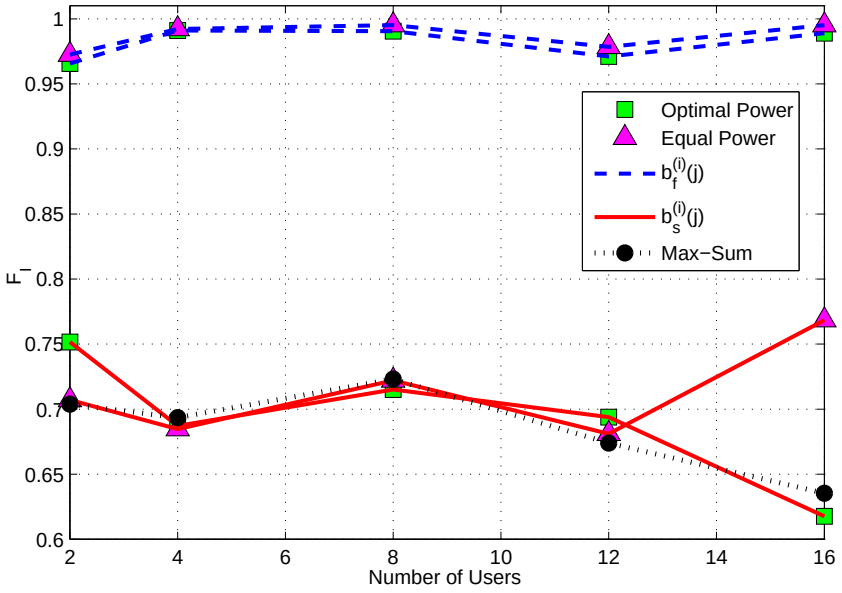

(c) Fairness Index F_1

Figure 9.5 The Sum Data Rate, T_I, and F_I for the Proposed Sequential Algorithm.

subcarriers assigned to her.

The bidding based on $b_s^{(i)}(j)$ achieves higher sum data rate compared to the bidding based on $b_f^{(i)}(j)$ as shown in **Figure 9.5(a)**. The bidding based on optimal power allocation at the source and relay nodes achieves higher sum data rate compared to the bidding based on uniform power allocation profile as expected. The throughput index T_I is shown **Figure 9.5(b)**. The maximum data rate $\sum_{i\in\mathcal{I}} \hat{v}_i$ is obtained with the assumption of zero duality gap and obtained by solving the dual problem (B.5).

Clearly, the proposed sequential auction algorithm with optimal power allocation using $b_s^{(i)}(j)$ as a bidding strategy asymptotically achieves the maximum sum rate. The difference in the achievable data rate is less than 2% compared to the sum data of (B.5) as illustrated by the throughput index, with less computational complexity for the proposed algorithm, since solving the dual problem requires large number of iterations to find the Lagrange multipliers. We use the subgradient method with three step sizes; a fixed step size with $\epsilon = .01$, about $200,000$ λ-evaluations are required, the

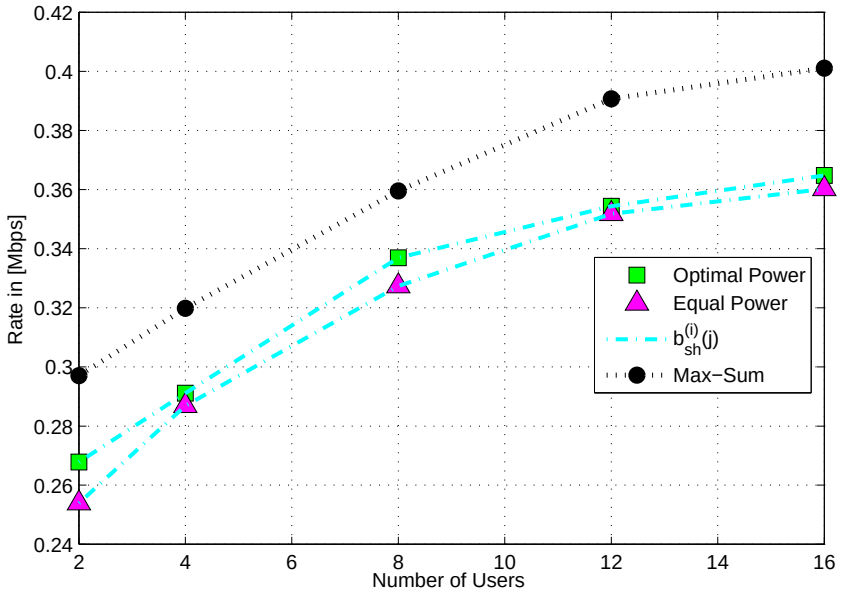

(a) Sum Data Rate

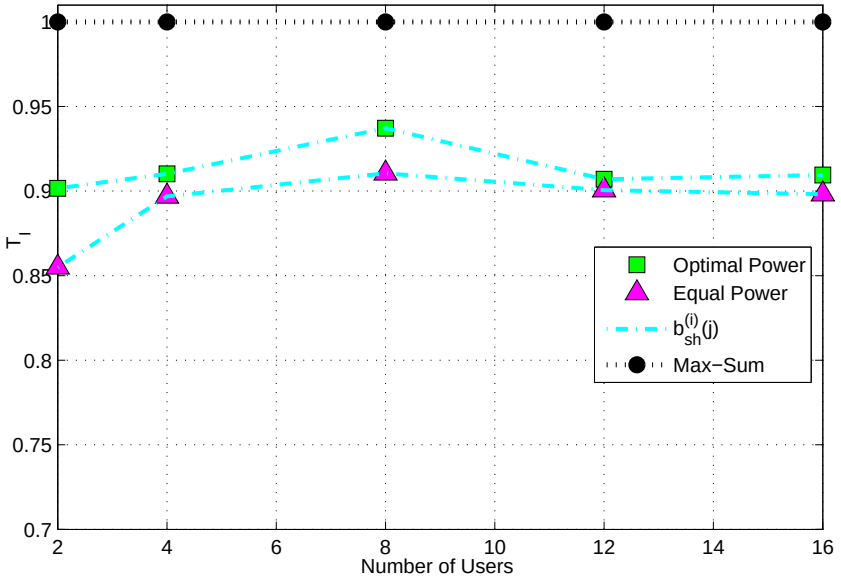

(b) Throughput Index T_1

diminishing step size $\epsilon = \frac{0.01}{\sqrt{t}}$, about $10,000$ λ-evaluations are required, and with a step size as in [143] $2,000$ λ-evaluations are required. The fairness index F_I is shown in **Figure 9.5(c)**. Clearly, the bidding based on $b_f^{(i)}(j)$ with optimal and uniform power allocation profiles achieves a very high fairness index independent of the number of users, and achieves a higher fairness index compared to the bidding based on $b_s^{(i)}(j)$. In addition, the fairness index of the maximum sum rate is shown for comparison purposes.

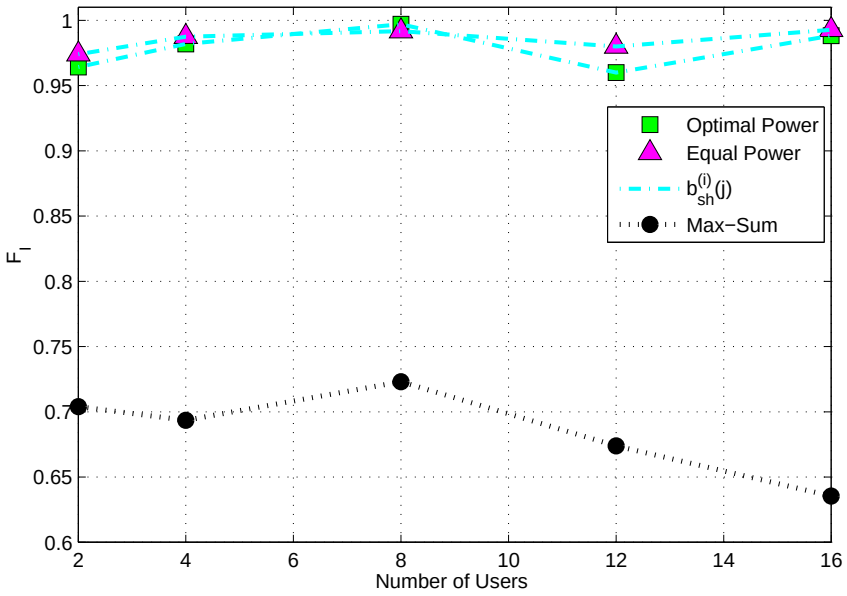

(c) Fairness Index F_1

Figure 9.6 The Sum Rate, T_I, and F_I for the Proposed One-shot Algorithm.

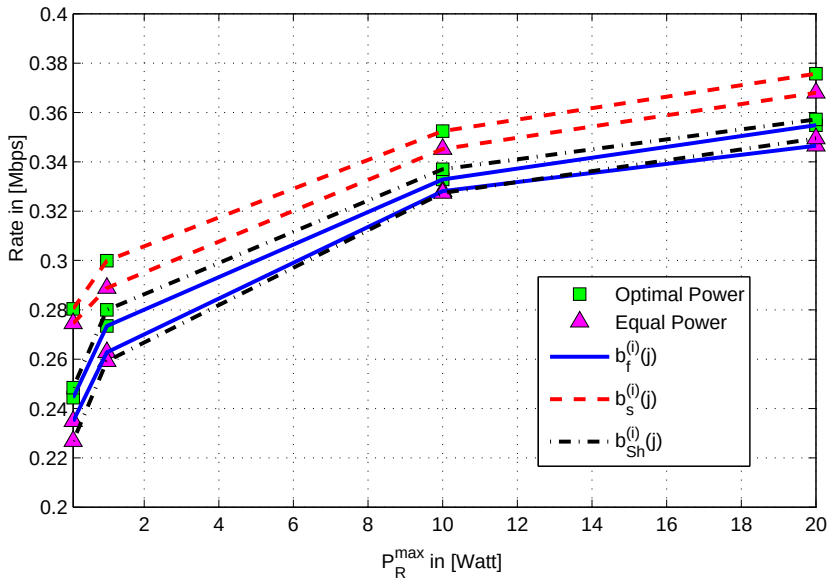

(a) Sum Data Rate

Figure 9.6 shows the sum data rate, the throughput, and the fairness indices as a function of the number of users for a single relay scenario for the one-shot subcarrier assignment auction with optimal and uniform power allocation profiles at the source and relay nodes for P_R^{max} = 10Watt. The sum data rate for the one-shot auction with optimal power allocation is higher than the sum data rate with uniform power allocation as shown in

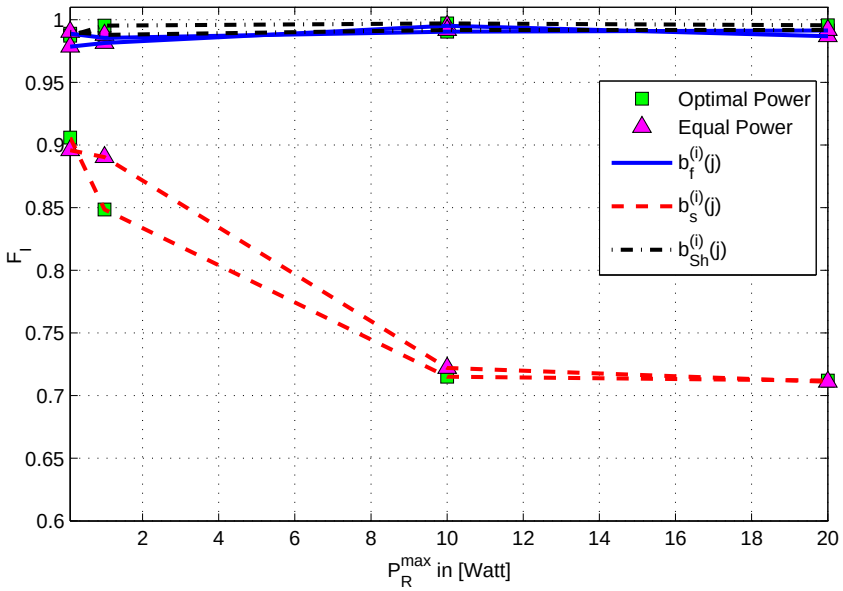

(b) Fairness Index F_1

Figure 9.7 The Sum Rate, and F_I for the Proposed Auction Algorithms as a Function of the Relay Maximum Transmitted Power P_R^{max} for $I = 8$ Users.

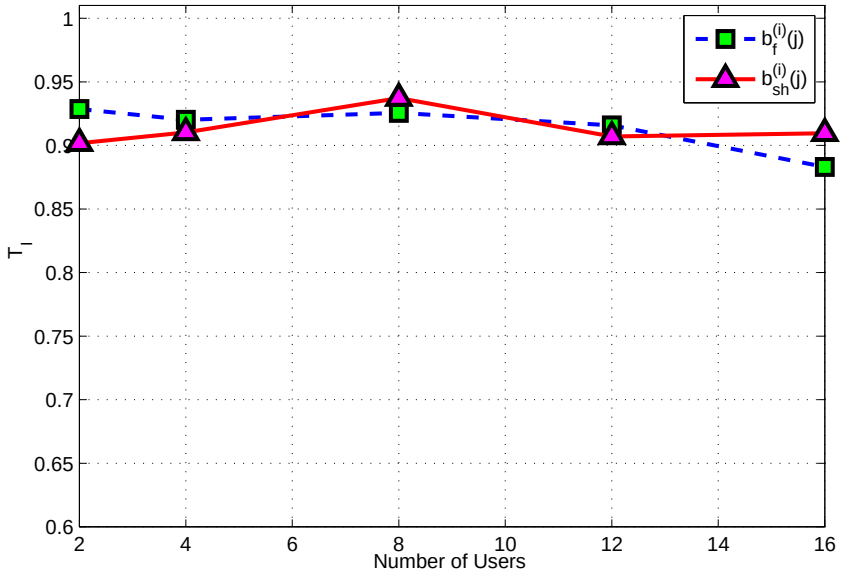

(a) Throughput Index T_I

Figure 9.6(a).

The one-shot auction using optimal power allocation achieves a throughput index $T_I \geq 90\%$ as shown in **Figure 9.6(b)**. The proposed one-shot auction algorithm achieves a very high fairness index $F_I \geq 95\%$ with optimal and uniform power allocation profiles as shown in **Figure 9.6(c)**.

Figure 9.7 shows the sum rate and fairness index for $I = 8$ users as a

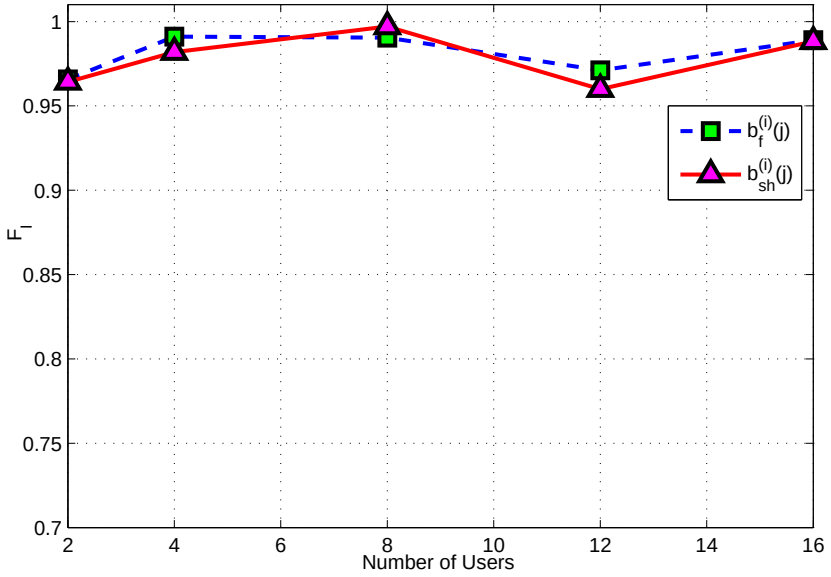

(b) Fairness Index F_1

Figure 9.8 T_I and F_I for the Proposed Auction Algorithms with Optimal Power Profiles.

function of the relay maximum transmit power P_R^{max}. The sum rate increases with the increase in the maximum transmit power P_R^{max} for all bidding strategies as shown in **Figure 9.7(a)**. The increase of the relay maximum transmit power P_R^{max} has marginal effect on the fairness index based on the bidding strategies $b_f^{(i)}(j)$ and $b_{sh}^{(i)}(j)$ as shown in **Figure 9.7(b)**. In addition, increasing the relay maximum transmit power P_R^{max} has a non-increasing effect on the fairness index for the bidding strategy $b_s^{(i)}(j)$. This is because the extra power will be allocated to the subcarriers with better channel conditions. The benefits of increasing P_R^{max} to the users with bad channel conditions are marginal.

Figure 9.8 compares the throughput and fairness indices as a function of the number of users with optimal power profiles for the bidding strategies $b_f^{(i)}(j)$ and $b_{sh}^{(i)}(j)$. Clearly, the difference in the fairness index is less than 2% and the difference in the throughput index is less than 5% for all cases (that is, different numbers of users).

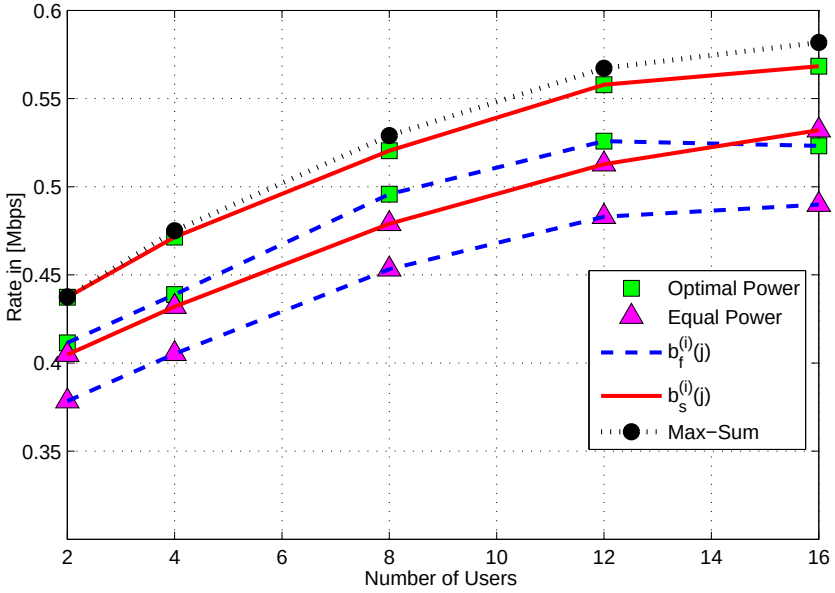

(a) Sum Data Rate

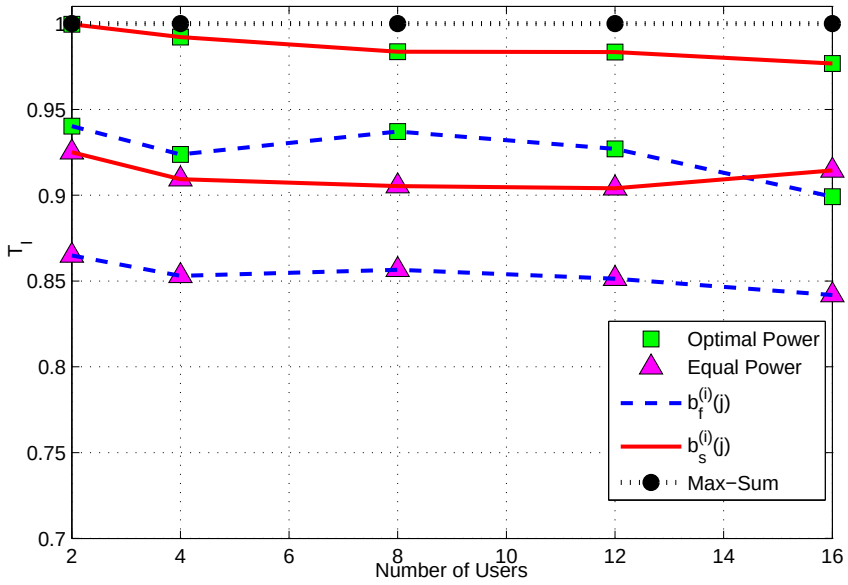

(b) Throughput Index T_1

9.5.2 Multiple Relays Scenario

The scenario under consideration consists of I sources (S_1, S_2, $\cdots$, S_I), 2 relays (R_1, R_2) and a common destination D as shown in **Figure 9.4(b)**. For the two relays scenario: relay R_1 is set at $(0, 0)$ and relay R_2 is set at $(0, 25)$m. The sources are distributed uniformly in the shaded area. The kth relay maximum transmit power is $P_{R_k}^{\max} = 5$Watt, $k \in \{1, 2\}$.

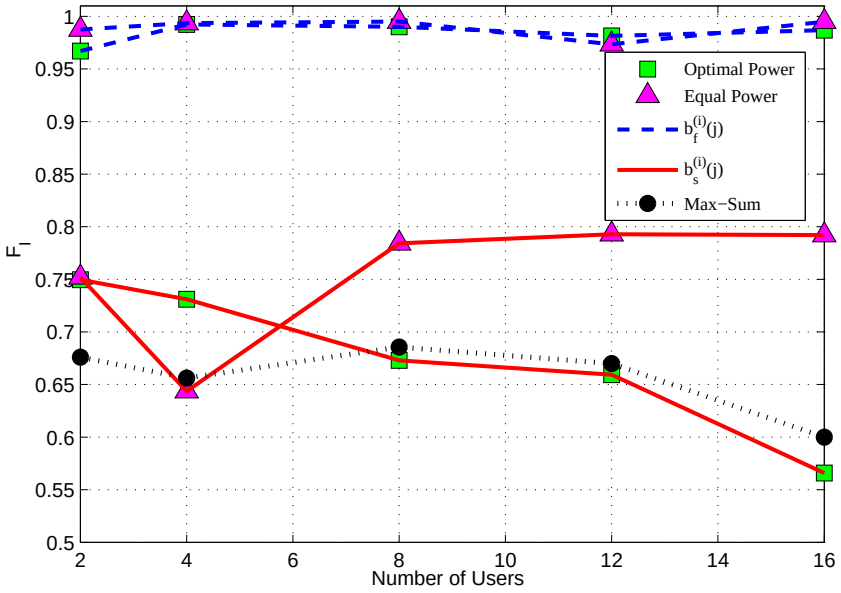

(c) Fairness Index F_1

Figure 9.9 The Sum Rate, T_I, and F_I for the Proposed Sequential Algorithm for Two Relays Scenario.

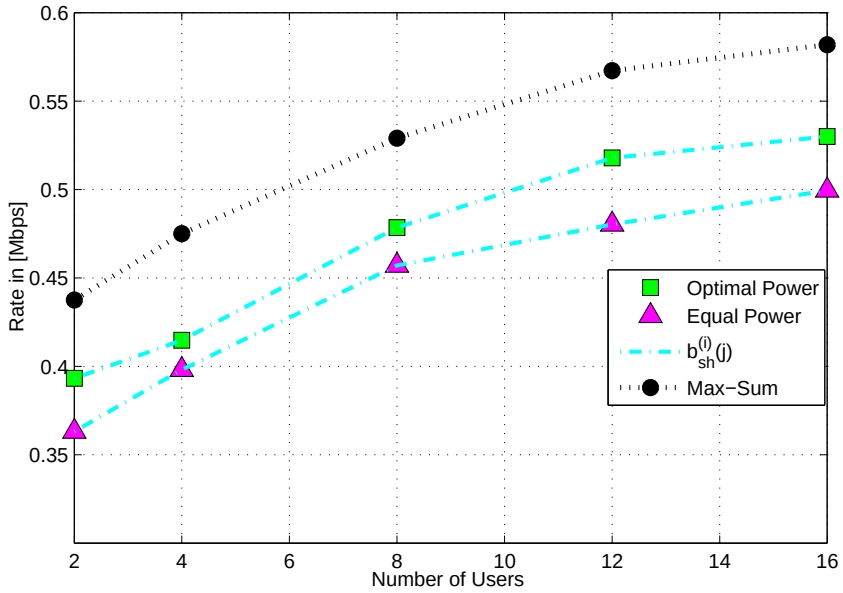

(a) Sum Data Rate

Figure 9.9 shows the sum data rate, the throughput, and the fairness indices as a function of the number of users for a two relays scenario for the proposed sequential subcarrier assignment auction for the two bidding strategies (aiming either to maximize the sum data rate, or to maximize the fairness index) with optimal and uniform power allocation profiles at the

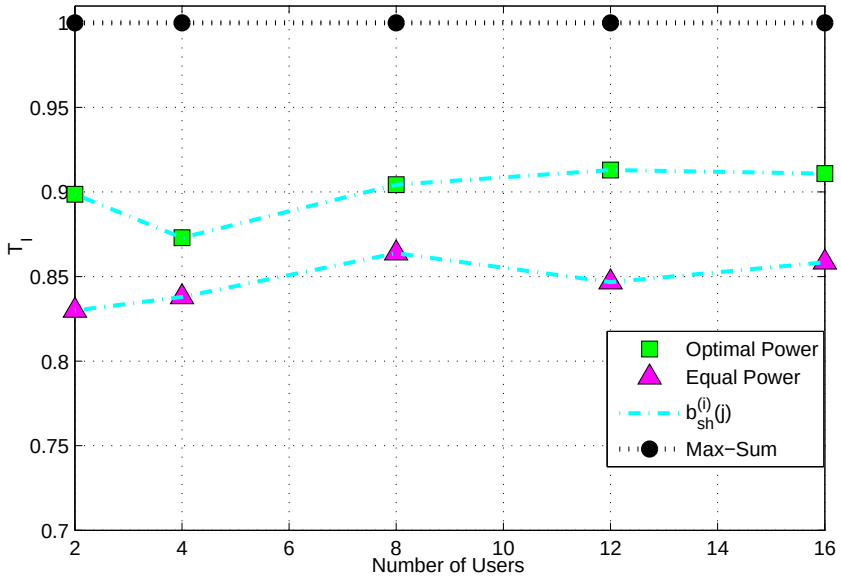

(b) Throughput Index T_1

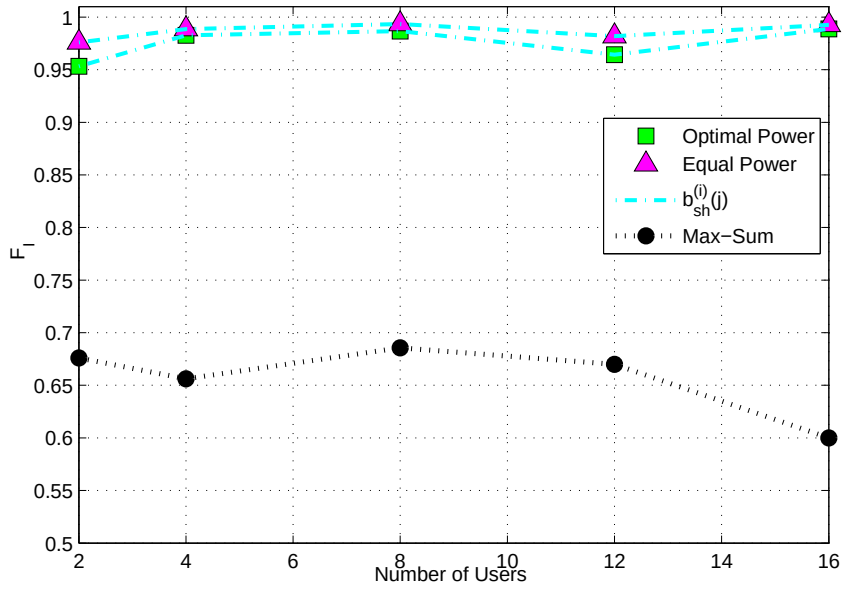

(c) Fairness Index F_1

Figure 9.10 The Sum Rate, T_I, and F_I for the Proposed One-Shot Algorithm for Two Relays Scenario.

source and relay nodes. Similar to the single relay scenario, the bidding based on $b_s^{(i)}(j)$ achieves a higher sum data rate and throughput index compared to the bidding based on $b_f^{(i)}(j)$ as shown in **Figure 9.9(a)**, and **Figure 9.9(b)**, respectively. The bidding strategy $b_f^{(i)}(j)$ achieves a very high fairness index with optimal and uniform power profiles similar to the one relay scenario as shown in **Figure 9.9(c)**.

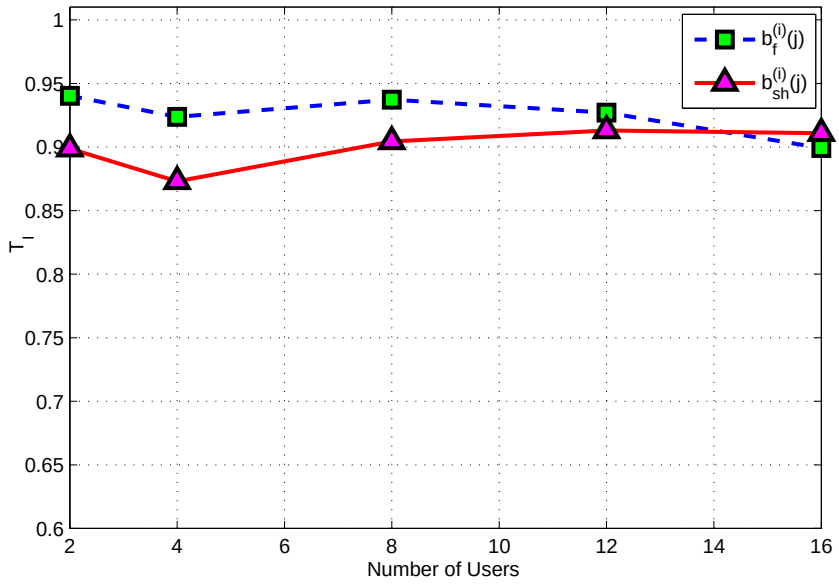

(a) Throughput Index T_I

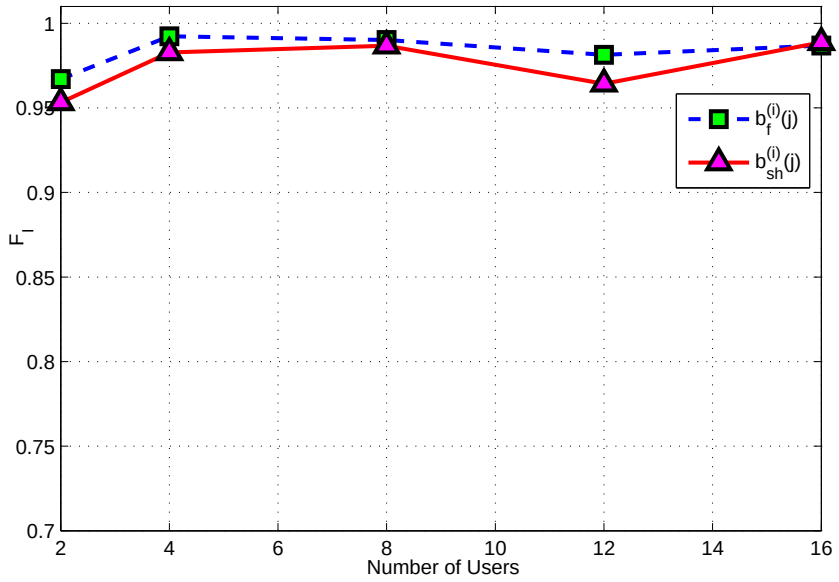

(b) Fairness Index F_1

Figure 9.11 T_I and F_I for the Proposed Auction Algorithm with Optimal Power Profiles for Two Relays.

Figure 9.10 shows the sum data rate, the throughput and fairness indices as a function of the number of users for two relays scenario for the one-shot subcarrier assignment auction with optimal and uniform power allocation profiles at the source and relay nodes. The sum data rate and the throughput index for the one-shot auction with optimal power allocation is higher than the sum data rate with uniform power allocation as shown in **Figure 9.10(a)**

and **Figure 9.10(b)**, respectively. The bidding strategy $b_{Sh}^{(i)}(j)$ achieves a very high fairness index similar to the one relay scenario as shown **Figure 9.10(c)**.

Figure 9.11 compares the throughput and fairness indices as a function of the number of users for the two relays scenario with optimal power profiles for the bidding strategies $b_{f}^{(i)}(j)$ and $b_{sh}^{(i)}(j)$. Similar to the single relay scenario, the difference in the fairness index is less than 2% and the different in the throughput index is less than 5% for all cases.

9.6 Conclusions

In this chapter, we investigate joint resource allocation for multiple users multiple relays AF-OFDMA cooperative communication systems in the presence of a direct link between the source and destination nodes. The subcarriers are assigned based on the auction framework. We propose subcarrier assignment algorithms based on the sequential auction framework. The base-station receives bids from all the users for the subcarrier, then the subcarrier is assigned to the user with the highest bid. Sequentially, the assignment progresses until all subcarriers are allocated. The bidding strategies of these algorithms are designed either to maximize the sum data rate or maximize the fairness index. Furthermore, we propose a subcarrier assignment algorithm based on a one-shot auction. The user submits bids to the base-station for all subcarriers at once based on an estimate of the Shapley value. An iterative algorithm is then used at the base-station to assign the subcarriers to the users to achieve rate fairness. Numerical simulation results show that the proposed algorithms achieve the proposed objective with high-performance measures; high-throughput index for maximizing the sum data rate and high fairness index for maximizing the fairness index. Uniform and optimal power allocation at the source and relay nodes are used within the auction framework. The throughput and the fairness indices for the uniform power allocation show similar trends to the through-

put and the fairness indices of optimal power allocation.

CHAPTER10

CONCLUSIONS AND FURTHER RESEARCH

In this chapter, conclusions are drawn in Section 10.1, and some suggestions for further research are introduced in Section 10.2.

10.1 Conclusions

In this dissertation, we investigate many resource allocation problems in relay aided cooperative communication systems. The main conclusions are summarized below.

- Sharing the two best ordered relays with equal power and equal bandwidth between the two users over Rayleigh flat fading channels achieves full diversity order for both users. Closed form expressions for the outage probability, and BEP performance measures for both AF and DF cooperative schemes are developed for different scenarios; AF/DF-orthogonal three time slots, AF-BF, DF-BF, and DF-STBC.

- Joint power and bandwidth allocation is proposed to maximize the sum rate for multi user single relay improved AF cooperative schemes. The improved AF cooperative communication scheme with optimal power and bandwidth profiles achieves a higher sum rate compared to full bandwidth relaying with optimal power allocation. A recursive algorithm alternating between a power allocation step for a given

power profile and a bandwidth allocation step for a given power profile is developed to solve the difficult joint optimization problem (non-convex). The proposed algorithm is extended to allocate the power and bandwidth profiles for the improved AF cooperative communication scheme over frequency selective fading channels.

- Stackelberg game is proposed to model the interactions between the users and the relay in AF cooperative communication systems, where the relay aims to maximize its benefits from selling its resources power and bandwidth to competing users, and the users aim to maximize their utility functions by selecting the power and bandwidth demands. The existence and uniqueness of Stackelberg Nash Equilibrium are proved for the proposed game. A distributed algorithm to reach the Stackelberg Nash Equilibrium is proposed. The stability conditions of the proposed algorithm are investigated.

- A low complexity algorithm is developed to select the mode of operation to maximize the sum rate over one OFDM symbol at high SNR regime for three scenarios: selective AF/OFDM, selective DF/OFDM, and hybrid AF-DF-OFDM scenarios, under two power constraint criteria; individual power constraint at the source node as well as the relay node, and total power constraint. The computation complexity of the proposed algorithm is of $O(N)$, which can be reduced further to $O(\log_2(N))$, using binary search algorithms compared to $O(2^N)$ for exhaustive search algorithm.

- The two band partition principle for two users OFDMA system can be applied to allocate subcarriers for two users AF/DF-OFDMA cooperative communication systems aiming to maximize the weighted sum rate. Low complexity algorithms are developed based on the two users scenario to allocate the subcarriers for multi user AF/DF-

OFDMA cooperative communication systems. Numerical simulations show that the proposed algorithms achieve approximately the sum rate of the dual approach with less computations.

- Sequential auction algorithm is proposed to allocate the subcarriers for multi relay multi user AF-OFDMA communication system, aiming to maximize either the sum rate or the fairness index in a competition fashion. The biding strategy is based on optimal power profiles at the source and relay nodes. The algorithm proceeds in a sequential fashion until all subcarriers are assigned. The subcarrier is assigned to the user who submits the highest bid. Numerical simulation results show that the proposed algorithm achieves the proposed objective with high-performance measures; high-throughput index for maximizing the sum data rate and high fairness index for maximizing the fairness index. To reduce the required synchronized interactions between the base-station and the users in sequential auction algorithms one-shot auction algorithm is devised to allocate the subcarriers for multi relay multi user AF-OFDMA communication system, aiming to maximize the fairness index. The biding strategy is based on optimal power profiles at the source and relay nodes. The user determines the most influential subcarriers based on an estimate of the Shapley value and bids on all subcarriers at once. The subcarriers are then allocated at the base station based on the submitted bids using an iterative algorithm developed to maximize the fairness index.

10.2 Further Research

This thesis opens promising doors for further research in wireless relay networks. Here, are some directions.

- *Optimal Resource Allocation for AF cooperative communication with Uncer-*

tainty in the Channel Gains

In Chapter 4, joint power and bandwidth allocation is performed with perfect CSI. It is also interesting to address joint power and bandwidth allocation with imperfect CSI.

- *Differential/ Dynamic Games for Resource Allocation*

  In Chapter 5, using Stackelberg framework, we assume a static model, i.e. the number of users do not change, channel gains do not vary, and the users do not move. It is interesting to extend the model to encompass the following:

  - The number of users is changing in the system; entering or leaving the system.
  - The user is moving with a certain speed.
  - The resources which are allocated to the user are changing based on the density of users and their class of service.
  - The channel is time variant.
  - The user can churn between different wireless networks.
  - The user can select different relays based on availability of resources or service prices.

  In this sense, the fit between differential games and resource management in a dynamic system is a promising one for further research.

- *Two Bands Partition with Subcarrier Pairing*

  In Chapter 8, the developed ordering function for AF/DF- OFDMA for subcarrier assignment is based on the assumption that the information at subcarrier j in the first time slot is forwarded on the same subcarrier in the second time slot. To utilize all available degrees of freedoms, further research is needed to find or modify the ordering

function to entail the possibility of using a different subcarrier to forward the information in the second time slot.

- *Two Bands Partition for low SNR for AF/DF-OFDMA Scenarios*

  In Chapter 8 and Chapter 7, the developed ordering function for AF/DF-OFDMA for subcarrier assignment is based on high SNR approximation. Further research is needed to explore the two-band partition approach for low SNR AF/DF-OFDM scenarios, and the possibility of developing an ordering function in this regime.

- *Two Bands Partition Principle with Beamforming*

  Further research is needed to explore the two band partition principle for multi relays with beamforming for AF/DF-OFDMA scenarios and developing the ordering function.

- *Resource allocation for AF/DF-OFDMA Multi User Two Way Relaying*

  Investigating subcarrier assignment and power allocation at the source and relay nodes for two way relaying AF/DF-OFDMA systems using auction framework is an interesting direction for further research.

- *Bundle Auction for AF/DF-OFDMA Relay Networks*

  In Chapter 9, each user submits bids either on a single subcarrier in the proposed sequential auction algorithm, or on all subcarriers in the proposed one-shot auction algorithm. Both algorithms are based on assigning one subcarrier at each step. It is interesting to develop auction algorithms where each user submits a bundle of bids based on optimal power profiles at the source and relay nodes. Bundling based on the Shapley value, is one promising direction for further investigation. The effect of the number of submitted bundles, and the characteristics of the submitted bundles on the throughput and fairness indices need to be investigated. Developing low complexity algorithms for bundle

auction AF/DF-OFDMA to solve the winner determination problem need to be explored further.

APPENDIX A

POWER AND BANDWIDTH ALLOCATION

The objective function for the exterior penalty method can be formulated as [109]:

$$\theta(\mu, \boldsymbol{P}, \boldsymbol{W}) = \sum_{i \in \mathcal{I}} R^{(i)} - \mu \sum_{i \in \mathcal{I}} (\max\{0, -P_i\})^2 - \mu \sum_{i \in \mathcal{I}} (\max\{0, -W_i\})^2 - \mu \sum_{i \in \mathcal{I}} (\max\{0, W_i - W\})^2 - \mu (\max\{0, (\sum_{i \in \mathcal{I}} P_i - P_{\max}\}))^2. \quad \text{(A.1)}$$

The dual problem can be formulated as [32]:

$$\mathcal{D} = \min_{\boldsymbol{\lambda} \geq 0} \max_{\boldsymbol{P}, \boldsymbol{W}} \sum_{i \in \mathcal{I}} R^{(i)} - \lambda_{sum}^{(P)} (\sum_{i \in \mathcal{I}} P_i - P_{\max}) + \sum_{i \in \mathcal{I}} \lambda_i^{(P)} P_i + \sum_{i \in \mathcal{I}} \lambda_i^{(WL)} W_i - \sum_{i \in \mathcal{I}} \lambda_i^{(WU)} (W_i - W), \quad \text{(A.2)}$$

where $\boldsymbol{\lambda} = [\lambda_{sum}^{(P)}, \lambda_i^{(P)}, \cdots, \lambda_I^{(P)}, \lambda_i^{(WL)}, \cdots, \lambda_I^{(WL)}, \lambda_i^{(WU)}, \cdots, \lambda_I^{(WU)}]$.

APPENDIX B

APPENDIX AF-OFDMA

B.1 Proof of Concavity

Define the function $R(P_S, P_R)$ as:

$$R(P_S, P_R) = \log\Big(1 + aP_S + \frac{P_S P_R}{bP_s + dP_R}\Big), \tag{B.1}$$

where a, b, and d are positive constants.

The second derivative test (Hessian) is used to show that $R(P_S, P_R)$ is a concave function [20]. The second partial derivative of $R(P_S, P_R)$ with respect to P_S is computed as:

$$\frac{\partial^2 R(P_S, P_R)}{\partial P_S^2} = \frac{-2bdP_R^2}{(1 + aP_s + \frac{P_S P_R}{bP_S + dP_R})(bP_S + dP_R)^3} - \frac{(a + \frac{dP_R^2}{(bP_S + dP_R)^2})^2}{(1 + aP_S + \frac{P_S P_R}{bP_S + dP_R})^2}, \tag{B.2}$$

the second partial derivative of $R(P_S, P_R)$ with respect to P_R is computed as:

$$\frac{\partial^2 R(P_S, P_R)}{\partial P_R^2} = \frac{-2bdP_S^2}{(1 + aP_s + \frac{P_S P_R}{bP_S + dP_R})(bP_S + dP_R)^3} - \frac{(bP_S^2)^2}{(bP_S + dP_R)^2(1 + aP_S + \frac{P_S P_R}{bP_S + dP_R})^2}, \tag{B.3}$$

and the second partial derivative with respect to P_R and P_S is computed as:

$$\frac{\partial^2 R(P_S,P_R)}{\partial P_R \partial P_S} = \frac{2dbP_SP_R(bP_S+dP_R)(1+aP_S+\frac{P_SP_R}{bP_S+dP_R}) - bP_S^2(bP_S+dP_R)(a+\frac{dP_R^2}{(bP_S+dP_R)^2})}{(bP_S+dP_R)^3(1+aP_S+\frac{P_SP_R}{bP_S+dP_R})^2}. \tag{B.4}$$

It is clear from (B.2) and (B.3) that $\frac{\partial^2 R(P_S,P_R)}{\partial P_S^2} < 0$ and $\frac{\partial^2 R(P_S,P_R)}{\partial P_R^2} < 0$, respectively. And it can be proved easily that $\frac{\partial^2 R(P_S,P_R)}{\partial P_S^2}\frac{\partial^2 R(P_S,P_R)}{\partial P_R^2} - \left(\frac{\partial^2 R(P_S,P_R)}{\partial P_R \partial P_S}\right)^2 > 0$. This proves the concavity of $R(P_S,P_R)$ in P_S and P_R.

B.2 Dual Problem

For AF-OFDMA scenario, the optimization problem after relaxing the total power constraints can be written as:

$$\begin{aligned}\max_{\boldsymbol{P}_S,\boldsymbol{P}_R,\boldsymbol{\Upsilon},\boldsymbol{\lambda}} \mathcal{R}(\boldsymbol{P},\boldsymbol{\Upsilon},\boldsymbol{\lambda}) =& \frac{W}{2N}\sum_{i\in\mathcal{I}}\sum_{j\in\mathcal{J}}\Upsilon_j^{(i)}\log\Big(1+\frac{\Gamma_{SD}^{(i)}(j)+\Gamma_{AF}^{(i)}(j)}{\Gamma\Upsilon_j^{(i)}}\Big)- \\ & \sum_{i\in\mathcal{I}}\lambda_i\Big(\sum_{j\in\mathcal{J}}P_S^{(i)}(j)-P_i^{\max}\Big)-\lambda_R\Big(\sum_{i\in\mathcal{I}}\sum_{j\in\mathcal{J}}P_R^{(i)}(j)-P_R^{\max}\Big), \\ \text{s.t. } & P_S^{(i)}(j)\geq 0, P_R^{(i)}(j)\geq 0,\ \Upsilon_j^{(i)}\geq 0,\ \lambda_R\geq 0, \lambda_i\geq 0,\end{aligned} \tag{B.5}$$

where λ_R, and λ_i are Lagrange multipliers. For a given subcarrier assignment $\boldsymbol{\Upsilon}$, the source and relay power profiles are given as in (8.12) and (8.14). Using the source and relay power profiles and the Lagrange multiplies λ_R and λ_i, $\forall i \in \mathcal{I}$, we can determine the jth subcarrier assignment, such that the subcarrier is assigned to the user that achieves the maximum rate in that subcarrier. This can be formulated as:

$$\Upsilon_j^i = \begin{cases} 1, & \text{if } i^* = \arg\max_{i\in\mathcal{I}} \tilde{R}_i(j), \\ 0, & \text{otherwise}, \end{cases} \tag{B.6}$$

where $\tilde{R}_i(j)$ is defined as:

$$\tilde{R}_i(j) = \frac{W}{2N}\log_2\left(1+\frac{\Gamma_{SD}^{(i)}(j)+\Gamma_{AF}^{(i)}(j)}{\Gamma}\right) - \lambda_i P_S^{(i)}(j) - \lambda_R P_R^{(i)}(j). \tag{B.7}$$

The power profiles $P_S^{(i)}(j)$ and $P_R^{(i)}(j)$ are obtained as $\arg \max_{P_S^{(i)}(j),\, P_R^{(i)}(j)} \tilde{R}_i(j)$. Problem (B.5) can be solved iteratively using the gradient or sub-gradient methods as [21]:

$$\boldsymbol{\lambda}^{(t+1)} = \left(\boldsymbol{\lambda}^{(t)} - \epsilon(\boldsymbol{P}_{max} - \boldsymbol{P})\right)^{+}, \tag{B.8}$$

where ϵ is the step size, t is the iteration index, $\boldsymbol{P}_{max} = [P_R^{\max}, P_1^{\max}, \cdots, P_K^{\max}]^T$, $\boldsymbol{P} = [\sum_{j\in\mathcal{J}}\sum_{i\in\mathcal{I}} Y_j^i P_R^{(i)}(j), \sum_{j\in\mathcal{J}} Y_j^1 P_S^{(1)}(j), \cdots, \sum_{j\in\mathcal{J}} Y_j^K P_S^{(K)}(j)]^T$, and $\boldsymbol{\lambda} = [\lambda_R, \lambda_1, \cdots, \lambda_K]^T$.

BIBLIOGRAPHY

[1] Agiza, H. N., Bischi, G.-I., and Kopel, M. (1999). A multistability in a dynamic cournot game with three oligopolists. *Mathematics and Computers in Simulation*, 51:63–90.

[2] Alamouti, S. (1998). A simple transmit diversity technique for wireless communications. *IEEE J. Sel. Areas Commun.*, 16(8):1451–1458.

[3] Alpcan, T., Basar, T., Srikant, R., and Altman, E. (2002). CDMA uplink power control as a noncooperative game. *Wireless Networks*, 8(6):659–670.

[4] Anghel, P. A. and Kaveh, M. (2004). Exact symbol error probability of a cooperative network in a Rayleigh-fading environment. *IEEE Trans. Wireless Commun.*, 3(5):1416–1421.

[5] Anghinolfi, D. and Paolucci, M. (2009). A new discrete particle swarm optimization approach for the single-machine total weighted tardiness scheduling problem with sequence-dependent setup times. *European Journal of Operational Research (EJOR)*, 193(1):73 –85.

[6] Annamalai, A., Deora, G., and Tellambura, C. (2006). Analysis of generalized selection diversity systems in wireless channels. *IEEE Trans. Veh. Technol.*, 55(6):1765–1775.

[7] Bai, Z., Yuan, D., and Kwak, K. (2008). Performance evaluation of STBC based cooperative systems over slow Rayleigh fading channel. *Computer Communications*, 31(17):4206–4211.

[8] Basar, T. and Srikant, R. (2002). Revenue-maximizing pricing and capacity expansion in a many-users regime. In *Proc. 21st Annual Joint Conference of the IEEE Computer and Communications Societies (INFOCOM 2002)*, pages 294–301, New York, NY, USA.

[9] Beaulieu, N. and Hu, J. (2006). A closed-form expression for the outage probability of decode-and-forward relaying in dissimilar Rayleigh fading channels. *IEEE Commun. Lett.*, 10(12):813–815.

[10] Belmega, E.-V., Lasaulce, S., and Debbah, M. (2009). Power allocation games for MIMO multiple access channels with coordination. *IEEE Trans. Wireless Commun.*, 8(6):3182–3192.

[11] Beres, E. and Adve, R. (2008). Selection cooperation in multi-source cooperative networks. *IEEE Trans. Wireless Commun.*, 7(1):118–127.

[12] Berhe, H. (2012). Penalty function methods using matrix laboratory MATLAB. *African Journal of Mathematics and Computer Science Research*, 5(13):209–246.

[13] Bertsekas, D. P. (2003). *Nonlinear Programming*. Athena Scientific, Belmont, Massachusetts, USA, 2nd edition.

[14] Biglieri, E., Calderbank, R., Constantinides, A., Goldsmith, A., Paulraj, A., and Poor, H. V. (2007). *MIMO Wireless Communications*. Cambridge University Press, New York, NY, USA.

[15] Biglieri, E., Goldsmith, A. J., Greenstein, L. J., Mandayam, N. B., and Poor, H. V. (2012). *Principles of Cognitive Radio*. Cambridge University Press.

[16] Bletsas, A., Shin, H., and Win, M. (2007). Cooperative communications with outage-optimal opportunistic relaying. *IEEE Trans. Wireless Commun.*, 6(9):3450–3460.

[17] Boche, H. and Schubert, M. (2009). Nash bargaining and proportional fairness for wireless systems. *IEEE/ACM Trans. Netw.*, 17(5):1453–1466.

[18] Boostanimehr, H. and Bhargava, V. (2011). Selective subcarrier pairing and power allocation for df ofdm relay systems with perfect and partial csi. *IEEE Trans. Wireless Commun.*, 10(12):4057–4067.

[19] Boyd, S. and Vandenberghe, L. (2003). Localization and cutting-plane methods. Stanford Engineering, Notes for EE392o.

[20] Boyd, S. and Vandenberghe, L. (2004). *Convex Optimization*. Cambridge University Press, New York, USA.

[21] Boyd, S., Xiao, L., and Mutapcic, A. (2003). Subgradient methoeds. Stanford Engineering, Notes for EE392o.

[22] Bu, T., Li, L., and Ramjee, R. (2006). Generalized proportional fair scheduling in third generation wireless data networks. In *Proc. 25th IEEE International Conference on Computer Communications (INFOCOM 2006)*, pages 1–12, Barcelona, Spain.

[23] Castro, J., Gmez, D., and Tejada, J. (2009). Polynomial calculation of the Shapley value based on sampling. *Computers and Operations Research*, 36(5):1726–1730.

[24] Chen, Y. and Kishore, S. (2008). A game-theoretic analysis of decode-and-forward user cooperation. *IEEE Trans. Wireless Commun.*, 7(5):1941–1951.

[25] Cheng, C.-M., Hsiao, P.-H., Kung, H. T., and Vlah, D. (2007). Maximizing throughput of UAV-relaying networks with the load-carry-and-deliver paradigm. In *Proc. IEEE Wireless Communications and Networking Conference (WCNC 2007)*, pages 4417–4424.

[26] Cho, Y., Kim, J., Yang, W., and Kang, C. (2010). *MIMO-OFDM Wireless Communications with MATLAB*. Wiley-IEEE Press, John Wiley & Sons (Asia) Pte Ltd, Singapore.

[27] Chong, E. K. P. and Zak, S. H. (2001). *An Introduction to Optimization*. John Wiley & Sons, Inc., 2nd edition.

[28] Cong, L., Zhao, L., Yang, K., Zhang, H., and Zhang, G. (2011). A Stackelberg game for resource allocation in multiuser cooperative transmission networks. *Wireless Communication and Mobile Computing*, 11(1):129–141.

[29] Cover, T. and Gamal, A. (1979). Capacity theorems for the relay channel. *IEEE Trans. Inf. Theory*, 25(5):572–584.

[30] Dang, W., Tao, M., Mu, H., and Huang, J. (2010). Subcarrier-pair based resource allocation for cooperative multi-relay OFDM systems. *IEEE Trans. Wireless Commun.*, 9(5):1640–1649.

[31] David, H. and Nagaraja, H. (2003). *Order Statistics*. John Wiley & Sons, Inc., Hoboken, New Jersey, USA, 3rd edition.

[32] Deb, K., Gupta, S., Dutta, J., and Ranjan, B. (2012). Solving dual problems using a coevolutionary optimization algorithm. *Journal of Global Optimization*, pages 1–43.

[33] Deng, H., Wang, Y., and Lu, J. (2010). Auction based resource allocation for balancing efficiency and fairness in OFDMA relay networks with service differentiation. In *Proc. IEEE 72nd Vehicular Technology Conference (VTC 2010) Fall*, pages 1–5, Ottawa, Canada.

[34] Dohler, M. (2000). *A Novel Statistical Indoor Model*. Diploma in electrical engineering, TU-Dresden, Dresden, Germany.

[35] Dohler, M. and Li, Y. (2010). *Cooperative Communications: Hardware, Channel & PHY*. Wiley Publishing, West Sussex, UK.

[36] Duval, O., Hasan, Z., Hossain, E., Gagnon, F., and Bhargava, V. (2010). Subcarrier selection and power allocation for amplify-and-forward relaying over OFDM links. *IEEE Trans. Wireless Commun.*, 9(4):1293–1297.

[37] Etkin, R., Parekh, A., and Tse, D. (2007). Spectrum sharing for unlicensed bands. *IEEE J. Sel. Areas Commun.*, 25(3):517–528.

[38] Feng, D., Jiang, C., Lim, G., Cimini, L.J., J., Feng, G., and Li, G. (2013). A survey of energy-efficient wireless communications. *IEEE Commun. Surveys Tuts.*, 15(1):167–178.

[39] Floudas, C. A. (1995). *Nonlinear and Mixed-Integer Optimization: Fundamentals and Applications*. Oxford University Press, USA.

[40] Fudenberg, D. and Tirole, J. (1991). *Game Theory*. The MIT Press, Cambridge, MA, London, England.

[41] Gallager, R. (1968). *Information Theory and Reliable Communication*. Wiley.

[42] Gao, Y., Chen, Y., and Liu, K. (2012). Cooperation stimulation for multiuser cooperative communications using indirect reciprocity game. *IEEE Trans. Commun.*, 60(12):3650–3661.

[43] Genc, V., Murphy, S., Yu, Y., and Murphy, J. (2008). IEEE 802.16J relay-based wireless access networks: an overview. *IEEE Wireless Commun. Mag.*, 15(5):56–63.

[44] Goldsmith, A. (2005). *Wireless Communications*. Cambridge University Press.

[45] Goldsmith, A. and Chua, S.-G. (1997). Variable-rate variable-power MQAM for fading channels. *IEEE Trans. Commun.*, 45(10):1218–1230.

[46] Gong, X., Vorobyov, S., and Tellambura, C. (2010). Joint bandwidth and power allocation in wireless multi-user decode-and-forward relay networks. In *Proc. IEEE International Conference on Acoustics Speech and Signal Processing (ICASSP 2010)*, pages 2498–2501, Dallas, Texas, USA.

[47] Goodman, D. J. and Mandayam, N. B. (2000). Power control for wireless data. *IEEE Personal Commun. Mag.*, 7(2):48–54.

[48] Hajiaghayi, M., Dong, M., and Liang, B. (2012). Jointly optimal channel and power assignment for dual-hop multi-channel multi-user relaying. *IEEE J. Sel. Areas Commun.*, 30(9):1806–1814.

[49] Hammerstrom, I. and Wittneben, A. (2006). On the optimal power allocation for nonregenerative OFDM relay links. In *Proc. IEEE International Conference on Communications (ICC 2006)*, volume 10, pages 4463–4468, Istanbul, Turkey.

[50] Han, Z., Ji, Z., and Liu, K. (2005). Fair multiuser channel allocation for OFDMA networks using Nash bargaining solutions and coalitions. *IEEE Trans. Commun.*, 53(8):1366–1376.

[51] Han, Z., Li, H., and Yin, W. (2013). *Compressive Sensing for Wireless Networks*. Cambridge University Press.

[52] Han, Z. and Liu, K. R. (2008). *Resource Allocation for Wireless Networks Basics, Techniques, and Applications*. Cambridge University Press, New York, NY, USA.

[53] Han, Z., Niyato, D., Saad, W., Basar, T., and Hjorungnes, A. (2012). *Game Theory in Wireless and Communication Networks theory, Models, and Applications*. Cambridge University Press, New York, NY, USA.

[54] Harrold, T. and Nix, A. (2000a). Capacity enhancement using intelligent relaying for future personal communication systems. In *Proc. IEEE 52nd Vehicular Technology Conference (VTC 2000) Fall*, volume 5, pages 2115–2120, Boston, Ma, USA.

[55] Harrold, T. and Nix, A. (2000b). Intelligent relaying for future personal communication systems. In *IEE Colloquium on Capacity and Range Enhancement Techniques for the Third Generation Mobile Communications and Beyond*, pages 1–9, London, UK.

[56] Hasna, M. and Alouini, M. (2003). End-to-end performance of transmission systems with relays over Rayleigh-fading channels. *IEEE Trans. Wireless Commun.*, 2(6):1126–1131.

[57] Hasna, M. and Alouini, M. (2004a). Optimal power allocation for relayed transmissions over Rayleigh-fading channels. *IEEE Trans. Wireless Commun.*, 3(6):1999–2004.

[58] Hasna, M. and Alouini, M. (2004b). A performance study of dual-hop transmissions with fixed gain relays. *IEEE Trans. Wireless Commun.*, 3(6):1963–1968.

[59] Hasna, M. O. and Alouini, M. (2002). Performance analysis of two-hop relayed transmissions over rayleigh fading channels. In *Proc. IEEE 56th Vehicular Technology Conference (VTC 2002) Fall*, volume 4, pages 1992–1996, Vancouver, Canada.

[60] Hayajneh, M. and Abdallah, C. (2004). Distributed joint rate and power control game-theoretic algorithms for wireless data. *IEEE Commun. Lett.*, 8(8):511–513.

[61] Himsoon, T., Siriwongpairat, W., Han, Z., and Liu, K. (2006). Lifetime maximization by cooperative sensor and relay deployment in wireless sensor networks. In *Proc. IEEE Wireless Communications and Networking Conference (WCNC 2006)*, volume 1, pages 439–444.

[62] Hong, Y. P., Huang, W.-J., and Kuo, C. J. (2010). *Cooperative Communications and Networking Technologies and System Design*. Springer, New York, NY, USA.

[63] Hossain, E., Kim, D. I., and Bhargava, V. K., editors (2011). *Cooperative Cellular Wireless Networks*. Cambridge University Press, New York, NY, USA.

[64] Hsu, C.-N., Lin, P.-H., and Su, H.-J. (2010). Joint subcarrier pairing and power allocation for OFDM two-hop systems. In *Proc. IEEE International Conference on Communications (ICC 2010)*, pages 1–5.

[65] Hu, J. and Chen, X. (2010). Performance of decode-and-forward cooperative communications with channel estimation errors over Rayleigh fading channels. In *Proc. 2nd International Conference on Future Computer and Communication (ICFCC 2010)*, volume 1, pages 164–167, Wuhan, China.

[66] Huang, J., Han, Z., Chiang, M., and Poor, H. (2008). Auction-based resource allocation for cooperative communications. *IEEE J. Sel. Areas Commun.*, 26(7):1226–1237.

[67] Huang, J., Subramanian, V., Agrawal, R., and Berry, R. (2009a). Downlink scheduling and resource allocation for OFDM systems. *IEEE Trans. Wireless Commun.*, 8(1):288–296.

[68] Huang, J., Subramanian, V., Agrawal, R., and Berry, R. (2009b). Joint scheduling and resource allocation in uplink OFDM systems for broadband wireless access networks. *IEEE J. Sel. Areas Commun.*, 27(2):226–234.

[69] Hunter, T., Sanayei, S., and Nosratinia, A. (2006). Outage analysis of coded cooperation. *IEEE Trans. Inf. Theory*, 52(2):375–391.

[70] Ibe, O. (2005). *Fundamentals of Applied Probability and Random Processes*. Elsevier Academic Press.

[71] Ibrahim, A., Sadek, A., Su, W., and Liu, K. (2008). Cooperative communications with relay-selection: when to cooperate and whom to cooperate with? *IEEE Trans. Wireless Commun.*, 7(7):2814–2827.

[72] Ikki, S. and Ahmed, M. (2007). Performance analysis of cooperative diversity wireless networks over Nakagami-m fading channel. *IEEE Commun. Lett.*, 11(4):334–336.

[73] Ikki, S. and Ahmed, M. (2008). Performance of multiple-relay cooperative diversity systems with best relay selection over Rayleigh fading channels. *EURASIP Journal on Advances in Signal Processing*, 2008(1).

[74] Ikki, S. and Ahmed, M. (2009a). On the performance of adaptive decode-and-forward cooperative diversity with the Nth best-relay selection scheme. In *Proc. IEEE Global Telecommunications Conference (GLOBECOM 2009)*, pages 1–6, Honolulu, Hawaii, USA.

[75] Ikki, S. and Ahmed, M. (2009b). On the performance of amplify-and-forward cooperative diversity with the Nth best-relay selection scheme. In *Proc. IEEE International Conference on Communications (ICC 2009)*, pages 1–6, Dresden, Germany.

[76] Ikki, S. and Ahmed, M. (2010a). On the performance of cooperative-diversity networks with the Nth best-relay selection scheme. *IEEE Trans. Commun.*, 58(11):3062 –3069.

[77] Ikki, S. and Ahmed, M. (2010b). Performance analysis of adaptive decode-and-forward cooperative diversity networks with best-relay selection. *IEEE Trans. Commun.*, 58(1):68–72.

[78] Jing, Y. and Hassibi, B. (2006). Distributed space-time coding in wireless relay networks. *IEEE Trans. Wireless Commun.*, 5(12):3524–3536.

[79] Jing, Y. and Jafarkhani, H. (2009). Single and multiple relay selection schemes and their achievable diversity orders. *IEEE Trans. Wireless Commun.*, 8(3):1414–1423.

[80] Karagiannidis, G. (2006). Performance bounds of multihop wireless communications with blind relays over generalized fading channels. *IEEE Trans. Wireless Commun.*, 5(3):498–503.

[81] Kelly, F., Maulloo, A., and Tan, D. (1998). Rate control for communication networks: Shadow prices, proportional fairness and stability. *J. Oper. Res. Soc.*, 49(3):237–252.

[82] Kennedy, J. and Eberhart, R. (1995). Particle swarm optimization. In *Proc. IEEE International Conference on Neural Networks*, volume 4, pages 1942–1948, Perth, Western Australia.

[83] Kong, Z., Kwok, Y.-K., and Wang, J. (2009). Auction-based scheduling in non-cooperative multiuser OFDM systems. In *Proc. IEEE 69th Vehicular Technology Conference (VTC 2009) Spring*, pages 1–4, Barcelona, Spain.

[84] Laneman, J. (2002). *Cooperative Diversity in Wireless Networks: Algorithms and Architectures*. Ph.d. thesis, Massachusetts Institute of Technology, Cambridge, MA.

[85] Laneman, J. (2004). Network coding gain of cooperative diversity. In *Proc. Military Communications Conference (MILCOM 2004)*, pages 106–112, Monterey, CA.

[86] Laneman, J. N., Tse, D. N., and Wornell, G. W. (2004). Cooperative diversity in wireless networks: Efficient protocols and outage behavior. *IEEE Trans. Inf. Theory*, 50(12):3062–3080.

[87] Larsson, P. and Rong, H. (2004). Large-scale cooperative relay network with optimal coherent combining under aggregate relay power constraints. In *Working Group 4, World Wireless Research Forum WWRF8 Meeting*.

[88] Lasaulce, S., Debbah, M., and Altman, E. (2009a). Methodologies for analyzing equilibria in wireless games. *IEEE Signal Process. Mag.*, 26(5):41–52.

[89] Lasaulce, S., Hayel, Y., El Azouzi, R., and Debbah, M. (2009b). Introducing hierarchy in energy games. *IEEE Trans. Wireless Commun.*, 8(7):3833–3843.

[90] Lasaulce, S. and Tembine, H. (2011). *Game Theory and Learning for Wireless Networks Fundamentals and Applications*. Elsevier Ltd., MA, USA.

[91] Lee, J., Wang, H., Andrews, J., and Hong, D. (2011). Outage probability of cognitive relay networks with interference constraints. *IEEE Trans. Wireless Commun.*, 10(2):390–395.

[92] Letaief, K. and Zhang, W. (2009). Cooperative communications for cognitive radio networks. *Proceedings of the IEEE*, 97(5):878–893.

[93] Li, M., Yang, Z., and Wenjing, L. (2011). Codeon: Cooperative popular content distribution for vehicular networks using symbol level network coding. *IEEE J. Sel. Areas Commun.*, 29(1):223–235.

[94] Liu, K., Sadek, A. K., Su, W., and Kwasinski, A. (2009). *Cooperative Communications and Networking*. Cambridge University Press, New York, NY, USA.

[95] Liu, Q., Ma, X., and Zhou, G. (2011). A general diversity gain function and its application in amplify-and-forward cooperative networks. *IEEE Trans. Signal Process.*, 59(2):859–863.

[96] Liu, Y. and Chen, W. (2012). Adaptive resource allocation for improved DF aided downlink multi-user OFDM systems. *IEEE Commun. Lett.*, 1(99):1–4.

[97] Liu, Y., Mo, J., and Tao, M. (2013). Qos-aware transmission policies for ofdm bidirectional decode-and-forward relaying. *IEEE Trans. Wireless Commun.*, 12(5):2206–2216.

[98] Maric, I. and Yates, R. (2010). Bandwidth and power allocation for cooperative strategies in gaussian relay networks. *IEEE Trans. Inf. Theory*, 56(4):1880–1889.

[99] Mesbah, W. and Davidson, T. (2008). Power and resource allocation for orthogonal multiple access relay systems. *EURASIP Journal on Advances in Signal Processing*, 2008(1):1–15.

[100] Molisch, A. F. (2011). *Wireless Communications*. John Wiley & Sons Ltd., West Sussex, United Kingdom, 2nd edition.

[101] Neel, J. (2006). *Analysis and Design of Cognitive Radio Networks and Distributed Radio Resource Management Algorithms*. Ph.D. thesis, Virginia Polytechnic Institute and State University.

[102] Ni, Q. and Zarakovitis, C. C. (2012). Nash bargaining game theoretic scheduling for joint channel and power allocation in cognitive radio systems. *IEEE J. Sel. Areas Commun.*, 30(1):70–81.

[103] Niyato, D. and Hossain, E. (2008). Competitive spectrum sharing in cognitive radio networks: A dynamic game approach. *IEEE Trans. Wireless Commun.*, 7(7):2651–2660.

[104] Nocedal, J. and Wright, S. J. (2006). *Numerical Optimization*. Springer, New York, NY, USA, 2nd edition.

[105] Osborne, M. and Rubinstein, A. (1994). *A Course in Game Theory*. The MIT Press, Cambridge, MA.

[106] P.-N., A. I. and Campalans, M. R. (2008). *Cross-Layer Resource Allocation in Wireless Communications: Techniques and Models from PHY and MAC Layer Interaction*. Academic Press.

[107] Papoulis, A. (1991). *Probability, Random Variables, and Stochastic Processes*. McGraw-Hill, Inc., New York, USA, 3rd edition.

[108] Phan, K. T., Le-Ngoc, T., Vorobyov, S. A., and Tellambura, C. (2009). Power allocation in wireless multi-user relay networks. *IEEE Trans. Wireless Commun.*, 8(5):2535–2545.

[109] Rao, S. S. (2009). *Engineering Optimization Theory and Practice*. John Wiley & Sons, Inc., Hoboken, New Jersey, USA.

[110] Ren., S. and van der Schaar, M. (2011). Pricing and distributed power control in wireless relay networks. *IEEE Trans. Signal Process.*, 59(6):2913–2926.

[111] Ribeiro, A., Cai, X., and Giannakis, G. (2006). Opportunistic multipath for bandwidth-efficient cooperative multiple access. *IEEE Trans. Wireless Commun.*, 5(9):2321–2327.

[112] Rosen, J. (1965). Existence and uniqueness of equilibrium points for concave N-person games. *Econometrica*, 33(3):520–534.

[113] Saad, W., Han, Z., Debbah, M., Hjorungnes, A., and Basar, T. (2009). Coalitional game theory for communication networks. *IEEE Signal Process. Mag.*, 26(5):77–97.

[114] Sadek, A., Su, W., and Liu, K. (2007). Multinode cooperative communications in wireless networks. *IEEE Trans. Signal Process.*, 55(1):341–355.

[115] Saraydar, C., Mandayam, N., and Goodman, D. (2002). Efficient power control via pricing in wireless data networks. *IEEE Trans. Commun.*, 50(2):291–303.

[116] Scaglione, A., Goeckel, D., and Laneman, J. N. (2007). *Distributed Antenna Systems: Open Architecture for Future Wireless Communications*, chapter Cooperative Communications in Mobile Ad-Hoc Networks: Rethinking the Link Abstraction. Auerbach Publications, CRC Press.

[117] Scutari, G., Barbarossa, S., and Palomar, D. (2006). Potential games: A framework for vector power control problems with coupled constraints. In *Proc. IEEE International Conference on Acoustics, Speech and Signal Processing (ICASSP 2006)*, pages 241–244, Toulouse, France.

[118] Scutari, G., Palomar, D., and Barbarossa, S. (2009). The MIMO iterative waterfilling algorithm. *IEEE Trans. Signal Process.*, 57(5):1917–1935.

[119] Sendonaris, A., Erkip, E., and Aazhang, B. (2003a). User cooperation diversity: Part I system description. *IEEE Trans. Commun.*, 51(11):1939–1948.

[120] Sendonaris, A., Erkip, E., and Aazhang, B. (2003b). User cooperation diversity: Part II implementation aspects and performance analysis. *IEEE Trans. Commun.*, 51(11):1939–1948.

[121] Seong, K., Mohseni, M., and Cioffi, J. (2006). Optimal resource allocation for OFDMA downlink systems. In *Proc. IEEE International Symposium on Information Theory*, pages 1394–1398.

[122] Serbetli, S. and Yener, A. (2008). Relay assisted F/TDMA Ad Hoc networks: node classification, power allocation and relaying strategies. *IEEE Trans. Commun.*, 56(6):937–947.

[123] Shannon, C. E. (1948). A mathematical theory of communication. *Bell System Technical Journal*, 27.

[124] Shaqfeh, M. and Alnuweiri, H. (2011). Joint power and resource allocation for block-fading relay-assisted broadcast channels. *IEEE Trans. Wireless Commun.*, 10(6):1904 –1913.

[125] Shen, Y., Feng, G., Yang, B., and Guan, X. (2012). Fair resource allocation and admission control in wireless multiuser amplify-and-forward relay networks. *IEEE Trans. Veh. Technol.*, 61(3):1383–1397.

[126] Shen, Z., Wang, X., and Zhang, H. (2009). Power allocation and subcarrier pairing for OFDM-based AF cooperative diversity systems. In *Proc. IEEE 69th Vehicular Technology Conference (VTC 2009) Spring*, pages 1–5, Barcelona, Spain.

[127] Shi, Y., Wang, J., Letaief, K., and Mallik, R. (2009). A game-theoretic approach for distributed power control in interference relay channels. *IEEE Trans. Wireless Commun.*, 8(6):3151–3161.

[128] Sidhu, G., Gao, F., Fan, L., and Nallanathan, A. (2011). A joint resource allocation scheme for relay aided uplink multi-user OFDMA system. In *Proc. IEEE Global Telecommunications Conference (GLOBECOM 2011)*, pages 1–5.

[129] Sierksma, G. (2001). *Linear and Integer Programming: Theory and Practice*. CRC Press, 2nd edition.

[130] Simon, M. and Alouini, M. (2000). *Digital Communication Over Fading Channels*. John Wiley & Sons, New York, NY, USA.

[131] Siriwongpairat, W., Sadek, A., and Liu, K. (2008). Cooperative communications protocol for multiuser ofdm networks. *IEEE Trans. Wireless Commun.*, 7(7):2430–2435.

[132] Stefanov, A. and Erkip, E. (2004). Cooperative coding for wireless networks. *IEEE Trans. Commun.*, 52(9):1470–1476.

[133] Stefanov, A. and Erkip, E. (2005). Cooperative space-time coding for wireless networks. *IEEE Trans. Commun.*, 53(11):1804–1809.

[134] Su, W., Sadek, A., and Liu, K. (2005). SER performance analysis and optimum power allocation for decode-and-forward cooperation protocol in wireless networks. In *Proc. IEEE Wireless Communications and Networking Conference (WCNC 2005)*, volume 2, pages 984–989.

[135] Su, W., Sadek, A., and Ray Liu, K. (2008). Cooperative communication protocols in wireless networks: Performance analysis and optimum power allocation. *Wireless Personal Communications*, 44(2):181–217.

[136] Su, X. and Chan, S. (2006). Max-min fair rate allocation in multi-hop wireless Ad Hoc networks. In *Proc. IEEE International Conference on Mobile Ad-hoc and Sensor Systems (MASS 2006)*, pages 513–516.

[137] Sun, J., Modiano, E., and Zheng, L. (2006). Wireless channel allocation using an auction algorithm. *IEEE J. Sel. Areas Commun.*, 24(5):1085–1096.

[138] Talha, B. and Patzold, M. (2010). On the statistical analysis of equal gain combining over multiple double rice fading channels in cooperative networks. In *Proc. IEEE 72nd Vehicular Technology Conference (VTC 2010) Fall*, pages 1–5.

[139] Tang, J. and Zhang, X. (2007). Cross-layer resource allocation over wireless relay networks for quality of service provisioning. *IEEE J. Sel. Areas Commun.*, 25(4):645–656.

[140] Tao, X., Xu, X., and Cui, Q. (2012). An overview of cooperative communications. *IEEE Commun. Mag.*, 50(6):65–71.

[141] Timus, B. (2009). *Studies on the Viability of Cellular Multihop Networks with Fixed Relays*. Ph.d. thesis, Royal Institute of Technology (KTH), Stockholm, Sweden.

[142] Torabi1, M., Ajib, W., and Haccoun, D. (2009). Performance analysis of amplify-and-forward cooperative networks with relay selection over Rayleigh fading channels. In *Proc. IEEE 69th Vehicular Technology Conference (VTC 2009) Spring*, pages 1–5, Barcelona, Spain.

[143] Tsiaflakis, P., Vangorp, J., Moonen, M., and Verlinden, J. (2007). A low complexity optimal spectrum balancing algorithm for digital subscriber lines. *Signal Processing*, 87(7):1735–1753.

[144] Uysal, M., editor (2010). *Cooperative Communications for Improved Wireless Network Transmission: Framework for Virtual Antenna Array Applications*. IGI Global, Hershey, New York, USA.

[145] van der Meulen, E. (1968). *Transmission of information in a T-terminal discrete memoryless channel*. Ph.D. thesis, Dept. of Statistics, University of California, Berkeley.

[146] Vandendorpe, L., Duran, R., Louveaux, J., and Zaidi, A. (2008). Power allocation for OFDM transmission with DF relaying. In *Proc. IEEE International Conference on Communications (ICC 2008)*, pages 3795–3800.

[147] Vandendorpe, L., Louveaux, J., Oguz, O., and Zaidi, A. (2009). Rate-optimized power allocation for DF-relayed OFDM transmission under sum and individual power constraints. *EURASIP Journal on Wireless Communications and Networking*, 2009(1):814278.

[148] w. Han, S. and Han, Y. (2007). A competitive fair subchannel allocation for OFDMA system using an auction algorithm. In *Proc. IEEE 66th Vehicular Technology Conference (VTC 2007) Fall*, pages 1787–1791, Baltimore, Maryland, USA.

[149] Wang, B., Han, Z., and Liu, K. R. (2009). Distributed relay selection and power control for multiuser cooperative communication networks using Stackelberg game. *IEEE Trans. Mobile Comput.*, 8(7):975–990.

[150] Wang, T. and Vandendorpe, L. (2011). Sum rate maximized resource allocation in multiple df relays aided ofdm transmission. *IEEE J. Sel. Areas Commun.*, 29(8):1559–1571.

[151] Wang, Z. and Giannakis, G. (2003). A simple and general parameterization quantifying performance in fading channels. *IEEE Trans. Commun.*, 51(8):1389 – 1398.

[152] Weeraddana, P. C., Codreanu, M., Latva-aho, M., Ephremides, A., and Fischione, C. (2012). *Weighted Sum-Rate Maximization in Wireless Networks: A Review*. Now Publishers Inc., Hanover, MA, USA.

[153] Wong, C. Y., Cheng, R., Lataief, K., and Murch, R. (1999). Multiuser OFDM with adaptive subcarrier, bit, and power allocation. *IEEE J. Sel. Areas Commun.*, 17(10):1747–1758.

[154] Wong, I. and Evans, B. (2008). *Resource Allocation in Multiuser Multicarrier Wireless Systems*. Springer, New York, NY, USA.

[155] Woradit, K., Quek, T., Suwansantisuk, W., Wymeersch, H., Wuttisittikulkij, L., and Win, M. (2009). Outage behavior of selective relaying schemes. *IEEE Trans. Wireless Commun.*, 8(8):3890–3895.

[156] Wu, D. and Cai, Y. (2009). Power allocation in interference relay channels based on non-cooperative game theory. In *Proc. International Conference on Wireless Communications Signal Processing (WCSP 2009)*, pages 1–5, Nanjing, China.

[157] Yaiche, H., Mazumdar, R., and Rosenberg, C. (2000). A game theoretic framework for bandwidth allocation and pricing in broadband networks. *IEEE/ACM Trans. Netw.*, 8(5):667–678.

[158] Yang, C., Zhao, S., Wang, W., and Peng, M. (2010). Performance of decode-and-forward opportunistic cooperation with the Nth best relay selected. In *Proc. 6th International Wireless Communications and Mobile Computing Conference (IWCMC 2010)*, pages 1253–1257, Caen, France.

[159] Yang, D., Fang, X., and Xue, G. (2011). Truthful auction for cooperative communications. In *Proc. ACM 12th International Symposium on Mobile Ad Hoc Networking and Computing*, pages 1–9, New York, NY, USA. ACM.

[160] Yang, D., Fang, X., and Xue, G. (2012a). Game theory in cooperative communications. *IEEE Wireless Communications*, 19(2):44–49.

[161] Yang, D., Fang, X., and Xue, G. (2012b). Truthful auction for cooperative communications with revenue maximization. In *Proc. IEEE International Conference on Communications (ICC 2012)*, pages 4888–4892.

[162] Yang, S. C. (2010). *OFDMA System Analysis and Design*. Artech House, Boston, London.

[163] Yao, H. and Zhong, S. (2011). Towards cheat-proof cooperative relay for cognitive radio networks. In *Proc. ACM 12th International Symposium on Mobile Ad Hoc Networking and Computing*, pages 1–11, New York, NY, USA. ACM.

[164] Yates, R. (1995). A framework for uplink power control in cellular radio systems. *IEEE J. Sel. Areas Commun.*, 13(7):1341–1347.

[165] Yiqing, L., Xigang, Y., and Yongjian, L. (2007). An improved PSO algorithm for solving non-convex NLP/MINLP problems with equality constraints. *Computers &amp Chemical Engineering*, 31(3):153–162.

[166] Yu, W. and Cioffi, J. (2002). FDMA capacity of Gaussian multiple-access channels with ISI. *IEEE Trans. Commun.*, 50(1):102–111.

[167] Yu, W. and Lui, R. (2006). Dual methods for nonconvex spectrum optimization of multicarrier systems. *IEEE Trans. Commun.*, 54(7):1310–1322.

[168] Zhang, D., Shinkuma, R., and Mandayam, N. B. (2010). Bandwidth exchange: an energy conserving incentive mechanism for cooperation. *IEEE Trans. Wireless Commun.*, 9(6):2055–2065.

[169] Zhang, G., Cong, L., Zhao, L., Yang, K., and Zhang, H. (2009). Competitive resource sharing based on game theory in cooperative relay networks. *ETRI Journal*, 31(1):89–91.

[170] Zhang, J. and Zhang, Q. (2009). Stackelberg game for utility-based cooperative cognitive radio networks. In *Proc. ACM 10th International Symposium on Mobile Ad Hoc Networking and Computing*, pages 23–32, New York, NY, USA. ACM.

[171] Zhang, R., Wang, L., Parr, G., Aliu, O., Awoseyila, B., Azarmi, N., Bhatti, S., Bodanese, E., Chen, H., Dianati, M., Dutta, A., Fitch, M., Giridhar, K., Hailes, S., Hari, K., Imran, M., Jagannatham, A., Karandikar, A., Kawade, S., Ali Khan, M., Kompalli, S., Langdon, P., Narayanan, B., Mauthe, A., McGeehan, J., Mehta, N., Millet, K., Moessner, K., Rajashekar, R., Ramkumar, B., Ribeiro, V., Vasudevan, K., Hanzo, L., and Bigham, J. (2013a). Advances in base- and mobile-station aided cooperative wireless communications: An overview. *IEEE Vehicular Technology Magazine*, 8(1):57–69.

[172] Zhang, X., Zheng, Z., Liu, J., Shen, X., and Xie, L.-L. (2012). Optimal power allocation and AP deployment in green wireless cooperative communications. In *Proc. IEEE Global Telecommunications Conference (GLOBECOM-2012)*, pages 4000–4005.

[173] Zhang, Y., Lee, C., Niyato, D., and Wang, P. (2013b). Auction approaches for resource allocation in wireless systems: A survey. *IEEE Trans. Control Syst. Technol.*, 15(3):1020–1041.

[174] Zhang, Z., Shi, J., Chen, H.-H., Guizani, M., and Qiu, P. (2008). A cooperation strategy based on Nash bargaining solution in cooperative relay networks. *IEEE Trans. Veh. Technol.*, 57(4):2570–2577.

[175] Zhao, Y., Adve, R., and Lim, T. (2006). Symbol error rate of selection amplify-and-forward relay systems. *IEEE Commun. Lett.*, 10(11):757–759.

[176] Zheng, G., Zhang, Y., Ji, C., and Wong, K.-K. (2009). Optimizing relay selection and power allocation for orthogonal multiuser downlink systems. In *Proc. International Conference on Wireless Communications Signal Processing (WCSP 2009)*, pages 1–5, Nanjing, China.

[177] Zhou, N., Zhu, X., Huang, Y., and Lin, H. (2009). Adaptive resource allocation for multi-destination relay systems based on OFDM modulation. In *Proc. IEEE International Conference on Communications (ICC 2009)*, pages 1–5.

[178] Zhou, Z., Zhou, S., Cui, S., and Cui, J.-H. (2008). Energy-efficient cooperative communication in a clustered wireless sensor network. *IEEE Trans. Veh. Technol.*, 57(6):3618–3628.

[179] Zhu, L., Yu, F. R., Ning, B., and Tang, T. (2013). A joint design of security and quality-of-service (QoS) provisioning in vehicular Ad Hoc networks with cooperative communications. *EURASIP Journal on Wireless Communications and Networking*, 2013(1):88.